EXPERIMENTAL PERFORMANCE INVESTIGATION OF GRAPHENE FERROCK CEMENT CONCRETE AND ITS COST ANALYSIS

Thesis Submitted for the Award of the Degree of

DOCTOR OF PHILOSOPHY

in

Civil engineering

By

Neha Singh

Registration Number: 12209870

Supervised By

Dr. Jaspreet singh (16659)

Department of civil engineering (Associate professor)

Lovely professional university

LOVELY PROFESSIONAL UNIVERSITY, PUNJAB

2025

DECLARATION

I, Neha Singh (12209870) hereby declared that the presented work in the thesis entitled "**Experimental Performance Investigation of Graphene Ferrock Cement Concrete and its Cost Analysis**" in fulfilment of degree of **Doctor of Philosophy (Ph.D.) in School of Civil Engineering** is outcome of research work carried out by me under the supervision of Dr. Jaspreet Singh, working as Associate Professor, in the School of Civil Engineering of Lovely Professional University, Punjab, India. The research work was completed in three years from 2022 to 2025. In keeping with general practice of reporting scientific observations, due acknowledgements have been made whenever work described here has been based on findings of another investigator. This work has not been submitted in part or full to any other University or Institute for the award of any degree.

(Signature of Scholar)

Name of the scholar:

Registration No.:

Department/school:

Lovely Professional University,

Punjab, India

CERTIFICATE

This is to certify that the work reported in the Ph.D. thesis entitled "**Experimental Performance Investigation of Graphene Ferrock Cement Concrete and its Cost Analysis**" submitted in fulfillment of the requirement for the award of degree of **Doctor of Philosophy (Ph.D.)** in the School of Civil Engineering, is a research work carried out by Neha Singh, 12209870, is Bonafide record of her original work carried out under my supervision and that no part of thesis has been submitted for any other degree, diploma or equivalent course. The experimental work was carried out from 2022 to 2025.

(Signature of Supervisor)	**(Signature of Co-Supervisor)**
Name of supervisor:	Name of Co-Supervisor:
Designation:	Designation:
Department/school:	Department/school:
University:	University

Abstract

Concrete is among the most widely used construction materials globally, and its demand is growing due to rapid infrastructure development with increase in an urban population that has led to a significant increase in cement production. As the primary binder in concrete, cement contributes substantially to strength development, but its production process is highly energy-intensive and a major source of CO_2 emissions—accounting for approximately 7% of global emissions. The process involves the combustion of fossil fuels and the calcination of raw materials, both of which contribute to environmental degradation. In addition, conventional concrete suffers from limitations such as porosity, chloride penetration, reduced workability, and low tensile strength. These challenges highlight the need for sustainable alternatives that reduce environmental impact while enhancing concrete performance.

India is currently second largest producer of crude steel after China with a market share of almost 6%. The Government of India is taking the initiative to promotes steel manufacturing by setting a target of 300 million tons crude steel in National steel policy 2017. This growth has led to the generation of large quantities of iron waste, which is often disposed of in landfills, contributing to soil pollution and environmental degradation this underscores the need for sustainable waste management solutions.

The present study addresses these two critical environmental challenges: the rising levels of atmospheric CO_2 because of increasing usage of cement and the increasing iron oxide waste generated from the steel industry. The production of cement significantly contributes to global CO_2 emissions, while finer iron waste often ends up in landfills, adversely affecting soil morphology. The incorporation of reduced graphene oxide (rGO) and ferrock into concrete aims to improve strength along with a reduction in cement usage.

Ferrock is a material that hardened through the carbonation of waste iron powder collected from steel industries to form strong composite with other pozzolanic materials. Ferrock contains iron oxide, fly ash, metakaolin, limestone and oxalic acid as raw materials. It utilizes iron oxide as the primary binder in

ferrock which reacts with CO_2 in the presence of oxalic acid to form complex iron carbonates which are responsible for its hardening. This hardening reaction uses CO_2 to form products that make ferrock works as a carbon-negative material. Recently the use of nano materials is increasing in construction due to their exceptional properties of large surface area and good tensile strength. rGO is a carbon-based nanomaterial derived from graphene oxide, exhibits a high surface area and tensile strength, making it highly suitable for enhancing cementitious composites. Its hydrophilic nature and water dispersibility support uniform dispersion in the concrete matrix. Its incorporation improves binding within the matrix, contributing to improved mechanical behavior.

The objective of this study is to investigate the individual and combined effects of rGO and ferrock as partial substitutes for cement. The aim is to reduce cement consumption, manage industrial waste effectively, and enhance the strength and durability of concrete, thereby contributing to sustainable construction practices.

Initially, the study focuses on the preparation of ferrock and investigates the optimal ratio of raw materials along with suitable CO_2 curing duration. This optimized composition and curing period are then used consistently throughout the research. The research explored the reactivity of iron oxide with CO_2 in the presence of oxalic acid, leading to iron carbonate formation, which enhanced binding properties and provides strength. Sixteen mixes were prepared with varying proportions of iron oxide, fly ash, metakaolin, limestone and carbon curing durations of 2,3,4,5 and 6 days followed by 3 days of air curing. The unconfined compressive strength test was performed to identify the optimal mix and carbon curing duration against the mix that gained highest strength among all the mixes. The results identified 62%, 20%, 10%, 6% and 2% as the optimum ratios of iron oxide, fly ash, metakaolin, limestone and oxalic acid respectively which achieved highest strength of 41.46 N/mm^2 at 4 days of CO_2 curing.

Energy Dispersive X-Ray Spectroscopy (EDS) confirmed a significant reduction in iron oxide content after four days of CO_2 curing compared to one day, indicating its reaction with CO_2 to form carbonation products. X- Ray Diffraction (XRD) analysis identified the mineral phases of iron, while Scanning

Electron Microscopy (SEM) revealed the particle morphology contributing to microstructural development.

The concrete mixes were prepared with rGO and ferrock as partial replacement of cement in ratio 0.1%, 0.2%, 0.4%, 0.6%, 0.8% and 5%, 10%, 15%, 20% respectively. Concrete mixes were prepared using a combination of rGO at 0.2% and ferrock at varying replacement levels of 5%, 10%, 15%, and 20%. During testing, the mix containing 0.2% rGO achieved the highest strength among all rGO-modified mixes; therefore, this proportion was consistently used in further combinations with ferrock.

All these mixes were tested for the fresh properties by slump cone test and compaction factor test to check the workability and compaction degree of fresh mix. The hardened properties of all mixes were determined by compressive, split tensile and flexural strength tests at 3 days, 7 days, 28 days, 56 days and 90 days. The samples with ferrock were initially cured in CO_2 environment for 4 days and then transferred to water tank for curing. Further durability of all concrete mixes was determined by total absorption test, water permeability test, initial surface absorption test and rapid chloride penetration test at 28, 56 and 90 days of curing. Microstructural analysis was conducted by SEM, EDS and XRD to study surface morphology, elemental composition and minerals peaks respectively. Carbonation tests were done on mixes which contain ferrock by using phenolphthalein as an indicator to provide visual interpretation for carbonated and non-carbonated areas of concrete and results reported.

The findings of the study concluded that 0.2% rGO showed highest improvement in compressive, split tensile, and flexural strength of 37.38%, 49.77% 29.06% respectively at 28 days of curing in all mixes of rGO. The mixes with ferrock showed 10% replacement showed the highest improvement of 36.51%, 37.55%, 19.38% for compressive, split tensile and flexural strength respectively at 28 days of curing among all mixes of ferrock. The mixes with rGO and ferrock combined showed optimum results with rGO 0.2% and ferrock 10%. This mix showed optimum improvement as 82.74%, 40.31%, and 54.75% for compressive, split tensile, and flexural strength respectively.

The durability tests were performed at 28 days, 56 days and 90 days of curing on all mixes and findings concluded that durability was improved with the inclusion of rGO and ferrock individually also together. Mixes with rGO exhibited less water and chloride penetration, with 0.8% rGO achieving the lowest absorption and penetration across all curing days. For chloride resistance, 0.6% showed the lowest permeability, classified as very low at 90 days. Increasing ferrock content in concrete enhances durability by reducing absorption (3.5% in FC5 to 2.33% in FC20) and penetration depth (27.2 mm to 17.6 mm). Initial Surface Absorption Test values dropped from 0.53 to 0.43 ml/m²/sec, and Rapid Chloride Penetration Test showed lesser chloride permeability, with FC10 decreasing from 1972 to 941 coulombs lie in low penetration zone. These results confirm the effectiveness of ferrock in improving concrete durability. The concrete matrix was found to be dense, compacted to enhance bonding between aggregates and other materials and reduce porosity. Increasing the ferrock ratio with constant 0.2% rGO enhanced durability by reducing water and chloride penetration in concrete. At 90 days, GC0.2F20 improved water penetration, absorption, and ISAT by 35.29%, 61.9% and 35.71%, respectively. The chloride penetration test showed GC0.2F10 had the highest chloride reduction of 72.47%, classified as low chloride penetration.

Microstructural and mineralogical analyses supported the performance enhancements observed in the modified concrete mixes. SEM revealed denser and more compact structures in samples with rGO, although excessive dosages led to visible agglomeration. Mixes containing ferrock exhibited reduced porosity, while the combination of rGO and ferrock showed complex hydrated crystal formations. EDS confirmed the presence of key elements such as silicon, Ca, and oxygen, which contribute to strength development. XRD analysis identified quartz as a common phase in all mixes, along with additional peaks such as SiO_2, CSH, and calcium carbonate. Notably, the combined mixes also showed the formation of iron carbonate, indicating beneficial mineralogical transformations that support both mechanical performance and durability.

The carbonation test was performed on mixes containing ferrock as CO_2 curing provided to samples contained ferrock only and results revealed that

concrete with ferrock absorbs CO_2. Phenolphthalein was used as an indicator, turning pink in non-carbonated areas and remaining colorless in carbonated areas. Concrete cubes were subjected to CO_2 curing for 4 days, followed by 28 days of water curing. The cubes with ferrock showed there was maximum carbonated part shows CO_2 was absorbed in ferrock. A sample with ferrock showed no pink coloration, suggesting complete CO_2 absorption due to the conversion of iron oxide into iron carbonates. Mixes FC5, FC10, FC15, and FC20 displayed varying degrees of carbonation, with FC5 showing the most pink area (least carbonation) and FC20 the least pink (highest carbonation). The results confirm the role of ferrock as a CO_2-absorbing material, with higher ferrock content enhancing CO_2 absorption.

Results found that strength and durability improved at all replacement ratios as compared to control sample. This research promotes sustainability by recycling iron oxide, which is waste generated from steel industries that would otherwise landfill or dumped, polluting soil morphology. The use of nano materials in concrete can improve properties of concrete in terms of durability and promote strength development. The incorporation of ferrock can improve strength with carbon absorbing concrete which can practically be used in various structures to form carbon negative structures. Their incorporation not only enhances mechanical strength and microstructural integrity but also contributes to sustainable construction and recycling industrial waste. Findings support the development of rGO ferrock concrete to form sustainable alternatives, promotes recycling of steel industrial waste dust, prevents landfilling, reduces CO_2 emissions as compared to conventional concrete by reducing the cement usage.

The objectives of this study are mentioned below.

Objectives:

1. To test the physical and chemical properties of graphene and ferrock to study their feasibility as an additive to cement concrete to improve its compressive strength.

2. To study the pore structure of concrete composite for mixing efficiency, compaction degree and strength development.

3. To prepare concrete having different proportions of graphene and ferrock as replacement of cement and testing the hardened composites samples for pore structure, tensile and compressive strength, and durability.

4. To carry out cost analysis of graphene- ferrock concrete developed.

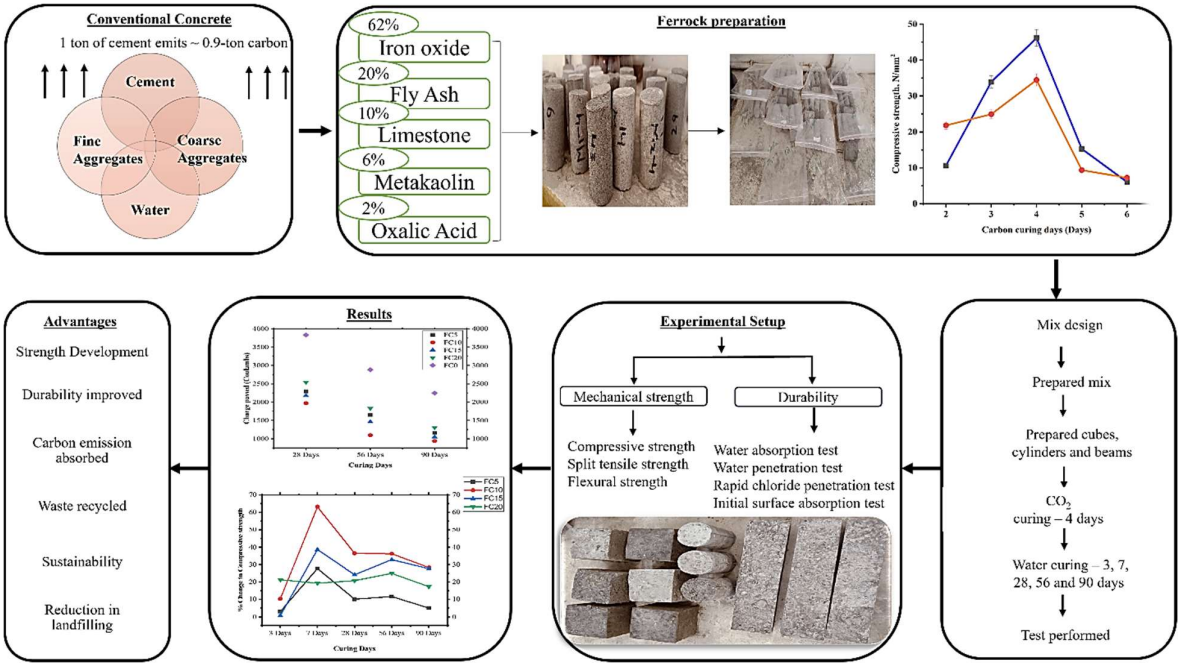

Acknowledgement

I am extremely grateful to the almighty for letting me through the difficulties and giving strength. I would like to express my gratitude and my appreciation to my supervisor Dr. Jaspreet Singh, Associate Professor, School of Civil Engineering, Lovely Professional University, Jalandhar India for their invaluable guidance, encouragement and personal concern throughout the study. The knowledge and enthusiasm towards work is highly appreciated. The help and support provided during the research period is greatly appreciated. It is also my enormous delight to give due gratitude to my parents and brother for their patience, acceptance and words of encouragement. I am grateful to the university for providing invaluable support throughout the study. I am extremely thankful to the people who have indirectly contributed to this research work presented in this thesis, even though they are not personally mentioned here.

Neha Singh

Table of Contents

List of Tables

List of Figures

Appendix

American Society for Testing and Materials	ASTM
Angle between the incident beam and a scattered beam of X - ray	2θ
Bureau of Indian Standards	BIS
By weight of cement	bwoc
Calcium aluminate hydrate	CAH
Calcium aluminate silicate hydrate	CASH
Calcium Hydroxide	$Ca(OH)_2$
Calcium Silicate Hydrate	CSH
Carbon	C
Carbon Dioxide	CO_2
Carbon Nano Tube	CNT
Compression Testing Machine	CTM
Compressive Strength	CS
Di calcium silicate	C_2S
Energy Dispersive X- ray Spectroscopy	EDS
Flexural Strength	FS
Fly Ash	FA
Functionalized Graphene Nanosheets	FGN
Gram	gm
Graphene Nanoplatelets	GNP
Graphene Oxide	GO
Green House Gases	GHG
Indian Standard	IS
Initial Surface Absorption Test	ISAT
Interfacial Transition Zone	ITZ
Iron Ore Tailings	IOT
Iron Oxide	IO
Kilogram	Kg
Limestone	LS
Mega Pascal	MPa

Metakaolin	MK
Metric Ton	Mt
Meter cube	m^3
Mili liter	ml
Mili meter	mm
Nano Silica	NS
Ordinary Portland Cement	OPC
Oxalic Acid	OA
Percentage	%
Rapid Chloride Penetration Test	RCPT
Reduced Graphene Oxide	rGO
Scanning Electron Microscopy	SEM
Self-Compacting Concrete	SCC
Silicon Dioxide	SiO_2
Sodium chloride	NaCl
Sodium hydroxide	NaOH
Split Tensile Strength	TS
Supplementary Cementitious Materials	SCM
Sustainable development goals	SDG
Tri calcium silicate	C_3S
Unconfined Compressive Strength	UCS
X-ray Diffraction	XRD

Chapter 1 Introduction

1.1 Background

Concrete is one of the most widely used construction materials valued for its versatility and efficiency. The construction industry significantly contributes to global Carbon Dioxide (CO_2) emissions, with cement production accounting for about 7% of total emissions. However, increasing demand for performance and durability in construction have led to a rise in concrete production [1]. Driven by an urbanization and increasing demand for modern infrastructure, the construction industry has become a major source of CO_2 emissions [2]. The construction sector is responsible for approximately 50% of total Green House Gas (GHG) emissions and 40% of global material consumption, positioning it as a major contributor to resource depletion and a critical challenge for achieving sustainability [3]. The building sector, which is accountable for more than 30% of the world's natural resource extraction and 25% of the creation of solid waste, plays a crucial role in global sustainability efforts [4]. United Nations assessment claims that the building sector is responsible for 38% of CO_2 emissions, which fuel climate change [5]. The environmental impact of cement production, an important component of concrete, is significant due to the emission of CO_2 [6] [7]. The production of cement produces approximately 1 ton of cement generating nearly 0.8 tons of CO_2 [8]. This raises serious concerns about the material's contribution to climate change and the global environmental crisis. These activities result in generate problems like excessive energy use, environmental damage, mostly from burning fossil fuels and the realization that cities account for almost 70% of worldwide CO_2 emissions [2]. Figure 1.1 presents the CO_2 emission by different sectors. These findings demonstrate the need for more scientific research to create a sustainable way of preparing concrete that is cost-effective and eco-friendly without compromising its strength and longevity.

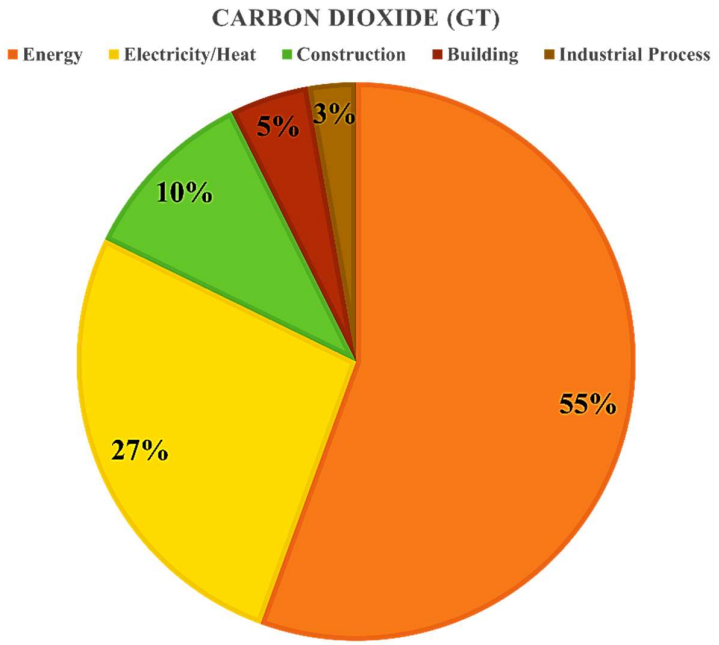

Figure 1.1 CO_2 emission by different sector

1.2 Need for sustainable materials in concrete

Over the years, there has been a consistent increase in cement production worldwide. "Mineral Commodity Summaries 2019" states that output increased from 0.94 billion tons to 2.284 billion tons between 1970 and 2005 [9]. Following that, there was a notable rise, reaching 4.05 billion tons in 2017, followed by a slight increase to 4.1 billion tons in 2018 [9]. Cement manufacturing is the third-largest industrial emitter of CO_2, accounting for around 7% of global CO_2 emissions annually [2] [10] [11] [12]. However, the environmental degradation resulting in this expansion in cement production is high, and it plays a major role in the problems that our world is now confronting. One of the most widely used materials of the construction industry is concrete. Concrete production requires large quantities of raw materials, primarily aggregates, cement and water. Cement, a fine grey powder, acts as a binding agent in concrete mixes. Alumina, lime, gypsum, and iron are the main basic elements used in the manufacturing of cement. The production process of cement involves the steps of

burning raw materials at high temperatures which impacts the environment by emitting large quantity of carbon emissions. One ton of CO_2 is released for every ton of Ordinary Portland Cement (OPC) produced, making this production process associated with substantial CO_2 emissions [1] [4]. Figure 1.2 presents CO_2 emissions by different countries illustrating the rise in emissions in recent years due to the construction industry. Given how extensively concrete is used in the building industry worldwide, this is a major contributor to environmental issues [13] [14] [15]. India is the third-largest emitter of CO_2 in the construction sector, with 559.2 metric tons in 2021 [16]. Among the major contributors to these environmental challenges, the cement industry stands out due to its significant carbon footprint and energy consumption. Reducing cement production is crucial and can be addressed by identifying sustainable alternatives to conventional cement that help in achieving the required strength and improving quality.

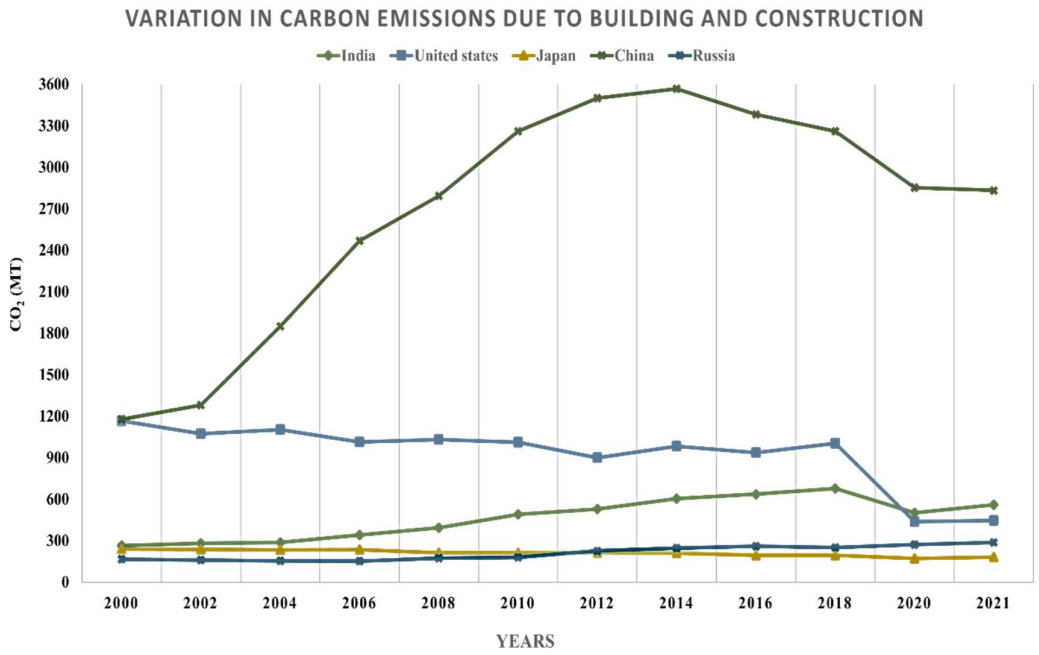

Figure 1.2 CO_2 emission by different countries

The necessity for environmentally friendly solutions to satisfy material needs without causing additional environmental deterioration is becoming more important. According to the Cement Sustainability Initiative (2006), cement production typically generates approximately 866 kg of CO_2 per ton of clinker. The primary source of carbon emissions in this process is clinker production. Therefore, substituting clinker with Supplementary Cementitious Material (SCM) presents an effective strategy for reducing CO_2 emissions [17]. Ongoing research focuses on incorporating various waste materials, including concrete composites, to enhance recycling and conserve raw resources. This approach significantly reduces the environmental impact commonly associated with cement production [18] [19] [20]. Previous studies incorporated agricultural waste [21] [22] [23], industrial waste [24] [25] and construction demolition waste [26] [27] [28] [29] primarily to reduce use of cement and promote waste recycling. In addition, researchers are exploring the potential of nano materials to enhance performance of concrete. These nanomaterials, when used in small quantities, can significantly improve the mechanical strength and durability of concrete, further contributing to sustainable construction practices.

Nano materials such as Graphene Oxide (GO) [30] [31] [32], Graphene Nanoplatelets (GNP) [33] [34] [35], reduced graphene oxide (rGO) [36] [37] [38] [39] [40], Carbon Nano Tube (CNT) [41] [42] [43] and Nano Silica (NS) [44] [45] [46] have been studied to enhance concrete's mechanical strength and durability. The effectiveness of several materials as partial cement replacement and the optimization of the replacement ratios are subjects of extensive study, analyzing important aspects such as strength development, durability and the overall sustainability of the resultant concrete [47] [48] [49]. The nanomaterials make the concrete structure denser and more compact due to the filler effect. Among the various alternative approaches, the utilization of industrial and agricultural waste materials offers a dual advantage of waste management and carbon reduction.

The issue of waste disposal is becoming more challenging due to increasingly stringent regulations and limited environmentally sustainable options present significant challenges. Consequently, recycling waste has become

essential for minimizing environmental impact and promoting sustainability. It is suggested that cement be partially replaced with environmentally friendly materials that nonetheless have a high bonding strength. Because of the beneficial results they have yielded, pozzolanic materials have been carefully examined in several research initiatives and studies. The incorporation of pozzolanic materials has been shown to improve concrete's workability, mechanical strength, and aggregate bonding. This environmental burden has prompted researchers and industry professionals to explore more sustainable alternatives to traditional cement. Alongside the use of waste materials, recent advancements in nanotechnology have paved the way for enhancing the performance of cementitious composites.

In concrete, different kinds of nanomaterials have been used, such as CNT, NS, GO, graphene nanosheets, and GNP. Graphene, a carbon-based nanomaterial, is widely recognized for its exceptional physical properties. In terms of thickness, it is a one-atom, two-dimensional carbon plane arranged in a hexagonal grid that is very good at conducting electricity, heat, and force [50]. Its length ranges from hundreds to thousands of nanometers (1000–100,000 nm) and its thickness is a few nanometers (1–7 nm). Study suggests that incorporating nanoparticles can significantly enhance the properties of concrete and mortar [51]. Nanomaterials exhibit high reactivity, altering chemical processes and the behavior of cement mixes. The incorporation of nanofillers significantly alters the properties of cement composites in both fresh and hardened states because of structure become more compact and denser [52]. Conventional concrete has significant Compressive Strength (CS), but it often lacks the requisite Flexural Strength (FS), Split Tensile Strength (TS) and durability for contemporary infrastructure due to its propensity to fracture and inadequate cohesion. Recent research indicates that incorporating nanoparticles into cementitious materials helps prevent the formation of fissures. Nanomaterials such as GO, nano-TiO_2, and nano-SiO_2 are increasingly used in construction due to their ultra-fine particle size, which enhances the strength and rheological behavior of cement paste [53] [54] [55]. The addition of nanoparticles added to cement pastes improves their properties

by filling pores and speeding up the pozzolanic reaction, which improves the total performance of the material [25]. The reduction process introduces some defects that enhance the bonding of rGO with the cement matrix. Graphene has a tensile strength of 50 GPa and an elastic stiffness of around 1 TPa. This indicates that it renders cement-based products less susceptible to fracture [56]. New construction materials are being made, which is a good sign for a future with lower cement production and environmental costs. Due to its unique properties—including a specific surface area of 2630 m^2/g, tensile strength of 130 GPa, and high thermal conductivity of 5300 $W \cdot m^{-1} \cdot K^{-1}$ GO is considered a promising material for reinforcing cement composites [52]. The presence of functional groups such as hydroxyl, epoxide, carboxyl, and carbonyl on the surface of GO enhances its mobility in water and promotes its integration with cement materials [57]. These oxygen functional groups not only enable GO to disperse effectively in water and other aqueous solutions characteristics not observed in pristine graphene—but also provide GO with superior dispersion compared to other carbon-based nanomaterials [58]. However, similar to other carbon-based nanomaterials, achieving uniform dispersion of GO within the concrete matrix remains a significant challenge [59]. Beyond graphene-based materials, research is also being conducted on various other nanomaterials to enhance the properties of concrete. Previous studies have shown that adding nano-silica to concrete in proportions of 1%, 1.5%, and 2% increased its CS by 2.2%, 29%, and 34%, respectively [60] [61] [62]. When NS was used in amounts of 4% and 3%, the compression strength went up by 31% and 21%, respectively [63] [64]. Studies found that very small amounts of CNT (0.02%, 0.05%, and 0.06%) were used to improve compression strength by 35.6%, 70%, and 11% respectively [65] [66] [67].

GO is converted into rGO, characterized by a layered architecture with nanoscale thickness and micrometer-scale breadth [68]. A lot of researchers are interested in GO because it disperses more easily than other derivatives of graphene [69] [70]. Recent studies indicate that incorporating rGO into cement paste can improve its strength, durability, and resistance to cracking [71]. GO

filled in tiny pores and dispersed easily with cement to make mix stronger and uniform [71]. The present study prefers rGO over other forms of graphene due to its notable advantages of rGO including its cost-effectiveness and excellent thermal conductivity. rGO sheets are capable of conducting heat at a rate of 1390 ± 65 W/(m·K) [72]. Research is ongoing into making cement mixtures with rGO so that they can be used for sustainable construction. Although rGO is not composed entirely of defect-free graphene, its water solubility allows it to enhance adhesion between cementitious components. The unique hydrophilic and water-dispersible properties of rGO make it easy to mix with cement to make a uniform mixture [73]. It has been shown that rGO changes how the pores are distributed in the cement composite material. Adding different sizes of rGO (1–200 mm^2) to the composite made the tiny pores (1–45 nm) bigger, but the pore volume in both PC and the rGO cement composite stayed the same between 45 and 80 nm [74]. Most of the gel pores in C-S-H that are smaller than 10 nm are gel pores. A greater proportion of gel pores in GO-cement indirectly indicates an increased presence of C-S-H (Calcium Silicate Hydrate) in the rGO-cement combination. An increase in the quantity of gel pores inside the mixture indirectly indicates the influence of graphene materials on the cement hydration process [75].

According to the Ministry of Steel, India recently became the world's second-largest producer of steel, with 99.56 million tons produced in 2020–2021 [76]. The Ministry of Steel has developed standard guidelines and norms for handling hazardous landfilled materials and encouraged the use of slag waste from the iron and steel industry in building to address the issue of generated wastes [77]. Millions of tons of metallic dust are frequently landfilled due to the low profitability of iron recovery and its potential adverse effects on soil morphology in disposal areas [78]. This waste often contains minerals such as wustite (FeO), hematite (Fe_2O_3), and magnetite (Fe_3O_4), which could be more effectively utilized. Steel demand has increased across various industries, including capital goods, railways, construction, and infrastructure. Per capita steel consumption has risen from 57 kg to 74 kg over the past five years [79]. The

government has set a target to increase rural per capita steel consumption from 19.6kg to 38kg by 2030–31. Infrastructure-related steel demand has grown by 6–7%, primarily driven by national highway construction projects and railway investments [80]. Research estimates that steel demand will increase by 40–45% in alignment with the ongoing 111-lakh crore infrastructure development plan. India's finished steel consumption stood at 119.17 MT in FY23 and increased to 138.5 MT in FY24 [81]. The Indian Steel Association (ISA) projects that steel demand will increase from 119.9 MT in the previous year to 128.9 MT in 2023–2024. The Ministry of Steel received Rs. 70.15 crore (US$ 8.6 million) from the government as part of the Union Budget 2023–2024 [76]. The amount of finished steel consumed in FY24 was 135.90 MT. In FY23, 86.7 kg of steel was consumed per person. According to ICRA, India's domestic steel demand is expected to increase by 9–10% in FY25 [79]. On the strength of expanding steel processes with a 29 MT capacity boost, steel producers are planning to resume expansion projects [82]. According to the most recent data from Global Energy Monitor, India overtook China as the leading developer of coal-based steel capacity in July 2023 for the first time ever. Indian Railways intends to purchase more than 11 lakh tons of steel from Steel Authority of India Limited in 2021 in order to install new lines and renovate existing tracks around the nation [83]. This increase reflects the growing reliance on steel across India, which directly contributes to the generation of steel dust in large quantity. To mitigate the environmental challenges of steel dust waste, innovative material like ferrock has been developed as potential solutions.

David Stone developed a material called Ferrock [84], which uses iron oxide as its main binding material. The composition of ferrock includes Iron Oxide (IO), Fly Ash (FA), Metakaolin (MK), and Limestone (LS) [85]. As steel production increases, so does the amount of iron oxide waste that would otherwise end up in landfills. Metallic dust, a byproduct of steel production, has traditionally been disposed of in landfills due to the economic impracticality of recycling the iron content [86]. Millions of tons of waste are landfilled worldwide at high costs, posing risks to soil morphology in disposal areas [83]. Ferrock

hardened as concrete after drying, providing comparable strength and flexibility, making it a promising material for sustainable construction. A comprehensive understanding of the role of iron oxide and other raw materials in ferrock is crucial for evaluating its structural performance and reactivity.

Iron oxide is the major binding element in ferrock, with the other pozzolanic components used to optimize the concrete's functionality [87]. Iron oxide comprises solid angular particles that enhance strength by filling voids in the composite matrix. When exposed to Oxalic Acid (OA), iron oxide particles react with CO_2 to generate a thick coating of iron carbonates [88]. FA is a source of silica, which is essential for strength in cement composites. FA slowly interacts with iron to generate silicate crystals, which increase both the durability and strength of ferrock [89]. Carbonation transforms the silica present in Ferrock, along with other pozzolanic materials, into calcium silicate, which plays a crucial role in filling voids within the Interfacial Transition Zone (ITZ) of concrete composites, thereby enhancing their overall performance [90] [91]. Iron oxide has an uneven structure; thus, MT is used to keep cement paste workable because it holds water and makes Ferrock paste thicker, stickier, and easier to distribute and trowel to a smooth surface [92]. MT has been found to be an effective pozzolanic substance derived from the heat and crushing of natural kaolin [93]. The material's early strength and compacted microstructure reduce chloride permeability, increasing the durability of the concrete [94]. MT and FA are aluminate-rich compounds that react with hydrated products, giving additional alumina to add to C-S-H [95] [96]. This iron oxide combines with CO_2 to produce rust, which forms iron carbonate, a rock-like matrix. In addition to the role of materials, the curing process also plays a pivotal role in shaping the microstructure and durability of cementitious composites.

CO_2 curing affects the microstructure of OPC as Ca^{2+} ions from cement hydration products—portlandite and C-S-H gel react with bicarbonate and carbonate ions produced during CO_2 dissolution, forming $CaCO_3$ [97]. Multiple studies have reported microstructural densification in OPC paste due to the rapid precipitation of calcite and C-S-H gel [98]. In OPC paste subjected to 3% CO_2

concentration, a C-S-H gel relationship with a lower Ca-to-silica ratio was observed [99]. Other work found that as the CO_2 concentration was increased to 10% and 100%, C-S-H completely disappeared from cement paste samples and was transformed into calcite. Thus, it can be said that CO_2 curing, is a significant process involving calcite precipitation, cement dissolution, and decalcified C-S-H, making it more resilient, long-lasting, and environmentally sustainable, offering an innovative approach in the construction sector [100] [98]. Among various supplementary materials, FA has been widely studied and applied due to its advantageous pozzolanic properties.

FA is a pozzolanic material that significantly reduces the environmental impact of concrete, thereby promoting sustainable construction practices [101] [102]. Additionally, FA enhances the long-term strength of concrete by facilitating continuous pozzolanic reactions over time. FA reacts with $Ca(OH)_2$ (Calcium Hydrate) produced during cement hydration to form supplemental C-S-H, which increases the strength and durability of concrete [103]. The spherical shape and fine particle size of FA enhance the fluidity of concrete mixtures, improving workability and ease of shaping during construction. Rice husk ash contains approximately 90% silica and exhibits enhanced pozzolanic properties due to its high surface area, amorphous nature, and compatibility with cementitious materials [104]. The pozzolanic reaction between FA and $Ca(OH)_2$ occurs at a slower rate than cement hydration, leading to a more gradual strength gain in FA concrete [105]. However, the formation of denser C-S-H structures contributes to greater long-term strength compared to conventional concrete. Amorphous silica, in FA, gradually reacts with iron to form specific silicate minerals that enhance the strength and durability of ferrock [106]. As the proportion of cement replaced with nano FA increases, both CS and TS rise by up to 40%, highlighting the significance of pozzolanic materials, particularly nano FA particles. However, when the percentage exceeded 40%, there was a slight decrease in strength [107]. This reduction could be attributed to excessive filler content and pozzolanic material saturation. Teixeira et al. [108] conducted life cycle assessment of using FA as cement replacement in production of concrete. Their study concluded that

FA minimizes the negative environmental impact of concrete as it acts as sustainable alternative to cement and an effective means of improving the environmental performance of the concrete industry. LS, an abundant and reactive material, the performance of concrete composites when used with FA.

The material must be natural LS rather than lime, which is derived from calcined LS and has a crystalline structure similar to iron carbonate. LS accelerates cement hydration, potentially reducing curing time [109]. The aluminate phases in cement react with $CaCO_3$ in LS to form additional Calcium Aluminate Hydrate (CAH), expediting concrete settings. This process supports LS integration by serving as a template for crystal growth. It also dissolves in acid, yielding CO_2, which provides additional carbonate for mineralization. Fine LS particles enhance the compactness of the cementitious matrix. Results in a denser microstructure and a decrease in cavities, which in turn improves strength, enhances workability and decreases permeability. LS acts as a reinforcing agent in composites, improving their permeability and durability. LS functions in two distinct ways in ferrock: Initially, it reacts with water and CO_2 produce calcium bicarbonate, which is water-soluble. Secondly, LS releases CO_2 when dissolved in OA, thereby increasing the availability of carbonate ions for mineralization. Moreover, it functions as a catalyst in the reaction, thereby accelerating the entire process [109] [84]. Chemically, LS is $CaCO_3$ and has the same mineral structure as iron carbonate. It facilitates the formation of crystals by serving as a template for crystal growth. LS fills pores to create dense structures, and when combined with FA, it produces calcium mono hemicarboaluminate, which is more durable and stronger [110]. The concept involves the use of pozzolanic compounds and recycled materials to enhance the bonding of aggregate cement paste and simplify the process of working with cement composites [111]. Study have demonstrated that the CS is not significantly altered by the substitution of 10% LS at any age [112] . The acceleration impact of LS filler in conjunction with the synthesis of CASH is the primary cause of this increase in strength, which may provide an explanation for the general increase in hydration rate. The LS powder in concrete was significantly influenced by the mineral composition of cement, particle size,

dosage, dissolution rate, polymorph of LS powder, and additional cementitious materials [113]. The effects were primarily characterized by filler, nucleation, dilution, and chemical effects. LS primarily exhibits a nucleation effect and a diluting impact when its particle size is smaller than that of cement particles. Likewise, MK—a thermally treated form of kaolin—has also demonstrated significant potential in enhancing the properties of Ferrock and cementitious materials.

Kaolin, also known as kaolinite, is a type of clay and MK is produced by heating kaolin to 600°C. This material possesses superior bonding capabilities with specific materials, such as the constituents of ferrock, and exhibits increased reactivity [114]. It also retains moisture, which results in a denser, stickier ferrock material that is easier to disseminate and trowel to a uniform finish. In both the early and later stages, MK enhances strength. It produces supplementary C-S-H, the primary constituent responsible for the strength of concrete, by interacting with $Ca(OH)_2$, a byproduct of cement hydration [115]. The formation of C-A-S-H, alumino-silicate gel, and C-A-H is facilitated by the combination of FA and MK. As MK is predominantly composed of alumina and silica, which are actively involved in these pozzolanic reactions, these phases contribute to early strength gain [116]. MK was produced from clay, which resulted in a decrease in $Ca(OH)_2$ and an increase in CSH levels. The incorporation of MK in the control mix was found to reduce the width of microcracks in microlevel experiments. The micro- and macro-level characteristics of the ideal substitution of MK were determined to be 10wt.% [93]. Pozzolans improve the performance of concrete by interacting with $Ca(OH)_2$ to generate secondary C-S-H gel. The overall porosity is reduced, and the pore architecture is enhanced by the development of secondary C–S–H gel, thereby increasing the strength and impermeability. The atomic Ca to silicon ratio of C-S-H is determined by the curing duration, combination proportions, and types of pozzolanic materials [117]. The long-term performance of concrete is improved using MK as a partial substitute for cement, which reduces permeability and increases durability.

1.3 Objectives of the study

This study investigates the partial replacement of cement in concrete using innovative combination of materials: rGO and Ferrock. rGO, a carbon-based nanomaterial, is synthesized by reducing the functional groups of GO. It has a high surface area and fine particle size, enabling it to occupy concrete pores and enhance density, thereby improving mechanical strength and durability. Ferrock, an iron-based binder, is derived from recycled iron oxide and other pozzolanic components. It offers multiple sustainability advantages, including carbon-negative properties, landfill waste reduction, and improved concrete composites through pozzolanic activity.

The study addresses two critical environmental concerns: rising atmospheric CO_2 levels and the increasing generation of iron oxide waste from the steel industry. Cement production is a major contributor to global CO_2 emissions, while fine iron waste, which is often discarded in landfills, poses significant environmental risks by altering soil morphology. With the continuous expansion of the steel industry, waste generation is increasing, yet only coarser steel particles are recycled, while finer iron oxide is not due to economic constraints. Disposing of fine iron oxide in landfills leads to soil contamination; therefore, recycling this waste in concrete not only mitigates environmental harm but also enhances concrete properties through pozzolanic interactions.

This research aims to evaluate the fresh, hardened, durability, and microstructural properties of concrete incorporating these alternative materials. A key focus is determining the optimal replacement ratio to maximize strength and durability while reducing cement consumption. The use of ferrock contributes to sustainable concrete production by lowering reliance on traditional cement while offering superior strength compared to conventional concrete mixtures. Similarly, the integration of rGO in minimal quantities significantly improves mechanical performance by refining the microstructural matrix.

By exploring these materials, the study advances sustainable construction practices by reducing CO_2 emissions, recycling industrial waste, and improving

concrete performance. The findings will contribute to the development of eco-friendly, high-performance cement alternatives, aligning with global sustainability efforts in the construction industry.

1.4 Scope of the research

Current research promotes sustainability by reducing carbon emissions, utilizing industrial waste, and conserving natural resources. Cement production significantly contributes to CO_2 emissions, but incorporating Ferrock—a carbon-negative material—helps mitigate this impact by absorbing CO_2 during curing. Additionally, recycling fine iron oxide from the steel industry minimizes landfill waste and soil contamination. The inclusion of rGO enhances concrete durability, extending the lifespan of structures and reducing material consumption. By integrating these eco-friendly materials, this study supports sustainable construction practices, promotes a circular economy, and contributes to the development of high-performance concrete, low-carbon concrete, aligning with global environmental goals.

Research Gap

- Previous research on rGO has predominantly focused on its incorporation into mortar matrices, with limited studies exploring its applicability in concrete. Notably, existing investigations on rGO in concrete have been confined to dosage levels either below 0.1% or exceeding 1% by weight of cement (bwoc). This study aims to address this gap by examining the effects of rGO incorporation in M25-grade concrete across a broader dosage range of 0.1% to 0.8%.
- While study on ferrock has been limited to Self-Compacting Concrete (SCC) only for strength improvement, its application in conventional concrete remains unexplored. This research expands its scope to durability, microstructure analysis and carbonation test.
- Additionally, the study expands its scope to investigate the combined impact of rGO and ferrock in concrete. This dual incorporation provides valuable insights into their synergistic effects on the mechanical properties and microstructural

characteristics of concrete, contributing to the advancement of sustainable construction materials.

1.5 Structure of thesis

The organization of this thesis is designed to systematically present the research conducted. **Chapter 1** introduces the study by providing background information, defining the research problem, outlining the objectives, and highlighting the significance of the work. **Chapter 2** presents a comprehensive review of existing literature, discussing relevant studies, identifying research gaps, and establishing the theoretical framework for this study. **Chapter 3** details the materials used, and the methodologies adopted for experimentation, including the procedures followed for data collection, sample preparation, and analysis. **Chapter 4** presents the results obtained from the experimental investigations, followed by an in-depth discussion interpreting these findings in relation to existing research and theoretical concepts. Finally, **Chapter 5** concludes the study by summarizing key findings, discussing their implications, and providing recommendations for future research, contributing to the advancement of sustainable construction materials.

Chapter 2 Literature Review

Studies have been carried out to investigate the impact of graphene derivatives and other cementitious materials as partial replacement of cement. The aim is to reduce the usage of cement with improved mechanical and durability properties of concrete to promote sustainability in the construction industry. Review of literature provides the gap which needs to be considered before performing further research. Studies found rGO is desirable nano material because of its dispersibility in water due to presence of functional groups. There is another material named ferrock which is prepared with waste steel dust as primary binding material with FA, LS and MK. There are studies that explored nano materials, iron forms, FA, MK and LS to improve properties of concrete. Detailed analysis of studies carried out are presented below-

Srivastava, A.et.al [118] conducted experimental analysis on incorporation of nano material i.e., titanium dioxide in a 2.5% ratio with plastic fibers as replacement of cement. The experiments were performed to analyze the impact of titanium dioxide and plastic fibers together. The tests were performed for water absorption, CS, TS and FS. Microstructural analysis performed by SEM which visualized surface morphology of concrete surface. Findings revealed that CS did not show a significant increase at all curing days. The FS improved by ~32.7% and TS by 16.88%. The optimum replacement ratio was found to be 2.5% nano titanium dioxide and 2% plastic fibers. The SEM images show denser and compacted microstructure of concrete matrix.

Amr E.Ali.et.al [119] studied the impact of NS, nano-aluminum and nano-glass materials as partial replacement for cement in 1%, 2% and 3% by weight. The properties of concrete were investigated as CS, chemical composition and microstructure. Findings showed that incorporating nano materials enhanced CS and microstructure properties. Optimum results showed by 1% replacement nano glass and NS. The SEM analysis found denser and compacted concrete matrix.

Khan K.et.al [63] studied the impact of NS into cementitious materials on mechanical properties. Increasing NS concentration to 2% and 3% enhances the mechanical properties and durability of cementitious materials owing to

pozzolanic reactivity, pore refinement, or pore filling. Nevertheless, concentrations of NS over 3% lead to a reduction in strength. The accumulation of NS grains results in porosity, microcracking, and a reduction in mechanical strength of the material. The pozzolanic activity of NS far exceeds that of silica fumes. NS-infused concrete exhibits superior CS at all ages, while significantly enhancing the flexural and TS qualities of the concrete. An increase in compressive and TS was seen at the optimal ratio of 3%, achieving 21% and 16.1%, respectively.

Gamal HA.et.al [120] investigated the effects of CNT as a partial substitute for cement in concrete composites and observed improved characteristics in concrete compared to the control mix. Small amounts of CNT improved concrete consistency; nevertheless, exceeding the optimal ratio resulted in a reduced slump. The use of 0.04% CNT in concrete enhanced CS by 26.4% relative to the control mix. The incorporation of 0.01% and 0.02% CNT in concrete enhanced flexural and TS by 15% and 40.4%, respectively. The use of 0.01% CNT in cement enhanced the maximum bond strength in corrosive settings relative to the control concrete. At increased percentages of CNT, the re-agglomeration process diminished the pozzolanic activity of concrete and the hydration reaction of cement at later ages, resulting in lower bond strength. The CNT % combinations exhibited slightly increased sorptivity and penetration depth compared to the control paste, whereas chloride penetration escalated comparably. SEM images indicate that CNT fill, bridge, and serve as nucleation sites for C-S-H gel.

Abd Elrahman M.et.al [64] performed experimental investigations to assess the influence of NS on the strength and properties of concrete. Four mixtures were formulated using NS at concentrations of 0%, 1%, 2%, and 4%. FS and CS were evaluated after 90 days of cure. The investigations show that even at minimal levels, NS influences the mechanical properties of concrete. The advantageous effects of NS were more pronounced when included into mixtures above 1 wt.%. NS enhanced solid content and refined the fine pore structure, therefore consolidating the concrete matrix and modifying the void system, which improved mechanical properties. Nonetheless, NS increased the viscosity of the

new combination while diminishing its consistency. A 4% enhancement in compressive and FS was noted; however, after a 31% advancement, no more increase was detected after 90 days.

Mohamed, Anwar M.et.al [121] performed an investigation to examine the influence of nanoparticles on the mechanical characteristics of concrete over time. Research has been conducted on NS, nano-clay, or a combination of both in varying proportions. Concrete prisms measuring 40 mm, 40 mm, and 160 mm were evaluated at 7, 28, and 90 days to examine the effect of nanoparticles on CS and FS. The research indicates that nanoparticles enhance the mechanical qualities of concrete, with NS outperforming nano-clay, and wet mix being superior to dry mix. The use of binary nanoparticles (NS combined with nano clay) enhanced concrete CS more effectively than the application of individual nanoparticles. Nano materials interact with $Ca(OH)_2$ crystals at the ITZ between hardened cement paste and aggregates, producing C-S-H gel and nanoparticles that fill and densify the microstructure. CS and FS reached their maximum at 3% NS, 25% nano clay, and 75% combined content.

Isuri Fonseka [122] investigated the performance of concrete containing 0.02-0.2% GO and FA at ratios of 10%, 20%, and 30%. The mixtures were evaluated for workability, CS, tensile strength, and FS. The results suggest that workability is reduced with an increase in GO concentration and improved with a higher FA ratio. After 28 days of curing with 0.12% GO and 30% FA substituting cement, the CS, tensile strength, and FS improved by 6%, 2%, and 3%, respectively. Microstructural research indicated that GO enhanced the concrete's microstructure.

Yuhang Yan [123] investigated graphene and its derivatives as nanomaterials, specifically focusing on graphene as additives in cement-based products. rGO could regain the remarkable features of graphene by diminishing its oxygen functional groups. Research showed that including 0.022 weight percent of modified rGO enhanced the CS of cement paste by 27% and the FS by 26% after 7 days. The FS of the mix, including 0.06%, increased by 22% after 28 days in comparison to the control sample.

Isuri Fonseka [70] indicated that including 0.12% bwoc and 0.14% bwoc in a concrete mixture enhanced CS by 33% after 28 days relative to a control mixture. This resulted from the advantageous material characteristics of GO-enhanced concrete, including reduced particle size, oxygen functional groups, superior graphitic structure, and an increased number of GO sheets and defects. The optimal mix exhibited a 7% enhancement in CS at 28 days relative to the control sample. The research revealed enhancements in indirect tensile strength, FS, and elastic modulus of 24%, 25%, and 30%, respectively, in comparison to the control combination.

P.M. Walunjkar and M.N. Bajad [124] illustrates the impact of graphene reinforcement enhances the properties of cement concrete. The SEM images of GO, rGO, and GNP are analyzed using suitable preparation techniques. The effect of carbon-based nanoparticles on the compressive and tensile strength of concrete with identical proportions is examined. GO and rGO have shown enhancements in the compressive and TS of concrete with equivalent mix ratios. The ideal dosage for GO ranges from 0.06% to 0.08%, whereas for rGO it is 0.5%, at which both concentrations markedly increase. GNP does not enhance the compressive and tensile strength of concrete; instead, it facilitates the improvement of pore structure.

Karthik Chintalapudi and Rama Mohan Rao Pannem [125] investigated the enhancement of CS in cement mortar by the incorporation of GO. Following 28 days of healing, GO dosages of 0.02% and 0.03% exhibited average increases in CS by 28.5% and 46.4%, respectively. The combination of GO with OPC produces flower-like polyhedron crystals, enhancing CS, toughness, and hydration rate via a complex pore structure. The increased hydration rate in 0.03% GO + OPC specimens yielded an average CS of 46.4% for Portland cement hydration products. The production of active crystals containing GO in the cement matrix is seen.

P.V.R.K Reddy and D.Ravi Prasad [126] conducted study to evaluate the influence of GO on the microstructure of concrete and its static mechanical characteristics. GO nanomaterial, with its remarkable range of physical properties, functions as a reinforcing agent in cement composites. Concrete

specimens were produced with varying GO concentrations from 0 to 0.1%, increasing by 0.025% relative to cement weight, while maintaining a constant water-to-cement ratio of 0.5. The CS, TS, and FS were evaluated after 7 and 28 days of curing. The results indicate that a little proportion of GO included into cement concrete significantly improved the microstructure of the composite and boosted its static mechanical characteristics.

Yahui Wang.et.al [127] performed research to examine the performance of GO and rGO in cement-based composites at 0.02, 0.04, and 0.06 wt% of cement. XRD and TGA measurements indicate that GO composites possess a higher concentration of $Ca(OH)_2$ and C-S-H compared to rGO composites at 1, 7, and 28 days. The maximum enhancements in FS were 75.7% for 0.04 wt% GO and 33.7% for 0.06 wt% rGO. Electrical resistivity increased with both additions, however water sorptivity decreased by 24.8% with GO and 4.7% with rGO in comparison to the control mix. GO decreased workability owing to its hydrophilic characteristics. Both GO and rGO expedited early-age hydration, with GO composites exhibiting enhanced dispersibility and robust chemical bonding, resulting in superior mechanical characteristics.

S.C. Devi.et.al [128] investigated the impact of GO on compressive and tensile strength. Results showed that the incorporation of GO into concrete reduced workability while enhancing compressive and tensile strengths by 21-55% and 16-38%, respectively. As the concentration of GO content rises, the ISAT and sorptivity diminish throughout a curing period of 28 to 90 days. The non-destructive technique indicates that the GO-reinforced concrete composite maintains homogeneity as concentration increases. The combination of 0.08% GO attained the maximum strength after 90 days of cure.

Xiangyu Li.et.al [129] conducted experiments on cement mortars with GO nanosheets. Findings revealed that they significantly improve the compressive, flexural, and tensile strengths of the mixture at all curing days. The addition of GO nano sheets at a concentration of 0.03% bwoc led to enhancements in compressive, flexural, and tensile strengths of 21.37%, 39.62%, and 53.77% respectively. However, the GO nano sheets did not affect the formation of flower-

like cement hydration crystals. The expanding space dramatically affected the morphology of hydrates so it can impact long term strength.

Cao, Ml.et.al [130] assesses mortar specimens reinforced with different types of GNP, subsequently comparing them to control samples. The study focused on the strength and durability of graphene-reinforced cementitious materials. Nano-scale characterization is performed to elucidate the reinforcing mechanisms of graphene, focusing on the microstructure of the cement paste around the GNP. The obtained microstructural morphology and modulus profile demonstrate that GNP significantly modifies the microstructure of cement paste. The findings indicated a 19.9% increase in strength with the addition of 0.1% GNP.

Teng Tong.et.al [131] investigated a 0.1% ratio of graphene and GO nanoparticles, which markedly improve the CS of mortar specimens. The 5 different mixes were prepared and for each group 12 cubes of size 50 mm, 3 cylinders (101.6 ×202.3 mm) and 3 beams (70×70×350 mm) were cast and cured for 28 days. These nanoparticles may mitigate chemical degradation from acidic solutions, hence improving the corrosion resistance of cementitious materials. Micro-characterization indicates that GNP substantially modifies the microstructure of cement paste, resulting in improved interfacial bonding between GNP and C-S-H gels during precipitation. Results found improved strength for all tests.

Zhu Pan.et.al [132] conducted on mortar including Functionalized Graphene Nanosheets (FGN) cement composites at mass fractions of 0.01% to 0.05%. The flow properties, mechanical properties, and microstructure of the cementitious material were further analyzed. The results indicate that the incorporation of FGN significantly improves the mechanical properties of cement-based composites, although with a little decrease in their fluidity. At an FGN level of 0.02%, the optimal strength was attained, yielding an FS of 12.917 MPa and a CS of 52.42 MPa after 28 days. Microstructural investigations indicate that FGN accelerates the hydration process to enhance the functioning of the composite.

A. Mohammed.et.al [133] investigated the durability of cement composites including GO. GO was incorporated into cement mortar at weight percentages of 0.01%, 0.03%, and 0.06% to manufacture GO cement composite. Experimental results indicate that a little quantity of GO (0.01%) effectively inhibits chloride ion entry. Furthermore, the incorporation of GO at a minimal concentration of 0.03% significantly enhances sorptivity. The mechanical strength was indicated to increase by up to 47% after 28 days of curing at 0.06%.

Gyanendra Kumar Chaturvedy [134] examined the effects of crumb rubber concrete with GO. The concrete used crumb rubber at 5%, 10%, and 15% as a substitute for sand, while rGO was utilized at 0.05%, 0.1%, and 0.15% to replace cement. Thirteen mixtures with varying ratios were created, and their workability, CS, tensile strength, and FS were evaluated. The findings indicated an increase in compressive, tensile, and FS of up to 18.7%, 3.86%, and 10%, respectively. Durability has been enhanced regarding water absorption and acid exposure.

N.Parthasarathi [135] performed study aims to minimize concrete CO_2 emissions by using zeolite powder as a partial substitute and rGO as an additive. Concrete mixtures were subjected to different quantities of zeolite and rGO. The research recommends incorporating zeolite and rGO into concrete at ideal ratios of 5% and 0.07%, using mechanical and microstructural studies. Reinforced concrete beams were used to evaluate load and deflection characteristics, resulting in enhancements.

Mohammad Valizadeh Kiamahalleh [136] assessed the influence of rGO on the mechanical and durability characteristics of waste-based concrete. Four dosages of rGO were incorporated, with the optimum concentration identified at 0.1%. This enhanced the concrete's CS, splitting tensile strength, and FS, while diminishing water absorption. Nonetheless, the properties of the concrete diminished with increased dosages. The addition of rGO at 0.3% weight percent decreased the workability of the concrete by 37%. The optimal dosage of rGO for enhancing the mechanical properties of concrete was 0.1%, resulting in increases of about 40%, 44%, and 42% in compressive, splitting tensile, and FSs, respectively.

Xiaonan Wang [137] investigated rGO as a reinforcing component in cement. Earlier studies used thick GNP, limiting their practical usefulness. A green chemical reduction and comprehensive washing without drying were used to produce high-quality rGO. Although the agglomeration of rGO in the pore solution, a mixture containing 0.05 wt% rGO enhanced the compressive and FS of the cement paste by 16.5% and 20.9%, respectively, demonstrating reinforcing efficiencies of 330% and 418%. Nonetheless, FS declined to 0.01 wt% rGO.

Shengtian Zhai [138] indicates that incorporating rGO suspension into concrete enhances its mechanical and functional properties. The use of rGO suspension enhances the compressive and FSs of mortar by 45% and 50% after three days, respectively, and also increases hydration heat and pore structure. Furthermore, the mortar's resistivity diminishes by 45%, while its thermal conductivity escalates by 23%. The coefficient of stress and strain sensitivity in mortar escalates with the concentration of rGO.

Ning Zhang [139] integrates rGO with cement to generate a self-sensing cement composite. The nucleation and morphological effects of rGO improve the microstructure of cement. The CS and FS of the rGO-paste improve by 23% and 45%, respectively. This produces a high-strength self-sensing cement composition with a FS of up to 49%.

Karthik Chintalapudi and Rama Mohan Rao Pannem [52] demonstrates that reducing the oxygen functional groups of GO into rGO enhances mechanical and durability performance. Despite the initial expense, substantial quantities of GO are already manufactured at an industrial scale. The uniform distribution of GO provides nucleation sites, enhancing the density of the cement matrix's microstructure. rGO produced by chemical or thermal reduction has pristine properties. Recent studies have investigated the mechanical properties, morphological changes, and chemical functional group modifications of geopolymer composites including rGO and GO.

Guojian Jing [140] examined the effects of rGO in cement mortar at different percentages of 0.1%, 0.2%, 0.3%, 0.4%, 0.5% and 0.6%. The results indicate that mechanical strength increases more after 3 days with up to 0.6 wt.% rGO doping, but no significant enhancement is reported after 28 days. The results

indicate that doping rGO is a viable method for alleviating stress and reducing fracture development. The incorporation of rGO or other graphene derivatives markedly enhances the properties of cement composites. The tensile strength and CS of mortar using rGO or GNP were enhanced.

Tanvir S.Qureshi [141] used GO because of its higher dispersibility compared to other graphene-based derivatives. Numerous research has presented their viewpoints about the influence of GO on the mechanical and durability properties of ceramic matrices. Five mixtures were formulated using GO at concentrations of 0%, 0.02%, 0.04%, 0.06%, and 0.08% bwoc. The mechanical and water permeability properties were examined. The combination with 0.08% GO exhibited superior compressive and tensile strength compared to the other mixes. The sorptivity and permeability of nano-reinforced concrete mixtures containing GO were seen to decrease with increasing GO content relative to the control mixture.

Jiangshan Zhao [78] investigated Iron Ore Tailings (IOT) as a partial substitute for cement in concrete; however, its CS decreased with more Iron Ore concentration. Although mechanical grinding improves the pozzolanic activity of iron ore, its hydration performance is still inferior to that of cement. Factors affecting the strength of iron ore include mixing techniques, concrete slump, and strength classification. When 80% of iron ore substituted NS by weight, the concrete's CS decreased by 20.25%. A 100% iron ore content led to a 1.31% decline. Present iron ore activation methods are costly and impractical for widespread use, necessitating continuous refinement. The use of high-volume iron ore influences the workability of concrete owing to its reduced particle sizes.

Alexandra Mallett and Prosanto Pal [142] suggests that India produces around 5% of the global steel supply, positioning it as the second-largest producer after China. India is projected to produce 227 million tons of steel by 2030, 347 million tons by 2040, and 489 million tons by 2050. In 2019–20, India produced around 111 million tons of crude steel.

Gabriel Lopez [86] investigates steel production has notably risen in recent decades, with crude steel output escalating from 200 million tons in 1950 to 1,804 million tons in 2018. Considering a 60% decrease in energy use, the

production of one ton of steel still necessitates 5.17 MWhth of raw energy. The industry emits 3.4 Gt of CO_2, or 9% of the global total of 36.4 Gt of direct anthropogenic CO_2 emissions. The output rate is anticipated to reach 2065 Mt by 2030, thereafter decelerating to 2336 Mt by 2040.

Jiangshan Zhao [78] investigated IOT as a partial substitute for cement in concrete; however, its CS diminishes with more Iron Ore concentration. Although mechanical grinding improves the pozzolanic activity of iron ore, its hydration performance is still inferior to that of cement. Factors affecting the strength of iron ore include mixing techniques, concrete slump, and strength classification. When 80% of iron ore substituted NS by weight, the concrete's CS decreased by 20.25%. A 100% iron ore content led to a 1.31% decline. Present iron ore activation methods are costly and impractical for widespread use, necessitating continuous refinement. The use of high-volume iron ore influences the workability of concrete owing to its reduced particle sizes.

Sumanta Das [85] investigated the iron oxide -based binder together with several supplemental cementitious materials as raw ingredients. This binder was cured in a CO_2 atmosphere to facilitate all reactions necessary for the hardening process and to ensure strength. Binder is designated as ferrock, using FA, LS, MK, and OA as raw ingredients. The hardening process absorbs CO_2 from the atmosphere, making it a carbon-negative material. Research indicates that ferrock has binding capabilities, demonstrating strength gains equivalent to those of OPC-based cubes. To facilitate its use in the building sector. Microstructural research indicates that prolonged carbonation decreases pore volume and CS, but critical pore size stays constant.

Sumanta Das [84] indicates that industrial waste, including iron powder, FA, LS powder, and MK, produces a binding material appropriate for construction purposes. CSs of 30-35 MPa were attained after four days of curing, resulting in a reduction of CO_2 emissions. The quantity of FA influences CS, but MK enhances cohesion, hence improving the mechanical characteristics and workability of the mixture. CO_2 exposure and air curing influence mechanical properties, with air exposure markedly enhancing CS at elevated levels.

Elnaz Khankhaje [143] aims to develop sustainable and eco-friendly concrete by substituting cement with ferrock at ratios of 5%, 10%, 15%, 20%, and 25%, while maintaining consistent aggregates and superplasticizers. Ferrock significantly improved concrete strength during simultaneous curing, elevating CSs by 21.9%, 25.9%, and 32.6%. Ferrock-based SCC exhibited superior mechanical strength compared to conventional SCC, attributable to enhanced compaction and density within the matrix. This indicates that ferrock SCC is favored and may be used in future building projects. The author investigated the use of FA as a partial substitute for cement, and the findings indicate a reduction in the pores seen in Portland cement. This results from the filler properties and pozzolanic activity of FA, which diminish overall permeability and void content. The optimal level of FA replacement is 10-30%; however, increasing it above 30-50% may impair hydration methods and hinder strength progression. Nonetheless, FA may reduce industrial waste and enhance the environment via waste recycling.

Dheeresh Kumar Nayak [144] studied the quantity of free lime influences the substitution of cement with FA in concrete. FA enhances the qualities of concrete, such as workability and strength. It also tackles storage and disposal concerns related to industrial waste. FA particles operate similarly to ball bearings, facilitating lubrication and decreasing viscosity. The optimal 10% FA significantly enhances CS by up to 36%. The use of finer cementitious particles expedites the pozzolanic reaction with $Ca(OH)_2$.

M. Jemimah Carmichael [107] examines the effects of varying proportions of nano FA in concrete. The findings indicated that increasing the cement replacement level with nano FA enhanced compressive and TS by up to 40%, underscoring the significance of pozzolanic materials. Nonetheless, if the percentage exceeded 40%, a marginal decrease in strength began. An ideal binder ratio of 0.33 yielded an 18.87% enhancement in CS and a 11.42% improvement in TS. The ratio of tensile to CS decreased as the proportion of nano FA enhanced.

J. Krithika [145] examines the influence of FA on concrete, with the objective of using economical sustainability measures. It was determined that substituting FA in cement at minimal percentages does not reduce strength,

enhances strength with time, and may ultimately surpass conventional concrete in the long run. FA further provide protection against sulfate attacks.

D.S. Vijayan [146] examined nano MK in cement mortar and discovered that it had the highest concentrations of Silicon Dioxide (SiO_2) and Al_2O_3, correlating with its significant pozzolanic activity. The appropriate proportion of nano MK enhances the CS of cementitious materials. Conversely, nano MK reduces its CS when its concentration exceeds the optimal level. As the proportion of nano MK replacement increased, the peak value of C–S–H shown an upward trend, however the CH content and the intensity of the XRD peak saw a little decline. The concentration of CH in the cement mix reduced by 6.7% due to the presence of nano MK. Unlike standard cement paste, no significant change in the CH content was observed when the replacement amount exceeded 10%.

Shahida Khan [147] investigated MK concrete as a sustainable and environmentally friendly alternative to traditional concrete. The study examined the feasibility of using MK as a partial substitute for cement to enhance its characteristics and diminish cement use. Cement was substituted with MK at 0%, 5%, 10%, 15%, 20%, and 25% in M35 concrete. The assessments conducted for mechanical strength, durability, and workability. The findings demonstrate that the optimal MK substitution was 15%, resulting in a 27.05% increase in CS and a 25% increase in TS. Durability was assessed at an optimal ratio of 25%, characterized by enhanced water permeability, reduced water absorption, and decreased chloride penetration. The workability was seen to diminish with increased MK concentration.

Deveshan L. Pillay [148] conducted research to examine the influence of MK on concrete performance. The research indicates that MK is an aluminosilicate substance with differing quantities of silica and alumina. The findings indicated a minor effect on FS but a substantial effect on long-term CS. MK enhances the pore structure of concrete, necessitating lower temperatures and producing less CO_2 emissions. Portland cement samples have a significant number of capillary voids, which is damaging to the durability of concrete. Samples containing MK exhibit a more cohesive matrix with C-S-H gels, suggesting enhanced concrete performance potential.

S. Elavarasan [149] explored MK in various ratios in concrete aims to study the impact on strength as compared with control samples. The results reveal that concrete with MK substitutions of 20% and 10% granulated blast furnace slag shows higher CS at 28 days compared to normal concrete. The CS increases up to 10% when granulated blast furnace slag is replaced, then falls. However, MK substitutions increase tensile strength by up to 20%. Concrete with 10% granulated blast furnace slag and 20% MK substitution has greater FS than standard concrete, despite granulated furnace slag having lower tensile strength.

Ramezan Ali Izadifard [150] examine the use of MK as a partial substitute for cement in concrete to enhance its characteristics. The research incorporates MK in proportions of 10%, 15%, and 20% of cement weight, and evaluates specimens at temperatures between 28 and 800°C. Elevated temperatures may compromise the mechanical properties and durability of ordinary concrete.

Snigdhajit Mukherjee [151] used LS as supplemental cementitious material used as an alternative in building materials for the advancement of a sustainable construction industry. The research examined LS calcined clay cement for lightweight self-compacting concrete with a goal strength of 25 MPa. The evaluation conducted for workability and microstructural analysis. The SEM study reveals that calcium hydrate, generated by the pozzolanic action, attains strength in the presence of LS. The microstructure of cementitious materials evolves over time due to cement hydration and the development of secondary C-S-H. The C-S-H formed at a later curing stage, influenced by the agglomerated water inside the pores, positively affected the aggregate-binder matrix. Comprehensive study indicates that costs and CO_2 emissions decreased by 12.6% and 16%, respectively, in comparison to the control mix.

Meenakshi Sharma [109] examines LS-based cements regarding density, which may be ascribed to the generation of a reduced amount of C-A-S-H, resulting in no notable alteration in density. The fineness of LS influences strength development and heat of hydration in the early stages owing to the filler effect and sulfate equilibrium. Increased proportion resulting from a greater volume proportion of low-density crystalline phases, which decreases permeability and enhances concrete durability. This decreased permeability also

decreases capillary sorption, chloride penetration, and enhances concrete durability.

Dehui Wang [152] investigated the use of LS powder as a replacement for portland cement in cementitious materials. The efficacy of the powder in cement-based products is determined by aspects like particle size, dose, dissolving rate, polymorph, and the mineral content of the cement. LS powder may decrease concrete shrinkage and serve as an inert filler, with its impact on setting time mostly determined by nucleation and dilution. Nonetheless, the influence of chemical additives and fillers on setting time is negligible, since their effects manifest post-setting of the concrete.

Abdurrahman A. Elgalhud [153] investigated the influence of LS on cement and examined its microstructure. Research indicates that the pore structure of Portland LS cement begins to deteriorate with the incorporation of LS up to a maximum of 25%. The features linked to pore structure (porosity, absorption, and sorptivity) of cementitious mixtures (paste, mortar, and concrete) stay unchanged thereafter. Integrating portland cement with LS to produce blended cement, commonly known as Portland LS cement.

Ahmed M. Diab [112] indicates that substituting LS cement diminishes concrete's CS owing to the dilutive effect of cement content. However, studies indicate that substituting 10% of LS does not dramatically affect CS. LS may enhance CS by as much as 10%. This is mainly attributable to the accelerating effect of LS fillers, which generate calcium carboaluminates hydrate and enhance the hydration rate. Moreover, the reduction in expansion and strength loss diminishes with the addition of LS, likely attributable to a decrease in hydration products such as gypsum and $Ca(OH)_2$.

Chapter 3 Methodology and Materials

3.1 Materials Used

The current investigation employed a range of raw materials, encompassing OPC, fine aggregates, coarse aggregates, rGO, ferrock and water. The preparation of ferrock involved the utilization of IO, FA, MK, LS and OA. Figure 3.1 provides a schematic representation of the materials employed, the characterization techniques implemented, and the procedural steps undertaken in preparation of ferrock. Both the aggregates and the constituent materials of ferrock were subjected to particle size distribution analysis and microstructural evaluation to ascertain surface morphology, elemental composition, and mineralogical phases. Subsequently, Unconfined Compressive Strength (UCS) testing was conducted to determine the mechanical performance of each mix design, with the formulation exhibiting the highest CS being identified as the optimal composition for subsequent analysis. This optimized mix was then further characterized through detailed microstructural examination and carbonation testing, wherein the phenolphthalein indicates carbonated and non-carbonated domains within the ferrock matrix.

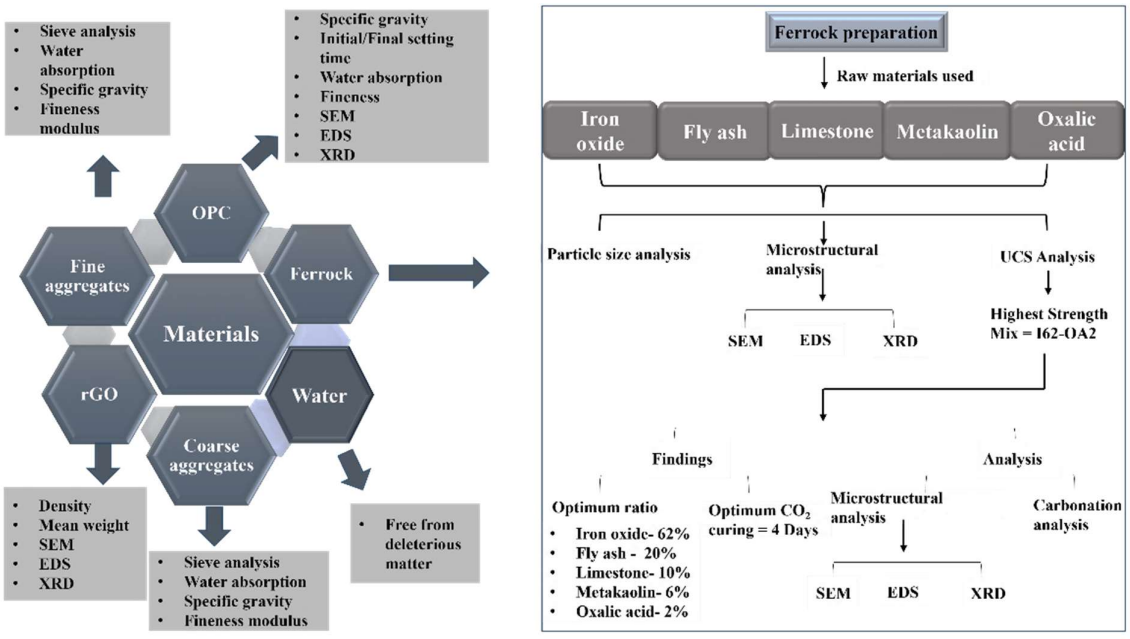

Figure 3.1 Raw materials used and ferrock preparation characterization

3.1.1 Cement

OPC of grade 43 used as the primary binder throughout the study for the preparation of specimens across the various experiments presented in figure 3.2. The physical properties of the OPC investigated in this study encompassed specific gravity, consistency, initial setting time, final setting time, fineness, and soundness. The results of these analyses, conducted in accordance with the specifications of BIS 4031 [Part 1 [154], Part 3 [155], Part 4 [156], and Part 5 [157]] respectively, are presented in table 3.1.

Figure 3.2 OPC grade 43 cement

Table 3.1 Physical properties of OPC

Material	Specific gravity	Fineness	Standard Consistency	Soundness	Initial setting time	Final setting time
OPC	3.15	97.5%	32%	1 mm	87 min	277 min

Microstructural analysis of OPC was conducted to study its surface morphology, texture, elemental composition and phases of minerals, as these properties significantly impact physical and chemical properties of concrete. Figure 3.3 illustrates the (a) SEM image, (b) XRD patterns indicating minerals phase, (c) EDS elemental peaks and (d)

elemental mapping of OPC. SEM images provided visual representation of the OPC's surface texture which exhibited an irregular morphology with rough edges and compacted structure. XRD analysis identified the primary crystalline phases as tricalcium silicate (Ca_3SiO_5), dicalcium silicate (Ca_2SiO_4), and SiO_2. The presence of elements such as silicon and Ca in OPC is crucial for strength development and durability in concrete composites. The elemental composition of the OPC, as determined by EDS and presented in table 3.2, revealed a calcium-to-silicon (Ca/Si) ratio of 4.85.

Table 3.2 Elemental composition of OPC

Elements (wt%)	O	Ca	Si	Al	Fe	K	Na	Mg
OPC	36.32	40.12	8.27	5.24	4.34	0.2	0.24	5.27

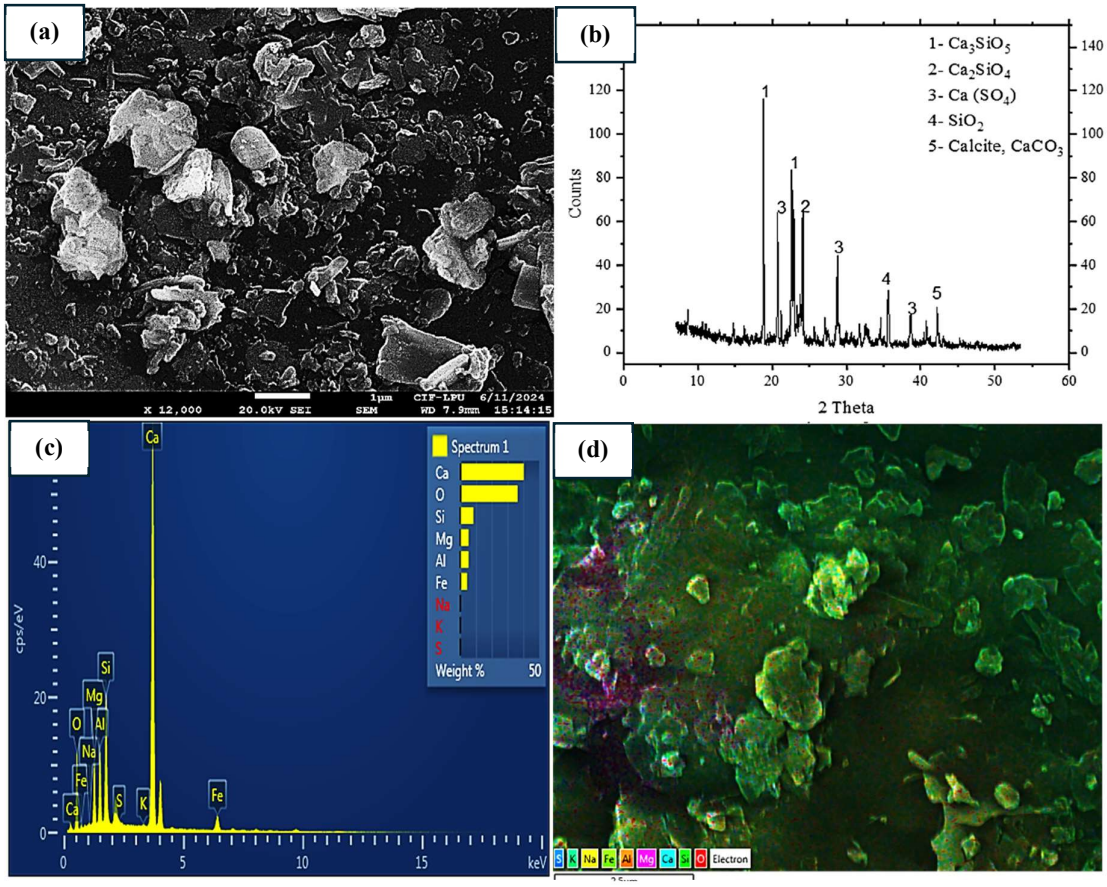

Figure 3.3 Microstructural analysis of OPC by (a) SEM, (b) XRD, (c) EDS peaks and (d) elemental mapping

3.1.2 Aggregates

The natural sand used as fine aggregate conformed to the Zone II grading requirement as specified in IS 383: 2016 [158]. The fine and coarse aggregates were sourced from Walia cement store Phagwara, Jalandhar India. The physical properties of the fine aggregate, including specific gravity, water absorption and fineness modulus of fine aggregates found as 2.65, 1% and 2.53 respectively followed BIS: 2386 (Part-3) [159]. The maximum nominal size of fine aggregates and coarse aggregates utilized in study was 4 mm and 20 mm respectively as depicted in figure 3.4. The specific gravity and fine modulus of coarse aggregates were found to be 2.64 and 6.8 respectively. The particle size distribution curve of both the fine and coarse aggregates are presented in figure 3.5 and 3.6 respectively as specified in BIS: 2386 (Part 1) (2002) [160].

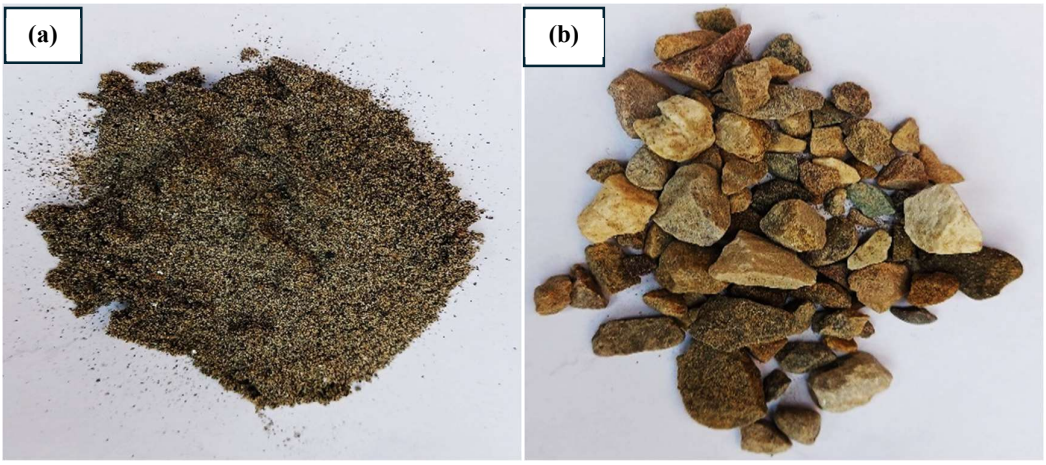

Figure 3.4 (a) Sand (b) Coarse aggregates

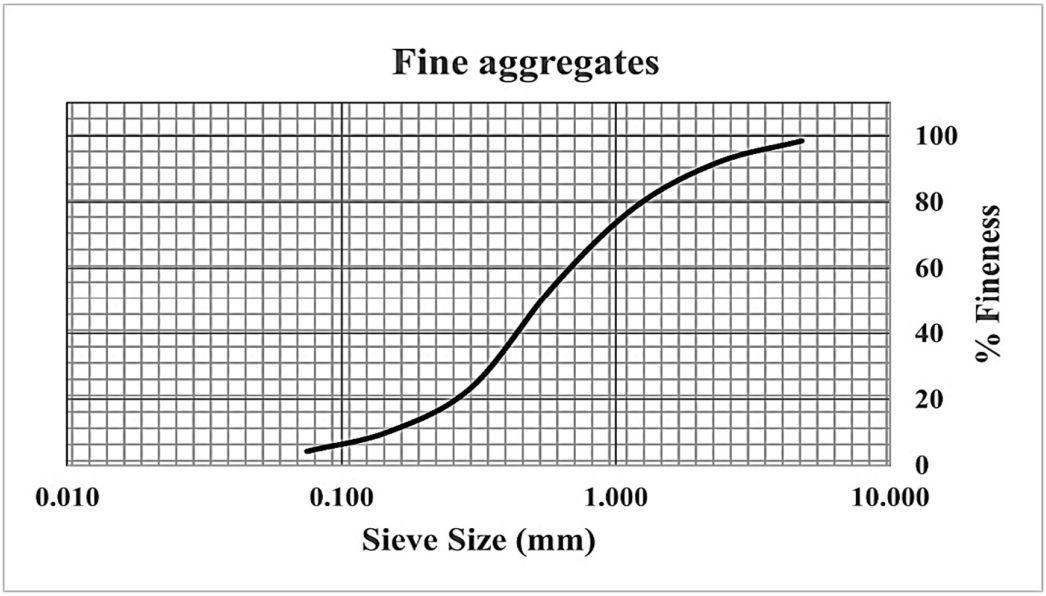

Figure 3.5 Particle size distribution curve of sand

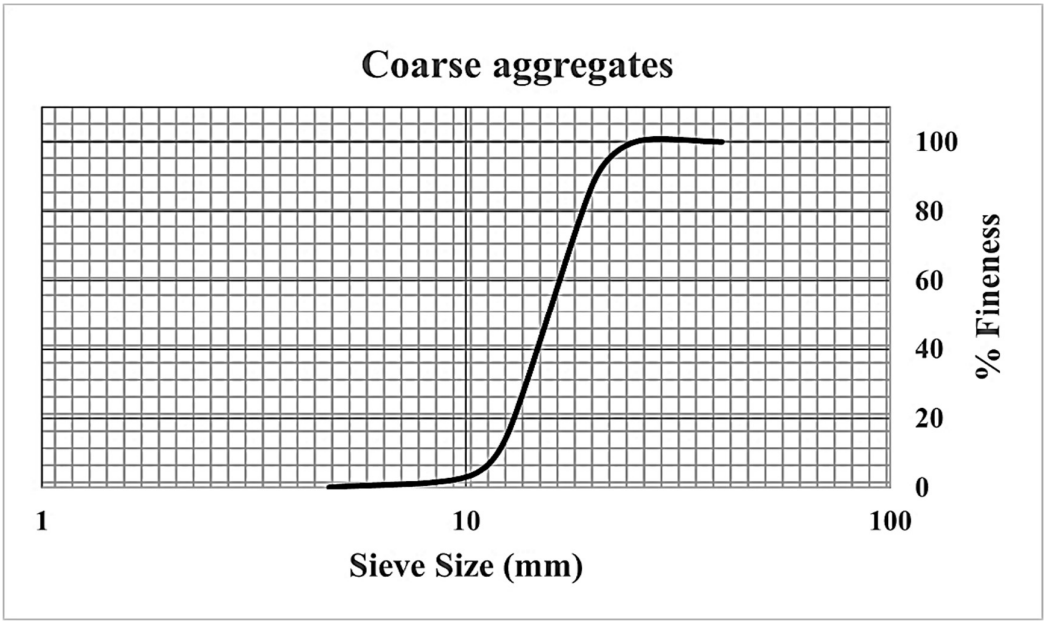

Figure 3.6 Particle size distribution curve of coarse aggregates

3.1.3 Water

Potable water, free from deleterious substances, was utilized for both the casting and curing of specimens, adhering to the specifications outlined in the IS 456:2000 [154]. A consistent temperature of 26 ± 2 °C was maintained throughout the duration of this study for the preparation of the concrete mix and the subsequent curing of samples.

3.1.4 Ferrock

Ferrock is an emerging carbon absorbing material that contains waste iron oxide as the main binder obtained from steel industries which otherwise landfilled [84] [85]. Its carbon-negative properties are attributed to the chemical reaction wherein IO interacts with CO_2 in the presence of OA. This reaction results in the formation of complex iron carbonate during the curing process, thereby sequestering CO_2 and enhancing the environmental sustainability of the material. The raw materials employed in the synthesis of ferrock include IO, FA, MK, and LS as illustrated in figure 3.7. These materials vary in particle size, with IO exhibiting a relatively coarser texture, while FA, MK, and LS consist of finer particles. All raw materials have finer particles as compared with IO to maintain workability of mix. When ferrock is mixed in concrete the coarser pores filled with IO and finer pores filled with FA, MK and LS to make denser and compacted concrete matrix. The concept used for hardening of ferrock as the CO_2 curing partially dissolved the tiny particles of steel dust by carbonic acid (H_2CO_3), which is what forms when CO_2 gas dissolves into water. The iron atoms that are released into the thin film of water around each particle of steel have a positive charge and are known as ferrous iron ions (Fe^{+2}). These positively charged ions are attracted to negatively charged carbonate ions (CO_3^{-2}) and combine with them to form iron carbonate ($FeCO_3$) with a balanced charge. Layers of iron carbonate form around each steel particle and build up into thicker shells. These growing shells of crystalline iron carbonate eventually connect and fuse together into what is called a mineral “matrix”, and this is how the ferrock cement locks any aggregate like sand and gravel into a solid mass.

Figure 3.7 (a) IO, (b) FA, (c) LS and (d) MK used as raw materials in ferrock

The current research primarily prepared ferrock and conducted experimental study with varying ratios of raw materials to conclude optimum ratio and curing days. To ensure precision in the further study, due to possible variations in the characteristics of the raw materials. The prepared samples were placed in airtight polybags and exposed to CO_2-enriched environment to initiate carbonation and facilitate product formation. UCS tests were conducted on all mixes to evaluate their mechanical strength. The mix exhibiting the highest CS was identified as the optimal formulation, establishing both the ideal ratio of raw materials and the required curing duration. This optimized mix design and curing period were subsequently used for preparing additional ferrock samples, which were later employed in further experiments involving concrete composites.

3.1.4.1 Raw materials

3.1.4.1.1 Iron Oxide

IO is used as the primary binding material in ferrock characterized by shiny black color and angular particles. The IO used in this study was bought from Herena instruments & engineers Chennai, India. SEM and EDS analyses were performed to study microstructural properties including surface texture, morphology and elemental composition of material. The figure 3.8 below presents the results of (a) SEM analysis, (b) XRD phases, (c) elemental peaks and (d) elemental mapping. The zoomed image of IO particle predominantly consisted of elongated, plate-like forms, hence affecting the rheological characteristics of the concrete mix. EDS analysis revealed Fe and O as major elements in IO as presented in table 3.3. Elements mapping further revealed presence and distribution of elements across IO. XRD analysis illustrated a prominent peak of Fe_2O_3, majorly because of the high concentration of Fe and O in IO. Iron oxide comprises solid angular particles which fill the voids to improve strength and denseness in composite matrix. Particles of iron oxide react with CO_2 when OA is present to form a dense layer of iron carbonates [88].

Table 3.3 Elemental composition of IO

Elements (wt%)	O	Fe	Ca	Mn	K	Cu
IO	27.56	72.13	0.05	0.07	0.04	0.14

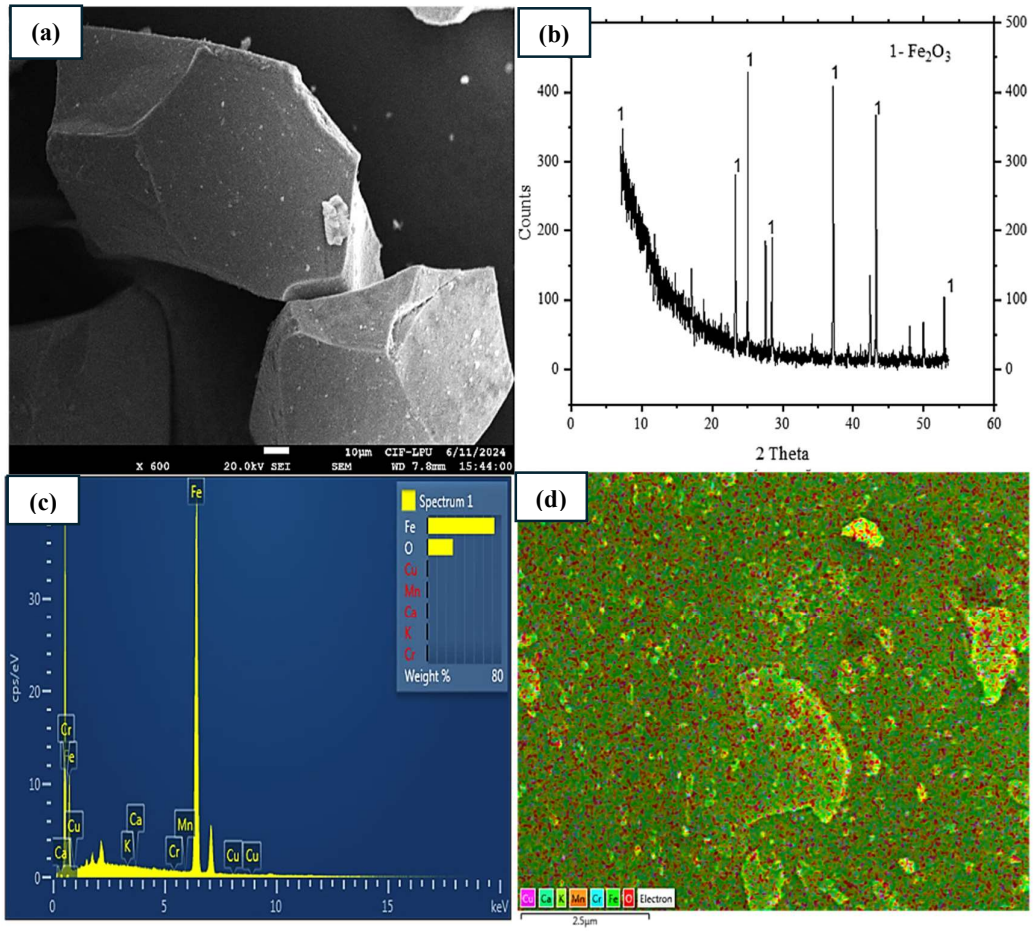

Figure 3.8 Microstructural analysis of IO by (a) SEM, (b) XRD, (c) EDS peaks and (d) elemental mapping

The particle size distribution curve of IO, presented in figure 3.9, was obtained through sieve analysis, as IO is a granular material. The curve exhibits a noticeable increase in the range of 0.1 mm to 0.2 mm, indicating a significant proportion of particles within this size range. Beyond 0.5 mm, the curve shows minimal variation, suggesting a limited presence of particles larger than 0.5 mm. The curve begins at approximately 0.05 mm, indicating the presence of finer particles in small quantities, which contributes to a more uniform distribution within the mix.

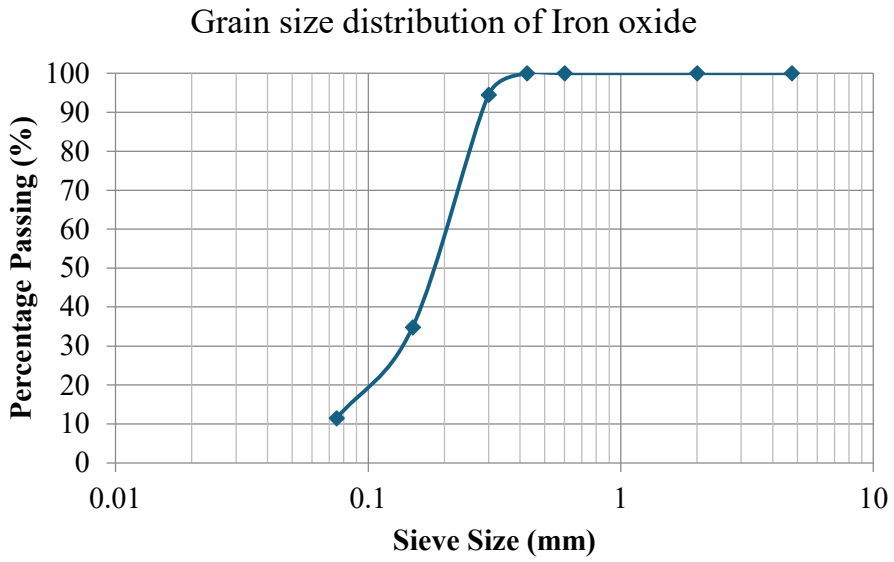

Figure 3.9 Particle size distribution of IO

3.1.4.1.2 Fly ash

Class F FA, as specified in ASTM C618 [161], was utilized as one of the raw materials in the preparation of ferrock to increase the silica content, thereby enhancing the overall strength of the material. FA forms iron silicate minerals when reacts with IO and these silicates can contribute to greater strength and durability to ferrock. The figure 3.10 presents the results of (a) SEM analysis, (b) XRD phase identification, (c) EDS analysis and (d) elemental mapping of FA. The SEM analysis revealed that FA particles exhibit smooth surface morphology and visualize the shape of particles which are spherical. The results of EDS revealed that the elemental composition of FA contains O and Si as major proportion as presented in table 3.4 below. Further the elemental mapping provided the visual representation of evenly distributed elements across the sample. XRD analysis demonstrated a prominent peak corresponding to SiO_2, consistent with the high concentrations of O and Si identified in the EDS analysis. FA slowly reacts with iron to form certain types of iron silicate minerals that add greater strength and durability to ferrock [89]. Ferrock incorporates various pozzolanic materials, each contributing uniquely to its properties. During the carbonation process, silica is transformed into calcium silicate, which plays a critical role in filling voids

within the ITZ of concrete composites, thereby enhancing their overall performance [90] [91].

Table 3.4 Elemental composition of FA

Elements (wt%)	O	Ca	Si	Al	Fe	K	Na	Mg
FA	49.16	1.42	25.15	20.35	1.87	1.27	0.06	0.72

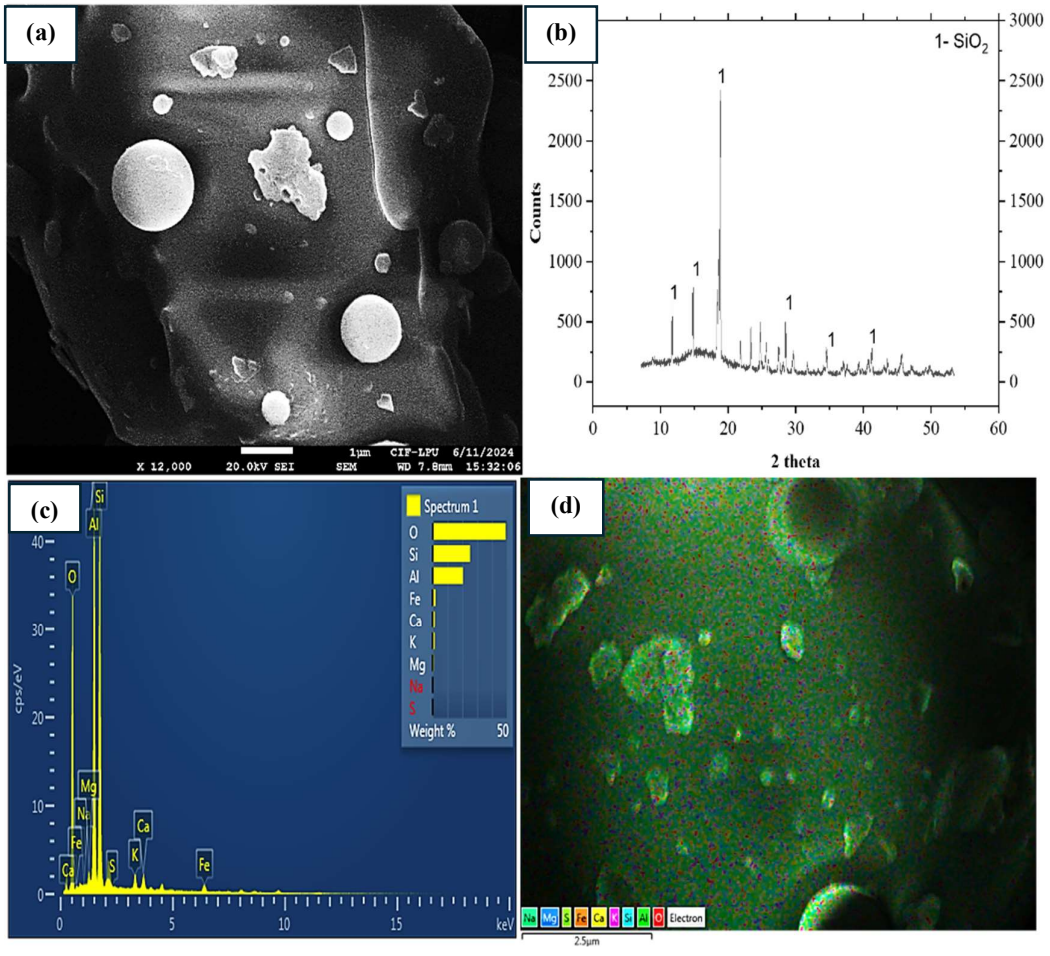

Figure 3.10 Microstructural analysis of FA by (a) SEM, (b) XRD, (c) EDS peaks and elemental mapping

The particle size distribution of FA was determined using the hydrograph analysis setup illustrated in figure 3.11, with the corresponding results presented in figure 3.12. The graph exhibits a pronounced peak around the 1 mm region, indicating that the majority of particles are concentrated at this size. Beyond 1 mm, the graph shows a gradual increase in particle size, suggesting the presence of coarser particles as well. The finer fraction of FA contributes to an increased surface area, thereby offering more active sites for pozzolanic reactions.

Figure 3.11 Setup of hydrograph analysis of FA

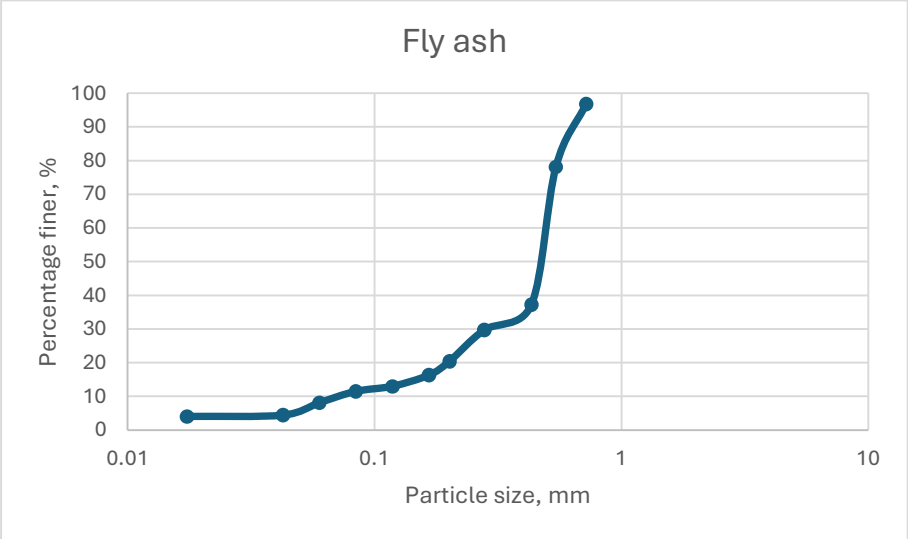

Figure 3.12 Particle size distribution of FA

3.1.4.1.3 Metakaolin

MK is a type of calcined clay used as a raw material in the production of ferrock as specified in ASTM C 618 [161]. It is produced by heating kaolin to approximately 600 °C, a process that enhances its reactivity and enables it to bond more effectively with other materials, including the constituents of ferrock. During current study MK sourced from Herenba instruments & engineers Chennai, India. Due to the irregular shape of IO dust particles, MK is employed to maintain the workability of the cementitious paste. Its water-retaining capacity contributes to a thicker and more cohesive ferrock paste, facilitating easier application and a smoother surface finish [148]. MK is an eco-friendly natural pozzolanic material obtained by heating kaolin to temperatures of 650–900 °C, a process that does not generate CO_2 production [162]. Figures 3.13 illustrate the results of (a) SEM analysis, (b) XRD phases, (c) EDS elemental peaks and (d) elemental distribution mapping. Image obtained from SEM revealed the smooth structure of particles in MK. EDS analysis revealed O, Ca and Si as major elements reported in table below 3.5. Further the elemental mapping visualizes the distribution of elements present in MK sample. Previous studies have confirmed MK as an effective pozzolanic material, produced by the thermal treatment and milling of natural kaolin [93]. Its incorporation into cementitious systems has been shown to

enhance chloride permeability resistance, increase early CS, and improve microstructural densification by reducing porosity. These characteristics contribute significantly to the durability and longevity of the resulting concrete [94]. Both MK and FA are rich in alumina, and their interaction with hydration products supplies additional alumina, which integrates into the formation of C-S-H, thereby improving the mechanical and durability properties of the composite material [95] [96].

Table 3.5 Elemental composition of MK

Elements (wt%)	O	Ca	Si	Al	Fe	K	Na	Mg
MK	49.31	0.22	25.74	24.32	0.22	0.04	0.08	0.06

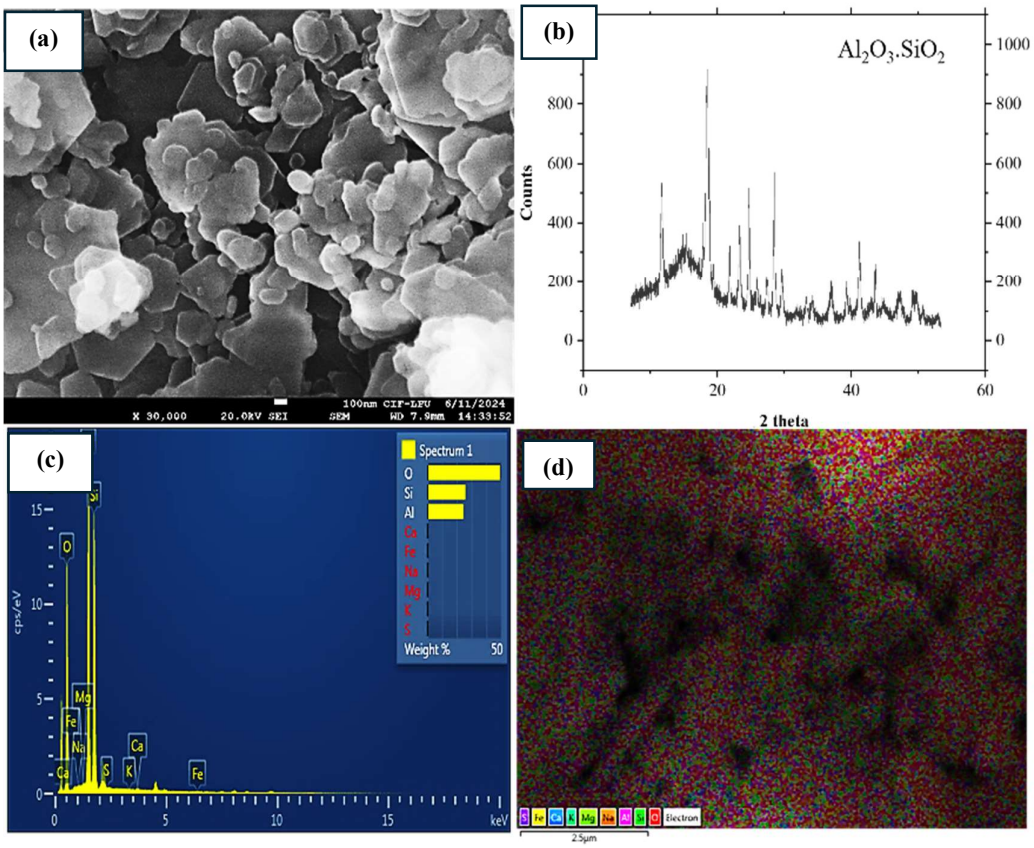

Figure 3.13 Microstructural analysis of MK by (a) SEM, (b) XRD, (c) EDS peaks and (d) elemental mapping

The particle size distribution of MK was determined through hydrometer analysis, with the experimental setup and resulting graph presented in figures 3.14 and 3.15, respectively. The distribution curve indicates that MK consists predominantly of very fine particles, as evidenced by the pronounced shift of the curve towards the finer end of the scale. The graph begins at a particle size of 0.001 mm, where approximately 5% of the particles are finer than this size. The curve reaches its upper plateau around 0.1 mm, corresponding to approximately 90% finer particles, suggesting that only 10% of the particles are coarser than this size. Overall distribution confirms that MK possesses a fine particle size, which is advantageous when blended with ferrock. The fine particles contribute to a higher surface area, thereby potentially enhancing the workability of the composite material.

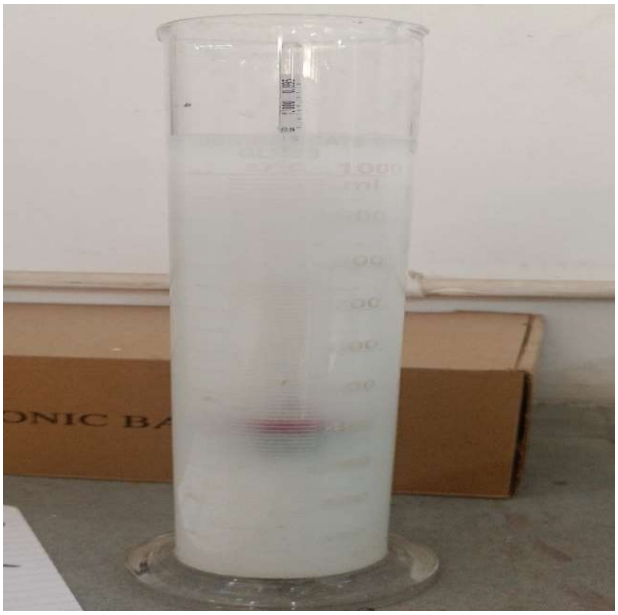

Figure 3.14 Setup for hydrograph analysis of MK

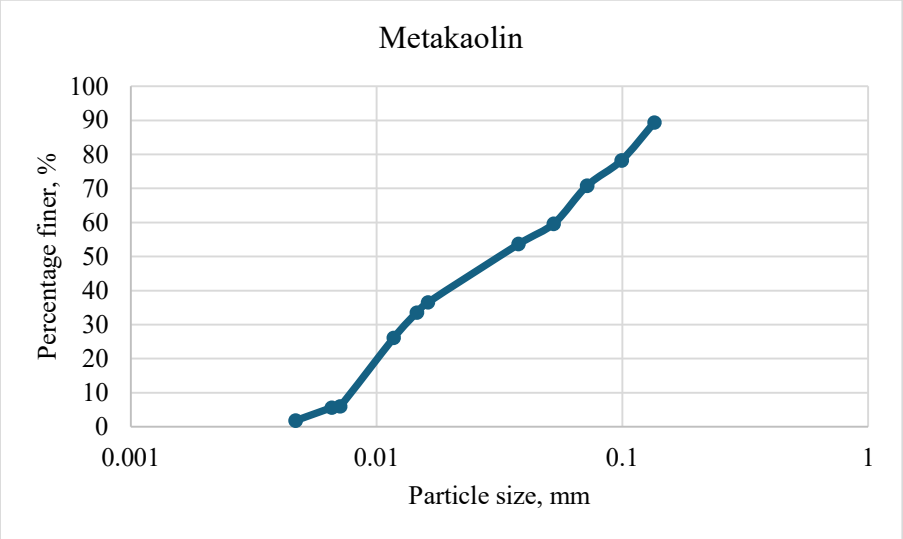

Figure 3.15 Particle size distribution of MK

3.1.4.1.4 Limestone

LS is utilized due to its composition of calcium carbonate, which facilitates crystal formation by serving as a template for nucleation and subsequent crystal growth as specified in ASTM C618 [161]. LS used as one of raw material in ferrock preparation bought from Hazur Singh & Grandsons Jalandhar, Punjab India. The role of LS involves its dissolution in water, during which it releases CO_2, thereby supplying additional carbonate ions that contribute to the mineralization process. SEM, XRD and EDS analysis including elemental mapping were conducted to study the microstructure of LS and results are depicted in figure 3.16. SEM images revealed the texture of the surface characterized by crystal boundaries and microfractures present within the LS structures. EDS analysis identified the elements present in LS as summarized in table 3.6 below while elemental mapping as visualize the spatial distribution of elements. XRD analysis indicated prominent peaks corresponding to $CaCO_3$ confirming that Ca and oxygen are two primary elements present in LS powder. Chemically, LS has the same mineral structure as iron carbonate and promotes its formation by providing a template for crystal growth. Furthermore, LS contributes to making structure dense by filling pores. When FA combine with FA it gives calcium mono hemicarboaluminate which enhances both the strength and durability of the composite material [110]. The

idea encompasses recycling materials and pozzolanic compounds to strengthen aggregate cement paste bonding and make cement composites more workable [163]. The use of LS as an ingredient in blended cement has a positive environmental impact, as it reduces the need for clinker production for the same quantity of cement. Consequently, this leads to lower energy consumption and a significant reduction in CO_2 emissions and other GHG associated with cement manufacturing [164]. Heterogeneous nucleation takes place since LS particles work as nucleation sites, raising the early hydration of cement and, consequently, creating an additional mixed-up crystallization of CSH [165].

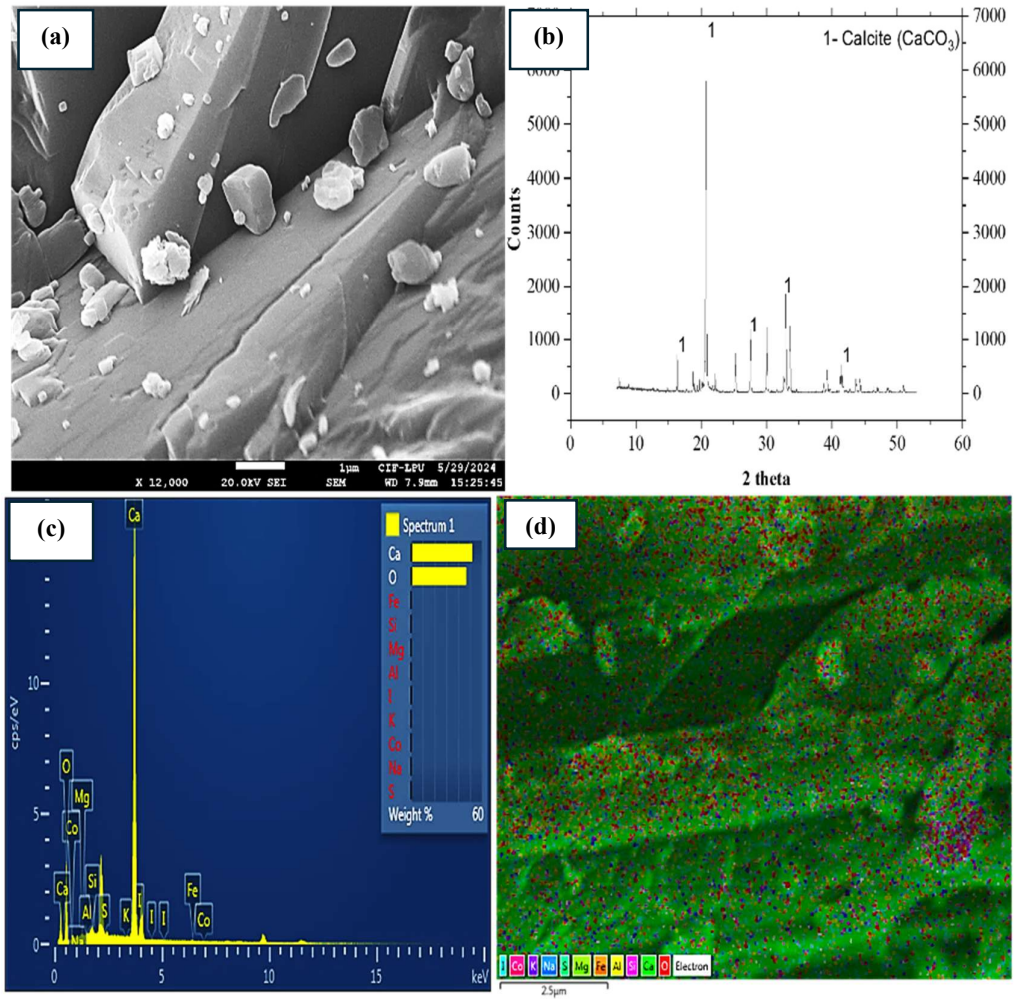

Figure 3.16 Microstructural analysis of LS by (a) SEM, (b) XRD, (c) EDS peaks and (d) elemental mapping

Table 3.6 Elemental composition of LS

Elements (wt%)	O	Ca	Si	Al	Fe	K	Na	Mg
LS	46.76	51.97	0.27	0.14	0.32	0.08	0.05	0.22

The particle size distribution of LS was analyzed using hydrometer analysis, with the experimental setup and the resulting graph presented in figures 3.17 and 3.18, respectively. The distribution curve begins at a particle size of 0.001 mm, where approximately 18% of the particles are finer than this size. The curve reaches its peak around 1 mm, with 95% to 98% of the particles being finer than this size, indicating that only 2% to 5% of the particles are coarser than 1 mm.

Figure 3.17 Setup of hydrograph analysis of LS

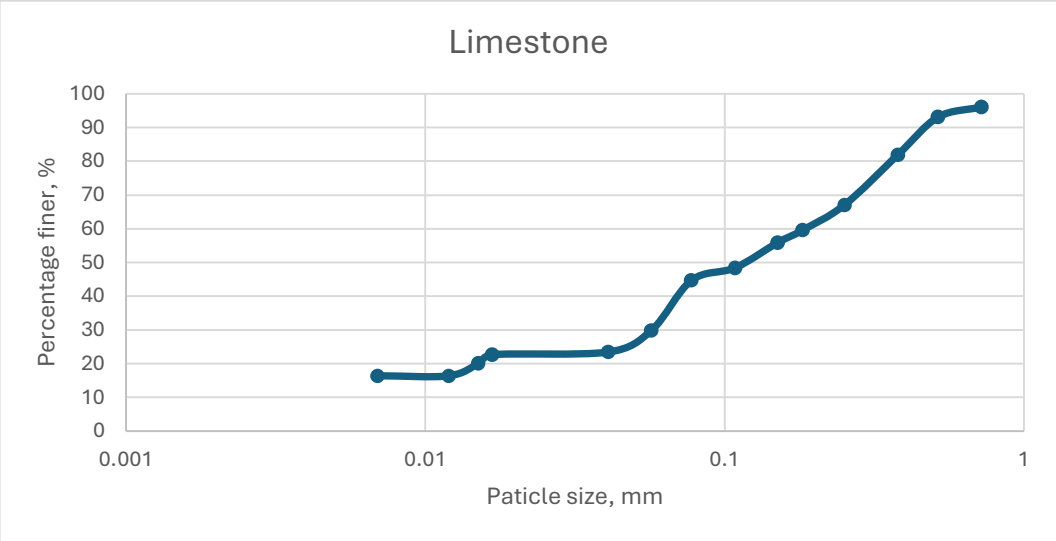

Figure 3.18 Particle size distribution of LS

3.1.4.1.5 Oxalic Acid

The OA used in this study was bought from Dee Jay Corporation, Jalandhar, Punjab. The reaction between iron oxide and CO_2 is chemically slow therefore to accelerate the rate of reaction OA was used as a catalyst [90]. Firstly, it facilitates the initial dissolution of steel dust by reacting with iron to form iron oxalate, which subsequently absorbs CO_2. Secondly, it inhibits the formation of IO, commonly referred to as rust, which can negatively impact the strength and durability of ferrock. Lastly, OA decomposes into carbonate ions, which further contributes to the formation of iron carbonate minerals, enhancing the overall mineralization process.

3.1.4.2 Optimum mixture proportions

A total of 16 different mixtures were prepared in the preliminary study, incorporating varying proportions of IO, FA, LS, MK, and OA, to identify the optimal mix based on UCS test results. The IO content ranged from 58% to 69% by mass, while FA, LS, and MK were varied within the ranges of 15–20%, 8–10%, and 6–10% by mass, respectively. The CS of each mixture was evaluated after CO_2 curing for durations of 2, 3, 4, 5, and 6 days. Table 3.7 below presents the mix proportions, expressed as

percentages of the raw materials used in the preparation of ferrock, along with their corresponding mix notations.

Table 3.7 Mix proportions of raw materials of ferrock with mix notation

Mix notation	IO (%)	FA (%)	LS (%)	MK (%)	OA (%)
I58-OA2	58	20	10	10	2
I58-OA4	58	20	10	10	4
I60-OA2	60	20	8	10	2
I60-OA4	60	20	8	10	4
I62-OA2	62	20	10	6	2
I62-OA4	62	20	10	6	4
I63-OA2	63	15	10	10	2
I63-OA4	63	15	10	10	4
I64-OA2	64	20	8	6	2
I64-OA4	64	20	8	6	4
I65-OA2	65	15	8	6	2
I65-OA4	65	15	8	6	4
I67-OA2	67	15	10	6	2
I67-OA4	67	15	10	6	4
I69-OA2	69	15	8	6	2
I69-OA4	69	15	8	6	4

3.1.4.3 Sample preparation

The mixing procedure involves the dry mixing of all materials i.e., IO, FA, LS, MK at the initial phase and then mix with water, leave it for some time to complete the reaction and with time mix thickened resulting in a consistent texture presented in figure 3.19. The stepwise procedure for preparing ferrock is given below, this method allows the different reactions to begin immediately. The sequence followed for the best results are mentioned below:

1. Weigh the raw materials in the ratio of mix design as ratios are mentioned in table 3.7.

2. First add FA in a tray, if FA contains hard lumps need to soften and break down to make fine powder.

3. Add IO and MK to the mix, then add LS powder and mix them properly to make uniform and dry mix.

4. Add OA and mix uniformly, then add water to make soft paste not slurry kind not hard, this should be like sample can be formed and stick to each other. Leave the mixture for 15 to 30 min to absorb water. The mix thickens over time.

5. As water mixed, bubbles started intensely as acid reacted with LS. The gas emitted CO_2 as acid dissolves some calcium carbonate and produces ($Ca(OH)_2$).

6. When mix was ready sample were prepared in cylindrical shape of dimension, diameter of 3.6 cm and a length of 7.6 cm for testing. After the respective durations of CO_2 exposure, the samples were placed in air at room temperature to allow the moisture to evaporate for 3 days. Now samples that were ready for UCS test and performed in accordance with IS 2720.10.2006 [166].

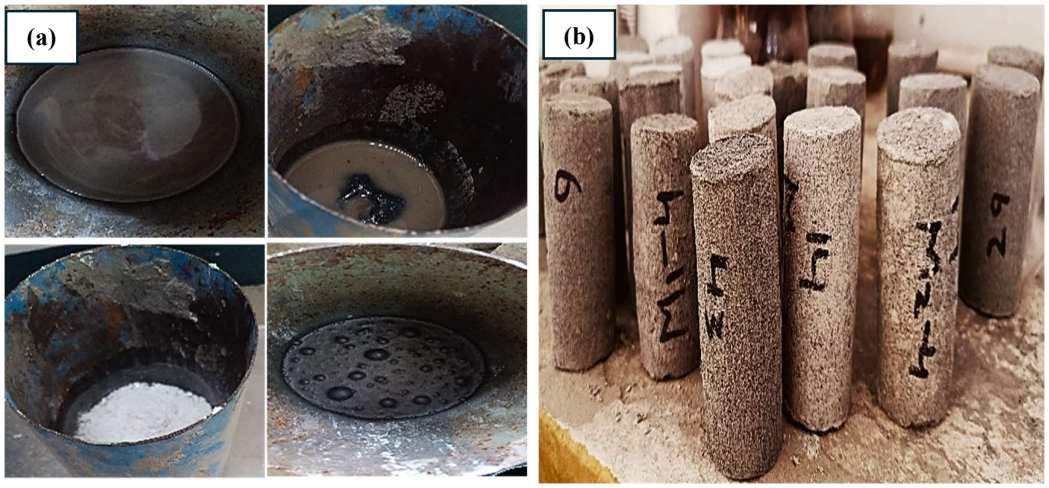

Figure 3.19 (a) Ferrock preparation process and (b) prepared sample of ferrock

3.1.4.4 Curing Procedure

Ferrock requires an additional carbonation reaction to fully cure and develop a solid matrix within a CO_2-rich environment. In this study, the specimens were placed in clear plastic bags filled with approximately 100% CO_2 at room temperature. To maintain CO_2 saturation, the bags were refilled after 12 hours, as illustrated in the corresponding figure 3.20. For the preliminary study, the specimens were exposed to a ~100% CO_2 atmosphere for 2, 3, 4, 5 and 6 days immediately after casting and demolding. Following this carbonation period, the specimens were cured in open air at room temperature for an additional 3 days to reduce moisture content and ensure proper hardening prior to UCS testing.

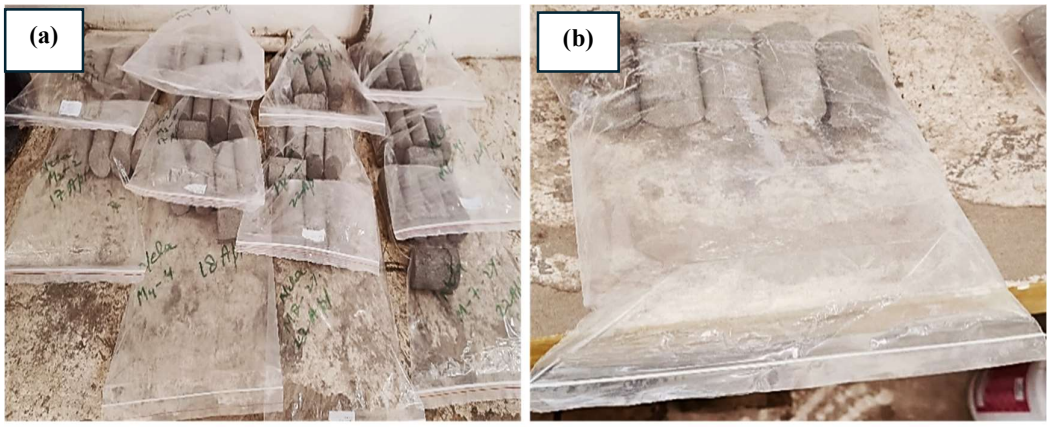

Figure 3.20 CO_2 curing of ferrock samples in airtight polybags

3.1.4.5 UCS test

A UCS test was performed in accordance with IS 2720.10.2006 [166] on every specimen of 16 mixes at different CO_2 curing of 2, 3, 4, 5 and 6 days followed by 3 days of air curing. The UCS test was conducted to determine the optimum proportions of raw materials for further investigation of ferrock as a potential substitute for conventional cement. Once the mix was prepared, the samples were molded into cylindrical specimens with a diameter of 3.6 cm and a length of 7.6 cm. The mixture was placed into the molds in three layers, with each layer compacted by tamping 25 times to ensure uniform density. The specimens were then immediately demolded using a specimen ejector. Following their respective durations of CO_2 exposure, the samples were kept at room temperature for an additional 3 days to allow moisture evaporation and to ensure proper hardening prior to testing.

The samples were subjected to CO_2 curing for 2, 3, 4, 5, and 6 days, followed by an additional 3 days of air curing at room temperature to allow excess moisture to evaporate and ensure proper drying. The CS of the various mixes was then evaluated and compared. The results are illustrated in figure 3.21, which presents UCS data for the following mix combinations: (a) I58-OA2 and I58-OA4, (b) I60-OA2 and I60-OA4, (c) I62-OA2 and I62-OA4, (d) I63-OA2 and I63-OA4, (e) I64-OA2 and I64-OA4, (f) I65-OA2 and I65-OA4, (g) I67-OA2 and I67-OA4, and (h) I69-OA2 and I69-OA4.

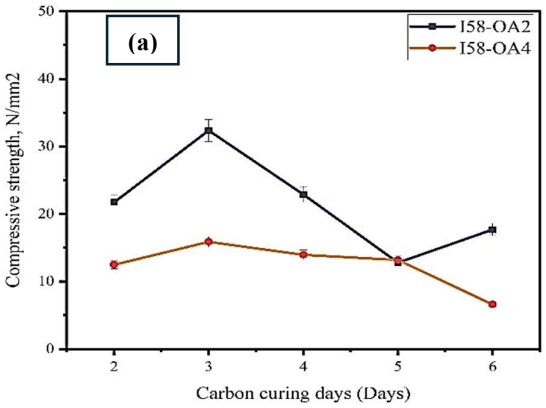
(a)
I58-OA2
I58-OA4
Compressive strength, N/mm2
Carbon curing days (Days)

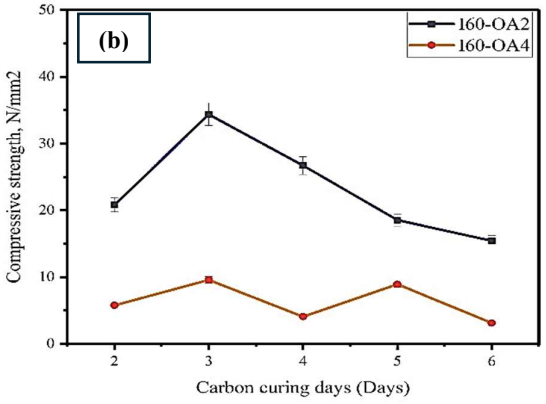
(b)
I60-OA2
I60-OA4
Compressive strength, N/mm2
Carbon curing days (Days)

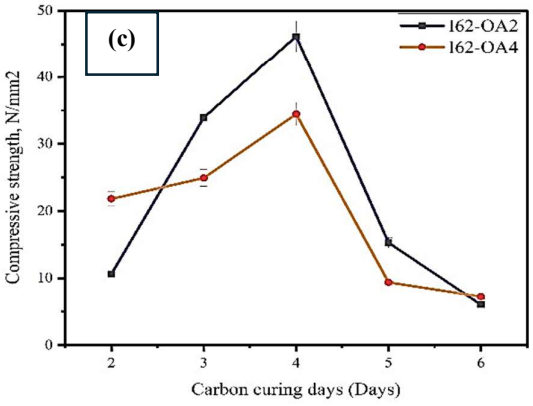
(c)
I62-OA2
I62-OA4
Compressive strength, N/mm2
Carbon curing days (Days)

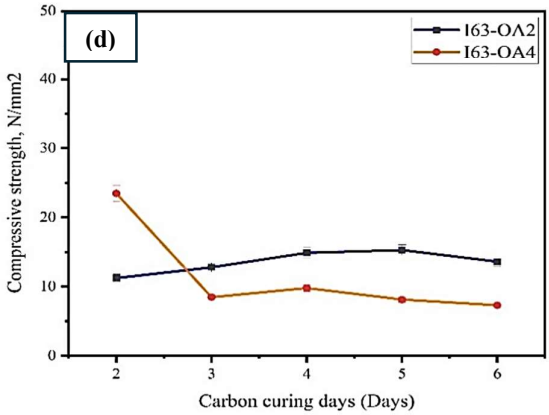
(d)
I63-OA2
I63-OA4
Compressive strength, N/mm2
Carbon curing days (Days)

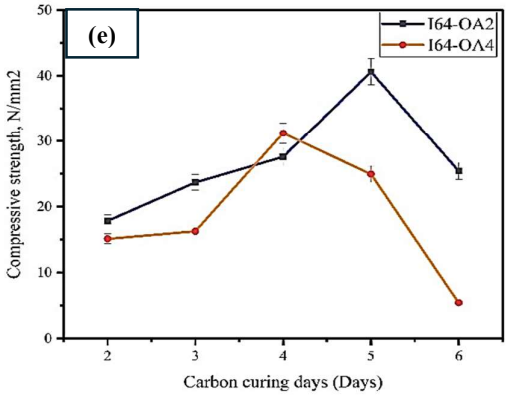
(e)
I64-OA2
I64-OA4
Compressive strength, N/mm2
Carbon curing days (Days)

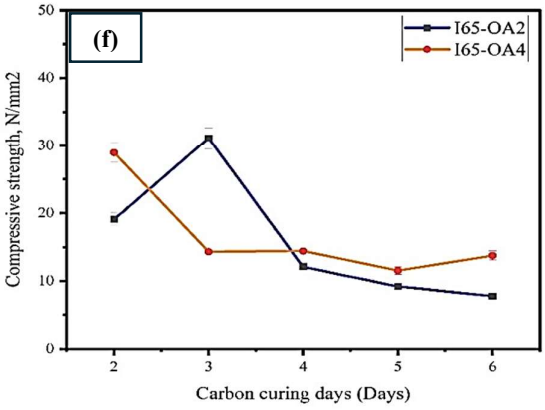
(f)
I65-OA2
I65-OA4
Compressive strength, N/mm2
Carbon curing days (Days)

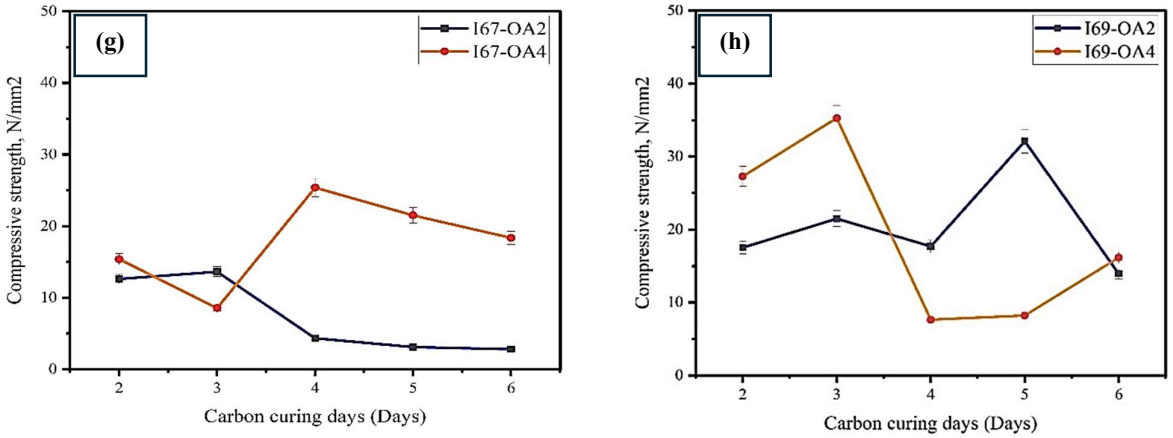

Figure 3.21 UCS results for mixes (a) I58-OA2 and I58-OA4, (b) I60-OA2 and I60-OA4, (c) I62-OA2 and I62-OA4, (d) I63-OA2 and I63-OA4, (e) I64-OA2 and I64-OA4 (f) I65-OA2 and I65-OA4 (g) I67-OA2 and I67-OA4 (h) I69-OA2 and I69-OA4

The results indicated that the mix I62-OA2 achieved the highest CS, followed by I64-OA2 and I69-OA4. The I62-OA2 mix achieved a peak CS of 46.15 MPa on the fourth day of CO_2 curing, followed by a sharp decline on the sixth day. This indicates that most of the reactions were likely completed within the initial four days. The I60-OA2 mix exhibited high early strength during the initial stages of CO_2 curing. However, a gradual decline in strength after the third day highlights the variability in the performance of FA and other supplementary materials under carbonation conditions. The overall results indicate a notable reduction in strength by the sixth day for all mixes, which attributed to the near completion of chemical reactions or increased porosity within the matrix. Both the highest strength mixes contain 20% FA concludes samples with 20% FA were stronger than others with same ratio of MK. With a constant high ratio of FA in mix I62-OA2 and I64-OA2 higher ratio of LS shows better results in strength. With constant low ratio of FA and constant MK in mix I69-OA2 and I67-OA2 with variable LS shows that mix with lower LS shows higher CS than higher LS value. The cohesive nature of MK and the synergistic action of silicates are likely to provide a denser matrix. The samples containing 20% FA exhibited similar strength, indicating that the variations in MK content influenced the overall strength. An increase in MK

content is linked to a notable but modest drop in CS values at lower FA content. In these systems, MK primarily serves as a rheology modifier, whereas the fine LS is anticipated to serve as a reaction product nucleation site [167]. The strength increased with the duration of CO_2 curing due to carbonation and product formation reactions. This enhancement in strength was attributed to the carbonation process and the formation of iron carbonates during the reaction. This implies that pores size decreases with increasing CO_2 curing. Higher carbonation leads to more reaction and more density as product fills the pores.

3.1.4.5.1 Stress strain behavior

Stress–strain analysis was performed on the mixes that exhibited the highest, second highest, and third-highest CS, with the results presented in figures 22(a), 22(b) and 22(c), respectively. The specimen I62-OA2C4 demonstrated a higher proportional limit compared to the others, indicating greater stiffness and lower deformation under applied stress. This suggests that the material is less ductile and more rigid. In contrast, the other two specimens showed lower stiffness and greater deformation, indicating more ductile behavior. The I62-OA2C4 mix exhibited enhanced elastic performance, making it more suitable for construction applications. After reaching the proportional limit, all mixes showed a drop in stress, marking the transition from elastic to plastic behavior. Notably, only I62-OA2C4 exhibited strain hardening, with the material reaching its ultimate tensile strength before failure. The other mixes showed minimal stress increase before failure, without significant hardening. Overall, I62-OA2C4 not only achieved the highest strength but also showed superior load-bearing behavior with reduced strain. The gradual stress drop before failure indicates a ductile failure mode, making it a more reliable option for structural use.

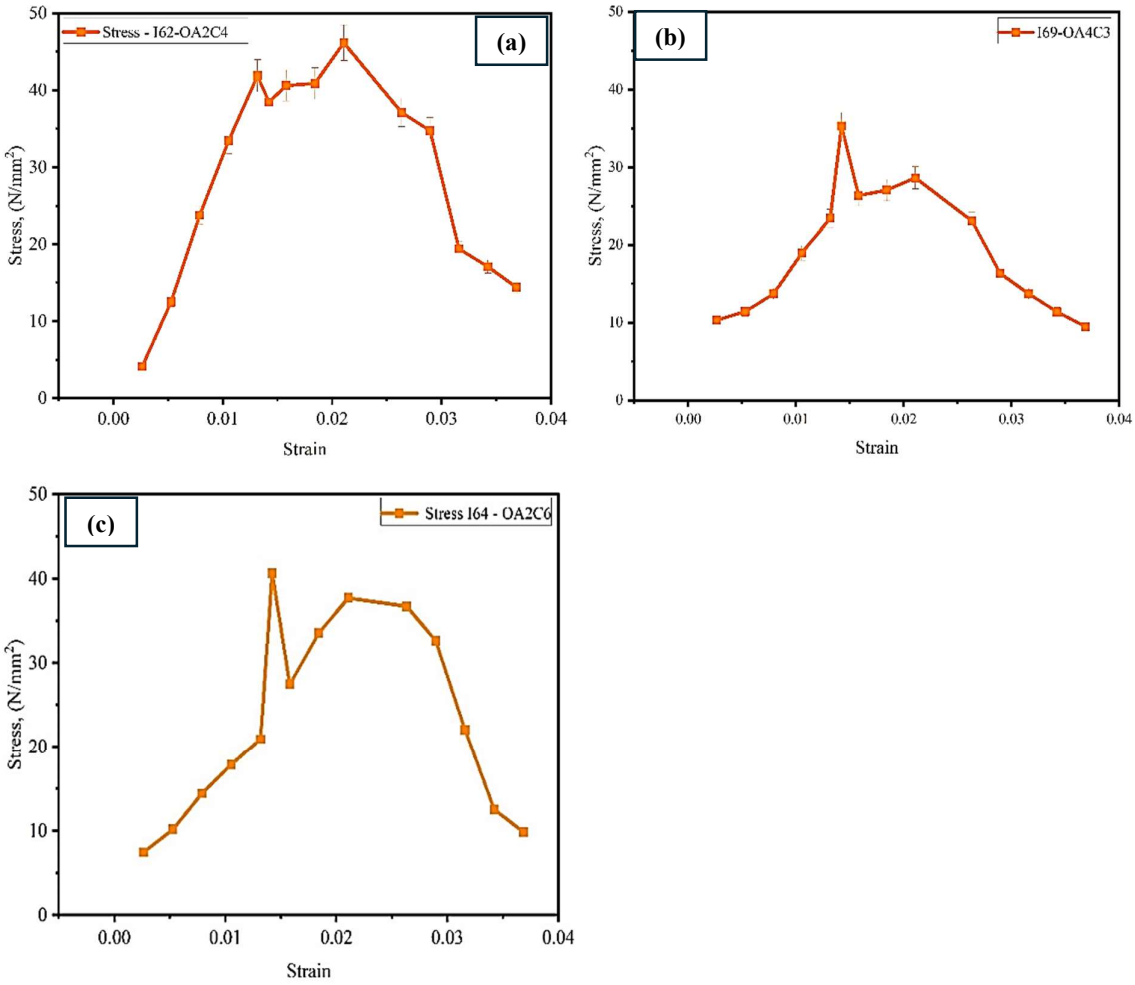

Figure 3.22 Stress strain graph for mix (a) I62-OA2C4 (b) I64-OA2C6 and (c) I69-OA4C3

3.1.4.5.2 Compressive strength test for OPC based binder

The CS of cubes prepared using ferrock was compared with that of cubes made using OPC and other binders to assess the binding capability of ferrock. For each mix, 50 mm cubes were cast, cured, and tested after 28 days of curing and results are presented in figure 3.23. Notably, the cube containing ferrock underwent CO_2 curing

for 4 days, followed by water curing for 28 days. The mix proportions and corresponding notations are detailed in table 3.8.

Table 3.8 Mix proportions of binder for CS comparison

Mix notations	C	FA	MK	Ferrock
100C	100	0	0	0
80C20FA	80	20	0	0
60C40FA	60	40	0	0
75C25MK	75	0	25	0
50C50MK	50	0	50	0
I62-OA2	0	0	0	100

While it is widely recognized that OPC-based composites continue to gain strength over time and may exhibit significantly higher long-term CS, the iron carbonate-based binder system in mix I62-OA2 already achieves strengths suitable for many construction applications. The values reported for the iron carbonate-based binder system in mix I62-OA2 fall within the range required for many construction applications. Mix 100C exhibited the highest strength, followed closely by mix I62-OA2, which showed only a 5.88% reduction—demonstrating a comparable performance. In the case of mix 80C20FA, which includes 20% FA replacement, a slight decrease in strength was noted. However, when FA content was increased to 40% in mix 60C40FA, a substantial strength reduction of 44.11% occurred. This suggests that excessive FA content negatively affects strength, likely due to slower formation of strength-contributing products, such as C-S-H gel, compared to pure cement hydration. For MK-based mixes, with 25% and 50% cement replacement in mixes 75C25MK and 50C50MK respectively, strength reductions of 20.5% and 49.21% were observed compared to the 100% cement mix. The lowest CS was recorded in the mix with 50% MK replacement. Excessive MK content may lead to binder matrix dilution, resulting in poor bonding and hydration processes, while increased porosity could further reduce

CS. High MK content may also increase porosity in the concrete matrix, introducing voids that weaken the internal structure.

The results indicate that the CS of the cube from mix I62-OA2 was comparable to that of the cube containing 100% cement. This similarity in strength can be related to the reaction of IO with CO_2, forming complex iron carbonates that contribute to the material's strength. These findings highlight the potential of ferrock as a sustainable alternative binder capable of partial cement replacement due to its resistance to compressive stress. Given its favorable mechanical performance and environmental advantages, Ferrock demonstrates promise as a viable component in green construction materials. Further investigations were undertaken to determine the optimal percentage of cement replacement with ferrock in concrete mixtures.

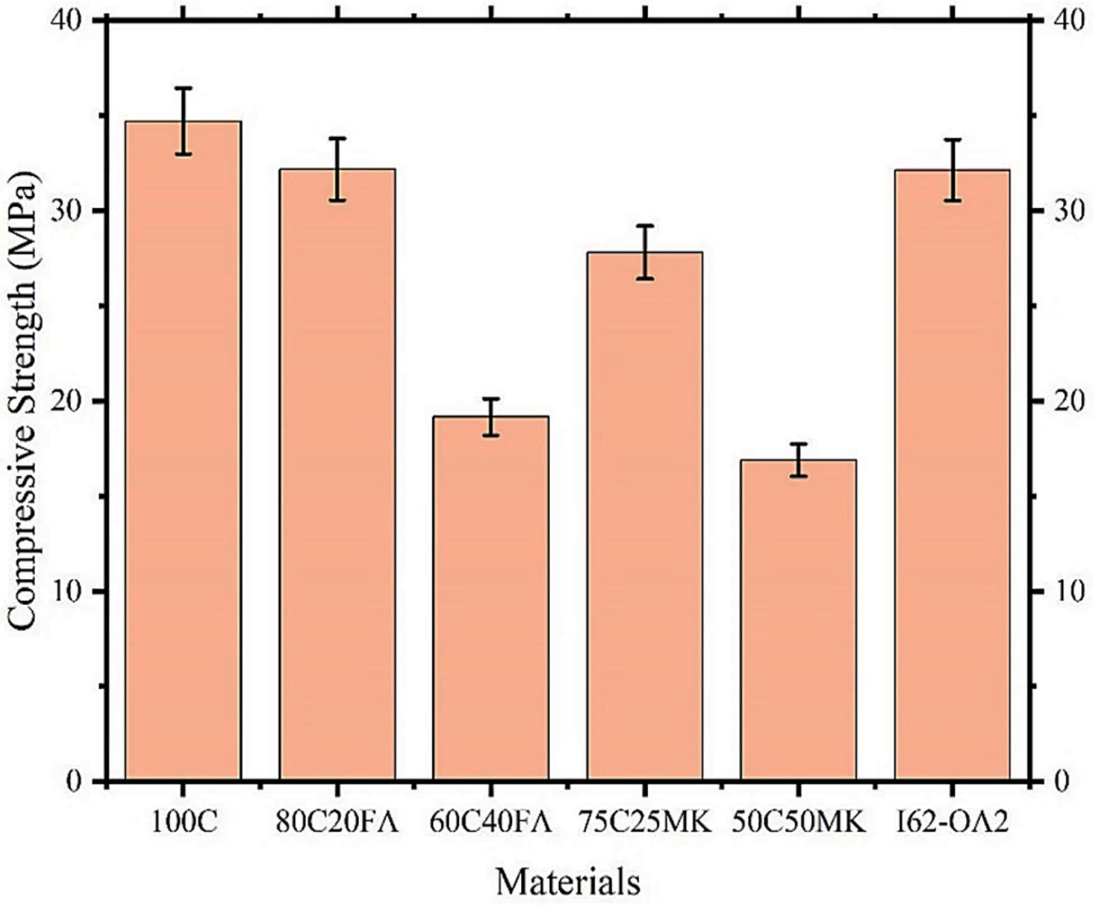

Figure 3.23 CS values of plain OPC and modified OPC mixtures for comparison

3.1.4.6 Microstructural analysis

3.1.4.6.1 SEM

The analysis was conducted to examine the microstructure of ferrock through high-magnification imaging. SEM was performed on the ferrock sample to investigate the pore structure of the iron carbonate binder, as it plays a critical role in influencing the material's mechanical properties. The analysis was performed using a SEM from JEOL, equipped with an Electron Detector for detailed mapping. For the SEM, the samples were crushed, and tiny bits of the core were adhered to the stub using epoxy resin. The SEM combines a semi-in-lens objective lens and an in-lens Schottky FEG to

provide ultrahigh resolution. The Gentle Beam mode improves resolution at low voltages, allowing observation of nonconductive samples. Mix I62-OA2 exhibited the highest CS, followed by mix I64-OA2, after 4 and 6 days of CO_2 curing, respectively. Based on these results, both mixes were selected for further microstructural analysis. Specifically, specimens labeled I62-OA2C2, I62-OA2C3, and I62-OA2C4, as detailed in table 3.7, correspond to CO_2 curing durations of 2, 3, and 4 days, respectively, with the 4-day curing period yielding the highest strength. SEM images, presented in figure 3.24, revealed that the microstructure was dense and well-compacted. The presence of rounded FA particles was also observed, indicating their role in the overall morphology. The formed products are iron oxalate carbonates complex which has less pores than control mix. The microstructure is heterogeneous, comprising angular iron particles, spherical FA particles, and porous reaction products. A thin film of reaction products is observed on the surfaces of the iron particles, indicating ongoing chemical interactions. Additionally, partial formation of reaction products is also noted on the surfaces of the FA particles.

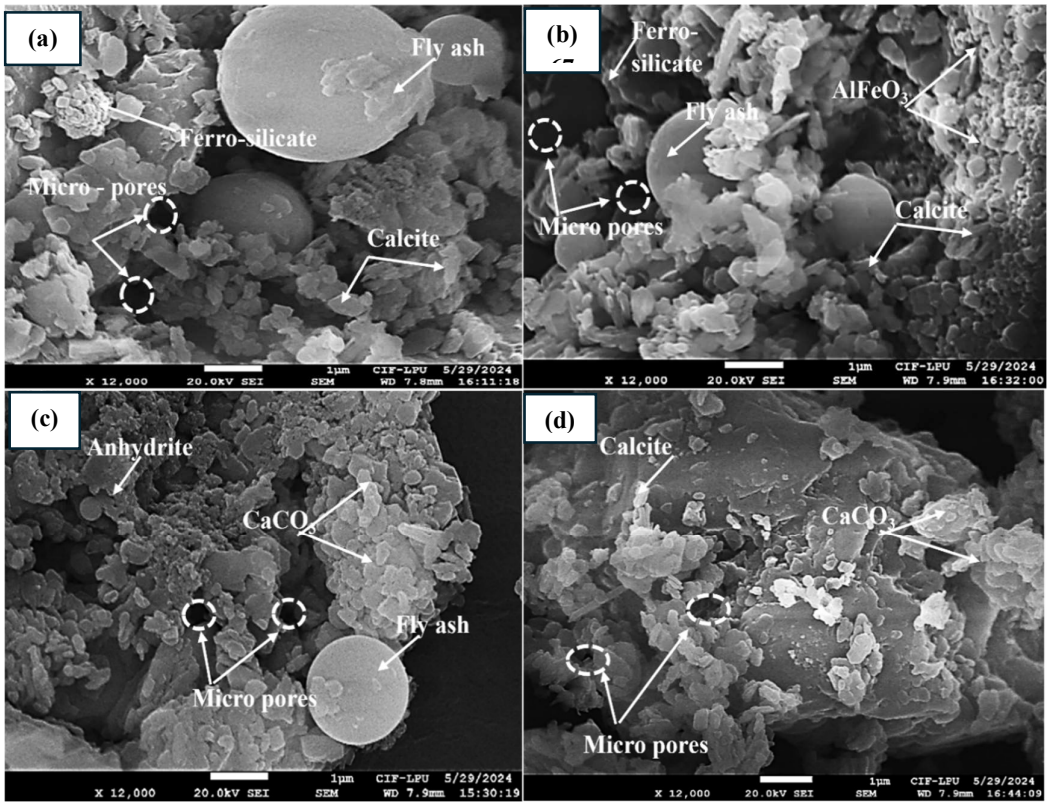

Figure 3.24 SEM images of mix (a) I62-OA2C2, (b) I62-OA2C3, (c) I62- OA2C4 and (d) I64-OA6

3.1.4.6.2 EDS

The analysis aimed to determine the elemental composition of mixes which showed the highest and second highest strength among all mixes. The specimens labeled I62-OA2C2, I62-OA2C3 and I62- OA2C4 corresponds to CO_2 curing durations of 2 days, 3 days and 4 days, respectively. The specimen labeled I64-OA2C6 achieved the second highest strength among the tested samples corresponds to a CO_2 curing duration of 6 days. The elemental composition of mixes as determined by EDS analysis are presented in table 3.9 below. This analysis suggests that the iron content in the I62-OA2 specimen is higher after 2 days of CO_2 curing compared to 3 and 4 days. This decrease in iron content with extended curing duration may be attributed to the progressive dissolution of IO, which facilitates carbonation and subsequent product formation. Also, only Fe, C and Si are present in EDS spectra confirms that no binding product formation occurs in the absence of dissolved CO_2. The microstructure exhibits

heterogeneity, consisting of angular iron particles, spherical FA particles, and porous reaction products. The product of reactions contains silica which enhances the concrete matrix and increases formation of product. The figure 3.25 showed results of EDS analysis in the form of peaks of elements present in composites. Although Al and Si are the dominant elements across all specimens, the Al/Si ratio varies among them. Specimens I62-OA2C2, I62-OA2C3, and I62-OA2C4 exhibit relatively similar Al and Si peak intensities, indicating a consistent Al/Si ratio. In contrast, specimen I64-OA2C6 shows a markedly stronger Al peak relative to Si, suggesting a higher aluminum content in this region. This variation in the Al/Si ratio may have implications for the material's properties, particularly its mechanical strength.

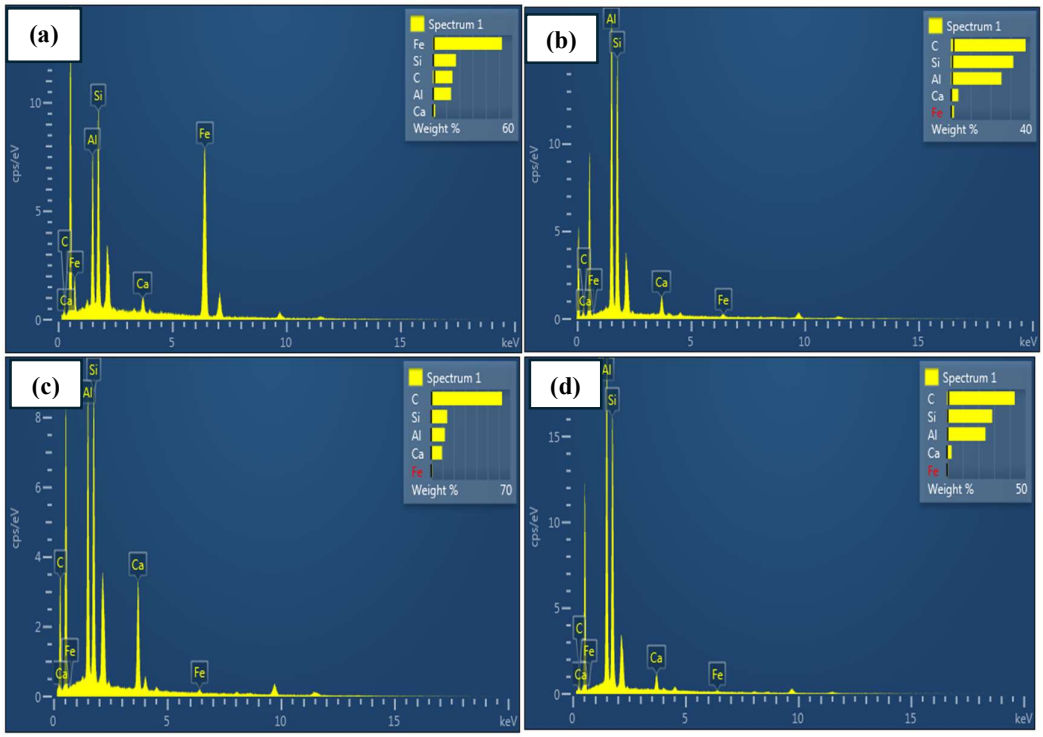

Figure 3.25 EDS peaks of mix (a) I62-OA2C2, (b) I62-OA2C3, (c) I62- OA2C4 and (d) I64-OA6

Table 3.9 Elemental composition of mix (a) I62-OA2C2, (b) I62-OA2C3, (c) I62-OA2C4 and (d) I64-OA6

Mix	C	Al	Si	Ca	Fe
I62-OA2C2	14.81	13.76	17.46	1.77	52.21
I62-OA2C3	37.73	25.54	31.48	3.74	1.5
I62- OA2C4	62.83	12.24	14.27	9.67	0.99
I64-OA2C6	43.13	24.51	28.8	2.92	0.63

Elemental mapping

Analysis provides visual representation of elemental distribution in samples and results are illustrated in figure 3.26. The specimens labeled I62-OA2C2, I62-OA2C3 and I62- OA2C4 represent CO_2 curing durations of 2 days, 3 days and 4 days, respectively. Distribution maps were acquired of iron, silicon, aluminum, Ca, and carbon. The brighter the color, the higher the concentration of the element shown for each map. Iron is observed at locations away from the particles also, aided by the organic dissolution agent. The distribution of carbon is uniform, except in regions occupied by the unreacted iron particles and the FA particles where it shows a higher concentration. It indicates that the reaction products which are formed away from the iron particles are also complex iron carbonates, although the stoichiometry could be locally different, this is not discounting the presence of carbon from the Ca. The specimen labeled I64-OA2C6 showed second highest strength with a CO_2 curing duration of 6 days. Sample I62-OA2C2 shows uneven distribution of IO because at 2 days of CO_2 curing few elements of IO already react and formed product. The two-day CO_2 curing period was insufficient for the completion of all reactions. However, after four days of curing, only a minimal presence of IO elements was observed, indicating that the reactions had largely concluded, ultimately contributing to strength development. The results indicate that as the number of curing days increases, IO continues to form products until all reactions are complete. Additionally, the

distribution of Ca is predominantly uniform, likely due to the small particle size (0.7 μm) of the calcium carbonate (LS) used in the matrix.

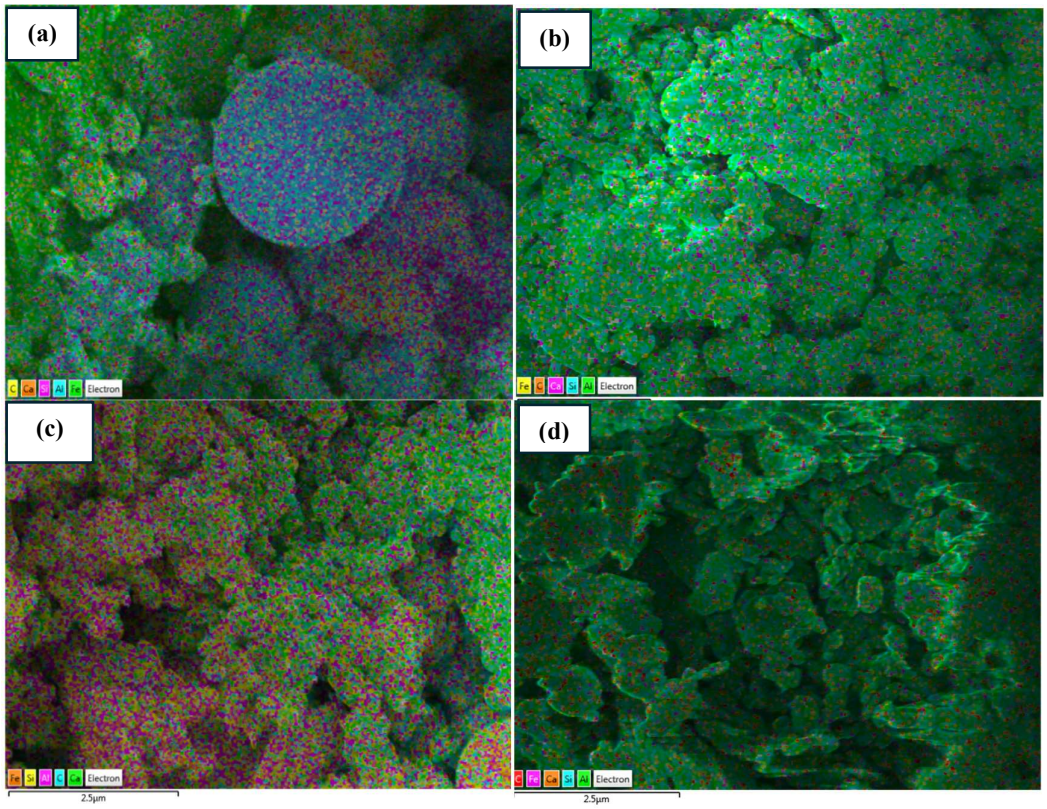

Figure 3.26 Elemental mapping of mix (a) I62-OA2C2, (b) I62-OA2C3, (c) I62-OA2C4 and (d) I64-OA6

3.1.4.6.3 XRD

XRD is a flexible analytical technique used to examine mineralogical attributes such as phase identification, crystal structure, and orientation samples. The LYNXEYE XE-T detector is equipped with a Motorized Anti-Scatter Screen and a Variable Active Detector Window. These features enable rapid data acquisition and effective filtering, ensuring precise low-angle measurements with minimal background interference. XRD analysis was conducted using Profex software to identify peaks and phases. The resulting data were then plotted using Origin Pro 2024 for graphical representation and reported in figure 3.27. The analysis revealed distinct mineralogical peaks in specimens I62-OA2C2, I62-OA2C3, I62-OA2C4, and I64-OA2C6, corresponding to 2, 3, and 4

days of CO_2 curing for mix I62-OA2, and 6 days of CO_2 curing for mix I64-OA2, respectively. The formation of hydrated and carbonated by-products with their peak composition are analyzed and compared. Since materials are composed of microscopic crystallites the effectiveness of the curing hours may influence the conversion of these metastable byproducts to a stable calcite form. Quartz was observed commonly in all specimens as major peaks. For the I62-OA2C2 sample, the XRD patterns revealed predominant peaks associated with Quartz, Kaolinite, Calcium Sulfate Anhydrate, Anhydrite, Manganosite, Dolomite, $Fe_3Si_2O_5(OH)_4$, Ferrihydrite, and various forms of Al_2O_3. These findings indicate a complex mixture of silicates, sulfates, and oxides, which are critical in understanding the sample's material properties. In the I62-OA2C3 sample, the analysis identified significant peaks corresponding to Metathenardite, AlF_3, Biotite, Beta-$MgSO_4$, Anhydrite, Illite, Calcium Sulfate Anhydrate, $AlFeO_3$, Epsomite, Ganophyllite, Albite, and Ferrihydrite. The variety of phases detected points to a rich mineralogical composition, which may contribute to the unique properties observed in this sample. The mineralogical phases of iron were found dominant under all reactions because of the inert nature of other materials (FA, MK and LS) in the mix. Further, C-S-H and C-A-S-H phases were abundant in all the samples due to the excess silicates and aluminates, which impart additional strength to the samples.

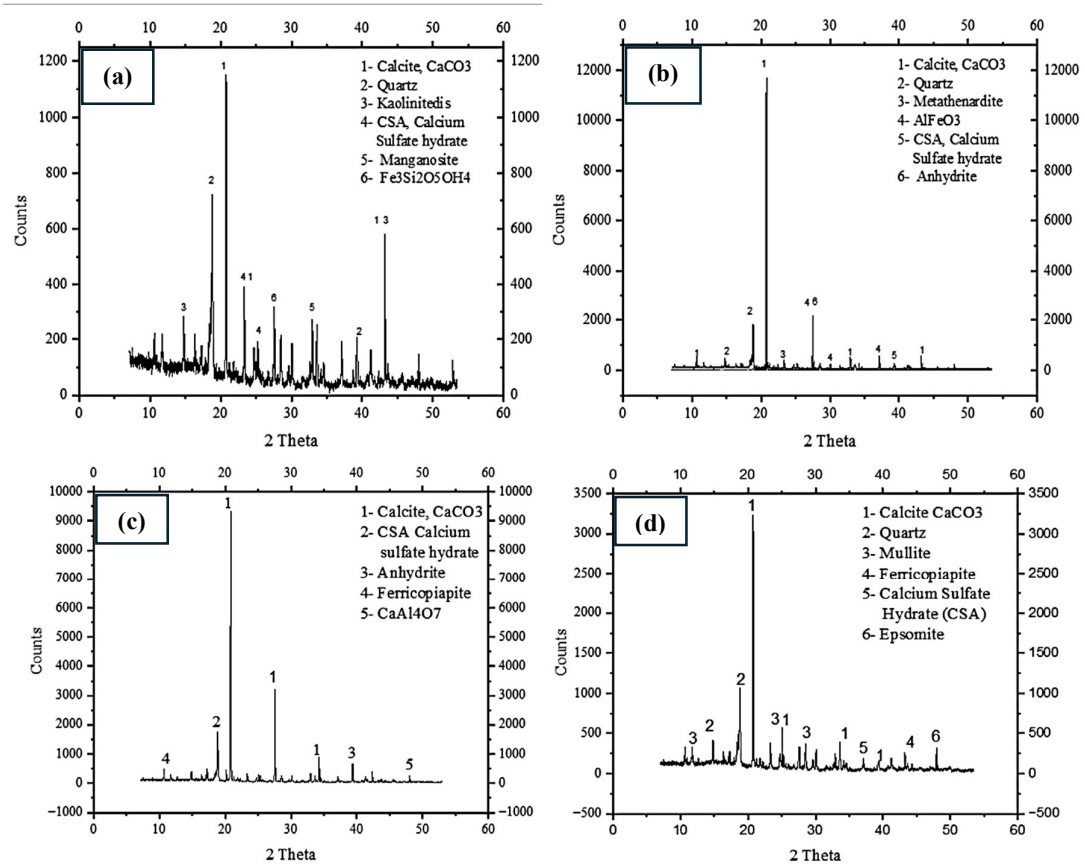

Figure 3.27 XRD peaks of mix (a) I62-OA2C2, (b) I62-OA2C3, (c) I62- OA2C4 and (d) I64-OA6

3.1.4.7 Carbonation Test

The carbonation test performed to get visual representation of carbonated and non-carbonated parts of concrete by using phenolphthalein as an indicator. A total of three types of specimens were cast: a cylindrical sample from UCS test, cube of size 50 mm with 100% ferrock and other cubes of size 50 mm with ferrock as a partial replacement of cement bwoc in ratio of 5%, 10%, 15% and 20%. Samples were kept in an airtight poly bag filled with a maximum CO_2, refilled after required time to maintain concentration. After cleaning the surface, phenolphthalein was sprayed over the recently split surface. A pink tint was obtained in the noncarbonated part of the sample, where the alkalinity of concrete was high. There was no coloring in the carbonated portion of the specimen, where

the alkalinity of concrete was lower. Calcite is created when Ca from $Ca(OH)_2$ and CSH combines with carbonation, which is caused by the dissolving of CO_2 in the concrete pore fluid. Further, the extent of carbonation was accessed visually, highlighting the vital role of CO_2 absorption during the carbonation process of hardened cement paste samples. This phenomenon occurs as CO_2 interacts with $Ca(OH)_2$, forming $CaCO_3$ in the presence of water. CO_2 infiltration initiates carbonation, lowering the alkalinity, and the pore water pH drops from 13.5 to about 9.0. After the complete carbonation of $Ca(OH)_2$, the pH drops further to around 8.0, showing a fading pink or no color.

In the case of the 100% ferrock specimens like cylinder and cubes, no pink coloration was observed on any of the samples. This indicates that carbonation had occurred throughout the entirety of the ferrock specimens, resulting in significant reduction in alkalinity. The complete absence of pink coloration suggests that the pH of the ferrock specimens dropped below the threshold (around pH 8.3) at which phenolphthalein changes color, confirming the full carbonation of the material.

The specimens of ferrock were cast 100% ferrock cubes of size 50mm in figure 3.28 (b), and cubes of different ferrock ratios as replacement of cement in figure 3.28 (c). Test showed that CO_2 was captured as there was no pink color found on specimens. Results showed that there is pink color partially on the surface of cube as there were some ratios of ferrock in concrete.

The results from the carbonation testing of the ferrock and concrete specimens provide clear insights into the carbonation process and the material's behavior under CO_2 exposure. After exposure to 100% CO_2, the freshly split surfaces of the specimens were treated with phenolphthalein pH indicator to assess the extent of carbonation.

In contrast, the concrete specimens exhibited partial pink coloration upon testing. The presence of pink color in some areas indicates that these parts of the concrete remained uncarbonated, retaining their high alkalinity. The areas without pink coloration reflect zones where carbonation had occurred, reducing the pH

and thus preventing the phenolphthalein from turning pink. This partial carbonation suggests that while the concrete's surface was affected by CO_2 exposure, the carbonation process had not fully penetrated through the material. Previous studies also used phenolphthalein for visualizing carbonated and non-carbonated parts of concrete [168] [169] [170].

These observations highlight the difference in carbonation resistance between ferrock and conventional concrete. The complete carbonation of ferrock suggests that it has a higher reactivity with CO_2 compared to traditional concrete, which exhibited only partial carbonation. This result is consistent with the chemical composition and behavior of ferrock, which, due to its different binder chemistry, may offer unique advantages or limitations in environments with high CO_2 exposure.

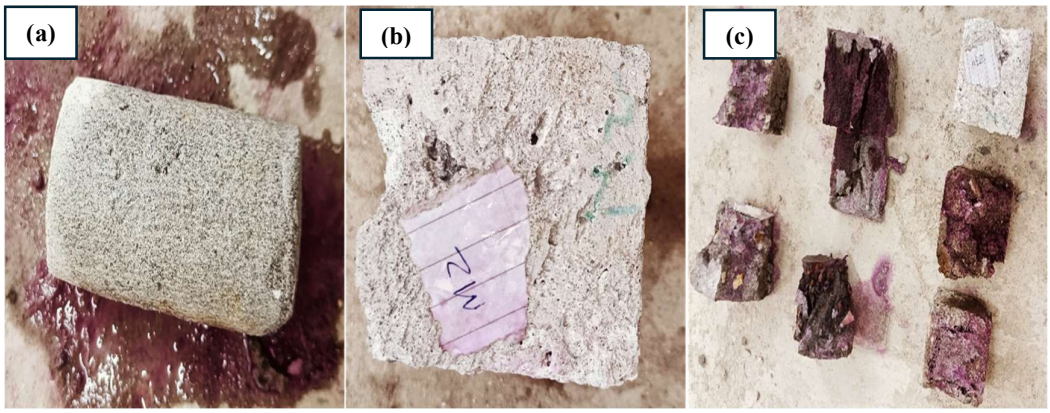

Figure 3.28 Carbonation test results of (a) Ferrock UCS sample, (b) Ferrock cube sample and (c) cubes with different ratios of ferrock

3.1.5 rGO

The rGO used in present study with an average particle size of 40 – 45 μm, density of 1.9 g/cm^3 and mean molecular weight of 12.01g/mol as depicted in figure 3.29 below. The rGO was purchased from the Sood Chemicals, Kurukshetra Haryana, India, is used solely for research purposes only. Microstructural analysis was performed at 28 days of curing using a resolution of 1 μm to visual representation of microstructure of rGO.

Figure 3.29 rGO used in study

Results of SEM, XRD, EDS peaks and elemental mapping are reported in the figure 3.30 (a), (b), (c) and (d) respectively. The SEM image revealed a wrinkled, irregular, plate-like structure of rGO, which contributed to enhanced binding within the concrete matrix. The surface appeared rough due to defects generated during the reduction of GO and the presence of residual functional groups. Densified hydrated cements with low density C–S–H in association with C–H is visible. Table 3.10 presents the elemental composition of rGO. The analysis confirmed that carbon is the predominant element, with a minor presence of oxygen, which aligns with its classification as a carbon-based nanomaterial. XRD analysis further revealed a prominent peak corresponding to carbon, indicating its dominance among the mineral phases present in rGO. The overall analysis suggests that rGO consists of ultra-fine particles with a large surface area, which enhances its ability to absorb water molecules.

Additionally, the material exhibits a bulky lateral size and a high-water retention capacity due to the formation of rGO clusters. Microstructural analysis provided insights into the surface morphology, elemental composition, and mineral phases, offering a comprehensive understanding of rGO at the microscopic level.

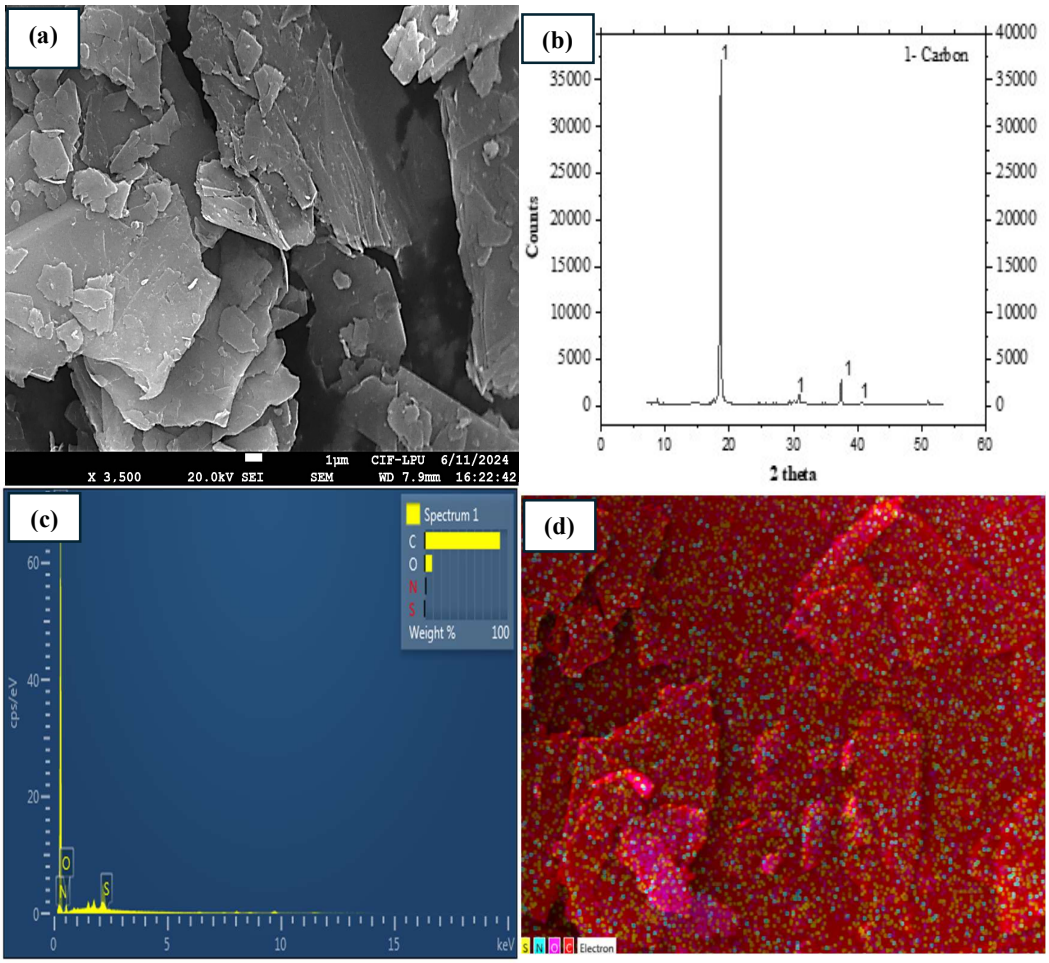

Figure 3.30 Microstructural analysis of rGO by (a) SEM, (b) XRD, (c) EDS peaks and (d) elemental mapping

Table 3.10 Elemental composition of rGO

Elements (wt%)	C	N	O	S	H
rGO	90.87	0	9.13	0	0

3.2 Mix Proportions

To investigate the effects of rGO and ferrock on concrete performance, a total of 14 different mix designs were prepared, incorporating varying proportions of rGO and ferrock both individually and in combination. Control samples without replacement of cement were prepared to test and compare the results of experiments. The experimental program included tests to assess fresh properties, hardened properties, durability, and microstructural characteristics using SEM, EDS, and XRD analyses. The control mix exhibited a slump value of 92 mm and a compacting factor of 0.91. A constant water-to-binder ratio of 0.5 was maintained throughout the study, with no additional plasticizer used, which may influence the strength characteristics of the mixes. The study focuses on investigating concrete mixes with the replacement of cement so that the amount of sand and coarse aggregate was consistently same as 707.6 kg and 1066.75 kg respectively. Table 3.11 contains the details of the quantities of OPC, rGO and ferrock used in each mix along with corresponding mix notations and replacement ratios of materials.

Table 3.11 Mix proportions of concrete

Mix Notations	**Description**	**Cement (kg)**	**rGO (kg)**	**Ferrock (kg)**
CSF0G0	OPC + Sand + Coarse aggregates	383.2	0	0
GC0.1	99.9% OPC + 0.1% rGO + Sand + Coarse aggregates	382.82	0.3831	0

GC0.2	99.8% OPC + 0.2% rGO + Sand+ Coarse aggregates	382.43	0.7664	0
GC0.4	99.6% OPC + 0.4% rGO + Sand+ Coarse aggregates	381.67	1.5324	0
GC0.6	99.4% OPC + 0.6% rGO + Sand + Coarse aggregates	380.90	2.2986	0
GC0.8	99.2% OPC + 0.8% rGO + Sand + Coarse aggregates	380.13	3.0648	0
FC5	95% OPC + 5% Ferrock+ Sand + Coarse aggregates	364.04	0	19.16
FC10	90% OPC + 10% Ferrock+ Sand + Coarse aggregates	344.88	0	38.32
FC15	85% OPC + 15% Ferrock+ Sand + Coarse aggregates	325.72	0	57.48
FC20	80% OPC + 20% Ferrock + Sand + Coarse aggregates	306.56	0	76.64
G0.2FC5	94.8% OPC + 0.2% rGO + 5% Ferrock + Sand + Coarse aggregates	363.28	0.7664	19.16
G0.2FC10	89.8% OPC + 0.2% rGO + 10% Ferrock + Sand + Coarse aggregates	343.73	0.7664	38.32
G0.2FC15	84.8% OPC + 0.2% rGO + 15% Ferrock + Sand + Coarse aggregates	324.95	0.7664	57.48

G0.2FC20	79.8% OPC + 0.2% rGO + 20% Ferrock + Sand + Coarse aggregates	305.79	0.7664	76.64

3.3 Methodology

The present study follows a systematic approach to investigate the properties of concrete with and without the partial replacement of cement by rGO and ferrock. The methodology illustrated in figure 3.31 through a flowchart encompasses the characterization of raw materials used, mix design, fresh and hardened properties, durability testing and microstructural analysis. Initially, the study involves the characterization of OPC, fine aggregates, coarse aggregates, and ferrock, including its raw materials. The concrete mixes were designed for partial replacement of cement using rGO, ferrock, and a combination of both materials. A control mix was prepared without any replacement of cement to compare results. Fresh properties of concrete mixes assessed by slump cone and compaction factor test. After curing the hardened mechanical properties were tested by CS, TS and FS at 3, 7, 28, 56 and 90 curing days. Further durability of concrete samples tested by total absorption, water penetration, initial surface absorption, RCPT and results were compared with control sample. Microstructural analysis of concrete analyzed the influence of rGO and ferrock in concrete mix by SEM analysis to study surface morphology and texture, EDS analysis to determine elemental composition and XRD to analyze mineralogical phases. All findings were systematically analyzed and compared with control mix and reported. In conclusion, the optimum replacement ratio was determined to achieve maximum strength and improved durability.

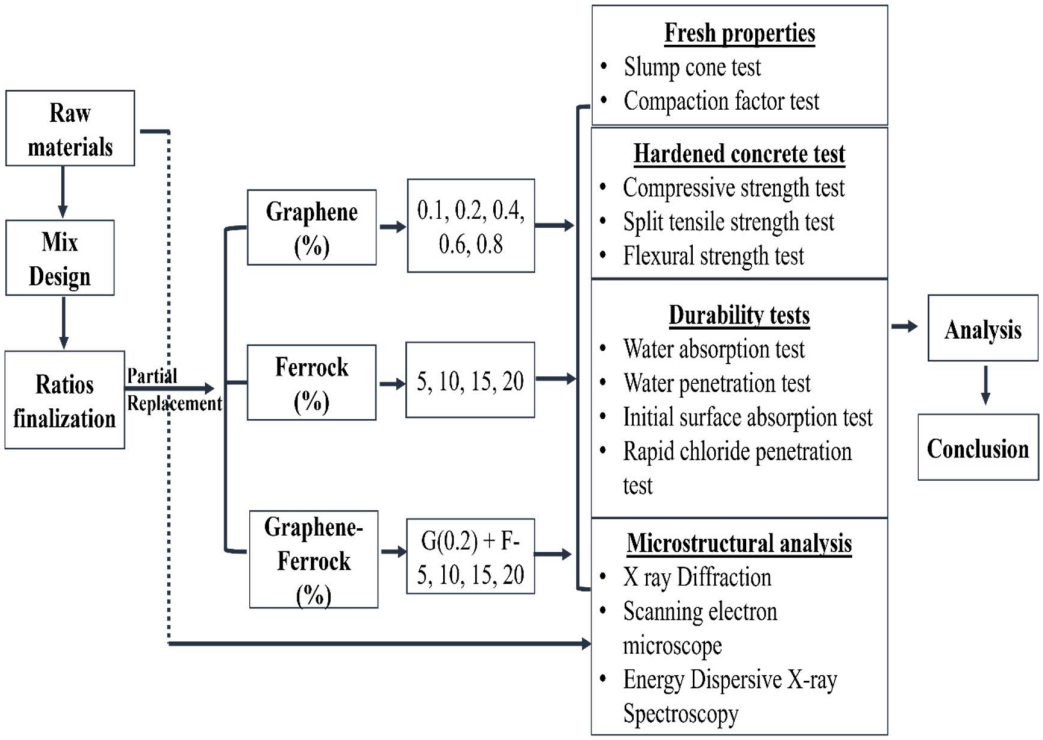

Figure 3.31 Methodology followed in study

The research methodology employed to accomplish the objectives of the present research work is explained in table 3.12 below. The analysis performed with apparatus used listed to study the properties of concrete.

Table 3.12 Research Methodology

Objective	Analysis to be done	Apparatus/ Software to be used
To test the physical and chemical properties of graphene and ferrock to study their feasibility as an additive to cement concrete to improve its compressive strength.	Sieve Analysis Hydrograph analysis XRD of raw materials SEM of raw materials EDS of raw materials	Sieve Hydrograph XRD SEM EDS

To study the pore structure of concrete composite for mixing efficiency, compaction degree and strength development	XRD of concrete mixes SEM of concrete mixes EDS of concrete mixes Slump test Compaction factor test	XRD SEM EDS Slump cone apparatus Compaction factor apparatus
To prepare concrete having different proportions of graphene and ferrock as replacement of cement and testing the hardened composites samples for pore structure, tensile and CS, and durability.	CS test TS test FS test Total absorption test Water penetration test Initial surface absorption test Rapid chloride penetration test	Compression Testing Machine (CTM) Absorption apparatus Water penetration apparatus Surface absorption apparatus Chloride penetration apparatus
To carry out cost analysis of graphene- ferrock concrete developed	Cost analysis of 1 Kg of ferrock Cost analysis for $1m^3$ of all concrete mixes	Cost compared as per purchased rate. The Economic Index used to compare mixes as cost and strength achieved.

3.3.1 General

The experimental test procedure includes tests for fresh properties, hardened properties and durability of concrete. Further microstructural analysis has been carried out to analyze the change in concrete microstructure due to rGO and ferrock.

3.3.2 Fresh Properties of concrete

3.3.2.1 Slump Test

The slump test is used to assess workability, which is defined as the ability to be mixed, transported, and placed with minimal loss of homogeneity according to IS: 1199- (2018) [171]. The slump value was measured using the slump cone test after filling the cone of dimension 200 mm, 100mm and 300mm in height in accordance with IS 7320: 1974 [172]. The cone filled with fresh concrete mix in four layers, each tamped 25 times, followed by lifting, and the height of the coned concrete was recorded. Findings for various mixtures were recorded, reported, and analyzed.

3.3.2.2 Compaction Factor Test

The compaction factor test used to assess the workability of concrete by determining the amount of compaction achievable under its own weight. The apparatus for testing has two conical hoppers positioned one above the other, with a cylindrical mold located underneath them. Freshly mixed concrete is dropped into the top hopper, let to descend into the lower hopper, and ultimately into the cylindrical mold in accordance with IS: 5515 (2004) [173]. The volume of concrete filling the mold was measured, and the weight of the partly compacted concrete was recorded. The same concrete is then compressed precisely and weighed again. The compaction factor is calculated as the weight of partly compacted concrete divided by the weight of completely compacted concrete.

3.3.3 Hardened properties of concrete

3.3.3.1 Compressive strength

Concrete cubes of size 150 mm evaluated for CS mentioned in IS: 10086 – 2021 [174] using a Compression Testing Machine (CTM). Fresh concrete was prepared according to the mix proportions mentioned in table 3.11 and poured into well-greased

cubical molds. Following a 24-hour curing period, the cubes were unmolded and placed in a tank for water curing. The figure 3.32 presents the setup and prepared samples for testing. The water temperature was maintained at 26° C ± 2 during curing. The CS was evaluated at 3, 7, 28, 56 and 90 days of curing as per IS: 516 – 2021 [175]. The concrete cubes containing ferrock were initially cured in a CO_2 atmosphere for four days in airtight container, since preliminary study on ferrock preparation on curing days and results of UCS testing found 4 days CO_2 as optimum. After that, the samples were transferred to a water tank for curing. The strength data were documented, analyzed, and presented.

Figure 3.32 (a) CS test setup and (b) Cubes of 150 mm for testing

3.3.3.2 Split tensile strength

TS tests conducted on cylindrical concrete specimens with a diameter of 150 mm and a height of 300 mm, as specified in IS: 10086 – 2021 [174]. Fresh concrete mix was prepared according to the mix proportions mentioned in table 3.11 and poured into well-oiled cylindrical molds. After 24 hours, the specimens were unmolded and then kept in a tank for water curing. The figure 3.33 presented the setup of samples. The concrete specimens containing ferrock underwent CO_2 curing for the first four days,

since preliminary research on ferrock preparation and results of UCS testing found 4 days as optimum days. After the CO_2 curing step, the samples were immersed in a water tank for further curing at temperature of 26° C ± 2. The strength of the specimens was evaluated at 3, 7, 28, 56 and 90 days by applying a diametral compressive load until failure as mentioned in IS 5816 – 1999 [176]. The findings were systematically recorded, analyzed, and presented.

Figure 3.33 TS test setup with samples

3.3.3.3 Flexural strength

Concrete beam specimens of size 100 mm × 100 mm × 500 mm were tested for FS using IS – 10086 – 2021 [174]. Fresh concrete was prepared as per proportions mentioned in table 3.11 and poured into thoroughly greased beam molds. After 24 hours, the specimens were carefully unmolded and placed in a tank filled with water maintaining temperature of 26° C ± 2. The figure 3.34 illustrates the test setup and specimens after testing. The concrete samples incorporating ferrock were initially cured in a CO_2 environment for four days, as this duration was determined to be optimal based on prior investigations into ferrock preparation and UCS testing results. Subsequently, the samples were transferred to a water tank for continued curing. The FS of specimens

was tested at intervals of 3 days, 7 days, 28 days, 56 days and 90 days using a three-point load system until failure occurred in accordance with ASTM C78/C78M-2016 [177]. The resulting data was processed, compared and reported.

Figure 3.34 (a) FS test setup and (b) tested beam samples

3.3.4 Durability

3.3.4.1 Total absorption

The total absorption test performed according to ASTM-C642-13 [178] as setup presented in figure 3.35. Cubes of dimension 150 mm were cast and kept for CO_2 curing for 4 days and then kept for water curing in the tank for 28 days, 56 days and 90 days. The samples containing ferrock were initially cured in a CO_2 environment for four days before being transferred to a water tank for further curing. To determine absorption % in concrete specimens, by measuring the increase in the mass of specimens were oven dried for 24 hours at 100 to 110 C, designate this value as A. Dry weight was noted after removal from the oven. After drying kept in water for 48 hours and noted weight of cubes, designate this value as B. Specimens were kept in boiling water for 5 hours in tank with adjustable curing temperature and leave for cooling by natural loss of heat for

not less than 14 hours and weight was noted, designate this value as C. Each time before taking weight remove excess water using cloth. By using eq (1) and eq (2) total absorption was calculated.

Total absorption after immersion, (%) = [(B - A)/A]*100 (1)

Total absorption after immersion and boiling, (%) = [(C - A)/A]*100 (2)

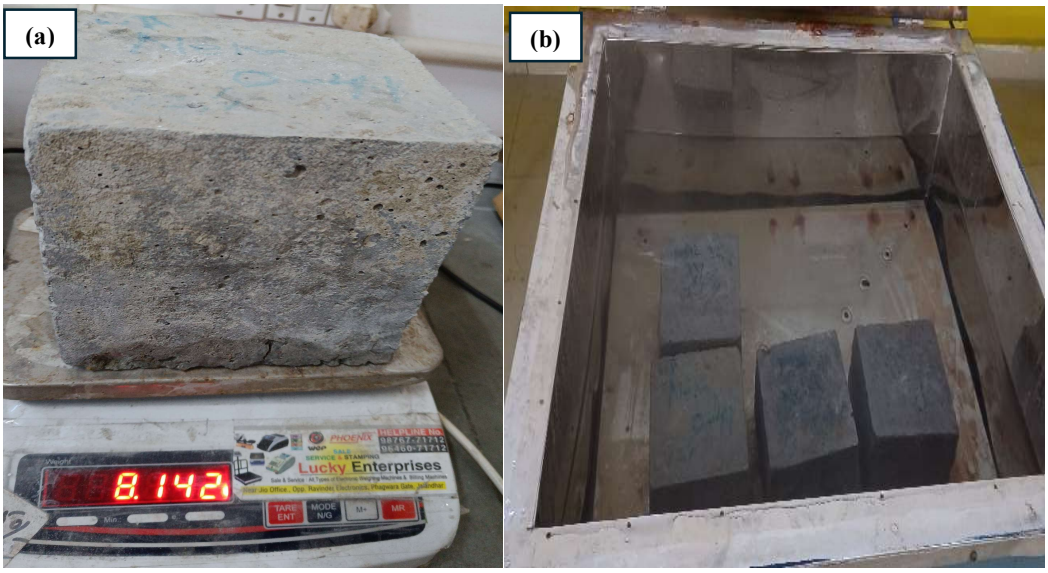

Figure 3.35 Total absorption test (a) sample and (b) test setup

3.3.4.2 Water Permeability

The water permeability test was performed as per BS EN 12390-8:2000 [179], using concrete cubes of 150 mm on each side as apparatus presented in the figure 3.36. These cubes were cast and tested after curing days of 28, 56 and 90 days. The ferrock-containing samples were first subjected to CO_2 curing for four days, after which they were placed in a water tank for continued curing at maintained temperature of 26° C ± 2. Cubes were subjected to a water pressure of 500 ± 50 kPa for a duration of 72 ± 2 hours to penetrate water. At the end of this period, the cubes were removed from the apparatus and split in half by using rod on top of cube and applying load perpendicular to the face on which the water pressure was applied by CTM. Excess water was wiped

so that penetration of water was clearly seen. The maximum penetration depth within the test area was measured and recorded to the nearest mm.

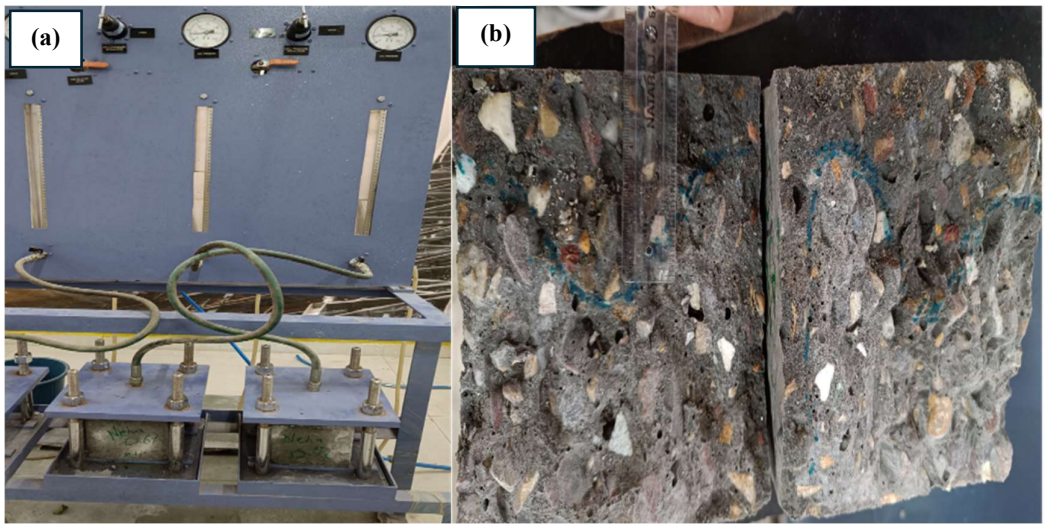

Figure 3.36 Water penetration test setup and measured depth

3.3.4.3 Initial Surface Absorption

ISAT gives the rate of flow of water into concrete per unit area at constant applied load. Estimation of the volume flow was obtained by measurement of the length of flow along a capillary of known dimension. Cubes of 150 mm side each were casted and tested at the curing age of 28 days, 56 days and 90 days according to BS 1881 – 208 [180] as illustrates in figure 3.37. The samples incorporating ferrock were initially cured in a CO_2 environment for four days before being moved to a water tank for further curing. The cubes were oven dried till the constant weight (difference was not more than 0.1%) was reached and allowed cubes to cool till room temperature. A plastic seal was used to prevent leakage. Water was introduced into the cell through inlet and outlet points with constant head of 200 mm by a funnel of diameter 78 mm. Water was introduced into the cell via a connecting point and maintained at a head of 180 mm to 200 mm using a filter funnel. A second connection point to the cap leads to a horizontal capillary tube. The connection to the reservoir was closed and the absorption was

measured by observing the movement of the end of the water line in the capillary tube with an affixed scale at 10 min. The rate of flow of water was noted in ml/m^2s.

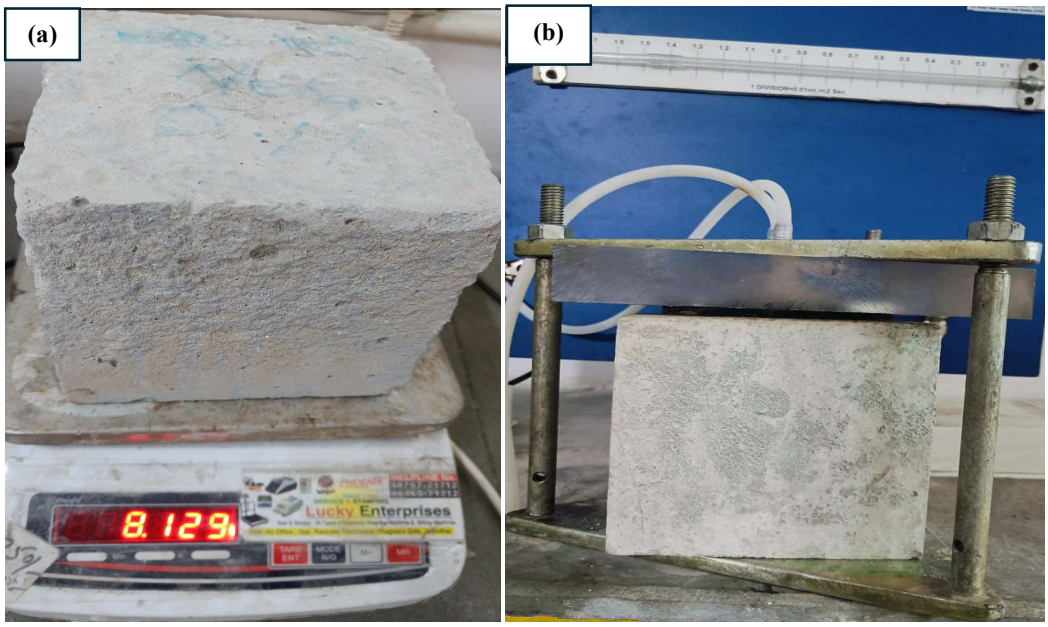

Figure 3.37 ISAT (a) sample and (b) test setup

3.3.4.4 Rapid Chloride Penetration

The RCPT determines penetration of chloride ion in concrete by electrical conductivity as described in ASTM-C1202 [181]. Cylindrical specimens with dimensions of 150 mm in length and 100 mm in diameter were cast to evaluate the effects of curing at 28, 56, and 90 days. The samples containing ferrock were first subjected to CO_2 curing for a duration of four days, after which they were transferred to a water tank for subsequent curing. After curing, each cylinder was cut into disc slices with a thickness of 50 mm and a diameter of 100 mm for further testing. These discs were then placed into RCPT molds with one side exposed to Sodium Chloride (NaCl) solution, the other in a Sodium Hydroxide (NaOH) solution , sides were sealed with epoxy compound to prevent leakage of chemicals. The NaCl solution was prepared by dissolving 3% (w/v) of distilled water and NaOH solution was prepared by dissolving 0.3N (normality) in distilled water. The NaOH side of mold was connected to positive terminal of power supply and NaCl side should connect negative terminal of power

supply A potential difference of 60 V was maintained across the specimen, the total amount of charge passed measured in coulombs, was used to determine the resistance of the specimen to chloride ion penetration. Figure 3.38 showed used apparatus and specimens in form of disc and disc after test showed brown coating due to chemical used. The test was conducted over a period of six hours, with readings recorded every 30 minutes.

Figure 3.38 RCPT test setup (a) vacuum, (b) disc preparation, (c) apparatus and (d) after chemical penetration

3.3.5 Microstructural Analysis

3.3.5.1 SEM

The SEM analysis of concrete samples provided valuable insights into the microstructure properties of materials by providing zoomed images of microstructure. Analysis studied the morphology, surface texture of the samples and the distribution of pores, cracks, and voids within the concrete matrix. The morphology of concrete samples is studied using JEOL field emission scanning electron microscopes. The samples were finely ground and examined under microscope to show the surface texture, roundness, and smoothness of the respective particles. A few nanometers thick Gold-coating was done on samples to get high resolution images. Secondary Electron, Back Scattered Electron were used as detectors. The sample of all mixes at 28 days of curing were analyzed, compared and reported.

3.3.5.2 EDS

Analysis helps in understand the change in elemental composition of concrete mixes with rGO and ferrock incorporation in concrete as compared to control sample. JEOL Field Emission electron microscopes have high power optics which produce fine electron probe used during analysis. The aperture angle control lens maintains a small probe diameter even at a larger probe current. Using these techniques elemental composition be detected by presence of elements down to boron through EDS by electron Back Scattered Detection attached with microscope. EDS analysis provided elemental composition (%) with distribution in the form of mapping of elements. The analysis was done at 28 days of curing for samples of all mixes.

3.3.5.3 XRD

The properties of concrete composites are directly affected by crystalline size, texture and mineralogical composition. The samples were finely grounded and analyzed using XRD. Data was processed by Profex (version 5.4.1) software for phase identification. The high-speed energy-dispersive LYNXEYE XE-T detector uniquely combines fast data collection with unprecedented filtering of fluorescence and Kβ radiation. Its proprietary variable active detector window and the Motorized Anti-Scatter Screen enable data collection from lowest 2θ angles without parasitic low-angle

background scattering, in particular air scattering. The identification of the phases formed during the curing process is pivotal in assessing and optimizing the performance of concrete mixes.

3.3.6 Carbonation test

The carbonation test on concrete was conducted to distinguish between carbonated and non-carbonated regions. Phenolphthalein was employed as a pH indicator to detect carbonation, consistent with methodologies reported in previous studies [168] [169] [182] [183]. After casting 100 mm concrete cubes kept them in CO_2 environment for 4 days and then 28 days of water curing for all mixes, the surface was broken to expose a fresh cross-section and sprayed with 0.1% phenolphthalein solution. Phenolphthalein turns pink in non-carbonated areas with a pH greater than 9, but it remains colorless in carbonated areas with a pH less than 9. This test provides a clear visual indication of the carbonated part in the concrete.

Chapter 4 Results and Discussion

4.1 Fresh Properties of concrete

4.1.1 Slump Test

4.1.1.1 Slump test for concrete with rGO

The Slump cone test was conducted on fresh concrete mixes containing rGO to determine their workability. The results for slump cone test for all mixes are presented in the figure 4.1 below along with their mix notations. The slump value for the control sample was measured 92 mm. The results indicated that as the ratio of rGO increased to 0.8%, the slump value decreased to 80 mm, representing the lowest value among all the mixes. This corresponds to a reduction of 13.04% compared to the control sample. The workability decreases with an increasing ratio of rGO due to the formation of agglomerations when rGO is present in excessive quantities. The reduction in slump value indicates a decrease in fluidity and viscosity; however, it remains within the practical application limits. Findings be concluded that mixes with higher rGO have lower concrete workability. Previous studies found that excessive quantity of rGO causes agglomeration and flocculation between cement particles and rGO [139] [184]. Due to the high surface area and strong van der waals force of rGO the water requirement is higher in mix the reason for decreasing slump values. As rGO acts as a filler in concrete mix which tends to bind water molecules reduce the available free water for flowability [124]. As denser mix has higher viscosity makes the concrete stiffer. The study revealed a 20% reduction in workability with the incorporation of GO into concrete [185]. GO caused the acceleration in hydration of Portland cement due to its plating profile [186]. Shang et al. studied the influence of GO on the cement mortar properties such as workability, segregation and bleeding and concluded that GO resulted in the betterment of properties [187].

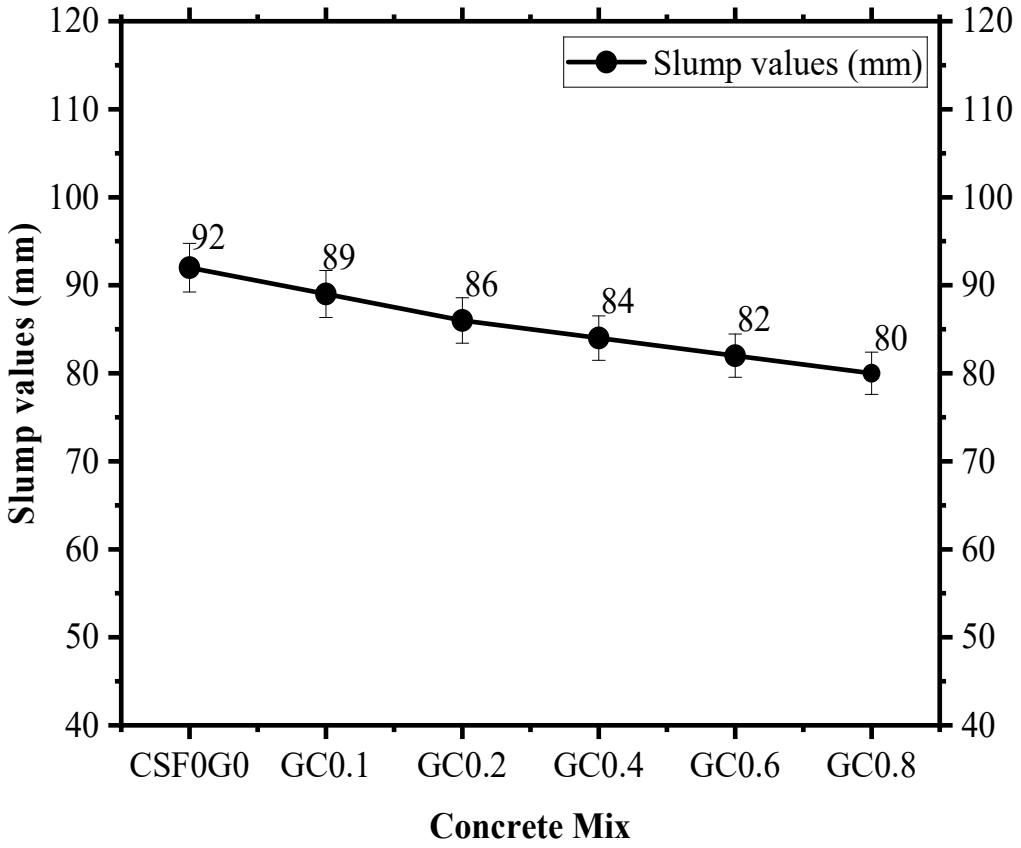

Figure 4.1 Results of slump test of concrete mix with rGO

4.1.1.2 Slump test for concrete with ferrock

Slump cone test conducted on fresh mixes of concrete for every mix containing ferrock to analyze its impact on workability. The results of slump test are reported in figure 4.2 which illustrate that workability was decreasing with the increasing ratio of cement replacement with ferrock. The samples with higher amount of ferrock showed lower workability. The slump value for control sample found 92 mm which reduced to 64 mm with cement replacement of 20% in mix FC20 which is the lowest among all mixes. The slump value decreased 4.34% and 30.43% for mix FC5 and FC20 respectively. The lower value of slump because rod like particle size of IO and water retention capacity of MK in ferrock [188]. This phenomenon is attributed to the presence of minerals, which enhance compaction and contribute to a denser matrix,

thereby reducing the flowability of the mix. Fine particles filling the voids in composites reduce pores and make mix workable by balancing the water content which is absorbed by the iron powder [90]. The reduction in slump value because of heavy IO particles which settle down at a place. The reaction of ferrock starts at an early age makes denser and stiffer mix reduces flow lowering slump values. Findings conclude that ferrock reduces the workability of concrete as higher amount of ferrock shows less workability. Previous study shows that nano MK in concrete reduced value of slump because nano MK has large specific surface area easy to form a flocculent network structure, shows poor dispersibility [189] and absorb more free water during wetting [190].

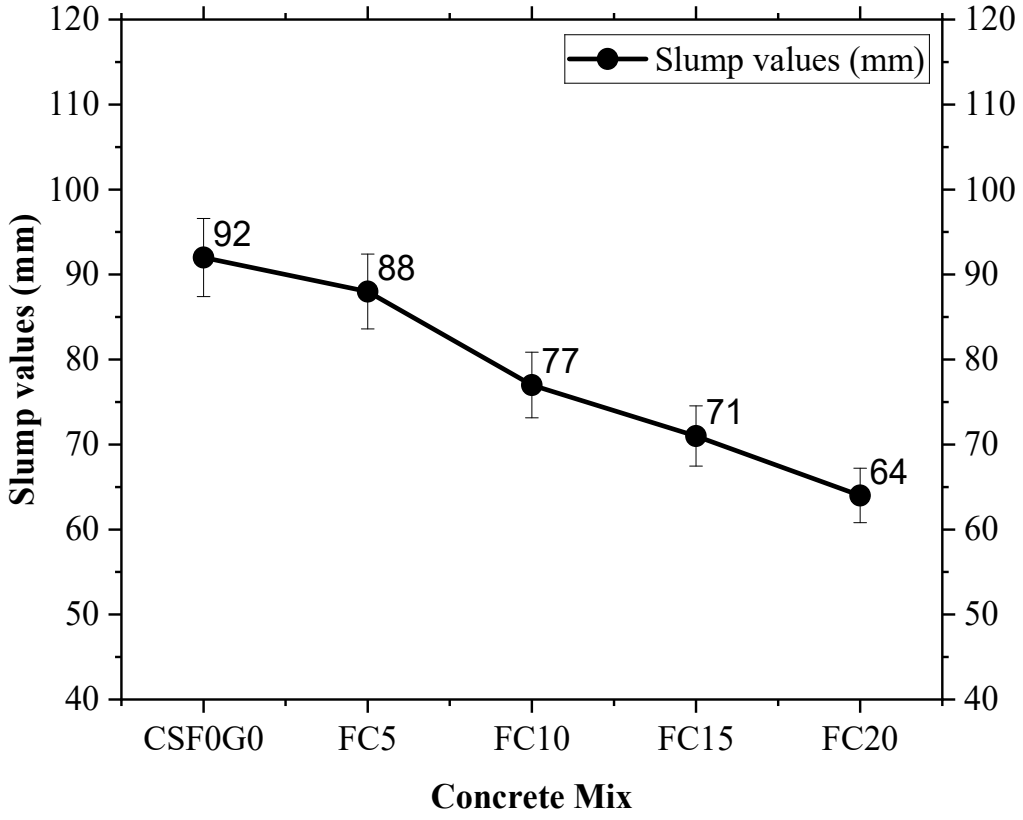

Figure 4.2 Result of slump test of concrete mix with ferrock

4.1.1.3 Slump test for concrete with rGO and ferrock together

Slump cone tests were conducted on fresh mix of concrete for every mix containing ferrock and rGO together to determine workability. rGO used as cement replacement in ratio of 0.2% constant throughout the study and ferrock used in ratio 5%, 10%, 15% and 20%. The results of slump test are presented in the figure 4.3 below along with mix notation. The workability decreased with the increase in cement replacement with ferrock and rGO. This decrease in workability was due to ferrock majorly. The mix G0.2FC5 and G0.2FC20 showed minimum and maximum reduction of 5.43% and 32.6% respectively as it remained within acceptable limits for practical construction applications. The observed reduction in slump with higher ferrock content is attributed to the increased surface area of the particles, which requires more water to maintain adequate flowability. The mix of two rGO and ferrock increases water retention because MK holds water and agglomerations created by rGO to make the mix stiffer. Decrease in workability is attributed to the adsorption of free water on the surface of nanomaterial. The increased surface area of rGO which is more than OPC makes it filler at nanoscale, refining the pore structure and increasing viscosity of concrete mix [36]. To minimize the decrease in fluidity caused by the addition of GO 0.2 wt% PC was added to all specimens to improve workability [191] [192]. Gong et al. [193] found that the inclusion of the GO sheets enhances the degree of hydration of the cement paste. The agglomeration of nanomaterials adversely affects their ability to improve the properties of concrete. Because GO can easily disperse in water, it is more likely than other nanomaterials to efficiently distribute throughout concrete [194]. As MK and LS contain fine particles to hold water also MK has the property of water holding to make paste stickier and viscous [195]. Findings report that the reduction in workability due to the combined effect of agglomeration of rGO and due to heavy weight of ferrock as workability was lesser with increasing content of ferrock. Recent study [196] has confirmed that the incorporation of GO as an additive in the mix can cause workability problems due to the agglomeration of the GO nanoparticles by the marked alkaline character of the cement mixture and the possible occurrence of undesired chemical reactions. Study suggests that incorporation of LS in concrete mix makes it decrease in slump because of friction between the solid particles [197].

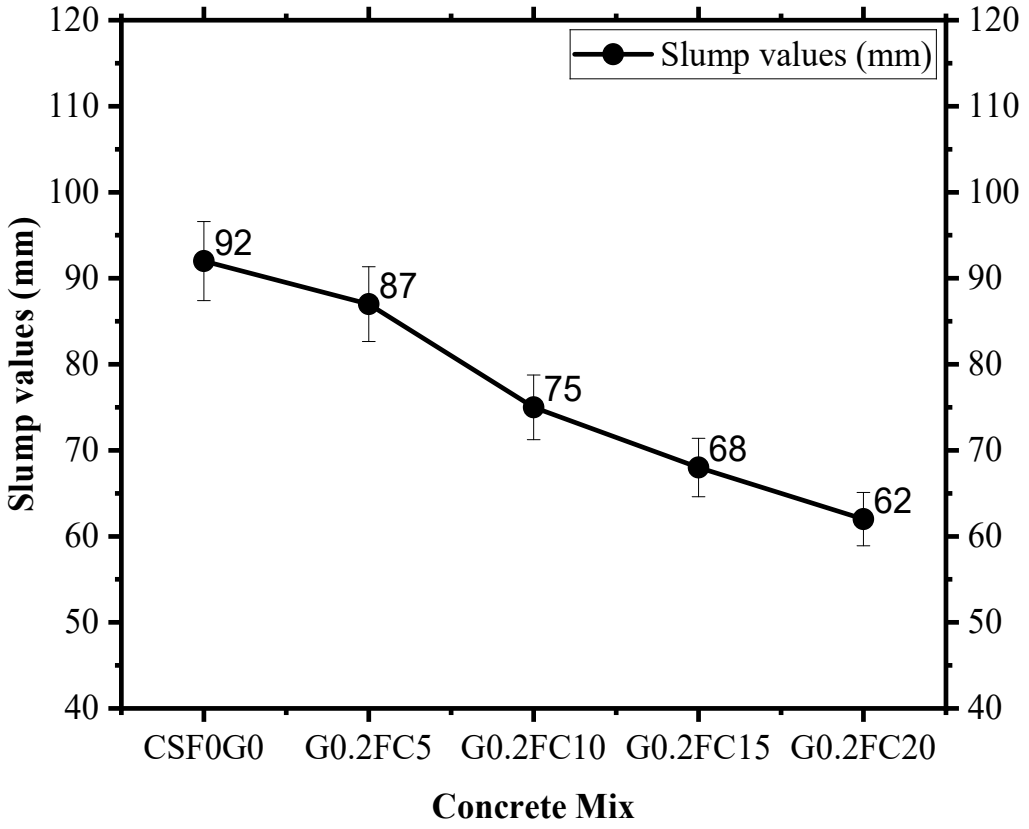

Figure 4.3 Result of slump test of concrete mix with rGO and ferrock together

4.1.2 Compaction Factor Test

4.1.2.1 Compaction factor for concrete with rGO

Compaction factor test conducted on fresh mix of concrete for every mix containing rGO to determine workability. The results of the compaction factor test are presented in figure 4.4 below along with mix notation reported that with increase in ferrock there was slight decrease in compaction factor value. The mix GC0.1 and GC0.8 shows maximum and minimum compaction factor value of 2.19% and 9.89% respectively. With the increasing rGO content the workability decreasing show low fluidity in mix. The decreasing compacting factor indicates the mix becomes stiffer with the increasing rGO quantity. As the surface area of rGO is quite higher than OPC so the

requirement of water is more but with higher amount rGO as it create agglomeration [136]. Findings showed that rGO does not impact workability as much. The use of rGO beyond optimum ratio causes agglomeration and reduces flowability. Previous studies suggest that incorporation of GO in concrete significantly increases viscosity and decreases workability of concrete [198]. GO not only acts as refined templates to aid the growth of reaction products in cement paste, but it also produces new nucleation sites within the pore space of fresh binder and promotes the formation of more hydration products [199]. Research has demonstrated that the inclusion of GO in concrete can enhance its strength while reducing workability [200]. This suggests that GO should be incorporated in an optimal ratio to achieve the desired balance of workability and strength. Furthermore, the addition of GO has been shown to enhance the structural integrity of concrete. A study reported a reduction in workability at all GO ratios, including the optimal ratio of 0.03% with a water content of 0.5. However, at this optimal ratio, the CS increased by 46%, indicating an enhancement in the degree of hydration of the cement paste [201]. The oxygen functionalities in GO decrease the Vander Waals forces between GO layers, increasing the electronic repulsion between them, thus allowing dispersion and reactivity of GO in the cement matrix [202].

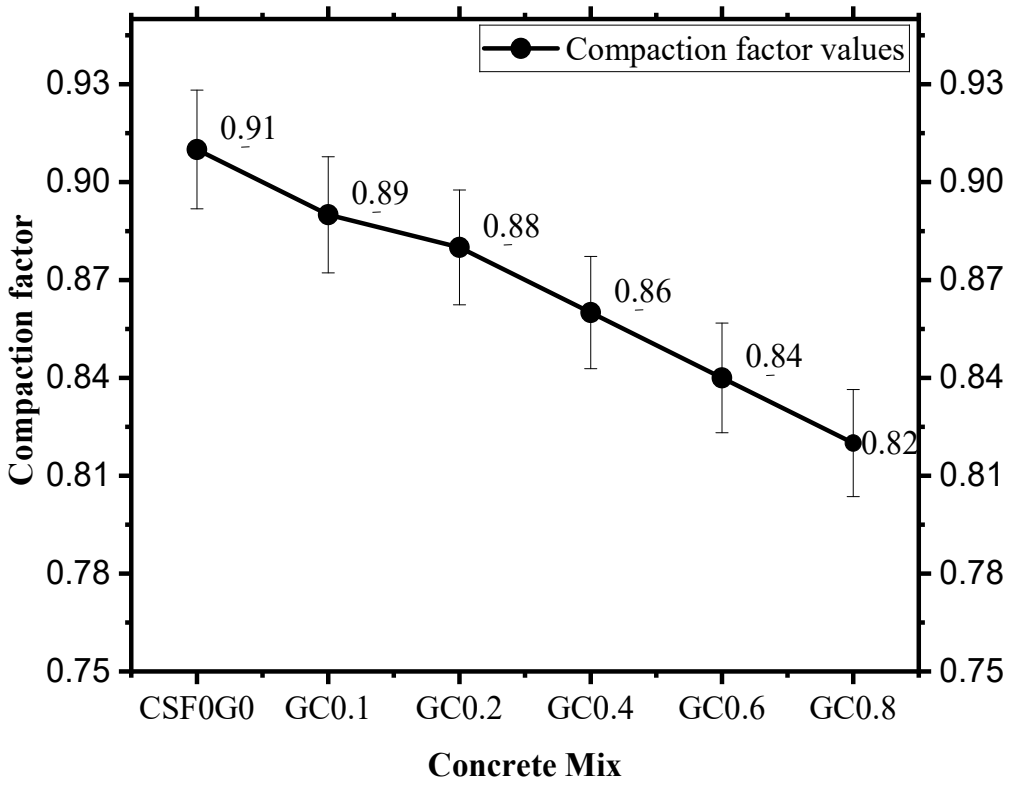

Figure 4.4 Result of compacting factor test values of concrete mix with rGO

4.1.2.2 Compaction factor for concrete with ferrock

Compaction factor test conducted on fresh mix of concrete for every mix containing ferrock to determine workability. The results of the compaction factor test are illustrated in figure 4.5 along with mix notation found that workability was decreasing with the increase in cement replacement with ferrock. The mix FC5 and FC20 showed minimum and maximum reduction of 4.0% and 18.0% respectively. The samples with higher amount of ferrock showed lower compaction value because of the thick and heavy paste formed by raw materials of IO, FA, MK and LS. Workability was decreasing due to the increasing ratio of ferrock while a lesser value provides a harder mix that may require higher energy for proper consolidation. The integration of FA, MT and LS, along with IO, forms a blend that enhances workability and minimizes water demand, and this combination balances the mix [195]. The filler effect of LS refined

and improves the porosity of the mix and in general terms results in lowering the water demand for a given workability [203]. Incorporating LS reduced the flowability of concrete. It was also reported that there was an optimum content of LS for the workability of concrete [22]. Effects of LS on the workability of concrete could be mainly attributed to the morphological effect, filler effect and dilution effect. Since its nucleation and chemical effects occur at several hours of hydration, they seem to have little effect on the workability of concrete [204].

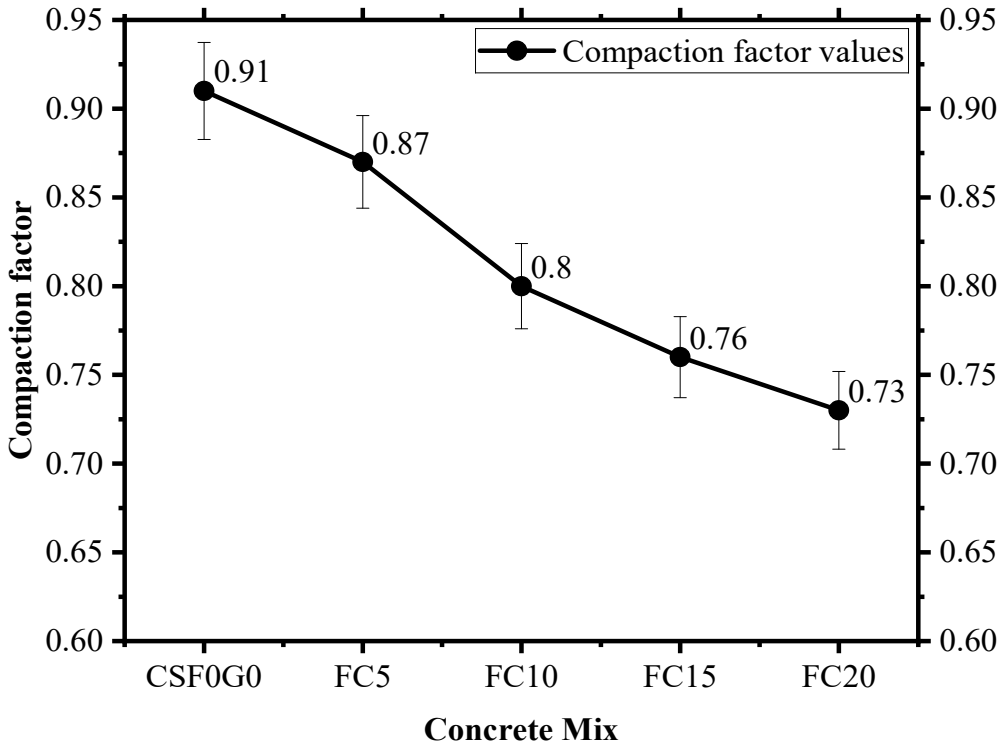

Figure 4.5 Result of compacting factor test values of concrete mix with ferrock

4.1.2.3 Compaction factor for concrete with rGO and ferrock together

Compaction factor test was performed on fresh mix of concrete for every mix containing ferrock and rGO together to determine workability. rGO was used as cement replacement in ratio of 0.2% constant throughout the study and ferrock was used in ratio 5%, 10%, 15% and 20%. The results of the compaction factor test are reported in figure

4.6 below along with mix notation. The mix G0.2FC5 and G0.2FC20 showed minimum and maximum reduction of 2% and 16% respectively. Findings suggest that due to combined effect of rGO and ferrock workability decreases because agglomeration of rGO and thick paste of ferrock. Workability decreases linearly with an increasing rGO content, with the most significant reduction of 0.8%, while 0.2% remains within an acceptable range. rGO should be used at an optimum ratio to avoid reduced workability, increased costs, and decreased strength at higher dosages. Previous studies indicate that the inclusion of GO in concrete mixtures reduces workability, as GO enhances the degree of hydration of the cement paste. However, despite this reduction in workability, the incorporation of 0.03% GO has been found to be beneficial. The improved performance is attributed to the refinement of the pore structure in the cement paste, which occurs due to the filler effect of GO agglomerates [201]. The reduction in workability is associated with water being trapped within the GO agglomerates. Furthermore, the incorporation of GO at ratios below 0.03% (w/c) has shown no significant positive effect on CS [205]. The inclusion of 0.05% GO in concrete mixtures has been found to reduce workability by 41.7%, while improving CS by 15–33% and FS by 41–59% [206]. Recent study [207] has confirmed that the incorporation of GO as an additive in the mix can cause workability problems due to the agglomeration of the GO nanoparticles by the marked alkaline character of the cement mixture and the possible occurrence of undesired chemical reactions that could involve the destabilization of the GO suspension.

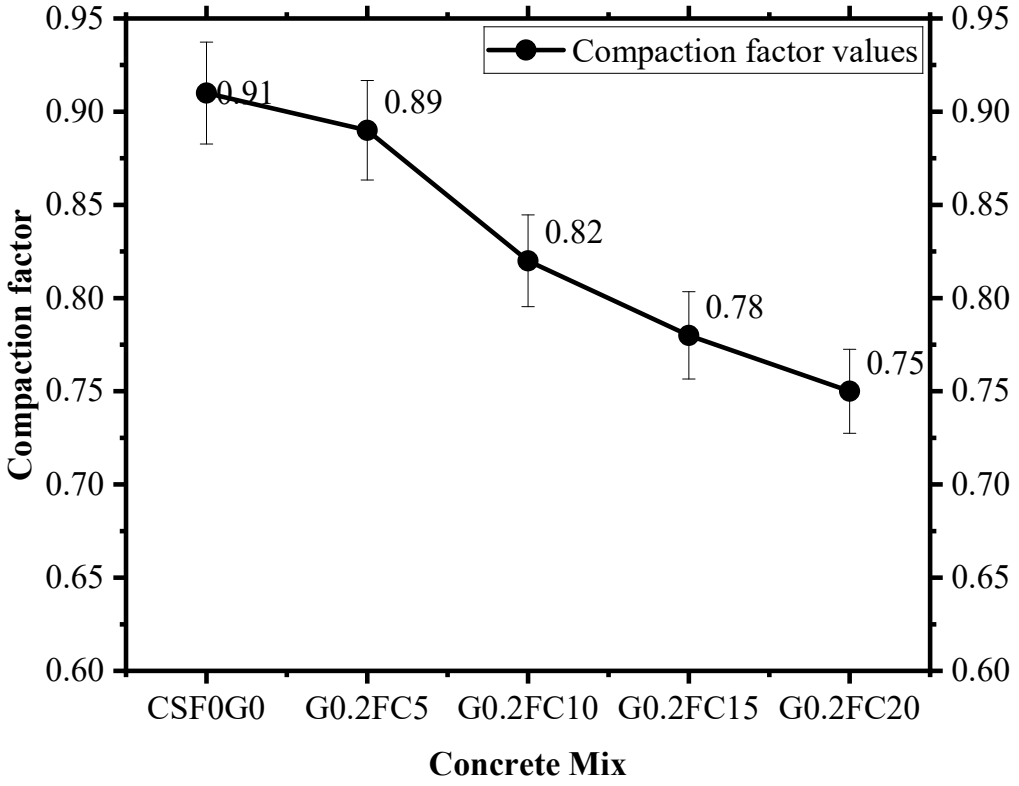

Figure 4.6 Result of compacting factor test values of concrete mix with rGO and ferrock together

4.2 Hardened Properties of concrete

4.2.1 Compressive strength test

4.2.1.1 CS of concrete with rGO

The CS test performed on hardened concrete with rGO as a partial replacement of cement in ratio of 0.1%, 0.2%, 0.4%, 0.6% and 0.8%. The figure 4.7 (a) presents the results of CS and 4.7 (b) % change in strength along with mix notations and curing days. The strength of all mixes of rGO concrete found improved as compared to control sample. The mix GC0.1 showed the lowest strength gain with a peak of 38.28MPa which improved by 25.09% as compared to CSF0G0 at 28 days of curing. The mix GC0.2 gained the highest strength with a peak of 42.04MPa with improvement of 37.38% as compared to CSF0G0 at 28 days of curing. Mix GC0.4 reported peak of

strength 41.34MPa which is 35.098% higher than CSF0G0. On increasing the ratio of rGO to 0.6% in mix GC0.6 the improvement in strength was 32.58% at 28 days of curing. On further increasing the ratio of rGO to 0.8% in mix GC0.8 the improvement in strength achieved was 28.98% than CSF0G0. Results found 0.2% of rGO to be optimum. With increasing amount of rGO strength started decreasing because of excessive addition of rGO cause the agglomeration of graphene layers in the concrete matrix to clump together [136]. Weak zones are likely to be formed in the concrete matrix by aggregating rGO particles. The gain in strength is attributed to its high surface area, which provides sites for hydration products, and to its nano-filling effect on reducing the pores in concrete [138]. rGO enhances the microstructure not only because of the nanofiller effect but also through pozzolanic reactivity, which in turn promotes cement hydration, formatting a higher amount of C-S-H gel [208]. The strength increased to the ratio 0.2% rGO because of the improvement in density of concrete matrix due to filling effect of rGO and then start decreasing because rGO agglomerates in pores when it presents in excess amount. Previous studies mentioned that with the inclusion of derivatives of graphene like GO [36] [72], graphene nanosheets [209] [55], GNP [33] [210] and pristine graphene [211] [212] the property of cement mortar and concrete improvement. Studies have reported that the incorporation of 1.5% NS in concrete enhances CS by 29% [60], while the addition of 3% NS results in an increase of 21% in CS and 16.1% in TS [44]. Lv et al. [191] investigated the incorporation of GO nanosheets into cement composites to improve their hardness, as they showed that the nanosheets were able to control the formation of cement hydration crystals and this resulted in a significant increase in cement hardness.

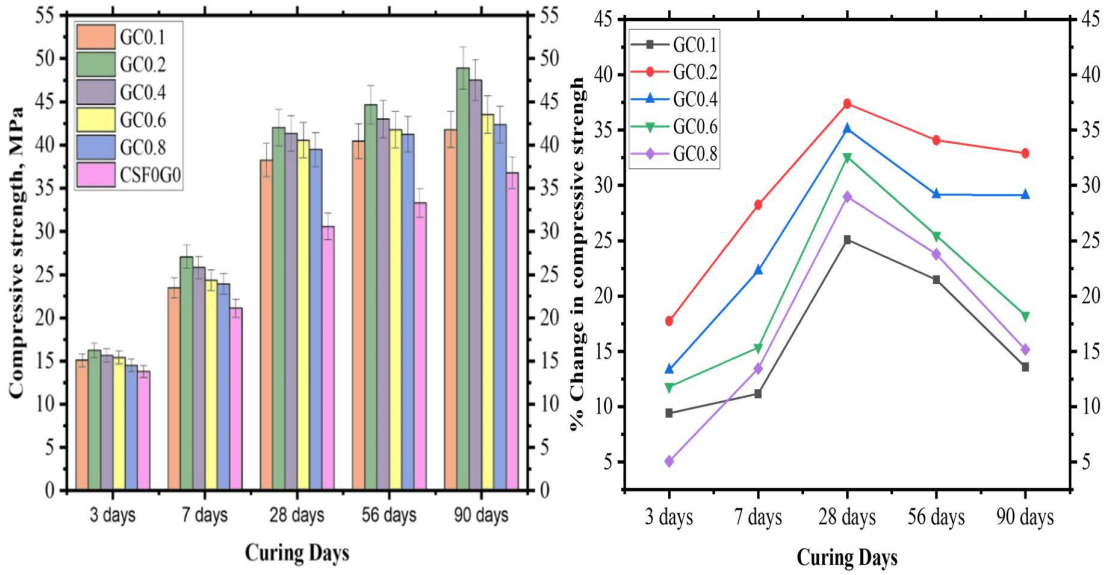

(a) **(b)**

Figure 4.7 (a) CS and (b) % change in CS of mixes with rGO

4.2.1.2 CS of concrete with ferrock

The CS of concrete tested on 150 mm cubes prepared with ferrock as a partial replacement of cement in ratio of 5%, 10%, 15% and 20% and results compared and presented. Results are illustrated in figures 4.8 (a) show CS for all mixes and the 4.8 (b) percentage change in strength due to ferrock respectively. Findings suggest that strength of all mixes with ferrock in concrete has been improved as compared to control sample. The mix FC10 showed the highest strength gain with a peak of 41.77MPa improved by 36.51% as compared to CSF0G0 at 28 days of curing. The mix FC5 achieve the lowest strength gain with a peak of 33.71MPa which is 10.16% higher than CSF0G0 at 28 days of curing. The raw materials such as FA, MK, and LS in ferrock thus improved the mechanical strength of the concrete by increasing the pozzolanic action with the cement hydrating materials [213]. Further, the presence of iron oxide in ferrock enhances the crushing value by making concrete dense and compact [214] [215]. The strength started increasing because when iron reacts with CO_2 it formed complex iron carbonates, so it fills in microstructure of concrete matrix and formed iron

carbonates and other pozzolanic materials helps in workability and early strength development of concrete [216]. When the ratio of ferrock increases more than 10% there is a slight decrease in strength, because of poor binding among ferrock and concrete composites. It was found that the curing of CO_2 at an early age improves the crystalline form of carbonates, thereby acquiring 40% of its strength at an early age. The reactions of calcium silicates such as Tri calcium silicate and Tri calcium silicate (C_3S and C_2S) when they get in contact with CO_2, contribute to earlier strength in CO_2-cured samples [85]. The LS cement replacement improves the CS to 10%. This improvement of strength is essentially due to the acceleration effect of LS filler related to the formation of calcium carboaluminates hydrate, which may be contributed to the overall increase in the rate of hydration [217] [218]. LS in combination with FA can improve the pore structure related properties such as porosity, absorption, and sorptivity, of cement paste, mortar and concrete. However, this improvement is limited to a certain level of addition beyond which the opposite happens [153]. The inclusion of nano MK enhances CS up to an optimum ratio. However, exceeding this ratio reduces strength, as excess nano MK tends to agglomerate and absorb onto cement particles, delaying the hydration reaction and decreasing the C_3S and β-C_2S phases in the matrix [219] [220]. CO_2 curing transforms $Ca(OH)_2$ into stable calcium carbonates, enhancing CS during CO_2 curing, as the carbonation reaction proceeds from the hydration process.

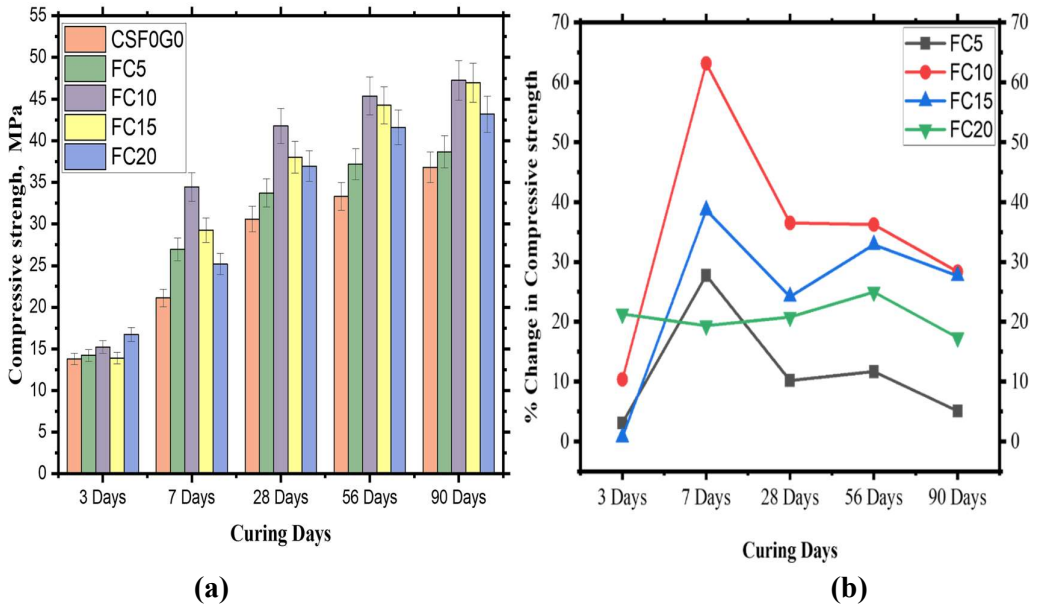

Figure 4.8 (a) CS and (b) % change in CS of mixes with ferrock

4.2.1.3 CS of concrete with rGO and ferrock together

The CS of hardened concrete cubes prepared with rGO and ferrock together as a partial replacement of cement in ratio 0.2% rGO and 5%, 10%, 15%, 20% ferrock and results are presented. Results are illustrated in figure 4.9 (a) CS and the 4.9 (b) percentage change in CS due to rGO and ferrock together with mix notations. Findings suggest that strength of concrete with rGO and ferrock have been improved as compared to control sample at all curing days. The mix G0.2FC5 showed the lowest strength gain with a peak of 42.92MPa with improvement of 40.26% as compared to CSF0G0 at 28 days of curing. The mix G0.2FC10 achieve the highest strength gain with a peak of 55.92MPa showed improvement of 82.74% as compared to CSF0G0 at 28 days of curing. By increasing the ratio of ferrock to 15% in mix G0.2FC15 gained strength 64.26% higher than control mix CSF0G0. However, on further increasing the ratio of ferrock in mix G0.2FC20 with improvement of 46.96% strength than CSF0G0. The combination of rGO and ferrock showed significant improvement in strength. This is due to the filler effect of rGO in concrete matrix and in ferrock has other pozzolanic

materials also to improve hydration in concrete along with iron as a binder [36]. It is indicated that the application of CO_2 at an early age improves the crystalline form of carbonates, by transforming $Ca(OH)_2$ into stable calcium carbonates thereby acquiring 40% of its strength at an early age [90]. The reactions of calcium silicates (C_3S and C_2S) when they get in contact with CO_2, contribute to earlier strength in CO_2-cured samples. This is the primary reason for enhancing the density and durability of carbonated samples. Upon addition of ferrock, the absorption and reaction get ameliorated, developing an additional stable ferrous compound ($FeCO_3$) which forms rust, acting like reinforcement for the concrete matrix [221]. This profound behavior of concrete under CO_2 curing was rapidly studied in recent times, with an outcome that increased time of exposure to CO_2 accelerates the carbonation reaction. Previous studies have confirmed that the inclusion of a small amount (0.02%) of graphene nanosheets results in a significant improvement in mechanical strength, with increases of 34.1% [209], 22% [222] and 23% [223] respectively.

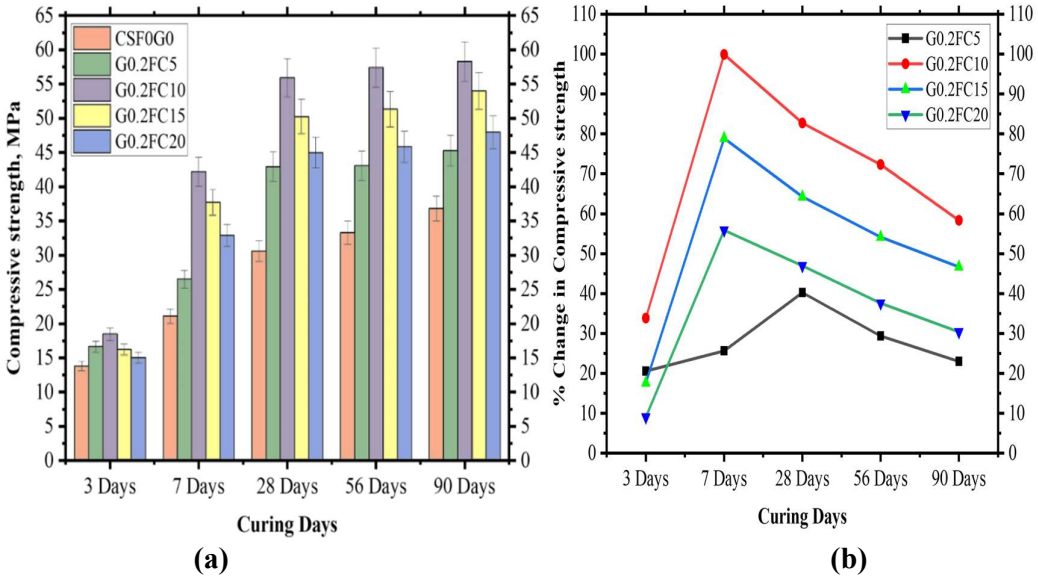

Figure 4.9 (a) CS and (b) % change in CS of mixes with rGO and ferrock together

4.2.2 Split tensile strength test

4.2.2.1 TS of concrete with rGO

The TS of hardened concrete tested on cylinders prepared with rGO as a partial replacement of cement in ratio of 0.1%, 0.2%, 0.4%, 0.6% and 0.8%. Results are illustrated in figures 4.10 (a) show CS and 4.10 (b) the percentage change in CS due to rGO respectively along with mix notations. Findings suggest that strength has been improved with inclusion of rGO in concrete as compared to control sample. Samples with the 0.1% of rGO in mix GC0.1 gained 40.27% improvement in strength at 28 days of curing. On increasing content of rGO in mix GC0.2 gain highest strength with a peak of 3.31MPa improvement of 49.77% as compared to CSF0G0 at 28 days of curing. In mix GC0.4 the strength gain was 48.42% which is similar with mix GC0.2 at 28 days of curing. On further increasing the ratio of rGO to 0.6% in mix GC0.6 concrete achieved strength 47.51% higher than control mix. The mix GC0.8 has the lowest strength gain with a peak of 2.99 MPa with the improvement of 35.29% as compared to CSF0G0 at 28 days of curing. The gain in strength because of accelerated hydration, refining the mechanical interlocking at the rGO reinforced cement matrix interface. Agglomerated rGO particles create a thick network that interferes with water flow and slows down hydration reactions [224]. Densification of microstructure caused due to the high aspect ratio and filler effect of rGO at nanoscale resulting in improved mechanical strength [37]. It is attributed to the strong interfacial bonding between the matrices arising from the two-dimensional crumpled structure with high specific surface area of rGO. Findings suggest 0.2% is the optimum ratio beyond then strength started decreasing because an excessive amount of rGO forms cluster results in inefficient rGO dispersion which hinders the binder's hydration process. Studies have concluded that the use of graphene derivatives improve tensile strength by 15% [129], 33% [193] and 15.19% [225] while carbon nanofibers improve 56% [226].

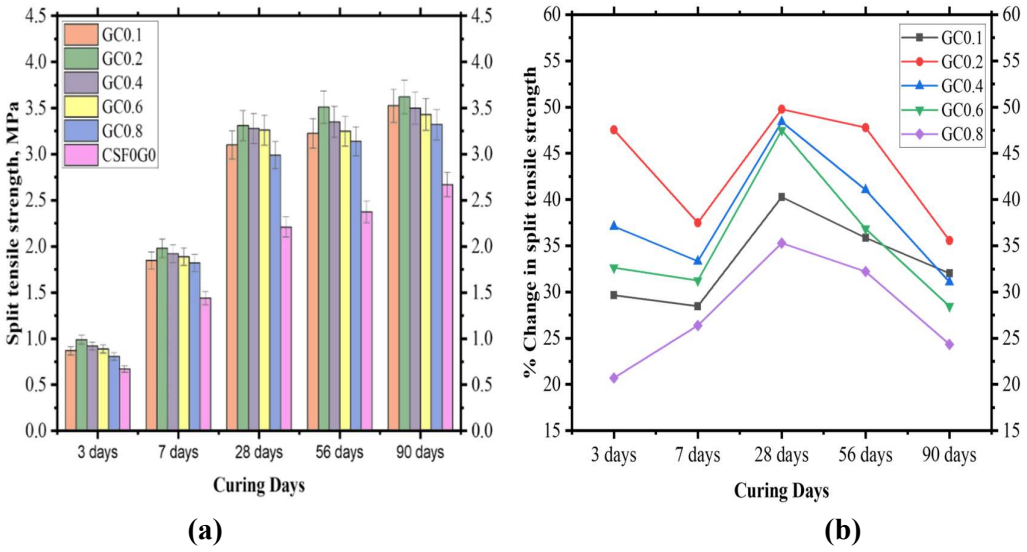

Figure 4.10 (a) TS and (b) % change in TS of mixes with rGO

4.2.2.2 TS of concrete with ferrock

The TS test of concrete tested with ferrock as a partial replacement of cement in ratio of 5%, 10%, 15% and 20%. Figure 4.11 (a) illustrates the results of TS and 4.11 (b) % change in strength at all curing days along with mix notations. Findings suggest that strength of ferrock concrete for all replacement ratios has been improved as compared to control sample. The mix FC5 showed the lowest strength gain with a peak of 2.75MPa improved by 24.43% as compared to CSF0G0 at 28 days of curing. The mix FC10 achieved the highest strength gain with a peak of 3.04MPa with improvement of 37.55% as compared to CSF0G0 at 28 days of curing. On increasing content of ferrock to 15% in mix FC15 the strength gain was 33.71% which is lower than mix FC10 but still higher than CSF0G0. However, on further increasing the ratio of ferrock to 20% in mix FC20 strength achieved was 28.05% more than CSF0G0. The early days improvement in strength because of CO_2 curing at initial days due to dilution and nucleation effect of particles. The quality of concrete is enhanced by the onsite reaction of iron particles with CO_2, producing a compound of ferric carbonate ($FeCO_3$), accelerating the disintegration of iron particles which further happens to fill the voids and pores neglecting strength loss. Another reason for strength improvement is the

shape of IO particles which are angular to enhance the bonding between the particles inside concrete matrix [90]. The iron particles having a rough surface texture form a sturdy ITZ, creating a solid bond between the cement matrix and aggregates thereby improving strength. Nevertheless, the fine particles in ferrock with its micro filling capacity and pozzolanic activity augment the formation of Ca and aluminum silicates in the silicate and amorphous phases and readily form hydrates empowering concrete [215]. Although, when FA and MK were combined in concrete, it may hinder the performance due to the lack of sufficient generation of $Ca(OH)_2$ necessary for the formation of C-S-H in the concrete matrix, because of which silica particles are left unreacted probably ending in strength reduction [90]. The observed reduction in strength attributed to the excessive silica content present in ferrock, which appears to have resulted in the dilution of the C_2S and C_3S phases, subsequently inhibiting the pozzolanic reaction [227]. Monshi and Asgarani [228] produced a kind of cement from steel slag (with 8%), iron slag and LS, which satisfied the requirement on CS for type I Portland cement. When steel slag is used in cement production, its adding amount is usually very small in order to insure the essential strength requirement of cement.

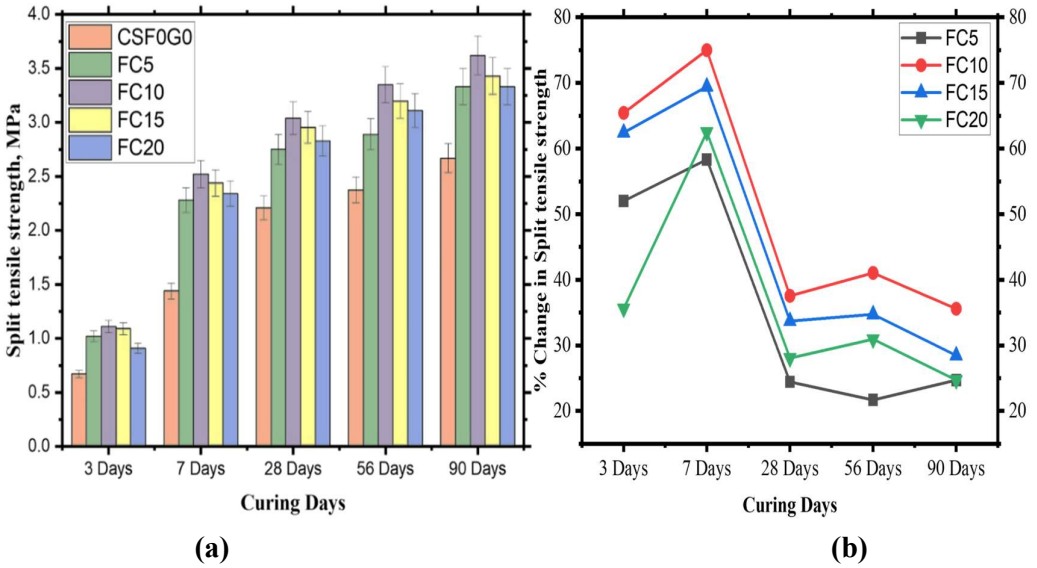

Figure 4.11 (a) TS and (b) % change in TS of mixes with ferrock

4.2.2.3 TS of concrete with rGO and ferrock together

The TS of concrete tested on cylinders prepared with rGO and ferrock together as a partial replacement of cement with constant ratio of 0.2% rGO and variable ratio of ferrock as 5%, 10%, 15% and 20%. Results are presented in figure 4.12 (a) and (b) for TS for all mixes and the % changes in strength respectively. Findings suggest that the strength of ferrock concrete for all mixes has been improved as compared to control sample. The mix G0.2FC5 gained the lowest strength improvement of 3.12MPa with improvement of 41.17% as compared to CSF0G0 at 28 days of curing. The mix FC10 achieved the highest strength gain with a peak of 3.42MPa with improvement of 54.75% as compared to CSF0G0 at 28 days of curing. On increasing the ratio of ferrock to 15% in mix FC15 of improvement of 52.94% which starts decreasing after 10% ferrock in mix FC10 at 28 days of curing. However, on further increasing the ratio of ferrock to 20% in mix FC20 gained 48.41% strength as compared with CSF0G0. The ferrock imparts additional strength to the concrete by the angular morphology of its iron particles. The iron particles having a rough surface texture form a sturdy ITZ, creating a solid bond between the cement matrix and aggregates thereby improving strength [90]. Additionally, the pozzolanic materials in ferrock concrete like FA, MK and micro sized LS powder enhanced the filling effect in the concrete and built a better bond between the aggregate and the cement paste [85]. Previous studies found that with the inclusion of small amount of GO like 0.03% [193], 0.12% [70], improve 33%, 24% of TS. Tsakiridis et al. [229] investigated the utilization of steel slag for Portland cement clinker production and revealed that the addition of steel slag did not negatively affect the quality of the produced cement with 10.5% addition of steel slag.

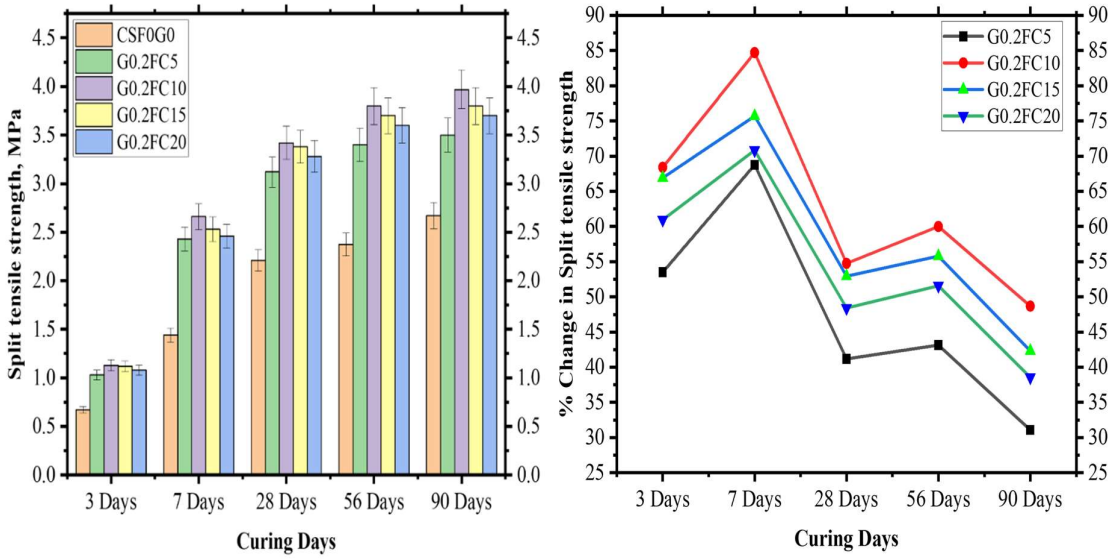

Figure 4.12 (a) TS and (b) % change in TS of mixes with rGO and ferrock together

4.2.3 Flexural strength Test

4.2.3.1 FS of concrete with rGO

FS of concrete performed on beams with rGO ratios of 0.1%, 0.2%, 0.4%, 0.6% and 0.8% after using rGO as a partial replacement of cement at 3days, 7days, 28 days, 56 days and 90 days of curing. Findings suggest that all ratios with rGO achieved better strength than control sample. The figures 4.13 (a) and (b) below illustrate the FS achieved for all mixes and percentage change in FS at all curing days. The mix GC0.1 exhibited improvement of 18.13% at 28 days curing. The mix GC0.2 has highest improved strength with a peak of 4.23MPa with 29.06% improvement in strength at 28 days of curing. On further increasing the ratio of rGO to 0.4% in mix GC0.4 the strength gain was 24.69 which is lower than mix GC0.2. In mix GC0.6 the achieved strength was 19.38% higher than control mix at 28 days of curing. The mix GC0.8 showed the lowest improved strength with 3.6MPa with 12.5% improvement in strength. According to the literature, rGO enhances the formation of C-S-H gel with a compact structure by filling its nanopores. Owing to the high efficiency of nanomaterials in improving the mechanical properties of cementitious materials. rGO also facilitates C-S-H hydration by providing nucleation sites because of their higher

surface area [230]. Microstructure observation confirmed that the functional group (carboxyl) of rGO interact with CH, generating an additional amount of gel hydrates [231]. On the other hand, it was reported that higher amounts of rGO limited the hydration of C-S-H gel because they reduced the amount of free water, which is crucial for hydration to proceed. The functional group present in rGO acts as an active site that attracts cement particles [232]. The high surface area to mass ratio of rGO assists the nucleation for formation of cement hydrates and develops strong covalent bonds at the interface of cement matrix and dispersed phase. Previous studies concluded that FS improved with incorporation of 0.01% of GNP by 7% [233] and with nanosheets of 0.022% 30.37% [209]. 0.03% of GO improve 8% of CS at 28 days of curing [225]. Pan et al. [32] also investigated the incorporation of GO in the cement paste, achieving an increase in concrete strength of 15–30% in compression tests and 40–60% in flexural tests. Li et al. [234] found that GO could efficiently accelerate cement hydration by accelerating the hydration of C_3S in cement. It is also noticed that excessive GO (exceed the optimal amounts) results in a decline in improvements in FS due to particle agglomeration

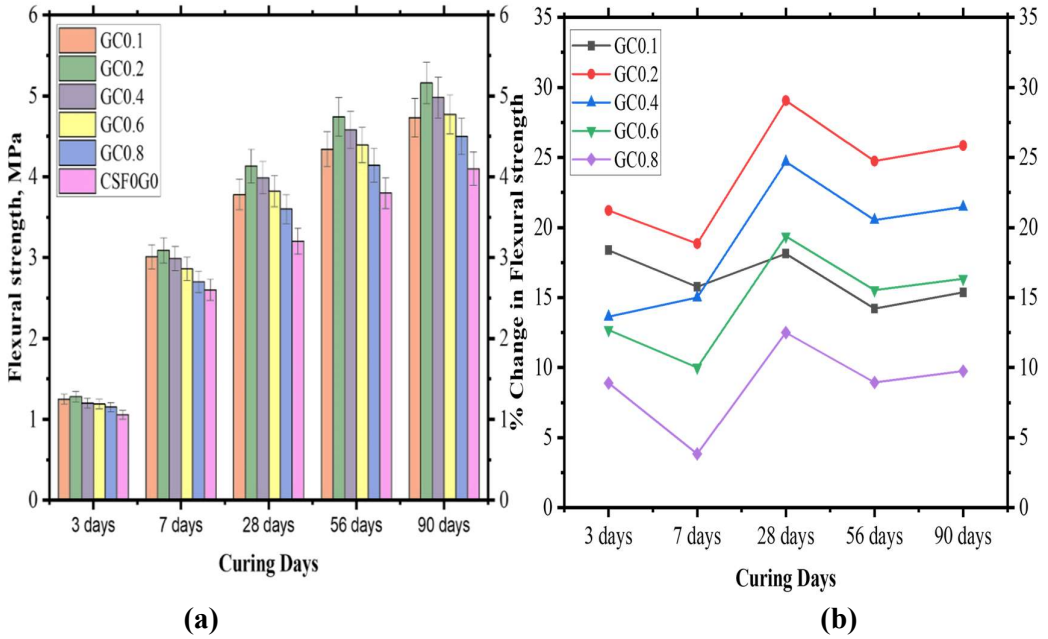

Figure 4.13 (a) FS and (b) % change in FS of mixes with rGO

4.2.3.2 FS of concrete with ferrock

FS of concrete beams with ferrock replacement ratios of 5%, 10%, 15% and 20% were tested at 3days, 7days, 28 days, 56 days and 90 days of curing. Findings suggest that all mixes with ferrock showed better strength than control sample. The figure 4.14 (a) below presents the FS achieved for all mixes and 4.14 (b) percentage change in FS with mix notations. The mix FC5 shows 13.75% improvement in strength at 28 days of curing. The mix FC10 illustrates the highest improved strength with a peak of 3.82MPa with 19.38% improvement in strength at 28 days of curing. On increasing the ratio of ferrock to 15% in mix FC15 has improved 15.94% at 28 days of curing. However, on further increasing the ratio of ferrock to 20% in the mix FC20 gained the lowest improved strength with 3.6MPa with 14.38% improvement in strength at 28 days of curing. When iron oxide in Ferrock is exposed to CO_2, it transforms into a solid material that is five times stronger than regular concrete and has a higher CO_2 absorption capacity. It is because of the contribution of nucleation sites by LS powder, improved silica content from FA and cohesive nature of MK imparted in the ferrock [195]. The reduction in strength is because of the reduction in the amount of $Ca(OH)_2$ crystallites due to accelerating hydration effect of iron fines in concrete [235]. It is worth noting that $Ca(OH)_2$ resulting from the hydration process is known to boost up the pozzolanic reactions at later ages. Ultimately, the reduction in $Ca(OH)_2$ during carbonation cannot activate the siliceous materials thereby reducing the C-S-H phases in the concrete matrix in later days, impeding the performance of SCC [236]. It was found that up to 15% of LS fines do not affect the strength performance of LS concrete manufacture [237]. Instead, due to the higher water absorption of FA, adding FA decreases the water necessary for the hydration of cement. Therefore, unfinished cement hydration reduced the connection between coarse aggregates and reduced the strength of PC [238]. Liu et al. (2019) studied the properties of PC containing 3%, 6%, 9%, and 12% FA. It was found that the addition of FA reduced the flexural and CS at the early time of the curing period (28 days). It is reported that by increasing the quantity of FA up to 12%, the CS 34% reduced. However, the result showed that with increasing curing period (up to 150 days) the strength of the FA-modified PC increased. As the curing time increased, the

rate of hydration enhanced progressively which resulted in the strong bonding between coarse aggregates [239].

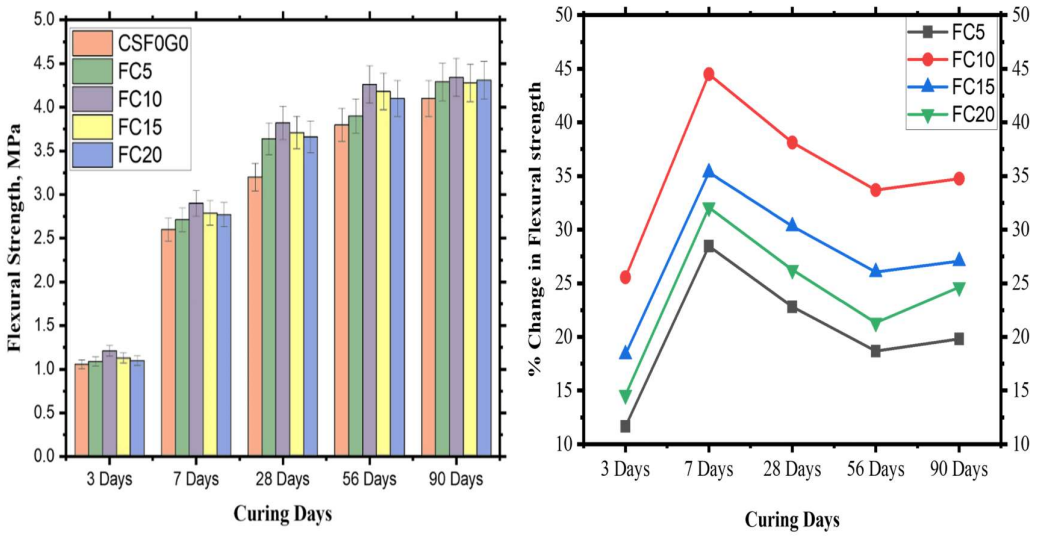

Figure 4.14 (a) FS and (b) % change in FS of mixes with ferrock

4.2.3.3 FS of concrete with rGO and ferrock together

FS performed on concrete beams with rGO and ferrock together as partial replacement of cement with constant ratio of 0.2% rGO and 5%, 10%, 15% and 20% of ferrock at 3days, 7days, 28 days, 56 days and 90 days of curing. Findings suggest that all mixes with rGO and ferrock showed better strength than control sample. The figures 4.15 (a) below illustrate the FS achieved for all mixes and 4.15 (b) percentage change in FS. The mix G0.2FC5 with the ferrock ratio 5% exhibited the lowest improvement with a peak of 4.19MPa of 30.94% as compared with CSF0G0 at 28 days of curing. The mix G0.2FC10 has the highest improved strength with a peak of 4.49MPa with 40.31% improvement in strength at 28 days of curing. On increasing the ratio of ferrock to 15% in mix FC15 with improvement of 36.88% as compared to control sample. However, on further increasing the ratio to 20% in mix FC20 which gained strength 35.44% higher than control mix at 28 days of curing. This improvement

is attributed to enhancements in the ITZ and the cementitious matrix within the concrete, facilitated by the pozzolanic reactions of silica with $Ca(OH)_2$, which leads to the formation of additional C-S-H [36]. This reaction refines the microstructure, resulting in a denser, more homogeneous concrete matrix and improved FS. Additionally, carbon curing enhances FS by accelerating the carbonation of $Ca(OH)_2$, leading to a denser microstructure and better resistance to bending forces [90]. rGO works as a filler in concrete matrix to make it dense and compacted. Results conclude that the combination of rGO and ferrock performed well and leads to higher strength as compared to control sample [68]. Previous studies also mentioned that small inclusion of nano material in cement composites improves strength, the inclusion of 0.01% of GNP improves 7% of FS [233]. It was observed that 0.06% of GNP improved by 20% [240] and 27.8% [241] of FS. Authors observed that with small inclusion of 0.04% GO improves 75.7% FS and microstructure of concrete composite [141]. Thus, the combined effect of rGO and ferrock enhanced the strength of concrete mixes at all curing days. It was found that the rate of increasing strength was lower initially and increased as the age increased when compared to conventional PC. This can be due to the development of cement hydration and the pozzolanic activity of the FA with free lime liberated from cement hydration. The gradual rate of pozzolanic properties results in a slower strength improvement in FA PC but noticeable strength achievement is typically detected from 28 to 90 day [242] [243] [244].

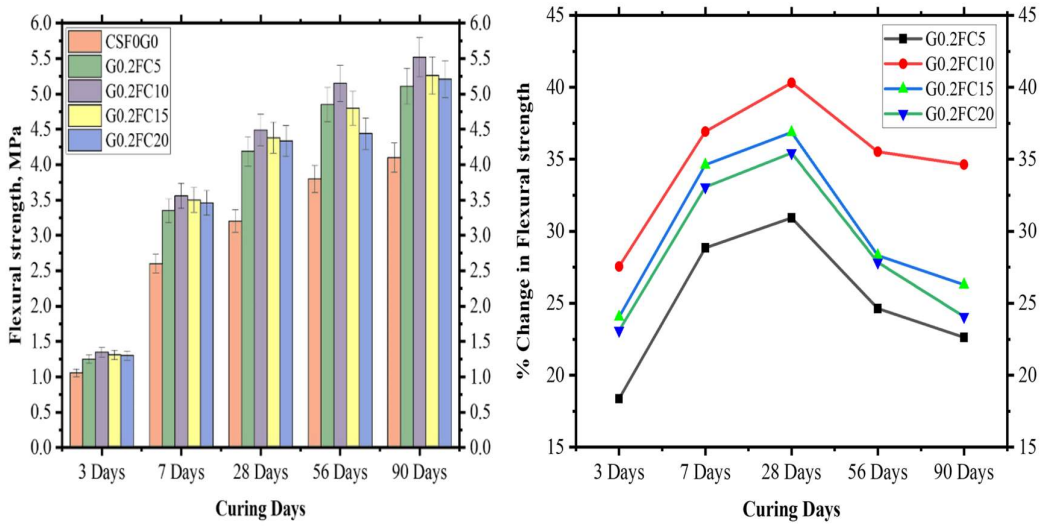

Figure 4.15 (a) FS and (b) % change in FS of mixes with rGO and ferrock together

4.3 Durability

4.3.1 Total absorption Test

4.3.1.1 Total absorption for concrete with rGO

Total absorption test conducted on hardened concrete cubes with rGO as a partial replacement of cement in ratios of 0.1%, 0.2%, 0.4%, 0.6% and 0.8% and tested at 28days, 56 days and 90 days of curing. Results of total absorption test are presented in figure 4.16 below along with mix notation and curing days. Mix GC0.1 showed less improvement with 12.9% and 12.36 % on 28 days and 90 days of curing. This is because there are pores left to be filled due to the small amount of rGO. The mix GC0.8 exhibited decrease of 48.27% and 43.6% at 28 days and 90 days of curing respectively which is lowest absorption of water among all mixes. Results found that with the increase in ratio of rGO the absorption rate is decreasing due to the surface area of rGO is much higher due to which it fills in pores easily and works as a filler in concrete matrix [245]. rGO makes composites denser and compacted due to which less water absorbed with higher amount of rGO [246]. Improved homogeneity and quality of

concrete hinders enhanced durability and mechanical performance of concrete. It is observed that with increase in rGO the concentration level of the porosity of the rGO reinforced concrete mixes have been reduced, i.e. the nucleation for formation of cement hydrates was indeed accelerated with rGO incorporation in the cement matrix [247]. rGO optimize the porosity of cement-based materials, greatly improve pore structure, and have the filling effect of micropores [36]. Increased durability and mechanical performance of concrete are restricted by improved homogeneity and quality of concrete. Increased mechanical performance and longevity of concrete are hampered by improved homogeneity and quality [37]. It is evident that the porosity of the rGO reinforced concrete mixes decreases as the concentration level of rGO increases; in other words, the integration of rGO into the cement matrix accelerated the nucleation to produce cement hydrates. With a further increase in the amount of GO beyond 0.075%, the water absorption was found to increase due to the agglomeration of GO, resulting in a non-uniform dispersion and thereby, leaving the pores vacant. The addition of GO and rice husk ash significantly reduced water absorption in concrete. The lowest absorption was achieved with 0.075% GO, resulting in a 25.4% decrease at 28 days without RHA, due to pore filling and densification. When 10% cement was replaced with RHA, absorption decreased by 14.5%, attributed to the filler effect and pozzolanic reaction. The optimal mix showed a 41.7% reduction at 28 days, as the combined effect of GO and RHA enhanced the formation of C–S–H gel, further reducing permeability [248]. The optimum mix of 0.3% GO showed a 23.3% decrease in water absorption due to the combined filler effect of RHA and GO [133].

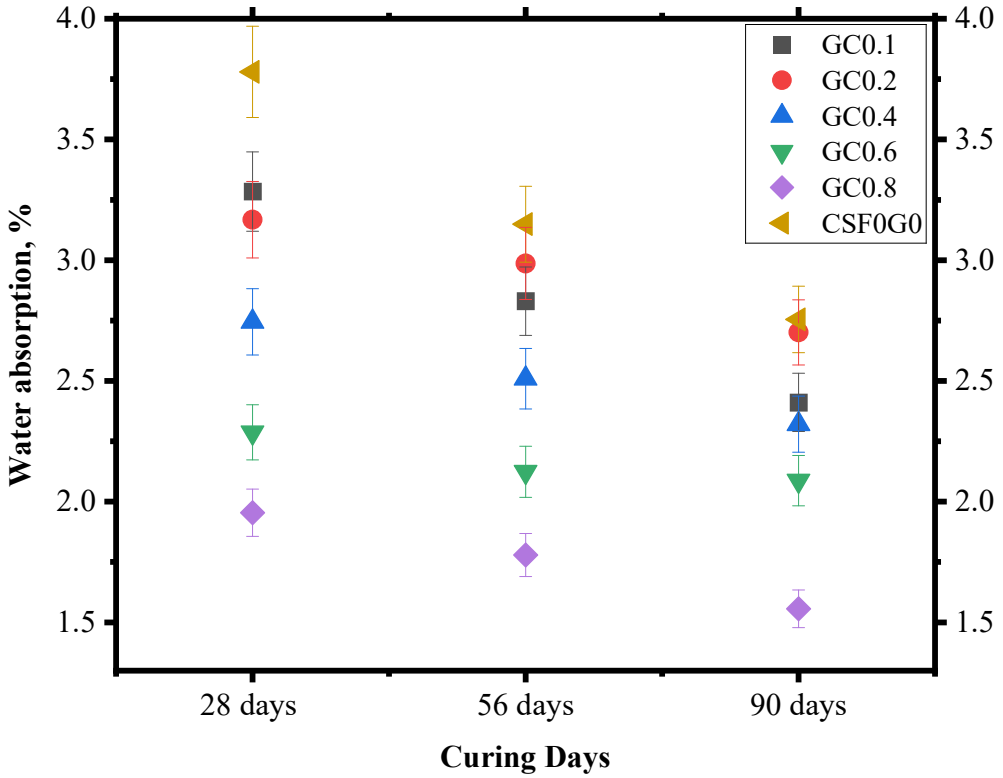

Figure 4.16 Results of total absorption for all concrete mixes with rGO

4.3.1.2 Total absorption for concrete with ferrock

Total absorption test was conducted on concrete cubes of size 150 mm with ferrock as a partial replacement of cement in ratios of 5%, 10%, 15% and 20% and tested at 28days, 56 days and 90 days of curing. Figure 4.17 presents the results of total absorption for concrete containing ferrock. The mix FC5 showed no improvement in 90 days in absorption of water in comparison with control sample. Further substitution ratio increased to 10% in mix FC10 resulted in reduction of water by 27.78%, 17.84% and 13.71% as compared with mix CSF0G0 at curing of 28, 56 and 90 days respectively. On increasing the replacement of cement to 15% in mix FC15 found 29.34%, 22.7% and 18.45% less absorption in comparison with mix CSF0G0 at 28, 56 and 90 days of curing respectively. On further increasing the replacement of cement to 20% in mix FC20 have 38.23%, 30.25% and 28.37% less absorption as compared to mix CSF0G0 at 28, 56 and 90 days of curing respectively. Results found that with an increase in ratio

of ferrock, the absorption rate is decreasing due to iron present in ferrock reacting with CO_2 and forming complex iron carbonates inside the concrete matrix to form denser and compacted composites [85]. With the increase in ratio of ferrock absorption rate started decreasing maybe because other pozzolanic materials were also present in ferrock to improve microstructure of concrete matrix [90]. The product of IO reaction with CO_2 in presence of OA forms complex iron carbonate which is dense and brittle structure which forms in concrete matrix [84]. Results suggest that ferrock makes structure more compacted and improved microstructure of composites. FA is a by-product of the combustion of pulverized coal and is a pozzolanic material. When it is mixed with Portland cement and water, it generates a product similar to that formed by cement hydration but has a denser microstructure that is less permeable [249]. The results indicated that the permeability and void ratio of PC decreased with increased percentages of FA due to the filler effect from FA and its pozzolanic activity, which created secondary C–S–H gels that resulted in cohesive activity, therefore decreasing voids and permeability [143].

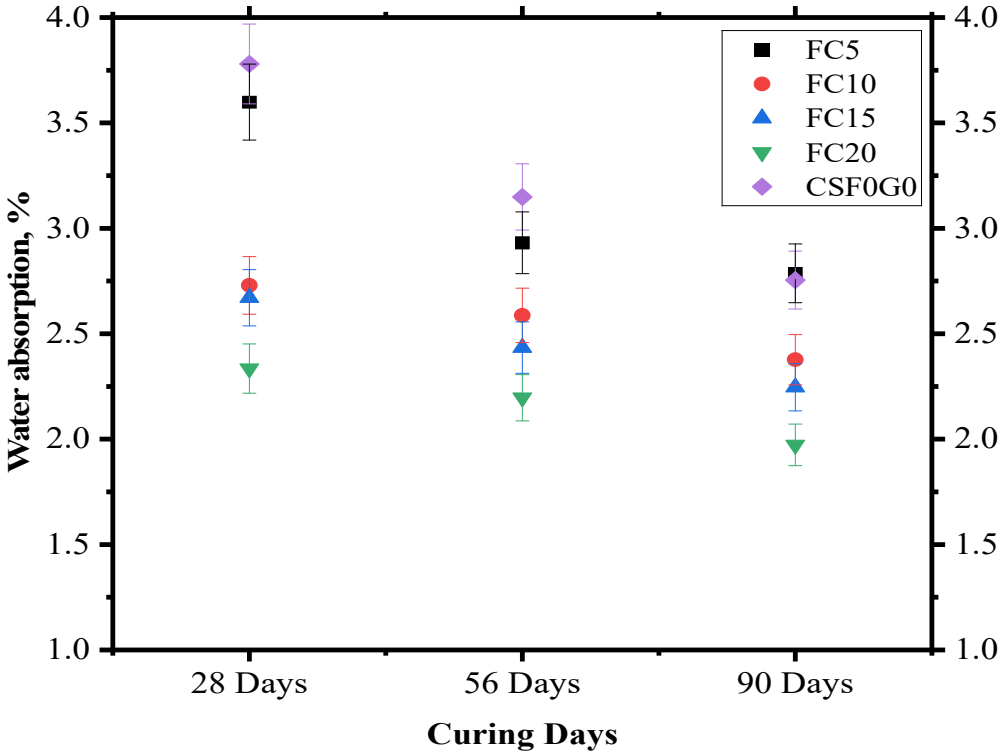

Figure 4.17 Results of total absorption for all concrete mixes with ferrock

4.3.1.3 Total absorption for concrete with rGO and ferrock together

The total absorption test conducted on 150 mm concrete cubes with rGO and ferrock as a partial replacement of cement as ferrock in ratio of 5%, 10%, 15% and 20% and rGO with constant ratio of 0.2% tested at 28days, 56 days and 90 days of curing. Findings, as reported in the figure 4.18 below, suggest that mix G0.2FC20 reduced absorption by 66.04% and 21.45% at 28 days and 90 days of curing respectively, which is the lowest absorption of water among all mixes. Mix G0.2FC5 exhibited less improvement with 30.23% and 21.45% at 28 days and 90 days of curing. With increasing the ratios of ferrock to 10% in mix G0.2FC10 reduced absorption by 2.53%, 2.21%, and 2.12% at 28, 56 and 90 days of curing respectively. With increasing the ratio of ferrock to 15% in mix G0.2FC15, absorbs 1.844%, 1.55% and 1.24% at 28, 56 and 90 days of curing respectively. With the replacement ratio of 20% in mix G0.2FC20 reduced water absorption 1.28%, 1.12% and 1.04% at 28, 56 and 90 days of curing,

respectively. The complex wrinkled architecture of the molecule indicates the presence of aggregated rGO, like the aggregated GO noted in the research [90]. Results indicate that with the increase in ratio of rGO the absorption rate is decreasing due to the filler effect of rGO and strong iron carbonate formation of ferrock with contains FA to improve microstructure of concrete [36]. The combining effect of rGO and ferrock to make composite denser and more compacted as surface area of rGO is large so it works as filler and fill in pores and product of ferrock make is dense as it contains pozzolanic material to improve its microstructure. rGO concentration leads to the rapid formation of cohesion and adhesion forces among adjacent rGO particles due to intermolecular forces such as van der Waals interactions, electric dipole interactions, and chemical bonding (hydrogen bonding), resulting in the aggregation of rGO particles [245]. As the amount of ferrock increases, the concrete matrix's ability to absorb water decreases, indicating a solid and compact concrete structure. Ferrock contains LS which acts as filler due to acceleration effect which forms calcium carboaluminates hydrate which enhance rate of hydration [153]. The maximum water absorption occurs within the first 28 days due to FGN, after which the rate decreases but continues. FGN also increases concrete shrinkage, though within permissible limits, both effects being linked to graphene's hydrophilic nature [250].

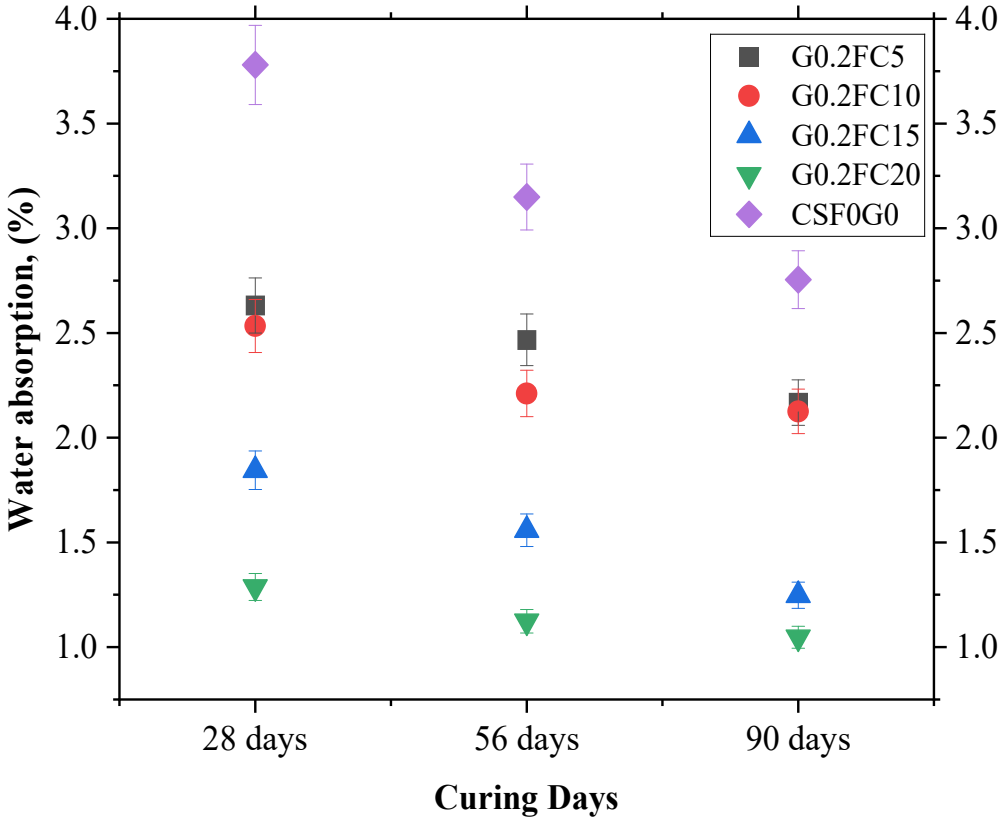

Figure 4.18 Results of total absorption for all concrete mixes with rGO and ferrock

4.3.2 Water Penetration Test

4.3.2.1 Water penetration for concrete with rGO

Water penetration test was conducted on concrete cubes of dimension 150 mm with rGO as a partial replacement of cement in ratios of 0.1%, 0.2%, 0.4%, 0.6% and 0.8% and tested at 28days, 56 days and 90 days of curing. Findings presented in the figure 4.19 below suggest that mix GC0.8 showed decrease in 47.81% and 56.33% at 28 days and 90 days of curing respectively which is lowest absorption of water among all mixes. Mix GC0.1 less improved with 9.7% and 7.84% at 28 days and 90 days of curing. Results indicate that with an increase in ratio of rGO water penetration rate is decreasing. This occurs as rGO enhances the microstructure by filling voids, improving

bonding between particles, and restricting water ingress. rGO reduces the capillary zone within the concrete composite to reduce the depth of water permeability [247]. This occurs as rGO enhances the microstructure by filling voids, improving bonding between particles, and restricting water ingress [137]. Study reported a considerable increase of compressive and FS, decrease in water permeability and at the same time enhanced electrical and thermal performance with the incorporation of graphene [250]. Thus, the mixes with rGO show less water penetration at all curing days in comparison to control mix leads to improved durability of concrete. The incorporation of 2.5% GNP bwoc in mortar significantly reduces the water penetration depth by 64%, the chloride diffusion coefficient by 70%, and the chloride migration coefficient by 31% [250].

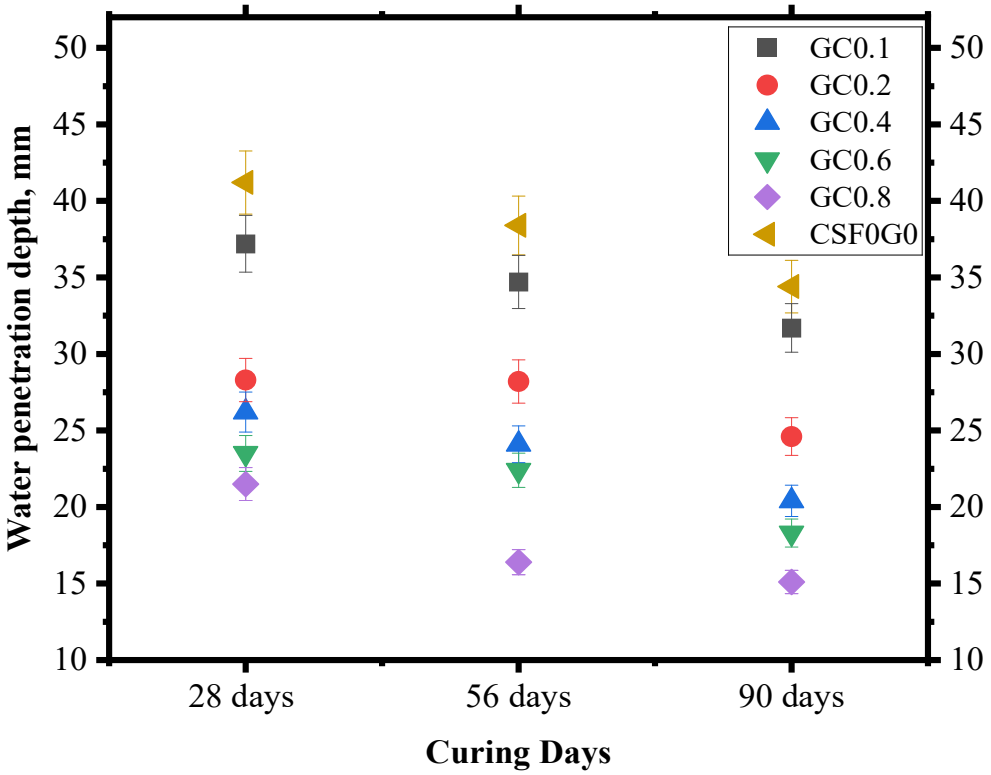

Figure 4.19 Results of water penetration for all concrete mixes with rGO

4.3.2.2 Water penetration for concrete with ferrock

Water penetration test was conducted on cubes of 150 mm with ferrock as a partial replacement of cement in ratios of 5%, 10%, 15% and 20% and tested at 28days, 56 days and 90 days of curing. Figure 4.20 presented the results of water penetration for concrete containing ferrock as partial replacement of cement. Findings interpret that 5% replacement of cement in mix FC5 has 3.88%, 9.38% and 10.78% decreased water penetration depth in comparison with the mix CSF0G0 at curing of 28, 56 and 90 days respectively. As the ratio increased to 10% in mix FC10 decreased water penetration by 18.37%, 23.67% and 16.17% as compared with mix CSF0G0 at 28, 56 and 90 curing days respectively. On increasing the ratio of ferrock in cement to 15% in mix FC15 exhibited 28.97%, 31.83% and 23.52% less water penetration depth in comparison to mix CSF0G0 at curing days of 28, 56 and 90 days respectively. On further increasing the replacement ratio of cement to 20% in mix FC20 reported 39.57%, 40% and 35.29% less water penetration as compared with mix CSF0G0 at 28, 56 and 90 days of curing respectively. Results found that with the increase in ratio of ferrock, water penetration depth is decreasing due to structure is denser and less capillary zone available as compared to control sample. The results indicate that FC20 formed the compact structure, likely due to the formation of iron carbonates that filled the micropores within the concrete matrix. The Fe_2O_3 in concrete able to fill voids in concrete to improve water permeability [251]. A study reports that the use of FA in concrete can reduce water permeability by 20% [252], with similar findings observed in another research also [253] [254] [255] [256]. When MK is used as a partial replacement of cement, it increases the long-term performance of the concrete through reduced permeability resulting in improved durability [257]. Previous studies have found a decrease in water penetration depth with an increase in LS content used as a replacement for cement [258] [259]. This is attributed to the filler effect of LS in the concrete mix. Similarly, Chen et al. [259] reported a significant reduction in water penetration depth as the LS content increased.

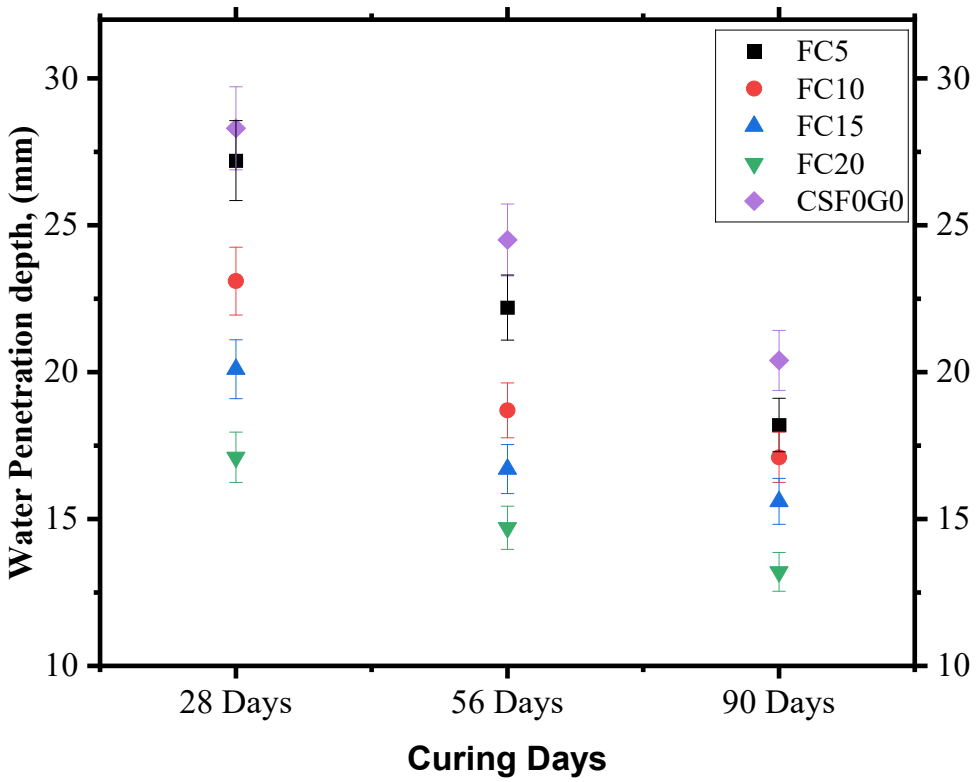

Figure 4.20 Results of water penetration for all concrete mixes with ferrock

4.3.2.3 Water penetration for concrete with rGO and ferrock together

Water penetration test was performed on hardened concrete cubes with rGO and ferrock together as a partial replacement of cement as ferrock in ratio of 5%, 10%, 15% and 20% along with rGO with constant ratio of 0.2% tested at 28days, 56 days and 90 days of curing as shown in figure 4.21. The WP depth in concrete was 1.7% lower in mix G0.2FC5 compared to CSF0G0. Increasing the replacement ratio to 10% in mix G0.2FC10 resulted in a 2.94% reduction in water penetration after 90 curing days. In mix G0.2FC15, the depth of penetration reduced by 25.98% compared to CSF0G0. After 90 days of curing, the penetration in mix G0.2FC20 was 35.29% lower than that of the control mix. The reduced degree of hydration with increasing rGO concentration may result from the aggregation of rGO sheets [260]. When the concentration of rGO is beyond the optimum threshold, the strong interlayer hydrogen bonds promote the stacking and agglomeration of rGO sheets, resulting in a significant decrease in the

interlayer distance of graphene [261]. The penetration depth for mix contains rGO and ferrock combined decreased because the composite was dense and compacted to reduce the pores to limit the penetration of water. Results conclude that this combination works effectively and there was significant difference in penetration depth. The results indicate that G0.2FC20 formed the compact structure, likely due to the formation of iron carbonates that filled the micropores within the concrete matrix. The incorporation of FA, MK, and LS resulted in a denser and more compact microstructure [195]. The study found that MK reduces the width of microcracks at the microstructural level and promotes the formation of secondary C-S-H gel, thereby reducing pore size [96]. Using LS to replace 0–8% of cement pastes significantly reduced the water permeability of concrete, primarily due to its filler effect. LS filled the pores, refined the pore structure, and decreased the permeable pores ultimately reduction in water penetration depth [262].

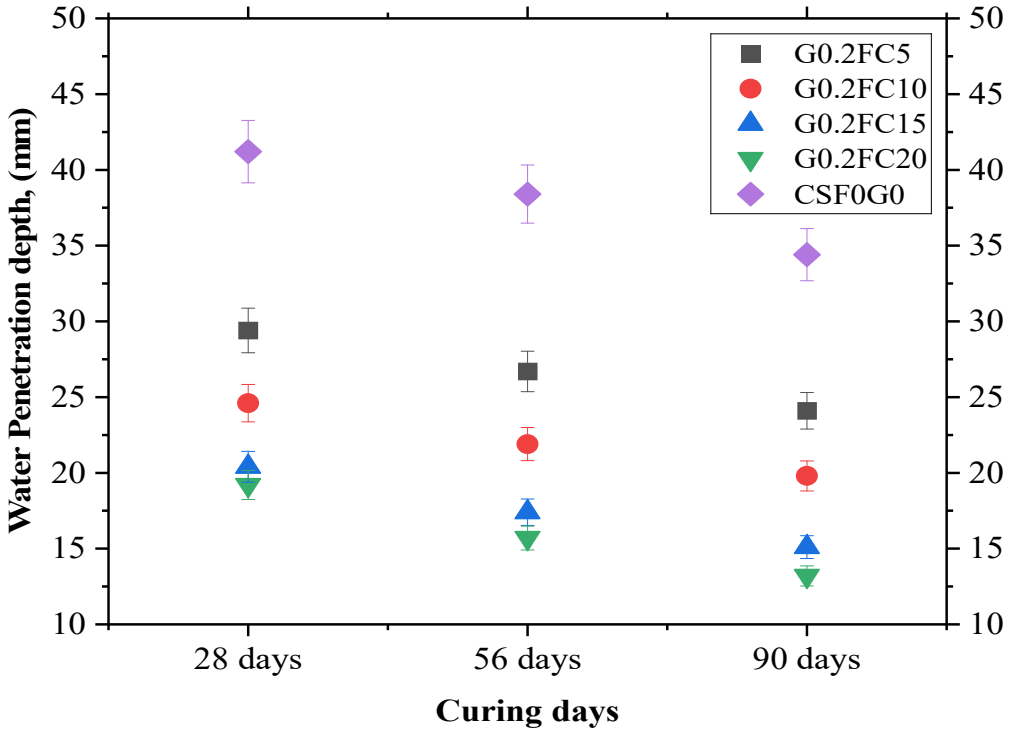

Figure 4.21 Results of WP for all concrete mixes with rGO and ferrock together

4.3.3 Initial Surface Absorption Test (ISAT)

4.3.3.1 ISAT for concrete with rGO

The ISAT was conducted on 150 mm concrete cubes with rGO as a partial replacement of cement in ratios of 0.1%, 0.2%, 0.4%, 0.6% and 0.8% and tested at 28days, 56 days and 90 days of curing. Findings presented in the figure 4.22 below suggest that cubes of mix GC0.8 decrease penetration depth by 26.56% and 26.78% at 28 days and 90 days of curing respectively which is the lowest surface absorption of water among all mixes. Mix GC0.1 exhibited less improvement with 3.1% and 7.1% followed by GC0.2, GC0.4, GC0.6 and GC0.8 at 28 days and 90 days of curing. Results indicate that with the increase in ratio of rGO surface absorption rate is decreasing. This is because of the decrease in pores inside the concrete matrix as rGO act as a filler and make structure dense [123]. The mixes with rGO show reduction in surface absorption as compared to control sample. A clear surface absorption reduction was observed by increasing rGO% with curing days. Because rGO fills voids at the nanoscale and increases density to restrict the pathways of water infiltration at specific intervals of time, the mixes containing rGO have therefore demonstrated lower surface absorption for the curing age when compared to CSF0G0. High density also implies that the concrete has better interlocking and cohesion which resists the water absorption [68]. With the inclusion of GO, the number of pores is greatly reduced, and the corresponding hydration products are closely inter woven and form a more compact structure compared to that of cement mortar without GO [263].

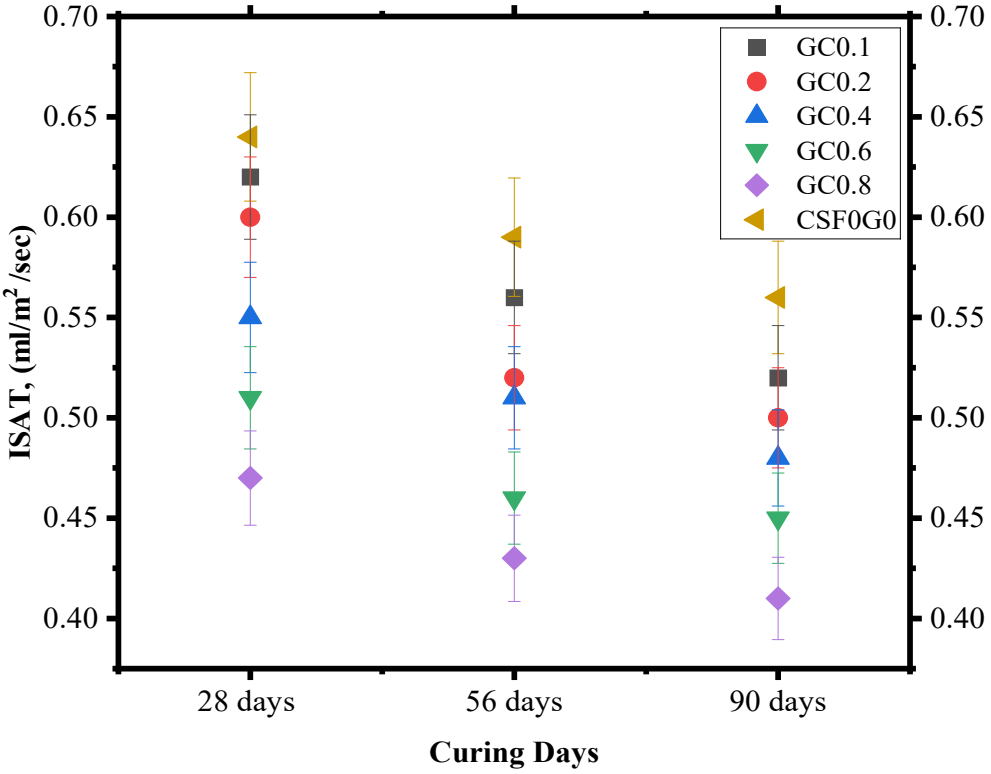

Figure 4.22 Results of ISAT for all concrete mixes with rGO

4.3.3.2 ISAT for concrete with ferrock

The ISAT was performed on hardened concrete cubes with ferrock as a partial substitute of cement in ratios of 5%, 10%, 15% and 20% and tested at 28days, 56 days and 90 days of curing. Figure 4.23 illustrates the results of ISAT for concrete containing ferrock. The results indicate that 5% replacement of cement in mix FC5 indicates 17.18%, 11.86% and 8.92% decreased absorption in comparison with the mix CSF0G0 at 28, 56 and 90 curing days respectively. As the replacement ratio increased to 10% in mix FC10 resulted in decrease of surface absorption by 23.43%, 20.33% and 19.64% as compared with mix CSF0G0 at 28, 56 and 90 days of curing respectively. On increasing the replacement of cement to 15% in mix FC15 indicate 26.56%, 23.72% and 23.21% less surface absorption in comparison with mix CSF0G0 at 28, 56 and 90 days of curing respectively. On further increasing the replacement of cement to 20% in mix FC20 the surface absorption decreased by 32.81%, 28.81% and 26.78% in

comparison with mix CSF0G0 at 28, 56 and 90 days curing days respectively. Results indicate that with an increase in ratio of ferrock, surface absorption is decreasing as ferrock makes structure denser and more compacted. As it contains other pozzolanic materials also i.e., FA, MK and LS to enhance the product formation and improve the microstructure of concrete matrix. Ferrock improved concrete's water resistance, while the control sample consistently had greater absorption values. This indicates a steady improvement in the concrete's water resistance as curing progresses. The iron particles have rough surface and angular shape to provide better binding ability with aggregates and other materials results in denser concrete matrix. Other materials with fine particles size such as MK, LS and FA act as filler for micro pores in concrete composite [123]. When FA and MK are used together in concrete, their combination may impair performance due to insufficient $Ca(OH)_2$ generation required for C-S-H formation in the concrete matrix, resulting in unreacted silica particles and potential strength reduction [264]. Muthaiyan and Thirumalai [265] observed that the replacement of class C FA (10–20%) reduced about 12–16% of the total voids compared to the control mix. It could be due to the micro-filler influence of FA. The filler effect of LS refined and improves the porosity of the mix and in general terms results in lowering the water demand for a given workability [203].

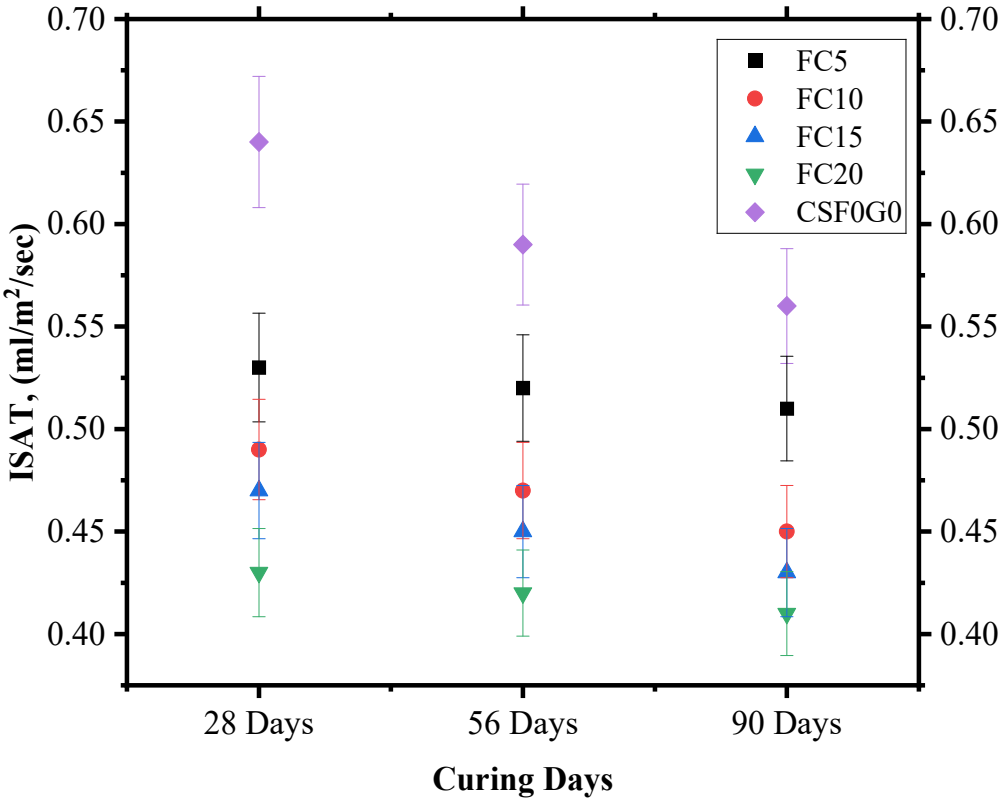

Figure 4.23 Results of ISAT for all concrete mixes with ferrock

4.3.3.3 ISAT for concrete with rGO and ferrock together

ISAT was conducted on concrete cubes with rGO and ferrock as a partial replacement of cement as ferrock in ratio of 5%, 10%, 15% and 20% and rGO with constant ratio of 0.2% tested at 28days, 56 days and 90 days of curing. Figure 4.24 shows the results of ISAT for concrete containing rGO and ferrock together. The G0.2FC5 mix indicates a 17.85% reduction in surface absorption at 90 curing days. With an increase in the ferrock ratio to 10% in the G0.2FC10 mix, the surface absorption measured 23.21% at 90 days of curing. Upon further raising the ferrock ratio to 15% in mix G0.2FC15, the absorption decreases to 30.35%. The replacement ratio in mix G0.2FC20 increased to 20%, resulting in a decrease of surface absorption of 35.71% at 90 days of curing. The reduced water absorption in the mixtures containing rGO attributed to the addition of micro voids and the reduction of capillary porosity

[266]. The improvements resulted from the formation of strong C–S–H bonds by the incorporation of rGO flakes into the mixture. Excessive rGO content may interfere with the binder's hydration process, as shown by the hydration degree results. The dense network formed by aggregated rGO particles may hinder water transport and block hydration activities [68]. The delay in the formation of cementitious compounds may result in reduced strength development and overall effectiveness of the concrete. Ferrock improved concrete's water resistance, while the control sample consistently had greater absorption values. This indicates a steady improvement in the concrete's water resistance as curing progresses. Overall, the findings suggest that adding more ferrock leads to progressively denser and less permeable concrete, with the 20% ferrock replacement offering the most significant reduction in absorption of water.

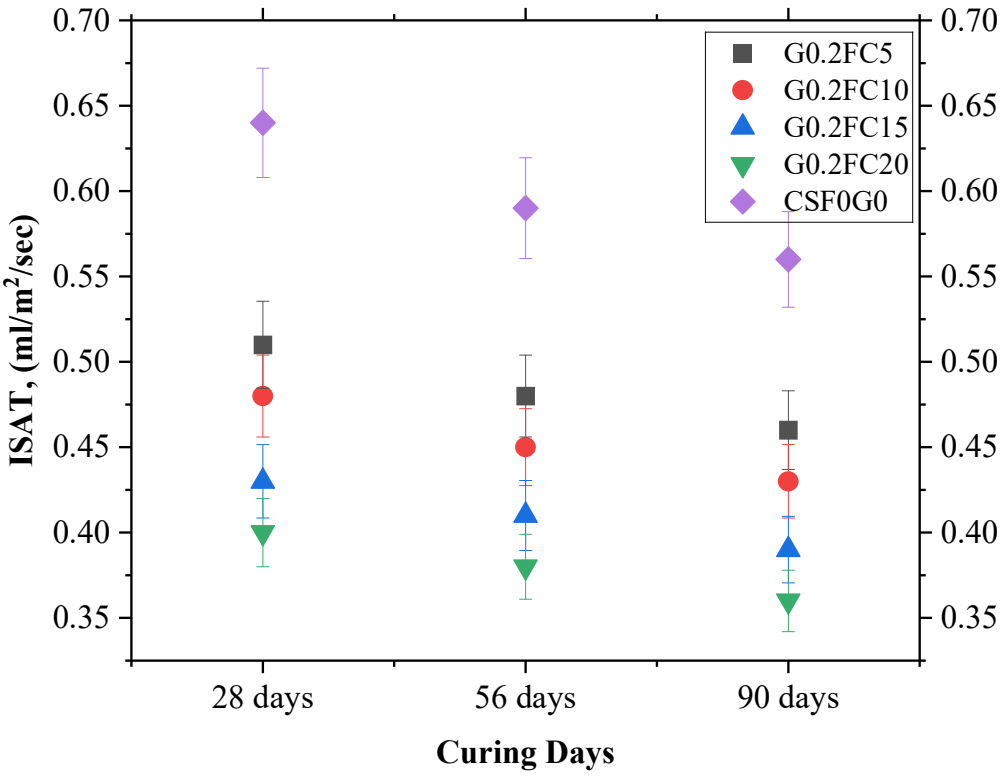

Figure 4.24 Results of ISAT for all concrete mixes with rGO and ferrock

4.3.4 Rapid Chloride Penetration Test

4.3.4.1 RCPT for concrete with rGO

The RCPT conducted on a concrete circular disc extracted from cylinder prepared with rGO as a partial replacement of cement in ratios of 0.1%, 0.2%, 0.4%, 0.6%, 0.8% and tested at 28days, 56 days and 90 days of curing. According to ASTM C1202 [181], the results were categorized based on the total charge passed through the samples: high permeability (>4000 coulombs), moderate permeability (2000–4000 coulombs), low permeability (1000–2000 coulombs), and very low permeability (<1000 coulombs). Findings as reported in the figure 4.25 below suggest that mix GC0.6 decrease chloride penetration by 21.07% and 55.89% at 28 days and 90 days of curing respectively, which is the lowest chloride penetration among all mixes. The mix CSF0G0 lies in range of moderate penetration and optimum ratio is 0.6% rGO lies in category of very low penetration of chloride at 90 days of curing. The mix GC0.6 indicates the lowest penetration of chloride followed by GC0.4, GC0.1, GC0.2 and GC0.8 at 90 days of curing. GC0.1 lies in category of moderate penetration of chloride and at 28 days of curing it lies in the same category with less chloride penetration but at 90 days of curing it reduces to low penetration. All mixes with rGO showed reduce chloride penetration in concrete in comparison with control sample. The optimum ratio of rGO was 0.6% after that chloride penetration slightly increased maybe because rGO starts agglomerates at some places irrespective of uniform distribution. The concrete's pore size is the essential key to its resistance to chloride-ion permeability. As previously indicated, because of the filling of nanoscale particles, rGO reduces porosity by blocking or stopping transit in addition to refining the structure to generate safe pores [68]. Conversely, rGO tends to agglomerate, which enhances its ability to react with $Ca(OH)_2$, leading to increased formation of additional C-S-H and improved development of microcrystalline structures that resist ion migration [247]. The high surface area and two-dimensional structure of GO fill in the voids and capillary pores in the concrete, leading to a more compact and less porous microstructure. The denser concrete matrix provides better resistance against abrasive forces and reduces surface wear [267]. Therefore, adding GO to concrete enhances its durability properties regarding abrasion resistance. The reduced porosity, improved strength, and enhanced

microstructure resulting because of GO incorporation [268]. With the increase in GO, the reduction in the charge passing through the mixes was probably because of the interconnected layers of GO and its ability to hold the chloride ions. Moreover, this reduction in the penetration depth of chloride ions was because of the formation of sponge-like structure, arising from well packed GO particles [269].

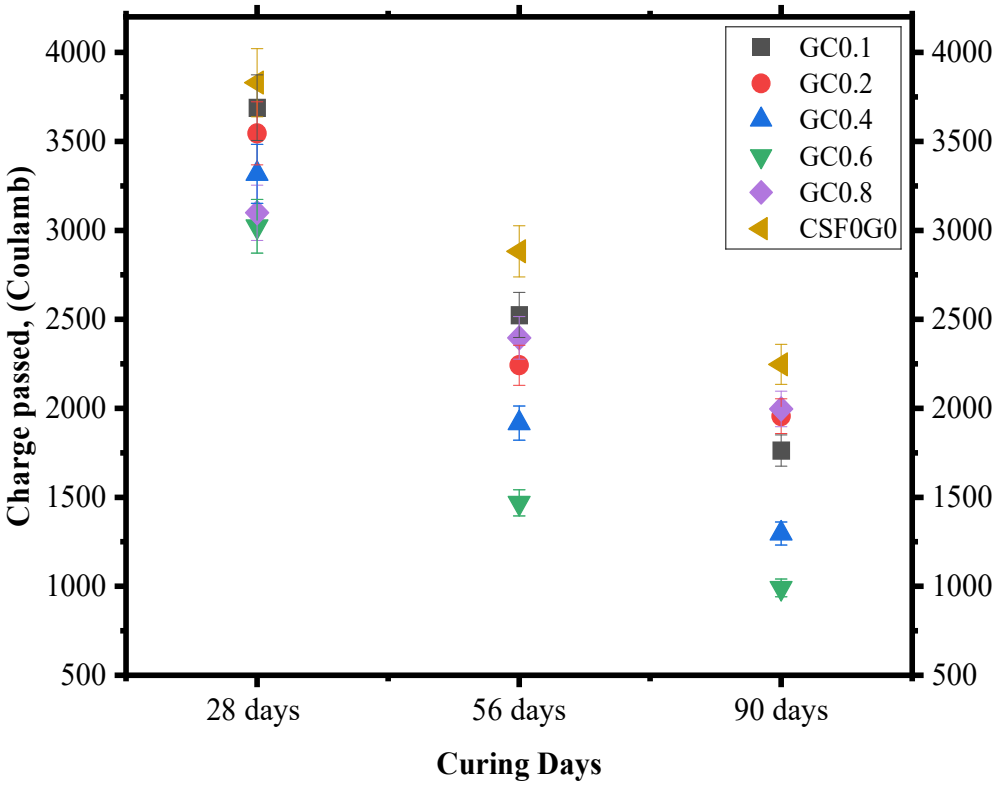

Figure 4.25 Results of RCPT for all concrete mixes with rGO

4.3.4.2 RCPT for concrete with ferrock

RCPT performed on the hardened concrete samples with ferrock as a partial replacement of cement in ratios of 5%, 10%, 15%, 20% and tested at 28days, 56 days and 90 days of curing. At 5% replacement of cement in mix FC5 showed 40.19%, 42.83% and 48.33% lower chloride penetration in comparison with the mix CSF0G0 at curing of 28, 56 and 90 days respectively. Findings presented in the figure 4.26 below suggest that the mix FC10 reported decrease in 48.5% and 58.12% at 28 days and 90 days of curing respectively which is the lowest chloride penetration among all mixes. The mix CSF0G0 lies in range of moderate penetration and the optimum ratio is 10% ferrock lies in category of very low penetration of chloride at 90 days of curing. On increasing the replacement of cement to 15% in mix FC15 reduced chloride penetration by 43.19%, 49.27% and 53.31% in comparison to the mix CSF0G0 at curing at 28, 56 and 90 days respectively. Mix FC20 has less improvement with 33.62% and 41.94% at 28 days and 90 days of curing. CSF0G0 lies in category of moderate penetration of chloride and at 28 days of curing it lies in the same category with less chloride penetration but at 90 days of curing it reduces to very low penetration. This is because of pozzolanic materials present in ferrock along with the product formed by the reaction of IO and CO_2. Results suggest that ferrock improve the durability of concrete in terms of chloride penetration by reducing it. The results conclude that incorporating ferrock into concrete significantly improves its resistance to chloride penetration, with the 10% ferrock replacement in mix FC10 providing the most effective performance. At every stage of curing, this ratio achieves the lowest chloride penetration values because it hits the ideal balance between matrix densification and pozzolanic activity. Higher replacement ratios, such as 15% and 20%, although beneficial, do not perform as well as the 10% ratio, due to the greater amount of silica present in ferrock affecting the concrete's overall performance. Thus, a 10% ferrock replacement is recommended for enhancing concrete durability in chloride-exposed environments. Replacing cement paste with LS reduced the chloride diffusion coefficient due to its filler and nucleation effects, which refined the concrete's pore structure [165] [270].

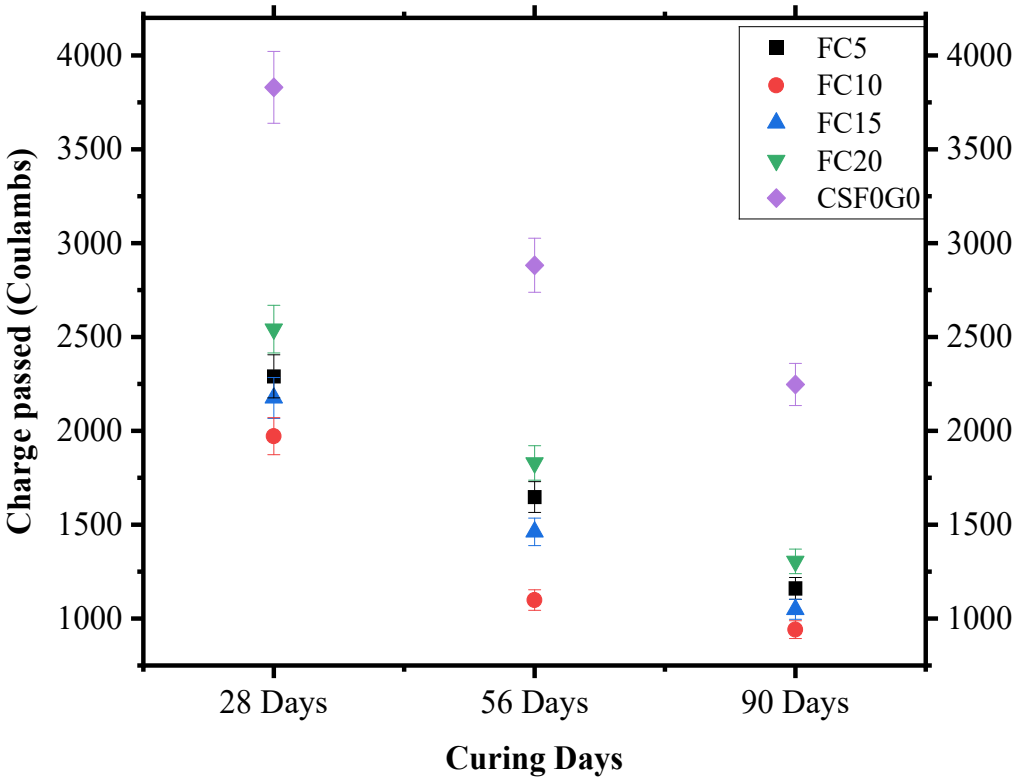

Figure 4.26 Results of RCPT for all concrete mixes with ferrock

4.3.4.3 RCPT for concrete with rGO and ferrock together

RCPT conducted hardened concrete samples with rGO and ferrock together as a partial replacement of cement as ferrock in ratio of 5%, 10%, 15% and 20% and rGO with constant ratio of 0.2% tested at 28days, 56 days and 90 days of curing. The penetration of chloride decreased by 64.75% in mix G0.2FC5 at 90 days of curing. Findings, reported in the figure 4.27 below, suggest that mix G0.2FC10 decrease the chloride penetration by 68.9% and 72.47% at 28 days and 90 days of curing respectively, which is the lowest chloride penetration among all mixes. The mix CSF0G0 lies in range of moderate penetration, and the optimum ratio is 10% ferrock lies in category of very low penetration of chloride at 90 days of curing. By increasing the replacement ratio to 10% in mix G0.2FC10, chloride penetration decreased by 72.47% compared to the control mix. On further increasing the ratio of ferrock in mix G0.2FC15 exhibited chloride penetration reduction of 68.06% compared to CSF0G0.

Mix G0.2FC20 indicate less improvement with 40.15% and 57.52% on 28 days and 90 days of curing. CSF0G0 lies in category of moderate penetration of chloride and at 28 days of curing it lies in the same category with less chloride penetration but at 90 days of curing it reduces to very low penetration. All mixes with ferrock lie in the category of very low chloride penetration at 90 days of curing with lowest value of G0.2FC10, followed by G0.2FC15, G0.2FC5 and G0.2FC20. The results suggest that the combination of rGO and ferrock showed good results by improving the durability of concrete as rGO fills the pores and ferrock to make denser structure and its pozzolanic material enhance the product formation [73]. The increase in hydration level is attributed to the interaction between rGO sheets and the paste constituents. rGO has many active functional groups, such as carboxyl, hydroxyl, and epoxy groups [141]. The increase in chloride penetration on further addition of GO was due to the further densification of the pore structure [271]. These functional groups may engage in chemical interactions with the clinker in cement, leading to a strong bond between graphene and cementitious materials. The thermal conductivity of rGO improves heat transfer, accelerating the hydration process and ultimately resulting in the formation of a dense structure during hydration [38]. The results conclude that incorporating ferrock into concrete significantly enhances its resistance to chloride penetration, with a 10% ferrock replacement in mix G0.2FC10 providing the most effective performance. This ratio achieves the lowest chloride penetration values at every curing stage due to the ideal balance between matrix densification and pozzolanic activity. Higher replacement ratios, like 15% and 20%, do not perform as well due to silica content.

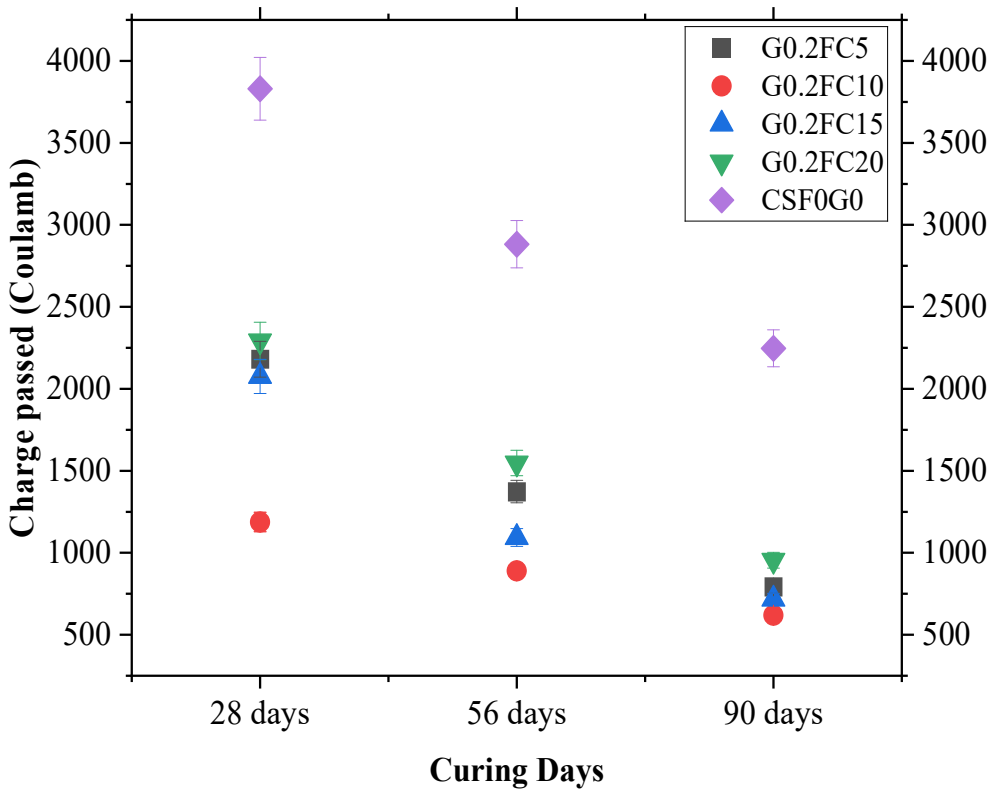

Figure 4.27 Results of RCPT for all concrete mixes with rGO and ferrock

4.4 Microstructural Analysis

4.4.1 Control mix

The microstructure analysis was performed for samples of mix CSF0G0 to compare results with other mixes. Figure 4.28 illustrates the results of SEM, XRD and EDS analysis at 28 days of curing. SEM analysis visualizes micropores in mix which make it porous matrix. Also, the visible morphology of control mix compared with the other SEM images of other mixes. The XRD analysis found major peaks of SiO_2, $Ca(OH)_2$ and C-S-H which are responsible for strength of concrete. The EDS analysis found elemental composition of samples with sharp peaks of Ca and O. The analysis identified key elements including C, oxygen (O), aluminum (Al), Si, Ca, iron (Fe), sodium (Na) and magnesium (Mg), with varying intensities that reflect their distribution within each mix. Elemental mapping visualizes distribution of all elements in particular sample found presence of Ca evenly in entire sample.

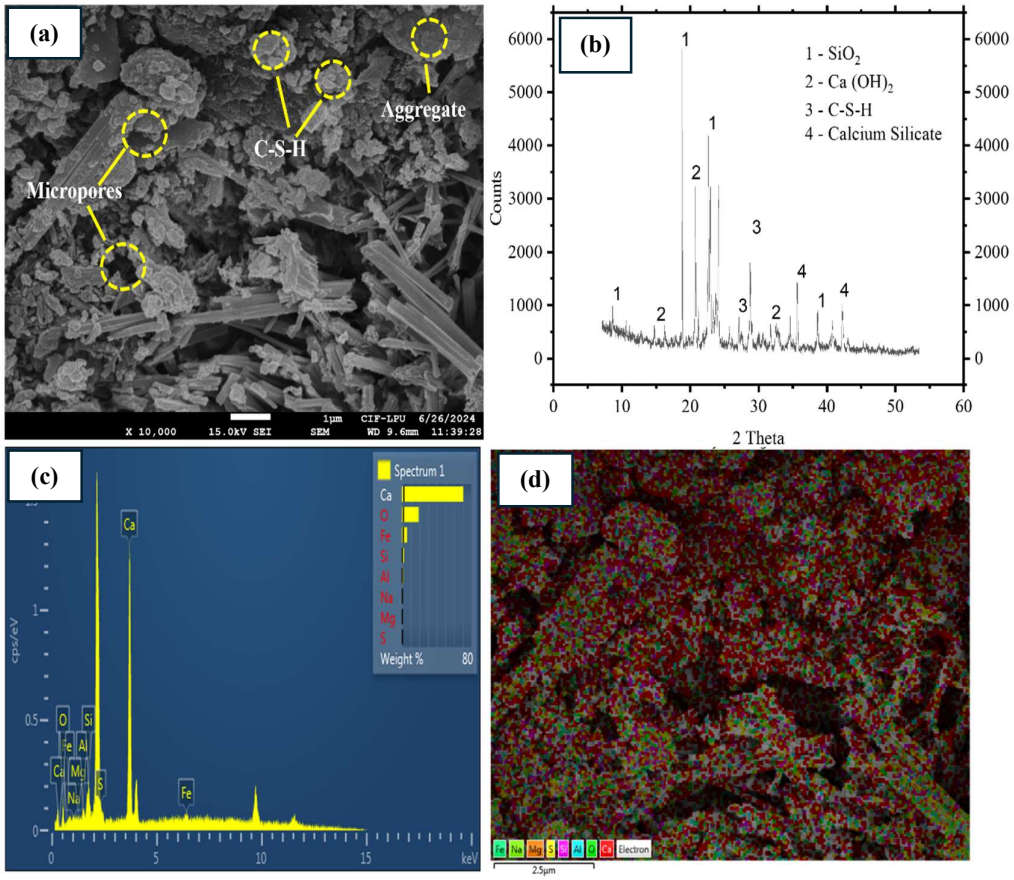

Figure 4.28 Microstructural analysis of control sample by (a) SEM, (b) XRD, (c) EDS peaks and (d) elemental mapping

4.4.2.1 SEM for concrete with rGO

The concrete samples from the mixes were finely ground and examined under SEM to visualize zoomed morphology and to compare with control samples. Figure 4.29 presents the SEM analysis results of mixes GC0.2 and GC0.1, comparing the morphology of mix with the highest strength and the mix with the lowest strength at 28 days of curing. The surface texture, roundness and smoothness of particles are visible in samples. The concrete mix with rGO represents denser and compacted structure when compared with control mix. The results present a clear picture of agglomerations which accumulate together to form clusters on surface. Previous study observed 0.02%

rGO to have dense platy cement hydrates associated with pores and hydrated crystals continue to become complex-stacking one over the other, massive and thicker. However, the microstructure of concrete mix with 0.06% GO inclusion undergoes significant improvement with densified hydrated crystals and lesser pores compared to mix with 0.04% and 0.08% GO content which attributed to C–S–H formation in conjunction with C–H platy crystals and ettringite (fibrous and needle shape crystals). With varying rGO concentration in the concrete composites, the hydrated crystals keep getting more complex stacking one on top of the other, huge, and thicker due to the nucleation effect of rGO on C–S–H [266]. The stronger bonding between rGO and cement paste, along with the hydrophilic groups on rGO's surface attracting hydration products, promotes crystal growth by acting as nucleation sites [272]. At the optimum replacement ratio in mix GC0.2, the microstructure of the concrete becomes denser. However, exceeding this ratio leads to agglomeration, which acts as a barrier, hindering water penetration and resulting in an irregular structure which ultimately causes a reduction in strength.

Lu et al. [271] confirmed the reaction between C–S–H of the cement matrix and carboxylic acid of GO, confirming the presence of hydration products. Furthermore, the acceleration of the hydration process was seen when GO reacts with $Ca(OH)_2$, thus producing C–S–H. It helped in enhancing the mechanical properties as resulted in a denser-more compact structure at a microscopic level with minimum amounts of $Ca(OH)_2$ crystals [273]. Thus, it can be concluded that GO acts as good reinforcing material in concrete. With 0.05 wt% GO, a variety of hydrates interwove with one another, forming a dense and uniform structure. Yet, there were large pores and cracks around with a small amount of flocculent C–S–H gel scatted on the surface. These pores and cracks should be the cause of the strength degeneration of GO–cement composites [132]. GO sheets can bridge cracks in the cement paste by acting as nano- reinforcement which finally inhibits crack propagation and enhances the overall durability of the concrete matrix [274]. GO can act as a nucleation site for hydrating crystals in GO. incorporated concrete. Therefore, hydration reactions continuously occur on the GO surface, forming numerous small C-S-H crystals attached to the GO surfaces [191]. GO can also serve as a growth template for C-S-H crystals, guiding their growth in specific

directions and facilitating additional growth and attachment of C-S-H crystals on the same GO surface because of this template effect. The oxygen functional groups on GO can interact with Ca 2+ ions, finally facilitating the formation of flower-like structures during the crystal growth process. When considering the SEM image of the GO-added concrete mix, it can be observed that the GO concrete microstructure has many flower-like hydration crystals attached to GO layers, and this has not been observed in the control mix. The concrete sample with GO has fewer pores within the microstructure than the control mix. This is due to the flower-like hydration crystals in GO-added concrete growing in the voids of the concrete matrix and decreasing concrete porosity from the nano-filling effect of GO [274]. After analyzing these SEM observations, a clear relationship exists between microstructural characteristics and mechanical properties of GO-incorporated concrete. The presence of GO leads to a refined microstructure, reduced crack propagation, decreased porosity, fewer pores, and the development of fully bloomed flower-like crystal formations.

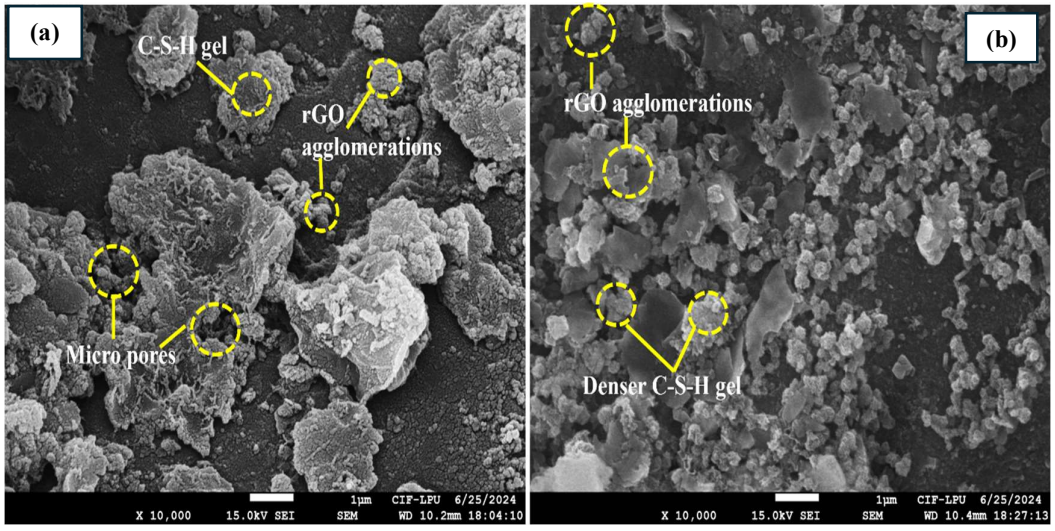

Figure 4.29 SEM images of mix (a) GC0.2 and (b) GC0.8

4.4.2.2 SEM for concrete with ferrock

The figure 4.30 presents the results of SEM analysis for mix FC5, FC10, FC15 and FC20 at 28 days of curing with 4 days of CO_2 curing at initial days. SEM analysis was done to visualize the impact of ferrock on microstructure of concrete matrix and results are presented in figure 4.30. As structure seems to be denser and more compacted for all mixes with ferrock. The mix FC5 illustrates microstructure with presence of voids to make microstructure porous. The morphology of mix FC10 looks quite denser than FC5 with pores in it. The surface of concrete seems compacted by increasing the ratio of ferrock in concrete. Result specifies the availability of denser C-S-H gel than control sample with amorphous phases of calcite and aragonite. However, improving the duration of CO_2 curing could sufficiently enhance the homogeneity of the carbonated specimens. The refinement in pore structure is due to the presence of micro-fillers in ferrock which significantly fills the gap between cement particles and supports pozzolanic reactions at later stages. It is clear from the micrographs that there are important hydrated phases present including portlandite, calcite and C-S-H. These phases are crucial for understanding the process of hydration and bonding between concrete matrixes. The analysis indicates that the structure of the concrete composite in these mixes is denser and more compact. Nevertheless, despite noticeable increase in density, the bonding between particles appears to be less than ideal. The images obtained from the SEM show the existence of pores that are extensively dispersed throughout the concrete matrix as well as the spread of hairline cracks. These imperfections suggest that while the concrete mixes exhibit increased density, there are notable issues with the internal cohesion and overall structural integrity. The observed hairline cracks and porous regions may affect the durability and strength of the concrete.

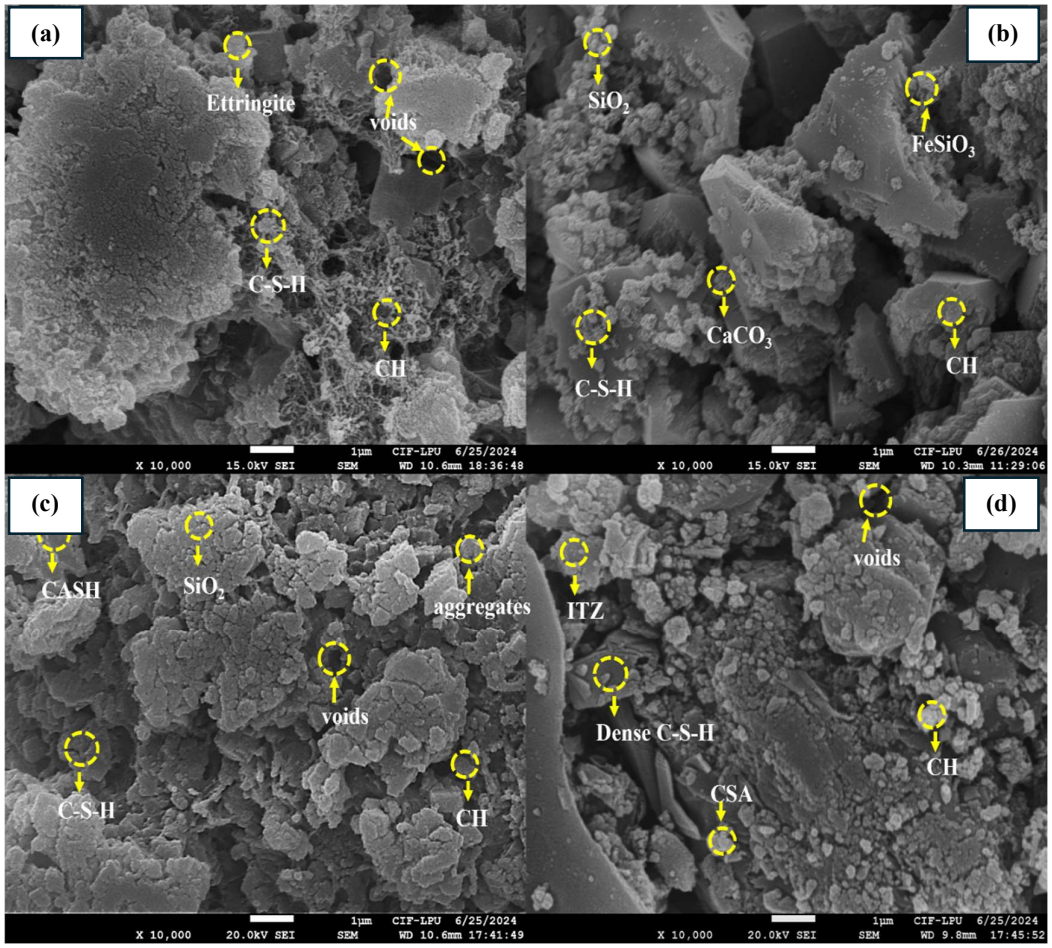

Figure 4.30 SEM images of mix (a) FC5, (b) FC10, (c) FC15 and (d) FC20

4.4.2.3 SEM for concrete with rGO and ferrock together

The visual representation of zoomed microstructure of concrete mix with partial replacement of cement with ferrock in ratio of 5%, 10%, 15% and 20% and rGO with constant ratio of 0.2% analyzed at 28 days of curing. Figure 4.31 presents the results of SEM analysis for the mix G0.2FC5, G0.2FC10, G0.2FC15 and G0.2FC20. Results show agglomeration of rGO on the surface when in excessive quantity. The mixes with ferrock show denser and more compacted structure than control sample. Results observed to have dense concrete composites with less pores which were improved as compared with CSF0G0 and with the mixes rGO and ferrock individually. The microstructure of control samples has pores and lower density because of less settlement of aggregates of less mechanical strength. Image of mix G0.2FC10 observed

to have denser and uniform structure because of large surface area of rGO filling the micropores and ferrock produces carbonates to fill larger pores leading to improvement in strength. Mix G0.2FC10 showed the hydrated crystals keep getting more complex stacking one on top of the other, huge, and thicker due to the nucleation effect of rGO on C–S–H. The stronger bonding between rGO and cement paste, along with the hydrophilic groups on rGO's surface attracting hydration products, promotes crystal growth by acting as nucleation sites. At the optimum replacement ratio, the microstructure of the concrete becomes denser. However, exceeding this ratio leads to agglomeration, which acts as a barrier, hindering water penetration and resulting in an irregular structure as shown in figure 4.31 causes a reduction in strength. It has been found that the addition of graphene enhances the hydration of cement, which makes the C-S-H crystal matrix denser [275]. GNP [276] is seen as an emerging nanomaterial [70] [33] [277] for use in cement composites as in increases the mechanical, durability, and sensing properties. In the context of hardened cement paste, the primary binder of the cement hydration process is the CSH gel (C-S-H: 3CaO.2SiO 2 .4 H 2 O), which is responsible for the strength gain of concrete [278] [279]. When introducing GO into the concrete matrix, it interacts with the cement hydration products within the microstructure. In GO-added concrete, the microstructure contains randomly distributed GO sheets [280]. The oxygen functional groups attached to these GO sheets have the potential to interact with cement hydration products. Specifically, the Ca ions (Ca^{2+}) within the C-S-H structure create covalent bonds with the oxygen functionalities of GO, which is known as the intercalation effect. Consequently, C-S-H crystals attached to one GO sheet interact with neighboring GO sheets. This interaction forms a three-dimensional grid structure connected by the -COO-Ca-OOC- component, which finally performs a high-density C-S-H gel within the concrete microstructure [70].

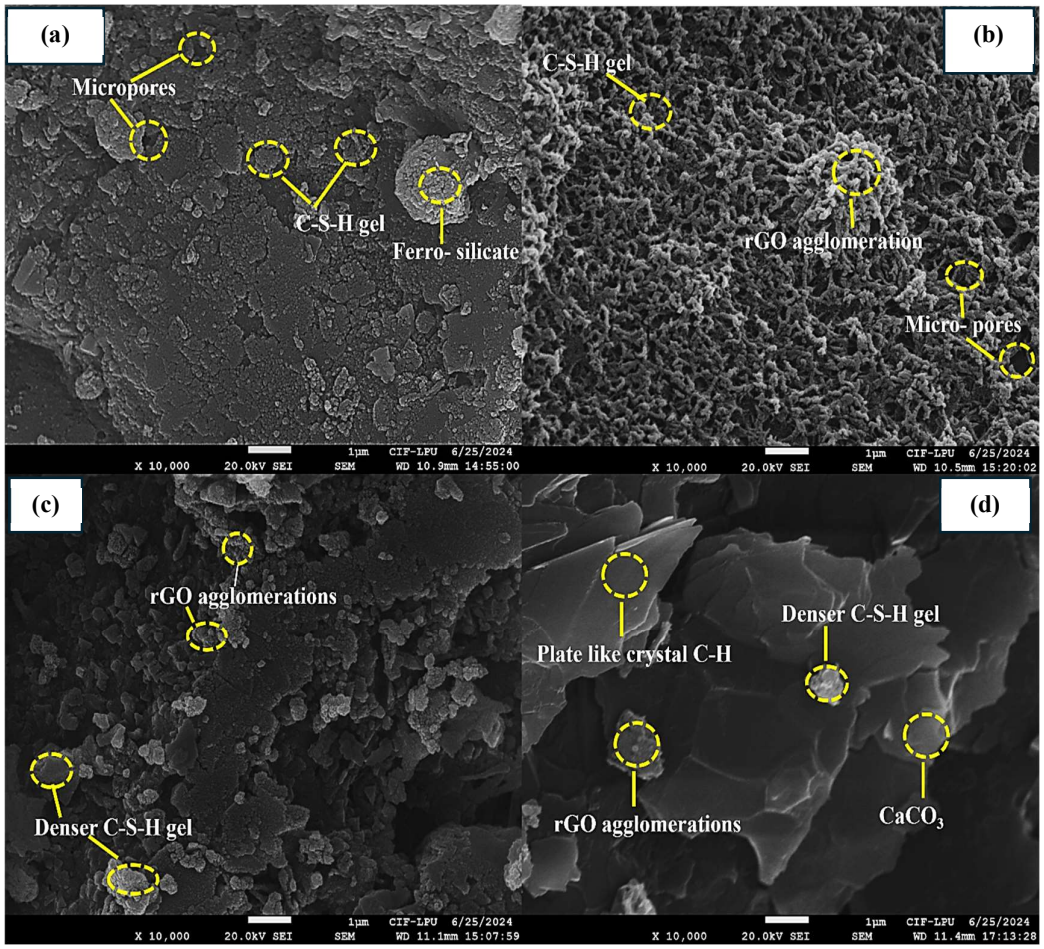

Figure 4.31 SEM images of mix (a) G0.2FC5, (b) G0.2FC10, (c) G0.2FC15 and (d) G0.2FC20

4.4.3 EDS Results

4.4.3.1 EDS for concrete with rGO

Analysis aims to find elemental composition of concrete mixes with or without rGO as elements present in concrete impacts mechanical strength and durability. The results are reported in table 4.1 below along with mix notation. EDS analysis was performed for highest strength and lowest strength mixes by mix GC0.2 and GC0.1 respectively at 28 days of curing. The Ca/Si ratio for control mix was found to be higher than other mix which specifies the hydrated products of the late stage of hydration. The Ca/Si ratio of mix GC0.2 is 2.18 which is less than the mix GC0.1 indicating the rapid

formation of C-S-H and C-H contributes to development of strength [281]. The minimum strength achieved by the mix GC0.1 which has a Ca/Si ratio 4.08 which is lower, the reason to achieve lower strength. Findings conclude that rGO, with 0.1%, helps unreacted cement particles to hydrate at later age which affect the mechanical and durability properties. The figure 4.32 provides visual representation of peaks of minerals with elemental distribution in concrete mix. Figure 4.32 presented EDS peaks of mix (a) GC0.2 and (c) GC0.1, with elemental mapping of mix (b) GC0.2 and (d) GC0.1.

Table 4.1 Elemental composition of concrete mixes with rGO

Elements (wt%)	C	O	Mg	Al	Si	Ca	Fe	Na
CSF0G0	0	19.26	0.07	1.51	2.44	70.62	5.81	0.27
GC0.2	21.07	30.4	0	2.11	12.68	27.74	1.11	0
GC0.1	13.26	40.43	0	5	8.13	33.19	1.5	0

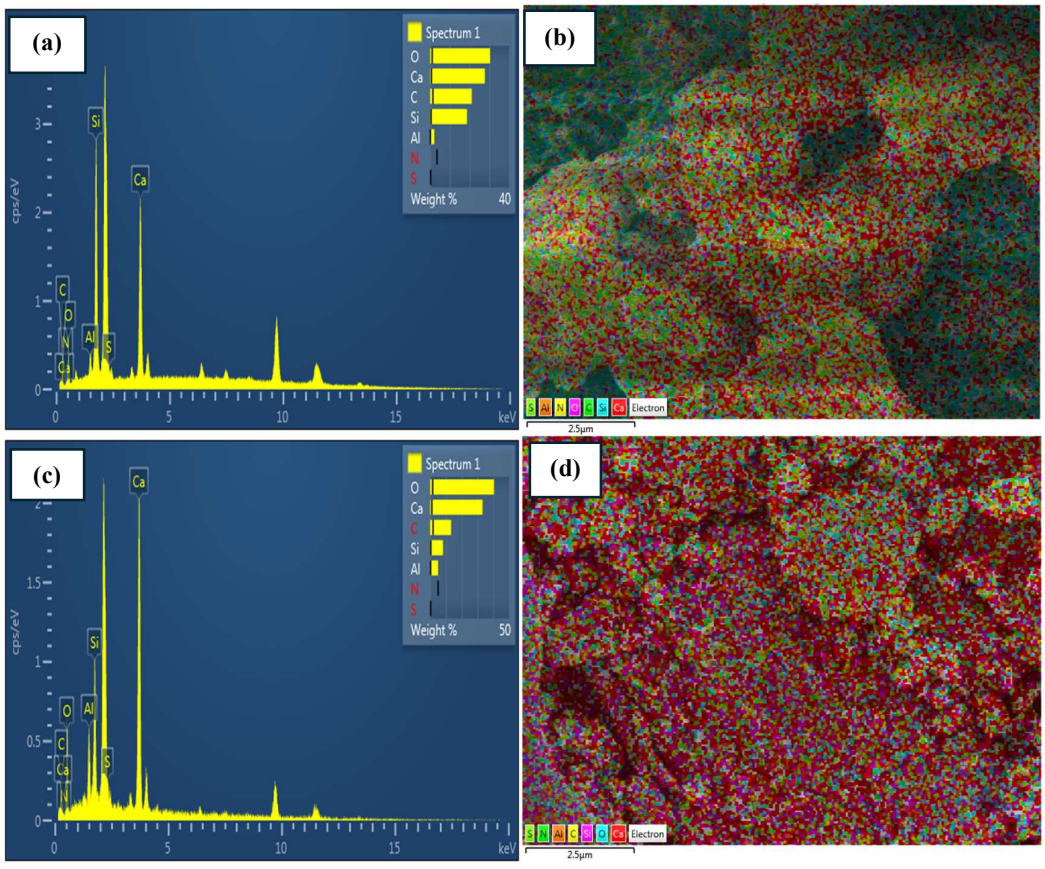

Figure 4.32 EDS peaks of mix (a) GC0.2 and (c) GC0.1, with elemental mapping of mix (b) GC0.2 and (d) GC0.1

4.4.3.2 EDS for concrete with ferrock

Analysis aims to determine elemental composition of concrete mixes with or without ferrock as elements present in concrete impacts mechanical strength and durability. The results are presented in table 4.2 below along with mix notation. The control mix exhibits the highest iron content, while the mix with the highest achieved strength has the lowest iron content. This reduction in iron content attributed to CO_2 curing, which facilitates the conversion of IO into iron carbonates, enhancing hardening and binding effects. Additionally, there was a notable increase in the presence of silica in the mixes compared to CSF0G0. The increase in silica contributes to the observed enhancement in the concrete's strength. Figure 4.33 (a), (b), (c) and (d) shows the peaks of elements present along with distribution of elements in figure 4.33 (e), (f), (g), (h) in concrete mix FC5, FC10, FC15 and FC20 respectively . The distribution of iron shows that with increasing CO_2 curing days it reduces the iron content. Results concluded that the ferrock concrete contains the necessary elements required for pozzolanic reaction. The Ca/Si ratio is lowest for mix FC10 which is one of the reasons for achieving highest strength improvement among all mixes. The lower value of Ca/Si indicated fast and more formation of CSH and CH results in improvement in properties [281].

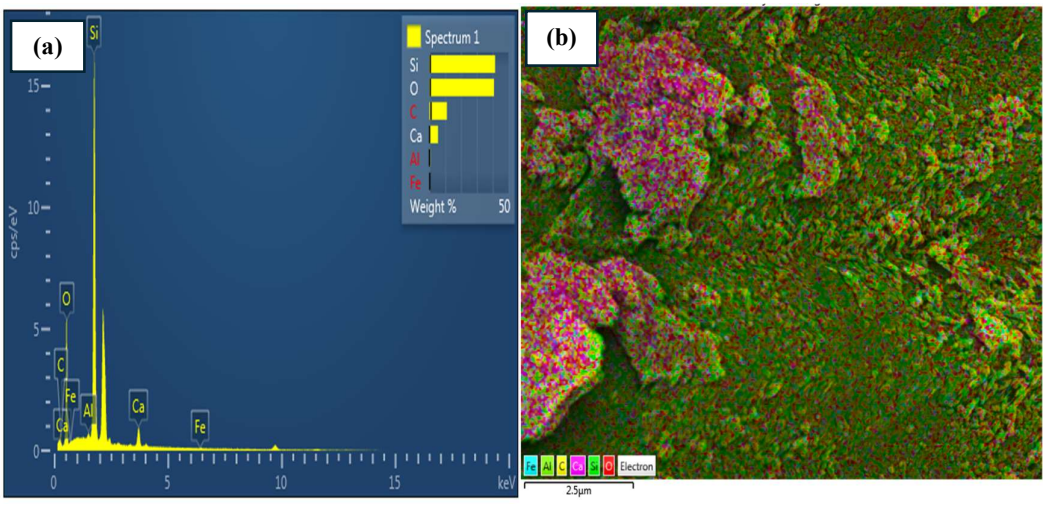

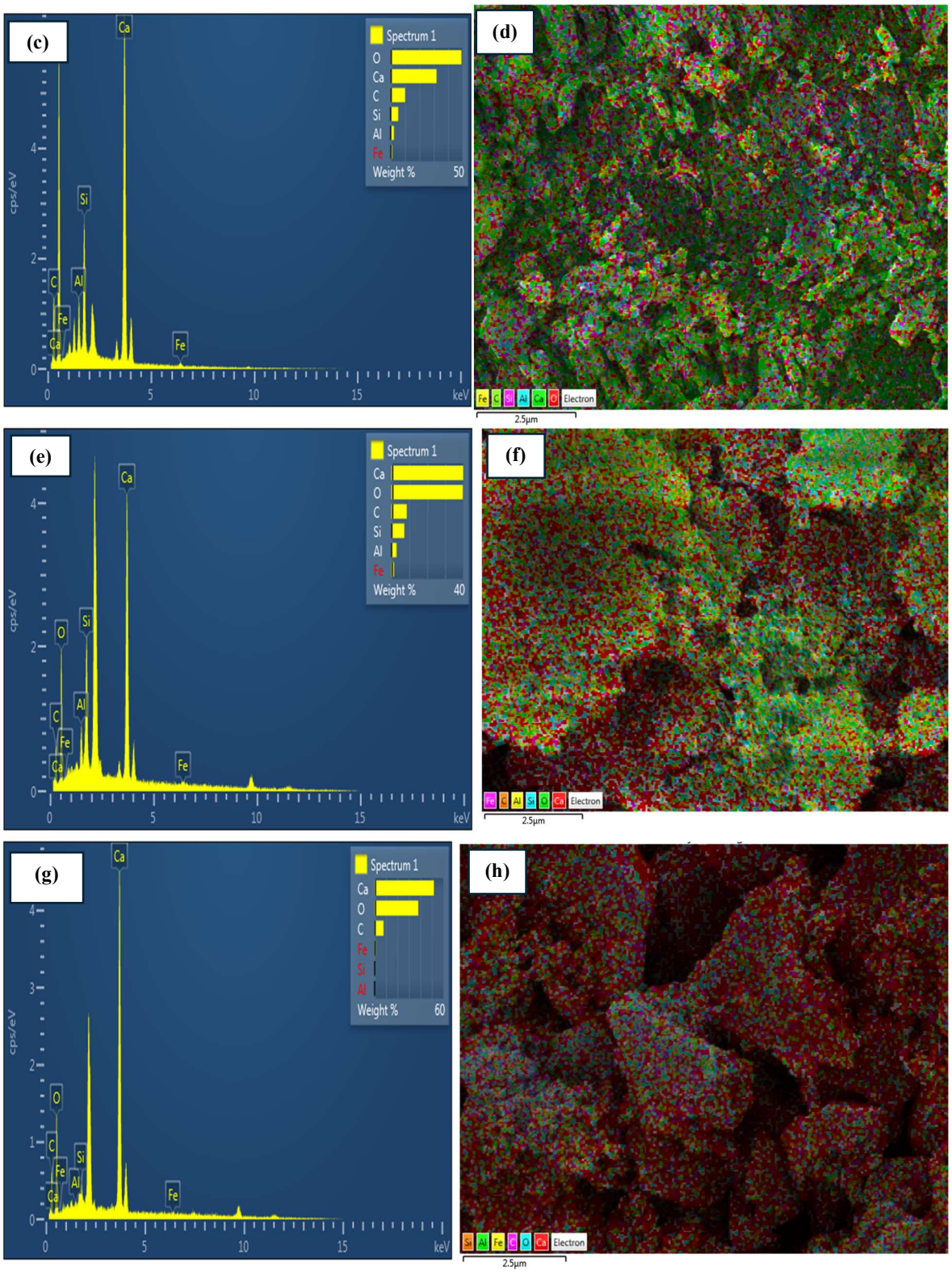

Figure 4.33 EDS peaks of mix (a) FC5, (b) FC10, (c) FC15, (d) FC20 with elemental mapping of mix (e) FC5, (f) FC10, (g) FC15 and (h) FC20

Table 4.2 Elemental composition of concrete mixes with ferrock

Elements (%)	C	O	Mg	Al	Si	Ca	Fe	Na
CSF0G0	0	19.26	0.07	1.51	2.44	70.62	5.81	0.27
FC5	11.07	40.87	-	0.62	5.44	41.6	0.4	-
FC10	8.59	39.74	-	2.92	7.27	39.98	1.5	-
FC15	10.03	49.25	-	2.27	5.3	31.99	1.15	-
FC20	7.77	38.09	-	0.45	0.65	51.72	1.31	-

4.4.3.3 EDS for concrete with rGO and ferrock together

The analysis aims to determine elemental composition of concrete mixes containing rGO and ferrock together and 0.2% rGO constantly used and variable ratio of 5%, 10%, 15%, 20% ferrock was used as partial replacement of cement in concrete. As elements present in concrete impacts mechanical strength and durability. The results are presented in table 4.3 below along with mix notation. The peaks of elements in mix are given in figure 4.34 below with distribution of elements in concrete. The EDS analysis showed that the mixes with rGO and ferrock contain the necessary elements required for pozzolanic reaction. The figure 4.34 (e), (f), (g), (h) visualizes the elements distribution mapping of mix G0.2FC5, G0.2FC10, G0.2FC15 and G0.2FC20 respectively which is compared with control sample. The optimum mix showed was G0.2FC10 which contains less iron among the other mixes illustrates that more product formation by conversion of IO into iron carbonate. The Ca/Si ratio is lowest for mix G0.2FC10 among all mixes which achieved highest strength among other mixes. The lesser value means higher amount of hydration in form of CSH and CH [281]. The control mix has much higher Ca/Si value shows less product formation.

Table 4.3 Elemental composition of concrete mixes with rGO and ferrock together

Elements (%)	C	O	Mg	Al	Si	Ca	Fe	Na
CSF0G0	0	19.26	0.07	1.51	2.44	70.62	5.81	0.27
G0.2FC5	5.5	22.75	0.29	0.84	2.92	65.82	1.88	0
G0.2FC10	26.73	41.6	1.7	4.72	10.55	13.92	0.79	0
G0.2FC15	7.79	24.97	1.26	2.91	8.47	51.03	3.57	0
G0.2FC20	22.99	51.8	1.07	5.07	9.72	7.64	1.7	0

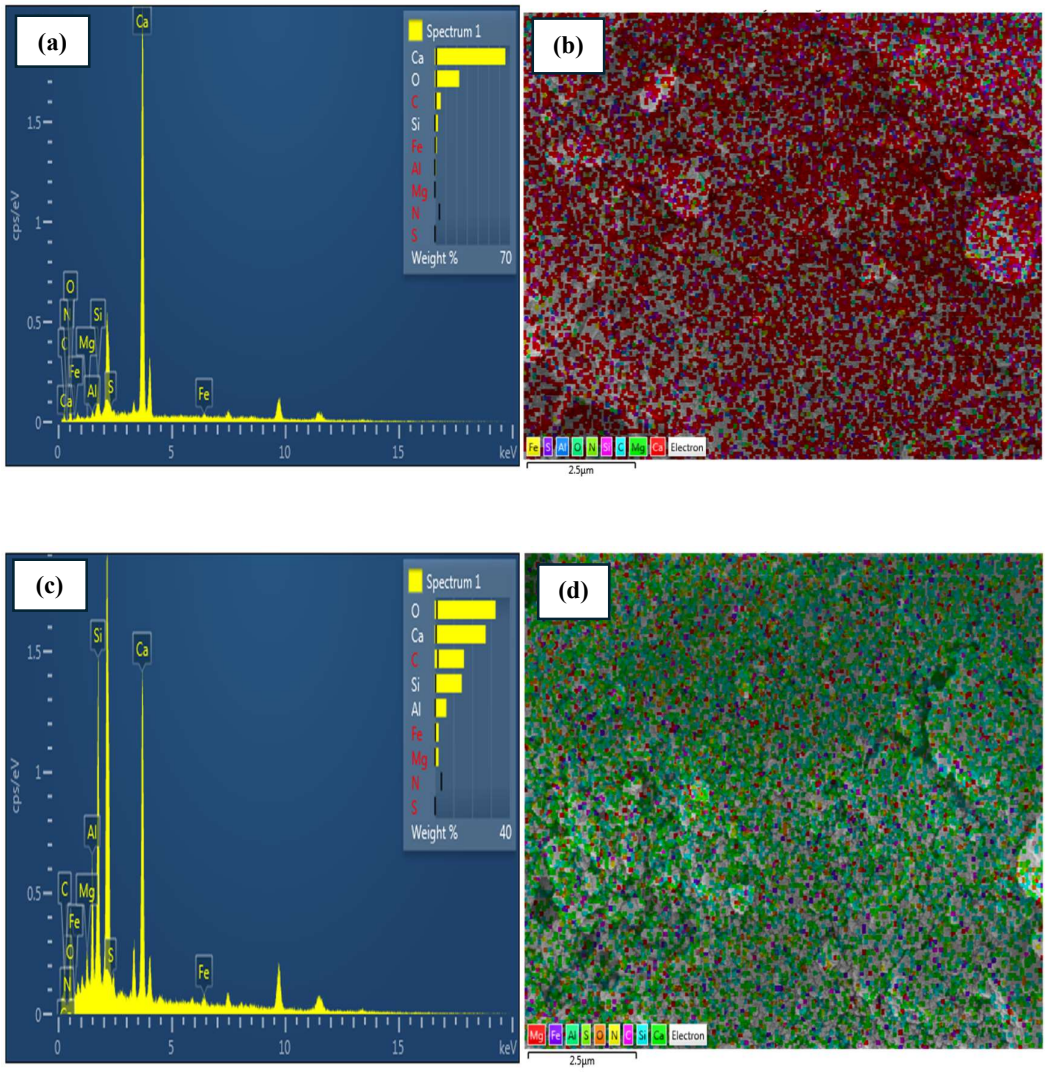

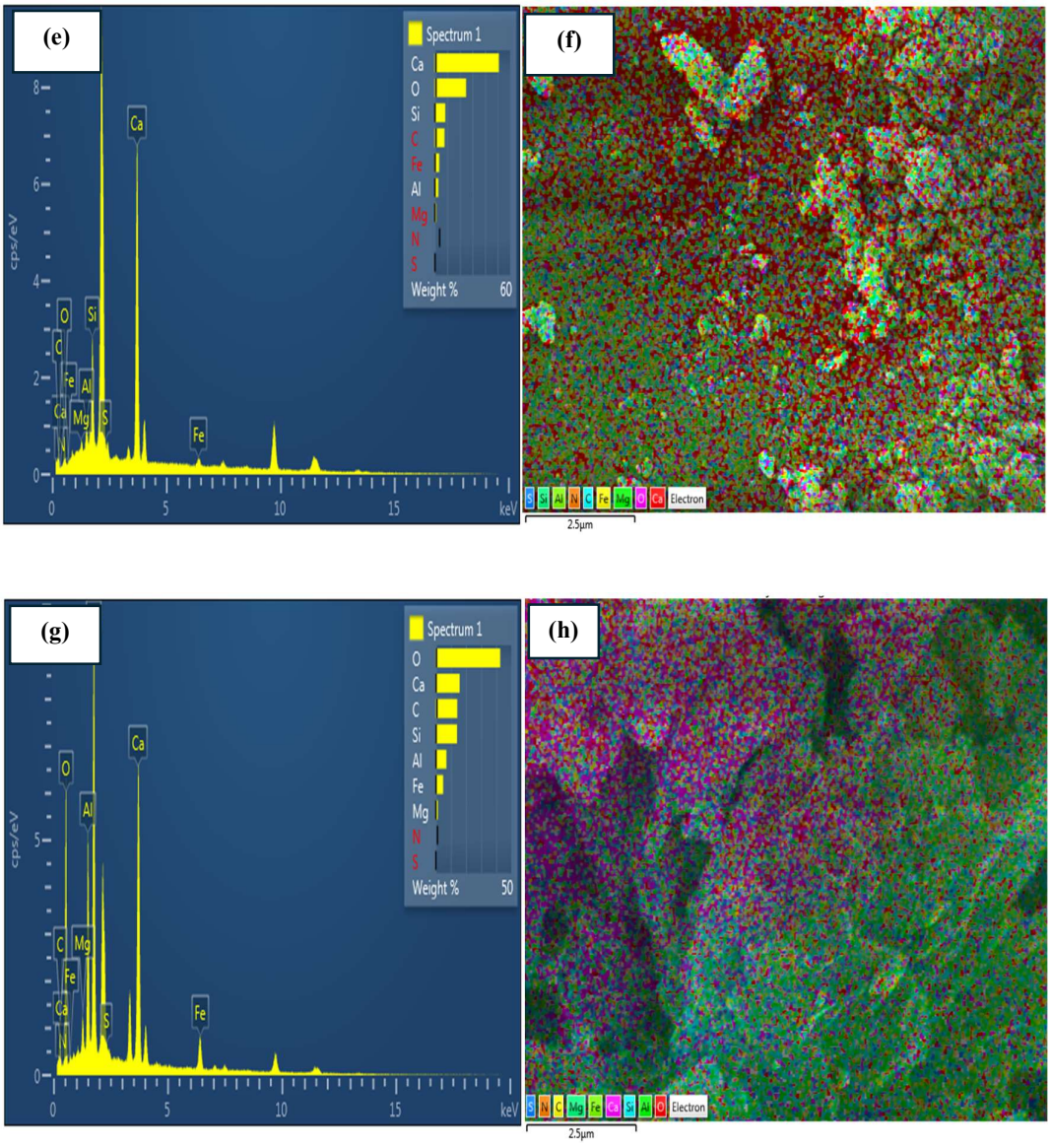

Figure 4.34 EDS peaks of mix (a) G0.2FC5, (b) G0.2FC10, (c) G0.2FC15, (d) G0.2FC20 with elemental mapping of mix (e) G0.2FC5, (f) G0.2FC10, (g) G0.2FC15 and (h) G0.2FC20

4.4.4 XRD Results

4.4.4.1 XRD for concrete with rGO

The analysis aims to study the XRD phases of concrete mixes with rGO as partial replacement of cement. The results are depicted in the figure 4.35 (a) and (b) at 28 days curing for concrete mix GC0.2 and GC0.1 respectively. The major minerals present in sample are SiO_2, $Ca(OH)_2$, CSH and calcium silicate. The most dominant peak at the angle of 2theta is SiO_2 in the samples of both mixes. The mix with rGO contains peaks of SiO_2, CSH, C_3S, C_2S and CH as major peaks of minerals. Other peaks are corresponding to the initiation of hydration and completion of crystallization (i.e. Portlandite (CH), C–S–H, C_3S, and C_2S), which is because of the introduction of a larger density of oxygen functionalities in the composite with a higher rGO dosage. Portlandite is formed during the reaction of C_2S and C_3S and its presence showing crystalline nature and leads to durability of concrete. The presence of CSH in both of mix the reasons for strength development. The increase in the interplanar spacing indicates that oxygen functional groups are inserted into carbon atom layers after the oxidization of graphite. Due to oxygen interaction with graphite through a covalent bond, the structure of the graphene sheets is modified, which further leads to the shift of GO diffraction peaks [263].

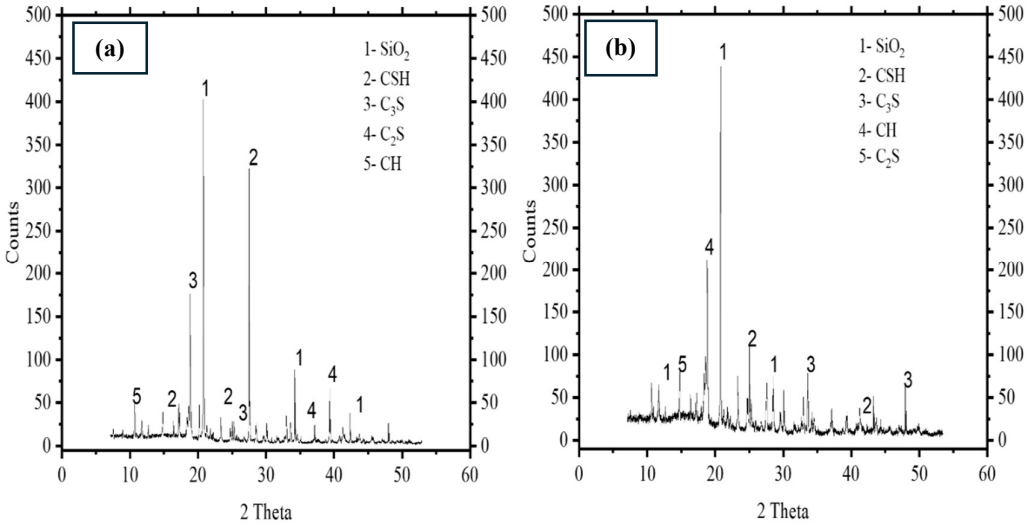

Figure 4.35 XRD peaks of mix (a) GC0.2 and (b) GC0.1

4.4.4.2 XRD for concrete with ferrock

The analysis compares the minerals phases of concrete mixes with ferrock, and the results are illustrated in the figure 4.36 (a), (b), (c) and (d) for concrete mix FC5, FC10, FC15 and FC20 at 28 days of curing respectively. The control mix contains SiO_2, $Ca(OH)_2$, CSH and calcium silicate majorly. The analysis highlighted several common minerals across all mixes, including SiO_2, which is crucial for the formation of C-S-H through pozzolanic reactions; $Ca(OH)_2$ (Portlandite), a byproduct of cement hydration; and $CaCO_3$, which was present in all mixes and indicates potential carbonation of $Ca(OH)_2$, contributing to the concrete's density and durability. C-S-H acts as the primary binder in concrete, facilitating the cohesion of aggregate particles. For the FC5 mix notable peaks included SiO_2, $Ca(OH)_2$, $CaCO_3$, ettringite, C-S-H, C-A-S-H (Calcium Aluminate Silicate Hydrate), and $(CO_3)_2$, with minor peaks of Manganosite, ferrihydrite, and Al_2O_3 etc. Mix FC10 have major peaks of SiO_2, $Ca(OH)_2$, $CaCO_3$ and CSH. Additionally contained ferrosilite ($FeSiO_3$), metathenardite, aluminum ferrite (AlF_3), biotite, and $AlFeO_3$, while FC15 featured C-A-S-H, ferrihydrite, ferricopiapite, albite, hydrohalite, and dolomite. The mix FC20 contains majorly SiO_3, $CaCO_3$, $MgCO_3$, CSH and calcium sulfate anhydrate etc. The presence of iron minerals in FC10 is indicative of improved strength and pozzolanic reactions due to these iron phases. Quartz was commonly present in all the samples at major peaks, which is the reason for strength improvement in all mixes with ferrock [90]. The presence of mineral calcite (CaCO3) because of carbonation and its effectiveness may influence the by- products of stable calcite form. The reaction of CO_2 formed CSH, CASH, magnesite and quartz which develop strong ITZ and denser and compacted concrete matrix. CO_2 curing at initial days accelerates the reactions and provides long term strength along with early-strength development. Results indicate that ferrock concrete contains important elements required for pozzolanic reaction. A previous study found for SCC with ferrock during carbonation to produce $FeCO_3$ results in carbonate of iron particles which indicate rusting of iron [282]. The present mineral in SCC makes microstructure denser by filling pores after the formation of CSH [282].

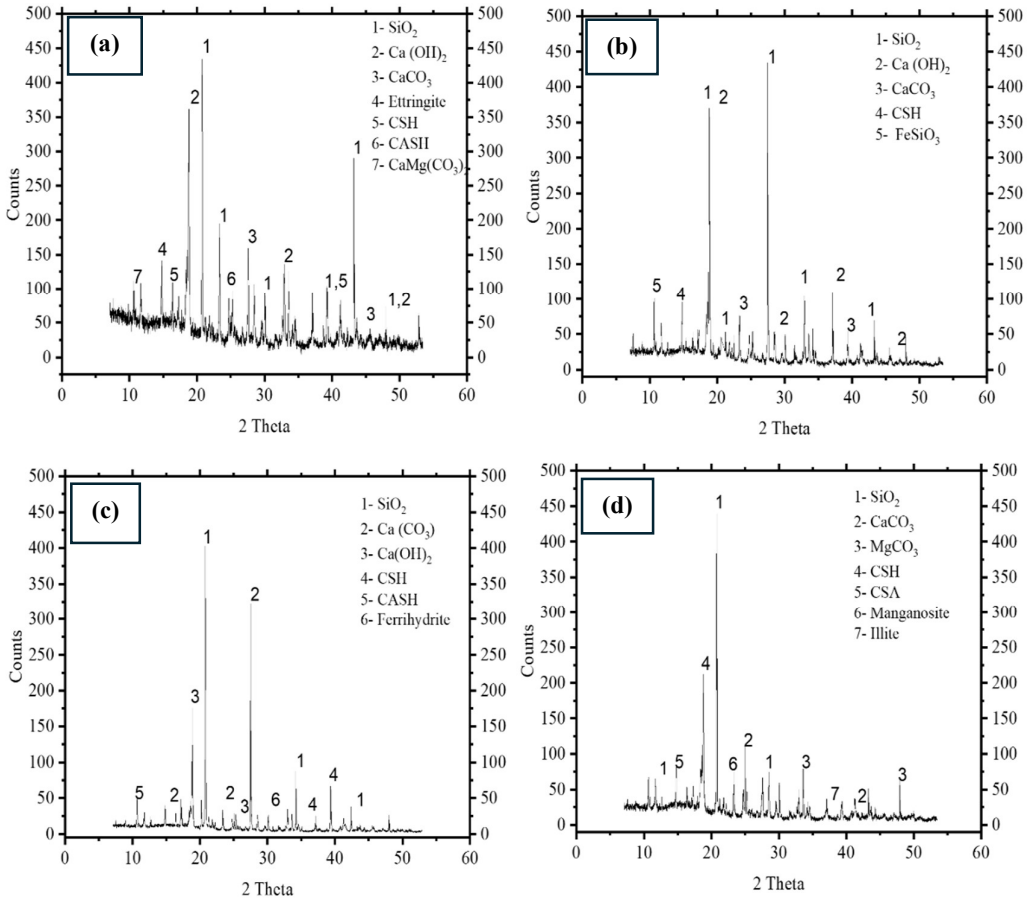

Figure 4.36 XRD peaks of mix (a) FC5, (b) FC10, (c) FC15 and (d) FC20

4.4.4.3 XRD for concrete with rGO and ferrock together

Analysis was performed to analyze the major and minor peaks of concrete mix with rGO and ferrock together and results are shown in figure 4.37 (a), (b), (c) and (d) for concrete mix GC0.2FC5, GC0.2FC10, G0.2FC15 and G0.2FC20 respectively. The control mix contains SiO_2, $Ca(OH)_2$, CSH and calcium silicate majorly. Analysis provides a comparison among mixes containing rGO and ferrock compared with the control mix. The analysis highlighted several common minerals across all mixes, including SiO_2, which is crucial for the formation of C-S-H through pozzolanic reactions; $Ca(OH)_2$ (Portlandite), a byproduct of cement hydration; and $CaCO_3$, which

was present in all mixes and indicates potential carbonation of $Ca(OH)_2$, contributing to the concrete's density and durability. Fe, Mg, Si, Al formed reactive compound in specimens of mixes along with peaks of $Ca(OH)_2$, CSH and Quartz. Whereas ferrock incorporated concrete possesses a traceable amount of hedenbergite ($CaFe_2Si_2O_6$), magnesium ferrite ($MgFe_2O_4$), and calcium - magnesium alumina silicate phases due to the prominent reaction of C_2S and C_3S with supplementary cementitious add-on material (ferrock) [90]. The carbonation reactions also support the formation of CSH, CASH, magnesite ($MgCO_3$) and quartz which facilitates the development of a strong ITZ and a dense matrix structure. Ferrock-based when undergoing carbonation tends to produce siderite ($FeCO_3$), a solid carbonate of iron particles, which often indicates the rusting of iron artefacts. Herein the study, this mineral composition tends to improve the microstructure by filling the voids left even after the formation of CSH, thereby improving the porous nature of the concrete matrix. The mineralogical phases of iron were found dominant under all reactions because of the inert nature of other materials (FA, MK and LS) in the mix. Further, C-S-H and C-A-S-H phases were abundant in all the samples due to the excess silicates and aluminates, which impart additional strength to the concrete.

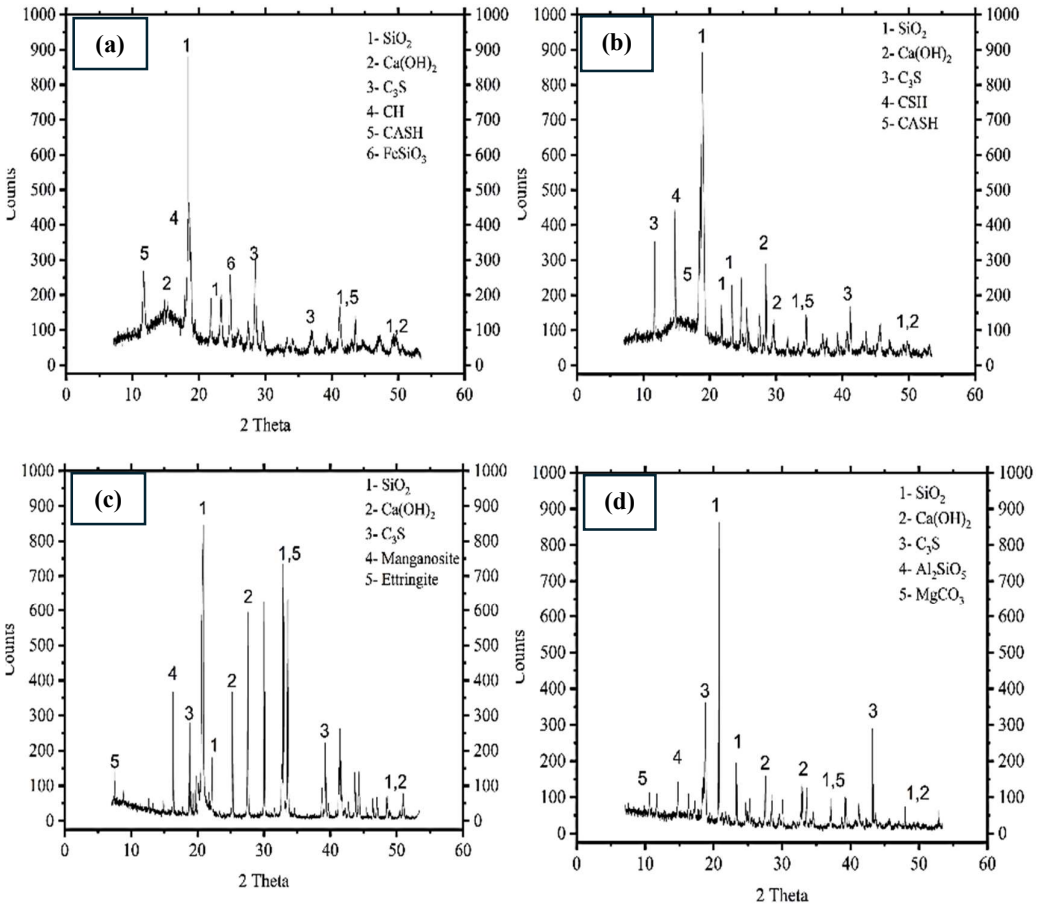

Figure 4.37 XRD peaks of mix (a) G0.2FC5, (b) G0.2FC10, (c) G0.2FC15 and (d) G0.2FC20

4.5 Carbonation Test

Carbonation test performed to visualize the carbonated and non-carbonated area of concrete with phenolphthalein as an indicator. The cubes of size 50 mm were cast and kept in CO_2 environment for 4 days curing and then transferred to water tank for 28 days curing. The results are visualized in the figure 4.38 (a), (b), (c) and (d) below for the mix of FC5, FC10, G0.2F5 and G0.2F10 respectively. The analysis performed for the lowest and highest strength achieved by mixes of ferrock and combination replacement ratios. After curing the cubes, the cube freshly split into two parts and spray phenolphthalein. The pink tint shows non-carbonated areas, and pink tint shows carbonated areas by

using phenolphthalein as an indicator. The solution is a colorless acid & base indicator, which turns purple when the pH is above 9, denoting the presence of $Ca(OH)_2$. It indicates the boundary at which the carbonated front meets the uncarbonated concrete, where concrete is alkaline [170]. The phenolphthalein solution changes its color in relation to the pH of the material: in the noncarbonated part of the specimen, where concrete has still a highly alkaline behavior (pH > 9), a purple-red coloration is obtained, whereas in the carbonated area of the specimen (pH < 9) no color change is observed signifying that the hardened cement paste can be considered carbonated [283] [183]. Results show that with the increasing content of ferrock in concrete the carbonated area increasing and non-carbonated area decreasing. The mix FC5 absorbs less CO_2 as content of ferrock in 5% with the increasing ferrock content the concrete able to absorb more CO_2. The reason is because higher ferrock leads to more content of IO which reacts with CO_2 to produce more product and hardening process requires more CO_2. The findings indicate that mix FC5 exhibited the most extensive pink coloration suggest lower carbonation as compared with FC10, FC15 and FC20. Previous results suggest that ferrock functions as CO_2 – absorbing material when cube of 100% ferrock tested and found whole cube carbonated. Ferrock enhances the strength of concrete and makes concrete CO_2 absorbing material. Previous studies also used phenolphthalein as an indicator for carbonation in concrete [168] [182]. The phenolphthalein-based method is the simplest way to determine the carbonation depth [169].

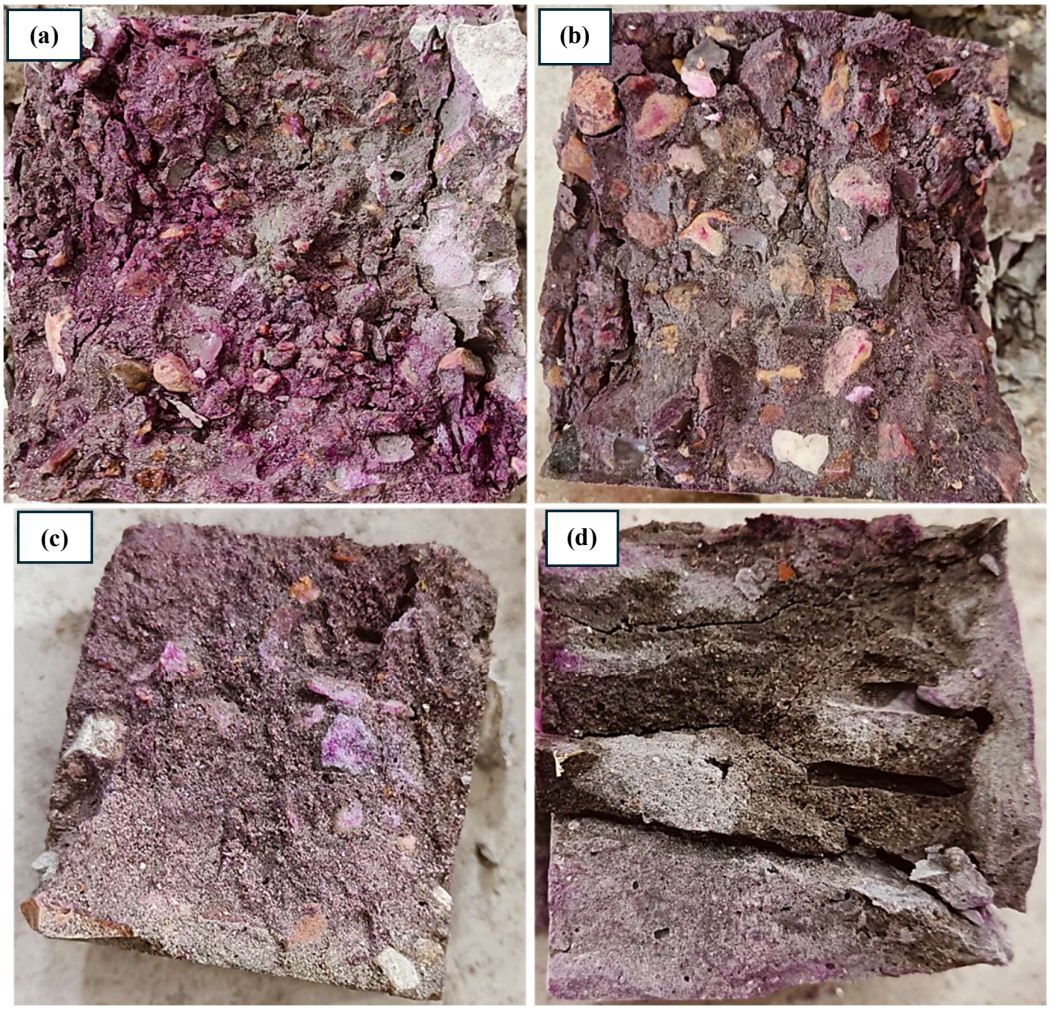

Figure 4.38 Carbonation test results of mix (a) FC5, (b) FC10, (c) G0.2FC5 and (d) G0.2FC10

4.7 Cost analysis

The cost analysis for all the mixes was conducted, compared, and presented in table 4.5. The cost of the materials was calculated based on their respective purchase rates. Table 4.4 displays the cost of producing 1 kg of ferrock, determined by the rates of the raw materials used. The proportions of the raw materials were based on the optimum ratio identified from the results of the UCS test. This same ratio was maintained throughout the subsequent experimental program. To evaluate the cost-effectiveness of each mix, the economy index (defined as the CS per unit cost per cubic meter) [128] was calculated and compared across all mixes. All mentioned quantities are reported in Kg.

Table 4.4 Cost analysis of 1Kg ferrock

Raw materials	Ratio (%)	for 1 kg	Cost/kg	Cost (Rs)
IO	62	0.62	90	55.8
FA	20	0.2	4	0.8
LS	10	0.1	8	0.8
MK	6	0.6	29	17.4
OA	2	0.2	336	67.2
				142

The cost required for $1m^3$ of concrete for all mixes is presented below in table 4.5. The results indicate that value of EI is decreasing by increasing the ratio of rGO and ferrock individually. The mixes contain the combination of rGO and ferrock the value of EI increased from 5% replacement to 10% replacement in mix G0.2F10 then decreased. The highest value of EI is for control mix indicates that the mixes with rGO and ferrock are expensive than conventional mix. The lowest value of EI is shown by mix G0.8, it means this mix is expensive with no relative strength gain. The most cost-

efficient mix is GC0.1 and FC5 with minimum ratio of replacements. The incorporation of rGO is expensive but the cost of ferrock can be lowered by utilizing ferrock in areas with steel industries so that the cost of IO can be reduced to a minimum.

Table 4.5 Cost analysis of concrete mix for $1m^3$

Mix Notations	OPC	Sand	Coarse aggregate	rGO	Ferrock	rGO + Ferrock		Total	EI=Strength/Cost
CSF0G0	3640.4	467	533.2	0	0	0	0	4640.6	0.00659
GC0.1	3636.76	467	533.2	2299.2	0	0	0	6936.16	0.00552
GC0.2	3633.12	467	533.2	4598.4	0	0	0	9231.719	0.00455
GC0.4	3625.84	467	533.2	9196.8	0	0	0	13822.84	0.00299
GC0.6	3618.56	467	533.2	13795.2	0	0	0	18413.96	0.0022
GC0.8	3611.28	467	533.2	18393.6	0	0	0	23005.08	0.00172
FC5	3458.38	467	533.2	0	2720.72	0	0	7179.3	0.0047
FC10	3276.36	467	533.2	0	5441.44	0	0	9718	0.0043
FC15	3094.34	467	533.2	0	8162.16	0	0	12256.7	0.0031
FC20	2912.32	467	533.2	0	10882.88	0	0	14795.4	0.0025
G0.2FC5	3451.1	467	533.2	0	0	4598.4	2720.72	11770.4	0.00365
G0.2FC10	3265.44	467	533.2	0	0	4598.4	5441.44	14305.5	0.00391

G0.2FC15	3087.06	467	533.2	0	0	4598.4	8162.16	16847.8	0.00298
G0.2FC20	2905.04	467	533.2	0	0	4598.4	10882.9	19386.5	0.00232

Chapter 5 Summary and Conclusions

5.1 Summary

The present study investigated the potential of rGO and ferrock for partial replacement of cement in different ratios. The experimental tests were performed to study the impact on fresh properties, hardened properties and microstructural analysis. rGO is a carbon-based nano material which acts as filler and ferrock is carbon negative material prepared with waste iron oxide with other pozzolanic materials. The incorporation of ferrock promotes sustainability by recycling waste which is usually landfilled and has ability to make concrete structure carbon negative to reduce carbon emission of environment. The key conclusions drawn from the experimental study are presented below-

1. The physical characteristics of rGO indicate surface morphology as rough wrinkled sheets with large surface area. The raw materials of ferrock have finer particles except iron oxide. The elemental composition revealed the presence of necessary elements like rGO contains carbon content and other materials with Si, Ca and iron content. XRD revealed the crystalline nature of ferrock and moderately amorphous nature of rGO. Particle size analysis revealed the presence of enough fine particles to replace cement in concrete.

2. The pore structure of concrete mixes with rGO and ferrock revealed to have denser and more compacted microstructure as compared to conventional concrete. rGO acts as nano filler due to large surface area and products formed during the ferrock preparation made composites. The incorporation of rGO and ferrock in concrete slightly reduced the workability tested by the slump and compaction factor value.

3. The results of hardened properties found enhancement in CS, TS and FS at all replacement ratios of cement with rGO and ferrock and combination of both. The results of durability test found a significant reduction in water absorption, water penetration, initial surface absorption and chloride penetration to improve durability of concrete at all curing days and replacement ratios. The

SEM analysis revealed denser and compacted microstructure of concrete with partial replacement of cement with rGO and ferrock. The essential elements found to be present in all concrete mixes with peaks of minerals which are responsible for strength development and improved durability. The optimum found to 0.2% rGO, 10% ferrock and on combination 0.2% rGO with 10% ferrock showed highest improvement in strength and durability.

4. The cost analysis performed for $1m^3$ of concrete mix compared on the basis of economic index. The mixes showed higher cost with the purchased raw materials as compared to areas with abundant steel dust. The production of ferrock is cost effective in areas near the steel industries to source steel dust at negligible cost.

5.2 Contribution to sustainable concrete development

The present study makes a significant contribution to sustainable concrete development by repurposing steel industry waste, specifically iron oxide, which is typically disposed of in landfills, contributing to soil pollution. By incorporating this waste material as the primary binder, along with other pozzolanic materials, the study introduces a novel material known as ferrock. A key environmental benefit of ferrock is its carbon-negative property, as it requires CO_2 for the hardening process, thereby absorbing atmospheric CO_2 during curing.

With the growing demand for modern infrastructure driven by population growth, the construction industry has become a major contributor to global carbon emissions. This study highlights the potential of rGO and ferrock as sustainable alternatives to cement in concrete production. The integration of these materials enhances the strength and durability of concrete composites while simultaneously reducing their carbon footprint, making the concrete carbon-absorbing.

By recycling industrial steel waste and incorporating nanomaterials, this research promotes environmentally responsible construction practices. The resulting carbon-negative concrete not only offers improved structural performance but also contributes to mitigating the environmental impact of the

construction sector. This study underscores the potential of innovative, sustainable materials in advancing the development of stronger, more durable, and eco-friendly concrete composites.

The present research aligns with the United Nations Sustainable Development Goal (SDG), specifically SDG 9 (Industry, Innovation, and Infrastructure), SDG 11 (Sustainable Cities and Communities), SDG 12 (Responsible Consumption and Production), and SDG 13 (Climate Action). This study contributes to SDG 9 by enhancing the durability of infrastructure through improved concrete properties while reducing cement consumption. SDG 11 is addressed by promoting the use of eco-friendly materials, thereby minimizing the environmental impact of urban development and contributing to the resilience of cities. Furthermore, SDG 12 is fulfilled by incorporating waste iron oxide as a recycled component in the construction binder, reducing landfill waste and promoting responsible resource utilization. Lastly, SDG 13 is supported through the utilization of ferrock, a carbon-negative binder that mitigates GHG emissions associated with conventional cement production. By integrating these sustainable practices, the study advances the development of climate-friendly materials, contributing to a more environmentally sustainable construction industry.

5.3 Limitations

The study has following limitations-

- The use of rGO increases the cost of the concrete, limiting its economic feasibility for large-scale applications.
- Ferrock concrete is limited for unreinforced structures, as the steel dust in ferrock may lead to corrosion and rusting when in contact with steel reinforcement.
- The transportation of steel dust is costly, making the use of ferrock concrete more viable only in regions with local steel industries, limiting its broader applicability.

5.4 Future suggestions/recommendations

- The optimization of the rGO ratio in concrete can be further investigated.
- Different ratios of ferrock and rGO can be explored across various grades of concrete.
- The impact of CO_2 curing on the reinforcement of concrete warrants further study.
- The effects of protective coatings on reinforcement, as well as alternative reinforcement materials, can be examined.
- The performance of rGO and ferrock concrete under extreme weather conditions should be assessed.

References-

[1] L. Barcelo, J. Kline, G. Walenta, and E. Gartner, “Cement and carbon emissions,” Mater Struct, vol. 47, no. 6, pp. 1055–1065, 2014, doi: https://doi.org/10.1617/s11527-013-0114-5

[2] E. Worrell, L. Price, N. Martin, C. Hendriks, and L. Ozawa-Meida, “Carbon Dioxide Emission from the Global Cement Industry,” Annu. Rev. Energy Environ, vol. 26, pp. 303–329, Nov. 2001, doi: https://doi.org/10.1146/annurev.energy.26.1.303

[3] Z. Duan, Q. Huang, and Q. Zhang, “Life cycle assessment of mass timber construction: A review,” Build Environ, vol. 221, p. 109320, 2022, doi: https://doi.org/10.1016/j.buildenv.2022.109320

[4] L. Huang, G. Krigsvoll, F. Johansen, Y. Liu, and X. Zhang, “Carbon emission of global construction sector,” Renewable and Sustainable Energy Reviews, vol. 81, pp. 1906–1916, 2018, doi: https://doi.org/10.1016/j.rser.2017.06.001

[5] K. Faldessai, S. Lawande, A. Kelekar, R. Gurav, and S. Kakodkar, “Utilization of ceramic waste as a partial replacement for cement in concrete manufacturing,” Mater Today Proc, 2023, doi: https://doi.org/10.1016/j.matpr.2023.06.453

[6] Z. Liu, Z. Deng, S. Davis, and P. Ciais, “Monitoring global carbon emissions in 2022,” Nat Rev Earth Environ, vol. 4, no. 4, pp. 205–206, 2023, doi: https://doi.org/10.1038/s43017-023-00406-z

[7] M. Segata et al., “The effects of MgO, Na2O and SO3 on industrial clinkering process: phase composition, polymorphism, microstructure and hydration, using a multidisciplinary approach,” Mater Charact, vol. 155, p. 109809, 2019, doi: https://doi.org/10.1016/j.matchar.2019.109809

[8] G. Liu, R. Chen, P. Xu, Y. Fu, C. Mao, and J. Hong, “Real-time carbon emission monitoring in prefabricated construction,” Autom Constr, vol. 110, p. 102945, 2020, doi: https://doi.org/10.1016/j.autcon.2019.102945

[9] “Mineral Commodity Summaries 2019,” Reston, VA, 2019. doi: https://doi.org/10.3133/70202434

[10] E. Worrell, L. Price, N. Martin, C. Hendriks, and L. O. Meida, “Carbon dioxide emissions from the global cement industry,” Annual Review of Energy and the Environment, vol. 26, no. 1, pp. 303–329, Nov. 2001, doi: https://doi.org/10.1146/annurev.energy.26.1.303

[11] B. N. U and J. Parikh, “Indicators of carbon emission intensity from commercial energy use in India,” 2000. doi: https://doi.org/10.1016/S0140-9883(99)00032-8

[12] Y. Wang, Z. Jiang, L. Li, Y. Qi, J. Sun, and Z. Jiang, “A Bibliometric and Content Review of Carbon Emission Analysis for Building Construction,” 2023. doi: https://doi.org/10.3390/buildings13010205

[13] C. Xu et al., “Carbon capture and storage as a strategic reserve against China’s CO2 emissions,” Environ Dev, vol. 37, p. 100608, 2021, doi: https://doi.org/10.1016/j.envdev.2020.100608

[14] X. Xu, P. Xu, J. Zhu, H. Li, and Z. Xiong, “Bamboo construction materials: Carbon storage and potential to reduce associated CO2 emissions,” Science of The Total Environment, vol. 814, p. 152697, 2022, doi: https://doi.org/10.1016/j.scitotenv.2021.152697

[15] P. Chastas, T. Theodosiou, K. J. Kontoleon, and D. Bikas, “Normalising and assessing carbon emissions in the building sector : A review on the embodied CO 2 emissions of residential buildings,” Build Environ, vol. 130, no. November 2017, pp. 212–226, 2018, doi: https://doi.org/10.1016/j.buildenv.2017.12.032

[16] A. A. Mahmoud, A. A. El-Sayed, A. M. Aboraya, I. N. Fathy, M. A. Abouelnour, and I. M. Nabil, “Influence of sustainable waste granite, marble and nano-alumina additives on ordinary concretes: a physical, structural, and radiological study,” Sci Rep, vol. 14, no. 1, p. 22011, 2024, doi: https://doi.org/10.1038/s41598-024-72222-4

[17] L. Barcelo, J. Kline, G. Walenta, and E. Gartner, “Cement and carbon emissions,” Mater Struct, vol. 47, no. 6, pp. 1055–1065, 2014, doi: https://doi.org/10.1617/s11527-013-0114-5

[18] S. J. R., H. D. N., and N. M. N. K., “Industrial Waste?Paper Sludge Ash as Partial Replacement to Cement in Making Concrete Paver Blocks,” Jun. 04, 2021. doi: doi: https://doi.org/10.1061/9780784483510.019

[19] I. Kula, A. Olgun, V. Sevinc, and Y. Erdogan, “An investigation on the use of tincal ore waste, fly ash, and coal bottom ash as Portland cement replacement materials,” Cem Concr Res, vol. 32, no. 2, pp. 227–232, 2002, doi: https://doi.org/10.1016/S0008-8846(01)00661-5

[20] S. Kadamba, S. Blesson, A. U. Rao, M. Kamath, and A. Tantri, “Mechanical, durability and microstructure properties of self-healing concrete utilizing agro-industrial waste: a critical review,” Journal of Building Pathology and Rehabilitation, vol. 9, no. 2, p. 153, 2024, doi: https://doi.org/10.1007/s41024-024-00501-8

[21] E. Aprianti, P. Shafigh, S. Bahri, and J. N. Farahani, “Supplementary cementitious materials origin from agricultural wastes – A review,” Constr Build Mater, vol. 74, pp. 176–187, 2015, doi: https://doi.org/10.1016/j.conbuildmat.2014.10.010

[22] I. Y. Hakeem, M. Amin, I. S. Agwa, M. H. Abd-Elrahman, and M. F. Abdelmagied, “Using a combination of industrial and agricultural wastes to manufacture sustainable ultra-high-performance concrete,” Case Studies in Construction Materials, vol. 19, p. e02323, 2023, doi: https://doi.org/10.1016/j.cscm.2023.e02323

[23] J. Gudainiyan and K. Kishore, “A review on cement concrete strength incorporated with agricultural waste,” Mater Today Proc, vol. 78, pp. 396–402, 2023, doi: https://doi.org/10.1016/j.matpr.2022.10.179

[24] S. Chandra and R. Choudhary, “Performance Characteristics of Bituminous Concrete with Industrial Wastes as Filler,” Journal of Materials in Civil Engineering, vol. 25, pp. 1666–1673, Nov. 2013, doi: https://doi.org/10.1061/(ASCE)MT.1943-5533.0000730

[25] N. K. Verma, “Influence of Partial Replacement of Cement by Industrial Wastes on Properties of Concrete BT - Recent Trends in Civil Engineering,” K. K. Pathak, J.

M. S. J. Bandara, and R. Agrawal, 2021, pp. 693–713.doi: https://doi.org/10.52783/jchr.v14.i2.3376

[26] P. Segui, M. Safhi, M. Amrani, and M. Benzaazoua, “Mining Wastes as Road Construction Material : A Review,” pp. 1–18, 2023. doi: https://doi.org/10.3390/min13010090

[27] M. Sofi, Y. Sabri, Z. Zhou, and P. Mendis, “Transforming Municipal Solid Waste into Construction Materials,” 2019. doi: https://doi.org/10.3390/su11092661

[28] M. Menegaki and D. Damigos, “A review on current situation and challenges of construction and demolition waste management,” Curr Opin Green Sustain Chem, vol. 13, pp. 8–15, 2018, doi: https://doi.org/10.1016/j.cogsc.2018.02.010

[29] Z. Ma, R. Hu, J. Shen, C. Wang, and H. Wu, “Chloride diffusion and binding capacity of sustainable cementitious materials with construction waste powder as cement replacement,” Constr Build Mater, vol. 368, p. 130352, 2023, doi: https://doi.org/10.1016/j.conbuildmat.2023.130352

[30] W.-J. Ong, L.-L. Tan, S.-P. Chai, and S.-T. Yong, “Graphene oxide as a structure-directing agent for the two-dimensional interface engineering of sandwich-like graphene/g-C3N4 hybrid nanostructures with enhanced visible-light photoreduction of CO2 to methane,” Chem. Commun., vol. 51, Nov. 2014, doi: https://doi.org/10.1039/C4CC08996K

[31] I. Fonseka, D. Mohotti, K. Wijesooriya, C.-K. Lee, and P. Mendis, “Influence of graphene oxide properties, superplasticiser type, and dispersion technique on mechanical performance of graphene oxide-added concrete,” Constr Build Mater, vol. 428, p. 136415, 2024, doi: https://doi.org/10.1016/j.conbuildmat.2024.136415

[32] 2015). (Pan Z et al., “Mechanical properties and microstructure of a graphene oxide–cement composite,” Cem Concr Compos, vol. 58, pp. 140–147, 2015, doi: https://doi.org/10.1016/j.cemconcomp.2015.02.001

[33] B. Wang, R. Jiang, and Z. Wu, “Investigation of the Mechanical Properties and Microstructure of Graphene Nanoplatelet-Cement Composite,” 2016. doi: https://doi.org/10.3390/nano6110200

[34] D. Wijerathne, Y. Gong, S. Afroj, N. Karim, and C. Abeykoon, “Mechanical and thermal properties of graphene nanoplatelets- reinforced recycled polycarbonate composites,” International Journal of Lightweight Materials and Manufacture, vol. 6, no. 1, pp. 117–128, 2023, doi: https://doi.org/10.1016/j.ijlmm.2022.09.001

[35] H. Du and S. Pang, “Enhancement of barrier properties of cement mortar with graphene nanoplatelet,” Cem Concr Res, vol. 76, Oct. 2015, doi: https://doi.org/10.1016/j.cemconres.2015.05.007

[36] A. Gholampour, M. Valizadeh Kiamahalleh, D. N. H. Tran, T. Ozbakkaloglu, and D. Losic, “From Graphene Oxide to Reduced Graphene Oxide: Impact on the Physiochemical and Mechanical Properties of Graphene–Cement Composites,” ACS Appl Mater Interfaces, vol. 9, no. 49, pp. 43275–43286, Dec. 2017, doi: https://doi.org/10.1021/acsami.7b16736

[37] A. Gholampour, M. Valizadeh Kiamahalleh, D. N. H. Tran, T. Ozbakkaloglu, and D. Losic, “From Graphene Oxide to Reduced Graphene Oxide: Impact on the Physiochemical and Mechanical Properties of Graphene–Cement Composites,” ACS Appl Mater Interfaces, vol. 9, no. 49, pp. 43275–43286, Dec. 2017, doi: https://doi.org/10.1021/acsami.7b16736

[38] G. Jing et al., “From graphene oxide to reduced graphene oxide: Enhanced hydration and compressive strength of cement composites,” Constr Build Mater, vol. 248, p. 118699, 2020, doi: https://doi.org/10.1016/j.conbuildmat.2020.118699

[39] G. Jing et al., “From graphene oxide to reduced graphene oxide: Enhanced hydration and compressive strength of cement composites,” Constr Build Mater, vol. 248, p. 118699, 2020, doi: https://doi.org/10.1016/j.conbuildmat.2020.118699

[40] A. Gutiérrez-Cruz, A. R. Ruiz-Hernández, J. F. Vega-Clemente, D. G. Luna-Gazcón, and J. Campos-Delgado, “A review of top-down and bottom-up synthesis methods for the production of graphene, graphene oxide and reduced graphene oxide,” J Mater Sci, vol. 57, no. 31, pp. 14543–14578, 2022, doi: https://doi.org/10.1007/s10853-022-07514-z

[41] S. Aodkeng, S. Sinthupinyo, B. Chamnankid, W. Hanpongpun, and A. Chaipanich, "Effect of carbon nanotubes/clay hybrid composite on mechanical properties, hydration heat and thermal analysis of cement-based materials," Constr Build Mater, vol. 320, p. 126212, 2022, doi: https://doi.org/10.1016/j.conbuildmat.2021.126212

[42] P. Li, J. Liu, H. Suh, E. Zal Nezhad, and S. Bae, "Understanding the role of graphene oxide nanoribbons–functionalized carbon nanotubes–graphene oxide (GNFG) complex in enhancing the fire resistance of cementitious composites," Constr Build Mater, vol. 348, p. 128637, 2022, doi: https://doi.org/10.1016/j.conbuildmat.2022.128637

[43] G. Li, P. Wang, and X. Zhao, "Mechanical Behavior and Microstructure of Cement Composites Incorporating Surface-Treated Multi-Walled Carbon Nanotubes," Carbon N Y, vol. 43, pp. 1239–1245, May 2005, doi: https://doi.org/10.1016/j.carbon.2004.12.017

[44] D.-H. Son, D. Hwangbo, H. Suh, B.-I. Bae, S. Bae, and C.-S. Choi, "Mechanical properties of mortar and concrete incorporated with concentrated graphene oxide, functionalized carbon nanotube, nano silica hybrid aqueous solution," Case Studies in Construction Materials, vol. 18, p. e01603, 2023, doi: https://doi.org/10.1016/j.cscm.2022.e01603

[45] N. Raveendran and V. Krishnan, "Engineering performance and environmental assessment of sustainable concrete incorporating nano silica and metakaolin as cementitious materials," Sci Rep, vol. 15, no. 1, p. 1482, 2025, doi: https://doi.org/10.1038/s41598-025-85358-8

[46] J. R. Oluremi, A. A. Raheem, R. O. Balogun, and A. A. Moshood, "Early strength development assessment of concrete produced from cement replaced with nano silica activated Corn Cob Ash," Mater Today Proc, 2023, doi: https://doi.org/10.1016/j.matpr.2023.02.191

[47] C. Singh and V. Aggarwal, "Experimental investigation of concrete strength properties by partial replacement of cement-sand with marble-granite powder," Mater

Today Proc, vol. 62, pp. 3734–3737, 2022, doi: https://doi.org/10.1016/j.matpr.2022.04.438

[48] W. Liu et al., "Evolution mechanism of mechanical properties of cemented tailings backfill with partial replacement of cement by rice straw ash at different binder content," Powder Technol, vol. 419, p. 118344, 2023, doi: https://doi.org/10.1016/j.powtec.2023.118344

[49] A. S. Ruviaro et al., "Characterization and investigation of the use of oat husk ash as supplementary cementitious material as partial replacement of Portland cement: Analysis of fresh and hardened properties and environmental assessment," Constr Build Mater, vol. 363, p. 129762, 2023, doi: https://doi.org/10.1016/j.conbuildmat.2022.129762

[50] T. Susan Ja, M. Mathew, and S. C. George, "Experimental investigations on the impact of graphene-based oxides in concrete," Mater Today Proc, 2023, doi: https://doi.org/10.1016/j.matpr.2023.08.071

[51] A. T. Smith, A. M. LaChance, S. Zeng, B. Liu, and L. Sun, "Synthesis, properties, and applications of graphene oxide/reduced graphene oxide and their nanocomposites," Nano Materials Science, vol. 1, no. 1, pp. 31–47, 2019, doi: https://doi.org/10.1016/j.nanoms.2019.02.004

[52] K. Chintalapudi and R. M. R. Pannem, "An intense review on the performance of Graphene Oxide and reduced Graphene Oxide in an admixed cement system," Constr Build Mater, vol. 259, p. 120598, 2020, doi: https://doi.org/10.1016/j.conbuildmat.2020.120598

[53] A. Anwar, X. Liu, and L. Zhang, "Nano-cementitious composites modified with Graphene Oxide – a review," Thin-Walled Structures, vol. 183, p. 110326, 2023, doi: https://doi.org/10.1016/j.tws.2022.110326

[54] I. H. Alvi, Q. Li, Y. Hou, C. C. Onyekwena, M. Zhang, and A. Ghaffar, "A critical review of cement composites containing recycled aggregates with graphene oxide nanomaterials," Journal of Building Engineering, vol. 69, p. 105989, 2023, doi: https://doi.org/10.1016/j.jobe.2023.105989

[55] M. Wang, R. Wang, H. Yao, Z. Wang, and S. Zheng, “Adsorption characteristics of graphene oxide nanosheets on cement,” RSC Adv, vol. 6, no. 68, pp. 63365–63372, 2016, doi: https://doi.org/10.1039/C6RA10902K

[56] Z. Pan et al., “Mechanical properties and microstructure of a graphene oxide–cement composite,” Cem Concr Compos, vol. 58, pp. 140–147, 2015, doi: https://doi.org/10.1016/j.cemconcomp.2015.02.001

[57] Y. Lin and H. Du, “Graphene reinforced cement composites: A review,” Constr Build Mater, vol. 265, p. 120312, 2020, doi: https://doi.org/10.1016/j.conbuildmat.2020.120312

[58] S. Chuah, Z. Pan, J. G. Sanjayan, C. M. Wang, and W. H. Duan, “Nano reinforced cement and concrete composites and new perspective from graphene oxide,” Constr Build Mater, vol. 73, pp. 113–124, 2014, doi: https://doi.org/10.1016/j.conbuildmat.2014.09.040

[59] L. Zhao, X. Guo, L. Song, Y. Song, G. Dai, and J. Liu, “An intensive review on the role of graphene oxide in cement-based materials,” Constr Build Mater, vol. 241, p. 117939, 2020, doi: https://doi.org/10.1016/j.conbuildmat.2019.117939

[60] H. M. Elkady, A. M. Yasien, M. S. Elfeky, and M. E. Serag, “Assessment of mechanical strength of nano silica concrete (NSC) subjected to elevated temperatures,” Journal of Structural Fire Engineering, vol. 10, no. 1, pp. 90–109, Jan. 2019, doi: https://doi.org/10.1108/JSFE-10-2017-0041

[61] H. H. Alqamish and A. K. Al-Tamimi, “Development and Evaluation of Nano-Silica Sustainable Concrete,” Applied Sciences, vol. 11, no. 7, 2021, doi: https://doi.org/10.3390/app11073041

[62] A. Hosan and F. U. A. Shaikh, “Influence of nano silica on compressive strength, durability, and microstructure of high-volume slag and high-volume slag–fly ash blended concretes,” Structural Concrete, vol. 22, no. S1, pp. E474–E487, Jan. 2021, doi: https://doi.org/10.1002/suco.202000251

[63] K. Khan, W. Ahmad, M. N. Amin, and S. Nazar, “Nano-Silica-Modified Concrete: A Bibliographic Analysis and Comprehensive Review of Material

Properties," Nanomaterials, vol. 12, no. 12, 2022, doi: https://doi.org/10.3390/nano12121989

[64] M. Abd Elrahman, S.-Y. Chung, P. Sikora, T. Rucinska, and D. Stephan, "Influence of Nanosilica on Mechanical Properties, Sorptivity, and Microstructure of Lightweight Concrete," Materials, vol. 12, no. 19, 2019, doi: https://doi.org/10.3390/ma12193078

[65] R. Kaur, N. C. Kothiyal, and H. Arora, "Studies on combined effect of superplasticizer modified graphene oxide and carbon nanotubes on the physico-mechanical strength and electrical resistivity of fly ash blended cement mortar," Journal of Building Engineering, vol. 30, p. 101304, Feb. 2020, doi: https://doi.org/10.1016/j.jobe.2020.101304

[66] P. Zhang, J. Su, J. Guo, and S. Hu, "Influence of carbon nanotube on properties of concrete: A review," Constr Build Mater, vol. 369, p. 130388, 2023, doi: https://doi.org/10.1016/j.conbuildmat.2023.130388

[67] A. Carriço, J. A. Bogas, A. Hawreen, and M. Guedes, "Durability of multi-walled carbon nanotube reinforced concrete," Constr Build Mater, vol. 164, pp. 121–133, 2018, doi: https://doi.org/10.1016/j.conbuildmat.2017.12.221

[68] A. Gholampour, M. Valizadeh Kiamahalleh, D. N. H. Tran, T. Ozbakkaloglu, and D. Losic, "From Graphene Oxide to Reduced Graphene Oxide: Impact on the Physiochemical and Mechanical Properties of Graphene–Cement Composites," ACS Appl Mater Interfaces, vol. 9, no. 49, pp. 43275–43286, Dec. 2017, doi: https://doi.org/10.1021/acsami.7b16736

[69] A. T. Smith, A. M. LaChance, S. Zeng, B. Liu, and L. Sun, "Synthesis, properties, and applications of graphene oxide/reduced graphene oxide and their nanocomposites," Nano Materials Science, vol. 1, no. 1, pp. 31–47, 2019, doi: https://doi.org/10.1016/j.nanoms.2019.02.004

[70] I. Fonseka, D. Mohotti, K. Wijesooriya, C.-K. Lee, and P. Mendis, "Influence of graphene oxide properties, superplasticiser type, and dispersion technique on

mechanical performance of graphene oxide-added concrete," Constr Build Mater, vol. 428, p. 136415, 2024, doi: https://doi.org/10.1016/j.conbuildmat.2024.136415

[71] S. Prabavathy, K. Jeyasubramanian, S. Prasanth, G. S. Hikku, and R. B. J. Robert, "Enhancement in behavioral properties of cement mortar cubes admixed with reduced graphene oxide," Journal of Building Engineering, vol. 28, p. 101082, 2020, doi: https://doi.org/10.1016/j.jobe.2019.101082

[72] J. Phiri, L.-S. Johansson, P. Gane, and T. Maloney, "A comparative study of mechanical, thermal and electrical properties of graphene-, graphene oxide- and reduced graphene oxide-doped microfibrillated cellulose nanocomposites," Compos B Eng, vol. 147, pp. 104–113, Apr. 2018, doi: https://doi.org/10.1016/j.compositesb.2018.04.018

[73] L. Serrano-Luján et al., "Environmental impact of the production of graphene oxide and reduced graphene oxide," SN Appl Sci, vol. 1, no. 2, p. 179, 2019, doi: https://doi.org/10.1007/s42452-019-0193-1

[74] T. S. Qureshi and D. K. Panesar, "Impact of graphene oxide and highly reduced graphene oxide on cement based composites," Constr Build Mater, vol. 206, pp. 71–83, 2019, doi: https://doi.org/10.1016/j.conbuildmat.2019.01.176

[75] G. Jing et al., "From graphene oxide to reduced graphene oxide: Enhanced hydration and compressive strength of cement composites," Constr Build Mater, vol. 248, p. 118699, 2020, doi: https://doi.org/10.1016/j.conbuildmat.2020.118699

[76] "Ministry of steel: Strategy and target to meet growing steel demand," New Delhi, Aug. 2024. https://pib.gov.in/PressReleaseIframePage.aspx?PRID=2040742

[77] "Government of India, Ministry of steel," Jul. 2024. https://steel.gov.in/sites/default/files/Monthly%20Summary%20for%20the%20month%20of%20July-2024.pdf

[78] J. Zhao, K. Ni, Y. Su, and Y. Shi, "An evaluation of iron ore tailings characteristics and iron ore tailings concrete properties," Constr Build Mater, vol. 286, p. 122968, 2021, doi: https://doi.org/10.1016/j.conbuildmat.2021.122968

[79] N. M, Y. M. Manjunath, and S. H. S. Prasanna, “Ferrock: A Carbon Negative Sustainable Concrete,” International Journal of Sustainable Construction Engineering and Technology, vol. 11, no. 4 SE-Articles, pp. 90–98, Feb. 2021, [Online]. Available: https://penerbit.uthm.edu.my/ojs/index.php/IJSCET/article/view/8084

[80] S. Karthika, A. Leema Rose, and G. Priyadarshini, “Sustainable Development on Ferrock Mortar Cubes,” J Phys Conf Ser, vol. 2040, no. 1, p. 12020, 2021, doi: https://doi.org/10.1088/1742-6596/2040/1/012020

[81] D. S. Vijayan, Dineshkumar, S. Arvindan, and T. Shreelakshmi Janarthanan, “Evaluation of ferrock: A greener substitute to cement,” Mater Today Proc, vol. 22, pp. 781–787, 2020, doi: https://doi.org/10.1016/j.matpr.2019.10.147

[82] “Ministry of Steel, Strategy and target to meet growing steel demand,” New Delhi, Aug. 2024. https://steel.gov.in/sites/default/files/Monthly%20Summary%20for%20August-2024.pdf

[83] V. S. Devi and B. K. Gnanavel, “Properties of Concrete Manufactured Using Steel Slag,” Procedia Eng, vol. 97, pp. 95–104, 2014, doi: https://doi.org/10.1016/j.proeng.2014.12.229

[84] S. Das, B. Souliman, D. Stone, and N. Neithalath, “Synthesis and Properties of A Novel Structural Binder Utilizing the Chemistry of Iron Carbonation.,” ACS Appl Mater Interfaces, vol. 6, May 2014, doi: https://doi.org/10.1021/am5011145

[85] S. Das, D. Stone, D. Convey, and N. Neithalath, “Pore- and micro-structural characterization of a novel structural binder based on iron carbonation,” Mater Charact, vol. 98, Dec. 2014, doi: https://doi.org/10.1016/j.matchar.2014.10.025

[86] G. Lopez, J. Farfan, and C. Breyer, “Trends in the global steel industry: Evolutionary projections and defossilisation pathways through power-to-steel,” J Clean Prod, vol. 375, p. 134182, 2022, doi: https://doi.org/10.1016/j.jclepro.2022.134182

[87] N. Shinde, R. Gobinath, S. Chidambaram, and M. Shewale, “An experimental investigation on concrete blocks using Ferrock as a green binding material,” Mater Today Proc, 2023, doi: https://doi.org/10.1016/j.matpr.2023.06.361

[88] G. Singh and R. Siddique, “Effect of iron slag as partial replacement of fine aggregates on the durability characteristics of self-compacting concrete,” Constr Build Mater, vol. 128, pp. 88–95, 2016, doi: https://doi.org/10.1016/j.conbuildmat.2016.10.074

[89] A. S. Tarek, E.-D. A. Salah, and T. M. Reda, “Effect of High-Volume Ceramic Waste Powder as Partial Cement Replacement on Fresh and Compressive Strength of Self-Compacting Concrete,” Journal of Materials in Civil Engineering, vol. 31, no. 2, p. 04018374, Feb. 2019, doi: https://doi.org/10.1061/(ASCE)MT.1943-5533.0002588

[90] J. Jeffy Pravitha, R. Ninija Merina, and N. Subash, “Mechanical properties and microstructural characterization of ferrock as CO2–negative material in self-compacting concrete,” Constr Build Mater, vol. 396, p. 132289, 2023, doi: https://doi.org/10.1016/j.conbuildmat.2023.132289

[91] Z. Liu, K. Takasu, H. Koyamada, and H. Suyama, “A study on engineering properties and environmental impact of sustainable concrete with fly ash or GGBS,” Constr Build Mater, vol. 316, p. 125776, 2022, doi: https://doi.org/10.1016/j.conbuildmat.2021.125776

[92] M. K. Mojdeh, M. Ehsan, O. Togay, and R. M. Mohammad, “Retracted: Durability Characteristics of Self-Compacting Concrete Incorporating Pumice and Metakaolin,” Journal of Materials in Civil Engineering, vol. 29, no. 11, p. 04017218, Nov. 2017, doi: https://doi.org/10.1061/(ASCE)MT.1943-5533.0002068

[93] B. B. Sabir, S. Wild, and J. Bai, “Metakaolin and calcined clays as pozzolans for concrete: a review,” Cem Concr Compos, vol. 23, no. 6, pp. 441–454, 2001, doi: https://doi.org/10.1016/S0958-9465(00)00092-5

[94] M. R. Jones, R. K. Dhir, and B. J. Magee, “Concrete containing ternary blended binders: Resistance to chloride ingress and carbonation,” Cem Concr Res, vol. 27, no. 6, pp. 825–831, 1997, doi: https://doi.org/10.1016/S0008-8846(97)00075-6

[95] J. Dweck, P. F. Ferreira da Silva, P. M. Büchler, and F. K. Cartledge, “Study by thermogravimetry of the evolution of ettringite phase during type II Portland cement

hydration," J Therm Anal Calorim, vol. 69, no. 1, pp. 179–186, 2002, doi: https://doi.org/10.1023/A:1019950126184

[96] O. R. Kavitha, V. M. Shanthi, G. Prince Arulraj, and P. Sivakumar, "Fresh, micro- and macrolevel studies of metakaolin blended self-compacting concrete," Appl Clay Sci, vol. 114, pp. 370–374, 2015, doi: https://doi.org/10.1016/j.clay.2015.06.024

[97] G. Mishra, A. Warda, and S. P. Shah, "Carbon sequestration in graphene oxide modified cementitious system," Journal of Building Engineering, vol. 62, p. 105356, 2022, doi: https://doi.org/10.1016/j.jobe.2022.105356

[98] X. Liu, P. Feng, Y. Cai, X. Yu, C. Yu, and Q. Ran, "Carbonation behavior of calcium silicate hydrate (C-S-H): Its potential for CO2 capture," Chemical Engineering Journal, vol. 431, p. 134243, 2022, doi: https://doi.org/10.1016/j.cej.2021.134243

[99] S. Siddique, A. Naqi, and J. G. Jang, "Influence of water to cement ratio on CO2 uptake capacity of belite-rich cement upon exposure to carbonation curing," Cem Concr Compos, vol. 111, p. 103616, Apr. 2020, doi: https://doi.org/10.1016/j.cemconcomp.2020.103616

[100] K. K. Das, R. Sharma, S. Dutta, J. Seo, and J. G. Jang, "Effects of curing regime, cement type, and water-to-cement ratio on the physicochemical, mechanical, and hydraulic properties of pervious mortar," Constr Build Mater, vol. 401, p. 132897, 2023, doi: https://doi.org/10.1016/j.conbuildmat.2023.132897

[101] R. R. Bellum, K. Muniraj, C. S. R. Indukuri, and S. R. C. Madduru, "Investigation on Performance Enhancement of Fly ash-GGBFS Based Graphene Geopolymer Concrete," Journal of Building Engineering, vol. 32, p. 101659, 2020, doi: https://doi.org/10.1016/j.jobe.2020.101659

[102] R. R. Bellum, K. H. K. Reddy, G. C. Reddy, M. V. R. K. Reddy, and S. Gamini, "Influence of steel slag on strength and microstructural characteristics of fly ash-based geopolymer concrete," Multiscale and Multidisciplinary Modeling, Experiments and Design, vol. 7, no. 6, pp. 5499–5514, 2024, doi: https://doi.org/10.1007/s41939-024-00541-0

[103] T. Kalra and R. Kumar, “Comparison of Normal and High Volume Fly Ash Concrete,” 2016.doi: https://www.academia.edu/89566789

[104] R. Khan, A. Jabbar, I. Ahmad, W. Khan, A. N. Khan, and J. Mirza, “Reduction in environmental problems using rice-husk ash in concrete,” Constr Build Mater, vol. 30, pp. 360–365, 2012, doi: https://doi.org/10.1016/j.conbuildmat.2011.11.028

[105] B. Uzbaş and A. Aydin, “Analysis of Fly Ash Concrete with Scanning Electron Microscopy and X-Ray Diffraction,” Advances in Science and Technology Research Journal, vol. 13, pp. 100–110, Dec. 2019, doi: https://doi.org/10.12913/22998624/114178

[106] B. Lothenbach, K. Scrivener, and R. D. Hooton, “Supplementary cementitious materials,” Cem Concr Res, vol. 41, no. 12, pp. 1244–1256, 2011, doi: https://doi.org/10.1016/j.cemconres.2010.12.001

[107] M. J. Carmichael, G. P. Arulraj, and P. L. Meyyappan, “Effect of partial replacement of cement with nano fly ash on permeable concrete: A strength study,” Mater Today Proc, vol. 43, pp. 2109–2116, 2021, doi: https://doi.org/10.1016/j.matpr.2020.11.891

[108] E. R. Teixeira, R. Mateus, A. F. Camões, L. Bragança, and F. G. Branco, “Comparative environmental life-cycle analysis of concretes using biomass and coal fly ashes as partial cement replacement material,” J Clean Prod, vol. 112, pp. 2221–2230, 2016, doi: https://doi.org/10.1016/j.jclepro.2015.09.124

[109] K. Scrivener, F. Martirena, S. Bishnoi, and S. Maity, “Calcined clay limestone cements (LC3),” Cem Concr Res, vol. 114, pp. 49–56, 2018, doi: https://doi.org/10.1016/j.cemconres.2017.08.017

[110] J. E. Rossen, B. Lothenbach, and K. L. Scrivener, “Composition of C–S–H in pastes with increasing levels of silica fume addition,” Cem Concr Res, vol. 75, pp. 14–22, 2015, doi: https://doi.org/10.1016/j.cemconres.2015.04.016

[111] R. Snellings, P. Suraneni, and J. Skibsted, “Future and emerging supplementary cementitious materials,” Cem Concr Res, vol. 171, p. 107199, 2023, doi: https://doi.org/10.1016/j.cemconres.2023.107199

[112] A. M. Diab, A. E. M. Abd Elmoaty, and A. A. Aly, “Long term study of mechanical properties, durability and environmental impact of limestone cement concrete,” Alexandria Engineering Journal, vol. 55, no. 2, pp. 1465–1482, 2016, doi: https://doi.org/10.1016/j.aej.2016.01.031

[113] D. Wang, C. Shi, N. Farzadnia, Z. Shi, and H. Jia, “A review on effects of limestone powder on the properties of concrete,” Constr Build Mater, vol. 192, pp. 153–166, 2018, doi: https://doi.org/10.1016/j.conbuildmat.2018.10.119

[114] A. S. Ruviaro et al., “Valorization of oat husk ash in metakaolin-based geopolymer pastes,” Constr Build Mater, vol. 367, p. 130341, 2023, doi: https://doi.org/10.1016/j.conbuildmat.2023.130341

[115] P. Zhan et al., “Utilization of nano-metakaolin in concrete: A review,” Journal of Building Engineering, vol. 30, p. 101259, 2020, doi: https://doi.org/10.1016/j.jobe.2020.101259

[116] B. Lothenbach, K. Scrivener, and R. D. Hooton, “Supplementary cementitious materials,” Cem Concr Res, vol. 41, no. 12, pp. 1244–1256, 2011, doi: https://doi.org/10.1016/j.cemconres.2010.12.001

[117] R. Siddique and J. Klaus, “Influence of metakaolin on the properties of mortar and concrete: A review,” Appl Clay Sci, vol. 43, no. 3, pp. 392–400, 2009, doi: https://doi.org/10.1016/j.clay.2008.11.007

[118] A. Srivastava, A. Mishra, and S. K. Singh, “An examination of the impact of waste plastic fibers and nanomaterials on concrete properties,” Discov Mater, vol. 5, no. 1, p. 72, 2025, doi: https://doi.org/10.1007/s43939-025-00248-0

[119] A. E. Ali, A. S. Faried, and K. M. Osman, “Effect of elevated temperature on properties of concrete containing different types of nanomaterials,” Constr Build Mater, vol. 438, p. 136988, 2024, doi: https://doi.org/10.1016/j.conbuildmat.2024.136988

[120] H. A. Gamal, M. S. El-Feky, Y. R. Alharbi, A. A. Abadel, and M. Kohail, “Enhancement of the Concrete Durability with Hybrid Nano Materials,” Sustainability, vol. 13, no. 3, 2021, doi: https://doi.org/10.3390/su13031373

[121] A. M. Mohamed, “Influence of nano materials on flexural behavior and compressive strength of concrete,” HBRC Journal, vol. 12, no. 2, pp. 212–225, 2016, doi: https://doi.org/10.1016/j.hbrcj.2014.11.006

[122] A. I. Madbouly, M. M. Mokhtar, and M. S. Morsy, “Evaluating the performance of rGO/cement composites for SHM applications,” Constr Build Mater, vol. 250, p. 118841, 2020, doi: https://doi.org/10.1016/j.conbuildmat.2020.118841

[123] Y. Yan, L. Tian, W. Zhao, S. A. M. Lazaro, X. Li, and S. Tang, “Dielectric and mechanical properties of cement pastes incorporated with magnetically aligned reduced graphene oxide,” Developments in the Built Environment, vol. 18, p. 100471, 2024, doi: https://doi.org/10.1016/j.dibe.2024.100471

[124] P. M. Walunjkar and M. N. Bajad, “Review on effect of graphene reinforcement on properties of cement concrete,” Mater Today Proc, vol. 77, pp. 1045–1051, 2023, doi: https://doi.org/10.1016/j.matpr.2022.11.386

[125] K. Chintalapudi and R. M. Rao Pannem, “Strength properties of graphene oxide cement composites,” Mater Today Proc, vol. 45, pp. 3971–3975, 2021, doi: https://doi.org/10.1016/j.matpr.2020.08.369

[126] P. V. R. K. Reddy and D. R. Prasad, “Investigation on the impact of graphene oxide on microstructure and mechanical behaviour of concrete,” Journal of Building Pathology and Rehabilitation, vol. 7, no. 1, p. 30, 2022, doi: https://doi.org/10.1007/s41024-022-00166-1

[127] Y. Wang, J. Yang, and D. Ouyang, “Effect of Graphene Oxide on Mechanical Properties of Cement Mortar and its Strengthening Mechanism,” 2019. doi: https://doi.org/10.3390/ma12223753

[128] S. C. Devi and R. A. Khan, “Effect of graphene oxide on mechanical and durability performance of concrete,” Journal of Building Engineering, vol. 27, p. 101007, 2020, doi: https://doi.org/10.1016/j.jobe.2019.101007

[129] X. Li et al., “Improvement of mechanical properties by incorporating graphene oxide into cement mortar,” Mechanics of Advanced Materials and Structures, vol. 25,

no. 15–16, pp. 1313–1322, Dec. 2018, doi: https://doi.org/10.1080/15376494.2016.1218226

[130] M. Cao, H. Zhang, and C. Zhang, “Effect of graphene on mechanical properties of cement mortars,” J Cent South Univ, vol. 23, no. 4, pp. 919–925, 2016, doi: https://doi.org/10.1007/s11771-016-3139-4

[131] T. Tong, Z. Fan, Q. Liu, S. Wang, S. Tan, and Q. Yu, “Investigation of the effects of graphene and graphene oxide nanoplatelets on the micro- and macro-properties of cementitious materials,” Constr Build Mater, vol. 106, pp. 102–114, 2016, doi: https://doi.org/10.1016/j.conbuildmat.2015.12.092

[132] Z. Pan et al., “Mechanical properties and microstructure of a graphene oxide-cement composite,” 2015, doi: https://doi.org/10.1016/j.cemconcomp.2015.02.001

[133] A. Mohammed, J. G. Sanjayan, W. H. Duan, and A. Nazari, “Incorporating graphene oxide in cement composites: A study of transport properties,” Constr Build Mater, vol. 84, pp. 341–347, 2015, doi: https://doi.org/10.1016/j.conbuildmat.2015.01.083

[134] G. K. Chaturvedy, K. Paras Krishna, and U. K. and Pandey, “Analyzing the effect of reduced graphene oxide on the physical, mechanical, and long-term durability performance of rubberized concrete,” Fullerenes, Nanotubes and Carbon Nanostructures, pp. 1–19, doi: https://doi.org/10.1080/1536383X.2025.2475977

[135] N. Parthasarathi, M. Prakash, and V. Subhash, “Enhancing environmental sustainability in concrete buildings with zeolite and reduced graphene oxide additives,” Innovative Infrastructure Solutions, vol. 9, no. 12, p. 468, 2024, doi: https://doi.org/10.1007/s41062-024-01792-z

[136] M. Valizadeh Kiamahalleh, A. Gholampour, Y. Tang, and T. D. Ngo, “Incorporation of reduced graphene oxide in waste-based concrete including lead smelter slag and recycled coarse aggregate,” Journal of Building Engineering, vol. 88, p. 109221, 2024, doi: https://doi.org/10.1016/j.jobe.2024.109221

[137] X. Wang, D. Feng, J. Zhong, and X. Shi, “Reinforcement of cement paste by reduced graphene oxide: effect of dispersion state,” Mater Struct, vol. 55, no. 1, p. 25, 2022, doi: https://doi.org/10.1617/s11527-021-01826-3

[138] S. Zhai et al., “Investigation on preparation and multifunctionality of reduced graphene oxide cement mortar,” Constr Build Mater, vol. 275, p. 122119, 2021, doi: https://doi.org/10.1016/j.conbuildmat.2020.122119

[139] N. Zhang, W. She, F. Du, and K. Xu, “Experimental Study on Mechanical and Functional Properties of Reduced Graphene Oxide/Cement Composites,” Materials, vol. 13, no. 13, 2020, doi: https://doi.org/10.3390/ma13133015

[140] G. Jing et al., “Introducing reduced graphene oxide to enhance the thermal properties of cement composites,” Cem Concr Compos, vol. 109, p. 103559, 2020, doi: https://doi.org/10.1016/j.cemconcomp.2020.103559

[141] T. S. Qureshi and D. K. Panesar, “Impact of graphene oxide and highly reduced graphene oxide on cement-based composites,” Constr Build Mater, vol. 206, pp. 71–83, 2019, doi: https://doi.org/10.1016/j.conbuildmat.2019.01.176

[142] A. Mallett and P. Pal, “Green transformation in the iron and steel industry in India: Rethinking patterns of innovation,” Energy Strategy Reviews, vol. 44, p. 100968, 2022, doi: https://doi.org/10.1016/j.esr.2022.100968

[143] E. Khankhaje, T. Kim, H. Jang, C.-S. Kim, J. Kim, and M. Rafieizonooz, “Properties of pervious concrete incorporating fly ash as partial replacement of cement: A review,” Developments in the Built Environment, vol. 14, p. 100130, 2023, doi: https://doi.org/10.1016/j.dibe.2023.100130

[144] D. K. Nayak, P. P. Abhilash, R. Singh, R. Kumar, and V. Kumar, “Fly ash for sustainable construction: A review of fly ash concrete and its beneficial use case studies,” Cleaner Materials, vol. 6, p. 100143, 2022, doi: https://doi.org/10.1016/j.clema.2022.100143

[145] J. Krithika and G. B. Ramesh Kumar, “Influence of fly ash on concrete – A systematic review,” Mater Today Proc, vol. 33, pp. 906–911, 2020, doi: https://doi.org/10.1016/j.matpr.2020.06.425

[146] D. S. Vijayan, Dineshkumar, S. Arvindan, and T. Shreelakshmi Janarthanan, “Evaluation of ferrock: A greener substitute to cement,” Mater Today Proc, vol. 22, pp. 781–787, 2020, doi: https://doi.org/10.1016/j.matpr.2019.10.147

[147] S. Khan, M. parveez, and M. A. Tantray, “Metakaolin-infused concrete for sustainable and durable building rehabilitation,” Journal of Building Pathology and Rehabilitation, vol. 10, no. 1, p. 66, 2025, doi: https://doi.org/10.1007/s41024-025-00578-9

[148] D. L. Pillay, O. B. Olalusi, M. W. Kiliswa, P. O. Awoyera, J. T. Kolawole, and A. J. Babafemi, “Engineering performance of metakaolin based concrete,” Clean Eng Technol, vol. 6, p. 100383, 2022, doi: https://doi.org/10.1016/j.clet.2021.100383

[149] S. Elavarasan, A. K. Priya, N. Ajai, S. Akash, T. J. Annie, and G. Bhuvana, “Experimental study on partial replacement of cement by metakaolin and GGBS,” Mater Today Proc, vol. 37, pp. 3527–3530, 2021, doi: https://doi.org/10.1016/j.matpr.2020.09.416

[150] R. A. Izadifard, M. Abdi Moghadam, and M. M. Sepahi, “Influence of metakaolin as a partial replacement of cement on characteristics of concrete exposed to high temperatures,” J Sustain Cem Based Mater, vol. 10, no. 6, pp. 336–352, Nov. 2021, doi: https://doi.org/10.1080/21650373.2021.1877206

[151] S. Mukherjee, R. Kumar, M. Behera, A. Goyal, and M. R. Rahman, “Rheology, mechanical properties and microstructure characterization of limestone calcined clay cement (LC3) incorporated sustainable lightweight self-compacting concrete,” Developments in the Built Environment, vol. 21, p. 100601, 2025, doi: https://doi.org/10.1016/j.dibe.2025.100601

[152] D. Wang, C. Shi, N. Farzadnia, Z. Shi, and H. Jia, “A review on effects of limestone powder on the properties of concrete,” Constr Build Mater, vol. 192, pp. 153–166, 2018, doi: https://doi.org/10.1016/j.conbuildmat.2018.10.119

[153] A. A. Elgalhud, R. K. Dhir, and G. Ghataora, “Limestone addition effects on concrete porosity,” Cem Concr Compos, vol. 72, pp. 222–234, 2016, doi: https://doi.org/10.1016/j.cemconcomp.2016.06.006

[154] Indian Standards, IS 4031 Part 1 (1996): Methods of physical tests for hydraulic cement, Part 1: Determination of fineness by dry sieving."

[155] Indian Standards, IS 4031 Part 3 (2005): Methods of Physical Tests for Hydraulic Cement, Part 3: Determination of Soundness," New Delhi, pp. 1–10, 2005.

[156] Indian Standard, IS 4031 Part 4 (2024): Methods of physical tests for hydraulic cement, Part 4: Determination of consistency of standard cement paste

[157] Indian Standards, IS 4031 Part 5 (1988): Methods of physical tests for hydraulic cement, Part 5:(Reaffirmed 2005)," 2005. doi: https://law.resource.org/pub/in/bis/S03/is.4031.5.1988.pdf

[158] Indian Standards, IS 383 2016, Reaffirmed 2021: Specification for Coarse and Fine Aggregates From Natural Sources For Concrete doi: https://www.services.bis.gov.in/tmp/tbl5_2024-11-10_11.pdf

[159] Indian Standard, IS 2386 (1963) Part III (Reaffirmed 2002), "Method of Test for aggregate for concrete. Specific gravity, density, voids, absorption and bulking," New Delhi

[160] Indian Standard, IS 2386 (1963) Part 1 (Reaffirmed 2002) "Methods of Test for Aggregates for Concrete: Particle Size and Shape.

[161] "Designation: C618 − 22 Standard Specification for Coal Fly Ash and Raw or Calcined Natural Pozzolan for Use in Concrete 1", doi: https://doi.org/10.1520/C0618-22

[162] E. Vejmelková, M. Keppert, S. Grzeszczyk, B. Skaliński, and R. Černý, "Properties of self-compacting concrete mixtures containing metakaolin and blast furnace slag," Constr Build Mater, vol. 25, no. 3, pp. 1325–1331, 2011, doi: https://doi.org/10.1016/j.conbuildmat.2010.09.012

[163] B. Lothenbach, G. Le Saout, E. Gallucci, and K. Scrivener, "Influence of limestone on the hydration of Portland cements," Cem Concr Res, vol. 38, no. 6, pp. 848–860, 2008, doi: https://doi.org/10.1016/j.cemconres.2008.01.002

[164] H. Sui, P. Hou, Y. Liu, K. Sagoe-Crentsil, F. Basquiroto de Souza, and W. Duan, "Limestone calcined clay cement: mechanical properties, crystallography, and microstructure development," J Sustain Cem Based Mater, vol. 12, no. 4, pp. 427–440, Apr. 2023, doi: https://doi.org/10.1080/21650373.2022.2074911

[165] G. İnan Sezer, "Compressive strength and sulfate resistance of limestone and/or silica fume mortars," Constr Build Mater, vol. 26, no. 1, pp. 613–618, 2012, doi: https://doi.org/10.1016/j.conbuildmat.2011.06.064

[166] Indian Standards, IS 2720-10 Part 10 (2006): Methods of test for soils: Determination of unconfined compressive strength doi: https://law.resource.org/pub/in/bis/S03/is.2720.10.1991.pdf

[167] P. Zhan et al., "Utilization of nano-metakaolin in concrete: A review," Journal of Building Engineering, vol. 30, p. 101259, 2020, doi: https://doi.org/10.1016/j.jobe.2020.101259

[168] S. Chinchón-Payá, C. Andrade, and S. Chinchón, "Indicator of carbonation front in concrete as substitute to phenolphthalein," Cem Concr Res, vol. 82, pp. 87–91, 2016, doi: https://doi.org/10.1016/j.cemconres.2015.12.010

[169] J.-I. Choi, Y. Lee, Y. Y. Kim, and B. Y. Lee, "Image-processing technique to detect carbonation regions of concrete sprayed with a phenolphthalein solution," Constr Build Mater, vol. 154, pp. 451–461, 2017, doi: https://doi.org/10.1016/j.conbuildmat.2017.07.205

[170] Y. Lo and H. M. Lee, "Curing effects on carbonation of concrete using a phenolphthalein indicator and Fourier-transform infrared spectroscopy," Build Environ, vol. 37, no. 5, pp. 507–514, 2002, doi: https://doi.org/10.1016/S0360-1323(01)00052-X

[171] Indian Standard, IS 1199 Part 2 (2018), "Fresh Concrete — Methods of Sampling, Testing and Analysis. weblink: www.standardsbis.in

[172] Indian Standards, IS 7320 (1974) Reaffirmed 2023: Specification for concrete slump test apparatus

[173] Indian Standards, IS 5515 (2004): Specification compacting factor apparatus

[174] Indian Standard, IS 10086 (2021): Moulds for Use in Tests of Cement, Concrete and Pozzolana-Specification

[175] Indian Standard, IS 516 (2021) Part 1: Hardened Concrete-Methods of Test-Testing of Strength of Hardened Concrete. weblink: www.standardsbis.in

[176] Indian Standards, IS 5816 (1999): Method of Test Splitting Tensile Strength of Concrete.

[177] Standard Test Method for Flexural Strength of Concrete (Using Simple Beam with Third-Point Loading), doi: https://doi.org/10.1520/C0078_C0078M-1

[178] ASTM C 642, Feb. 01, 2013, ASTM International, West Conshohocken, PA. doi: https://doi.org/10.1520/C0642-13

[179] EN 12390- 208 (2009), Testing hardened concrete. Part 8, Depth of penetration of water under pressure. BSI, 2009.

[180] Indian Standards, "BIS 1881- part 208 (1996). Recommendations for the determination of the initial surface absorption of concrete. doi: https://dl.azmanco.com/standards/BS/BS%201881-part%20208-96.pdf

[181] ASTM 1202, (2022), Standard Test Method for Electrical Indication of Concrete's Ability to Resist Chloride Ion Penetration, doi: https://doi.org/10.1520/C1202

[182] Y. Lo and H. M. Lee, "Curing effects on carbonation of concrete using a phenolphthalein indicator and Fourier-transform infrared spectroscopy," Build Environ, vol. 37, no. 5, pp. 507–514, 2002, doi: https://doi.org/10.1016/S0360-1323(01)00052-X

[183] N. Giulietti et al., "Automated measurement system for detecting carbonation depth: Image-processing based technique applied to concrete sprayed with phenolphthalein," Measurement, vol. 175, p. 109142, 2021, doi: https://doi.org/10.1016/j.measurement.2021.109142

[184] K. Chintalapudi and R. M. R. Pannem, "An intense review on the performance of Graphene Oxide and reduced Graphene Oxide in an admixed cement system," Constr

Build Mater, vol. 259, p. 120598, 2020, doi: https://doi.org/10.1016/j.conbuildmat.2020.120598

[185] T. M. Sheikh et al., "Chemical interference between graphene oxide and polycarboxylate superplasticizer, and the resulting impact on the concrete strength, workability, and microstructure," J Sustain Cem Based Mater, vol. 13, no. 12, pp. 1782–1794, Dec. 2024, doi: https://doi.org/10.1080/21650373.2024.2411303

[186] Y. Shang, D. Zhang, C. Yang, Y. Liu, and Y. Liu, "Effect of graphene oxide on the rheological properties of cement pastes," Constr Build Mater, vol. 96, pp. 20–28, 2015, doi: https://doi.org/10.1016/j.conbuildmat.2015.07.181

[187] Shang, Wei, Yanbo Wen, Jinrong Yang, and Jinghong Liu. 2025. "Effect of Graphene Oxide on Mechanical Properties and Durability of Steel Fiber Reinforced Concrete under Different Corrosion Environments." European Journal of Environmental and Civil Engineering, March, 1–21. doi: https://doi.org/10.1080/19648189.2025.2479119

[188] K. Vance, M. Aguayo, T. Oey, G. Sant, and N. Neithalath, "Hydration and strength development in ternary portland cement blends containing limestone and fly ash or metakaolin," Cem Concr Compos, vol. 39, pp. 93–103, 2013, doi: https://doi.org/10.1016/j.cemconcomp.2013.03.028

[189] Deveshan L. Pillay, Oladimeji B. Olalusi, Moses W. Kiliswa, Paul O. Awoyera, John Temitope Kolawole, Adewumi John Babafemi, Engineering performance of metakaolin based concrete, Cleaner Engineering and Technology, 6, 2022, https://doi.org/10.1016/j.clet.2021.100383

[190] Pei-min Zhan, Zhi-hai He, Zhi-ming Ma, Chao-feng Liang, Xiao-xiang Zhang, Annulo Addisayehu Abreham, Jin-yan Shi, Utilization of nano-metakaolin in concrete: A review, Journal of Building Engineering, https://doi.org/10.1016/j.jobe.2020.101259

[191] S. Lv, Y. Ma, C. Qiu, T. Sun, J. Liu, and Q. Zhou, "Effect of graphene oxide nanosheets of microstructure and mechanical properties of cement composites," Constr Build Mater, vol. 49, pp. 121–127, 2013, doi: https://doi.org/10.1016/j.conbuildmat.2013.08.022

[192] Y. Shang, D. Zhang, C. Yang, Y. Liu, and Y. Liu, “Effect of graphene oxide on the rheological properties of cement pastes,” Constr Build Mater, vol. 96, pp. 20–28, Oct. 2015, doi: https://doi.org/10.1016/j.conbuildmat.2015.07.181

[193] K. Gong et al., “Reinforcing Effects of Graphene Oxide on Portland Cement Paste,” Journal of Materials in Civil Engineering, vol. 27, p. A4014010, Feb. 2015, doi: https://doi.org/10.1061/(ASCE)MT.1943-5533.0001125

[194] S. Sharma and N. C. Kothiyal, “Influence of graphene oxide as dispersed phase in cement mortar matrix in defining the crystal patterns of cement hydrates and its effect on mechanical, microstructural and crystallization properties,” RSC Adv, vol. 5, no. 65, pp. 52642–52657, 2015, doi: https://doi.org/10.1039/C5RA08078A

[195] R.-S. Lin, Y. Han, and X.-Y. Wang, “Experimental study on optimum proportioning of Portland cements, limestone, metakaolin, and fly ash for obtaining quaternary cementitious composites,” Case Studies in Construction Materials, vol. 15, p. e00691, 2021, doi: https://doi.org/10.1016/j.cscm.2021.e00691

[196] C. Liu et al., “Advance on the dispersion treatment of graphene oxide and the graphene oxide modified cement-based materials,” vol. 10, no. 1, pp. 34–49, 2021, doi: https://doi.org/10.1515/ntrev-2021-0003

[197] O. Esping, “Effect of limestone filler BET(H2O)-area on the fresh and hardened properties of self-compacting concrete,” Cem Concr Res, vol. 38, no. 7, pp. 938–944, 2008, doi: https://doi.org/10.1016/j.cemconres.2008.03.010

[198] T. Susan Ja, M. Mathew, and S. C. George, “Experimental investigations on the impact of graphene-based oxides in concrete,” Mater Today Proc, 2023, doi: https://doi.org/10.1016/j.matpr.2023.08.071

[199] J. Park, Y. S. Cho, S. J. Sung, M. Byeon, S. J. Yang, and C. R. Park, “Characteristics tuning of graphene-oxide-based-graphene to various end-uses,” Energy Storage Mater, vol. 14, pp. 8–21, 2018, doi: https://doi.org/10.1016/j.ensm.2018.02.013

[200] Y. Sui, S. Liu, C. Ou, Q. Liu, and G. Meng, “Experimental investigation for the influence of graphene oxide on properties of the cement-waste concrete powder

composite," Constr Build Mater, vol. 276, p. 122229, 2021, doi: https://doi.org/10.1016/j.conbuildmat.2020.122229

[201] G. Kai et al., "Reinforcing Effects of Graphene Oxide on Portland Cement Paste," Journal of Materials in Civil Engineering, vol. 27, no. 2, p. A4014010, Feb. 2015, doi: https://doi.org/10.1061/(ASCE)MT.1943-5533.0001125

[202] P. K. Akarsh, D. Shrinidhi, S. Marathe, and A. K. Bhat, "Graphene oxide as nano-material in developing sustainable concrete – A brief review," Mater Today Proc, vol. 60, pp. 234–246, 2022, doi: https://doi.org/10.1016/j.matpr.2021.12.510

[203] E. F. Irassar, "Sulfate attack on cementitious materials containing limestone filler — A review," Cem Concr Res, vol. 39, no. 3, pp. 241–254, 2009, doi: https://doi.org/10.1016/j.cemconres.2008.11.007

[204] A. Yahia, M. Tanimura, and Y. Shimoyama, "Rheological properties of highly flowable mortar containing limestone filler-effect of powder content and W/C ratio," Cem Concr Res, vol. 35, no. 3, pp. 532–539, 2005, doi: https://doi.org/10.1016/j.cemconres.2004.05.008

[205] X. Li et al., "Effects of graphene oxide agglomerates on workability, hydration, microstructure and compressive strength of cement paste," Constr Build Mater, vol. 145, pp. 402–410, 2017, doi: https://doi.org/10.1016/j.conbuildmat.2017.04.058

[206] Z. Pan et al., "Mechanical properties and microstructure of a graphene oxide–cement composite," Cem Concr Compos, vol. 58, pp. 140–147, 2015, doi: https://doi.org/10.1016/j.cemconcomp.2015.02.001

[207] Q. Wang, G. Qi, Y. Wang, H. Zheng, S. Shan, and C. Lu, "Research progress on the effect of graphene oxide on the properties of cement-based composites," New Carbon Materials, vol. 36, no. 4, pp. 729–750, 2021, doi: https://doi.org/10.1016/S1872-5805(21)60071-9

[208] S. Zhai et al., "Investigation on preparation and multifunctionality of reduced graphene oxide cement mortar," Constr Build Mater, vol. 275, p. 122119, 2021, doi: https://doi.org/10.1016/j.conbuildmat.2020.122119

[209] E. Shamsaei, F. B. de Souza, X. Yao, E. Benhelal, A. Akbari, and W. Duan, "Graphene-based nanosheets for stronger and more durable concrete: A review," Constr Build Mater, vol. 183, pp. 642–660, 2018, doi: https://doi.org/10.1016/j.conbuildmat.2018.06.201

[210] H. Du and S. D. Pang, "Enhancement of barrier properties of cement mortar with graphene nanoplatelet," Cem Concr Res, vol. 76, pp. 10–19, 2015, doi: https://doi.org/10.1016/j.cemconres.2015.05.007

[211] A. Gholampour, M. Sofi, H. Alipooramirabad, and Y. Tang, "Performance of concrete containing pristine graphene-treated recycled concrete aggregates," Resour Conserv Recycl, vol. 199, p. 107266, 2023, doi: https://doi.org/10.1016/j.resconrec.2023.107266

[212] O. Abiodun, C. Kabubo, R. Mutuku, and O. Ejohwomu, "The Effect of Pristine Graphene on the Mechanical Properties of Geopolymer Mortar," 2023. doi: https://doi.org/10.3390/su15021706

[213] M. A. S. Anjos, A. Camões, P. Campos, G. A. Azeredo, and R. L. S. Ferreira, "Effect of high volume fly ash and metakaolin with and without hydrated lime on the properties of self-compacting concrete," Journal of Building Engineering, vol. 27, p. 100985, 2020, doi: https://doi.org/10.1016/j.jobe.2019.100985

[214] G. Singh and R. Siddique, "Strength properties and micro-structural analysis of self-compacting concrete made with iron slag as partial replacement of fine aggregates," Constr Build Mater, vol. 127, pp. 144–152, 2016, doi: https://doi.org/10.1016/j.conbuildmat.2016.09.154

[215] F. Han, Y. Zhou, and Z. Zhang, "Effect of gypsum on the properties of composite binder containing high-volume slag and iron tailing powder," Constr Build Mater, vol. 252, p. 119023, 2020, doi: https://doi.org/10.1016/j.conbuildmat.2020.119023

[216] Md Jihad Miah, "Effect of Recycled Iron Powder as Fine Aggregate on the Mechanical, Durability, and High Temperature Behavior of Mortars, Materials 13(5), 2020. doi: https://doi.org/10.3390/ma13051168

[217] A. P. Barker and D. W. Hobbs, “Performance of Portland limestone cements in mortar prisms immersed in sulfate solutions at 5 °C,” Cem Concr Compos, vol. 21, no. 2, pp. 129–137, 1999, doi: https://doi.org/10.1016/S0958-9465(98)00009-2

[218] E. F. Irassar, V. L. Bonavetti, and M. González, “Microstructural study of sulfate attack on ordinary and limestone Portland cements at ambient temperature,” Cem Concr Res, vol. 33, no. 1, pp. 31–41, 2003, doi: https://doi.org/10.1016/S0008-8846(02)00914-6

[219] A. Hakamy, F. U. A. Shaikh, and I. M. Low, “Characteristics of nanoclay and calcined nanoclay-cement nanocomposites,” Compos B Eng, vol. 78, pp. 174–184, 2015, doi: https://doi.org/10.1016/j.compositesb.2015.03.074

[220] M. Ghazy, M. Elaty, and R. Elkhoriby, Performance of Blended Cement Mortars Incorporating Nano-Metakaolin Particles at Elevated Temperatures. 2015.

[221] H. M. Nadir, A. Ahmed, J. West, and A. Ahmed, “Experimental Investigation of Engineering Properties of Iron-Based Binary and Ternary Pozzolanic Supplementary Cementitious Materials,” Journal of Materials and Polymer Science, vol. 3, pp. 1–13, 2022, doi: https://doi.org/10.47485/2832-9384.1024

[222] M. Muthu, M. Santhanam, S. Sen Gupta, P. Thalappil, and S. Shah, “Influence of 2D rGO nanosheets on the properties of OPC paste,” Cem Concr Compos, vol. 70, Mar. 2016, doi: https://doi.org/10.1016/j.cemconcomp.2016.03.005

[223] M. Murugan, M. Santhanam, S. Sen Gupta, T. Pradeep, and S. P. Shah, “Influence of 2D rGO nanosheets on the properties of OPC paste,” Cem Concr Compos, vol. 70, pp. 48–59, 2016, doi: https://doi.org/10.1016/j.cemconcomp.2016.03.005

[224] C. Lin, W. Wei, and Y. H. Hu, “Catalytic behavior of graphene oxide for cement hydration process,” Journal of Physics and Chemistry of Solids, vol. 89, pp. 128–133, 2016, doi: https://doi.org/10.1016/j.jpcs.2015.11.002

[225] G. K. Chaturvedy, U. K. Pandey, and H. Kumar, “Effect of graphene oxide on the microscopic, physical and mechanical characteristics of rubberized concrete,” Innovative Infrastructure Solutions, vol. 8, no. 6, p. 163, 2023, doi: https://doi.org/10.1007/s41062-023-01133-6

[226] W. Meng and K. H. Khayat, “Mechanical properties of ultra-high-performance concrete enhanced with graphite nanoplatelets and carbon nanofibers,” Compos B Eng, vol. 107, pp. 113–122, 2016, doi: https://doi.org/10.1016/j.compositesb.2016.09.069

[227] R. Choudhary, R. Gupta, and R. Nagar, “Impact on fresh, mechanical, and microstructural properties of high strength self-compacting concrete by marble cutting slurry waste, fly ash, and silica fume,” Constr Build Mater, vol. 239, p. 117888, 2020, doi: https://doi.org/10.1016/j.conbuildmat.2019.117888

[228] A. Monshi and M. K. Asgarani, “Producing Portland cement from iron and steel slags and limestone,” Cem Concr Res, vol. 29, no. 9, pp. 1373–1377, 1999, doi: https://doi.org/10.1016/S0008-8846(99)00028-9

[229] P. E. Tsakiridis, G. D. Papadimitriou, S. Tsivilis, and C. Koroneos, “Utilization of steel slag for Portland cement clinker production,” J Hazard Mater, vol. 152, no. 2, pp. 805–811, 2008, doi: https://doi.org/10.1016/j.jhazmat.2007.07.093

[230] X. Li et al., “Effects of graphene oxide agglomerates on workability, hydration, microstructure and compressive strength of cement paste,” Constr Build Mater, vol. 145, pp. 402–410, 2017, doi: https://doi.org/10.1016/j.conbuildmat.2017.04.058

[231] S. Zhai et al., “Investigation on preparation and multifunctionality of reduced graphene oxide cement mortar,” Constr Build Mater, vol. 275, p. 122119, 2021, doi: https://doi.org/10.1016/j.conbuildmat.2020.122119

[232] S. Zhai et al., “Investigation on preparation and multifunctionality of reduced graphene oxide cement mortar,” Constr Build Mater, vol. 275, p. 122119, 2021, doi: https://doi.org/10.1016/j.conbuildmat.2020.122119

[233] I. Papanikolaou, N. Arena, and A. Al-Tabbaa, “Graphene nanoplatelet reinforced concrete for self-sensing structures – A lifecycle assessment perspective,” J Clean Prod, vol. 240, p. 118202, 2019, doi: https://doi.org/10.1016/j.jclepro.2019.118202

[234] L. Wengui, L. Xiangyu, C. S. Jian, L. Guangcheng, L. Y. Ming, and D. W. Hui, “Effects of Nanoalumina and Graphene Oxide on Early-Age Hydration and Mechanical

Properties of Cement Paste," Journal of Materials in Civil Engineering, vol. 29, no. 9, p. 04017087, Sep. 2017, doi: https://doi.org/10.1061/(ASCE)MT.1943-5533.0001926

[235] H. M. Nadir, A. Ahmed, J. West, and A. Ahmed, "Experimental Investigation of Engineering Properties of Iron-Based Binary and Ternary Pozzolanic Supplementary Cementitious Materials," Journal of Materials and Polymer Science, vol. 3, no. 1, 2022, doi: https://doi.org/10.47485/2832-9384.1024

[236] A. A. E. Elzokra, A. al Houri, A. Habib, M. Habib, and A. Malkawi, "Shrinkage Behavior of Conventional and Nonconventional Concrete: A Review," Civil Engineering Journal, vol. 6, pp. 1839–1851, Sep. 2020, doi: https://doi.org/10.28991/cej-2020-03091586

[237] P. R. da Silva and J. de Brito, "Durability performance of self-compacting concrete (SCC) with binary and ternary mixes of fly ash and limestone filler," Mater Struct, vol. 49, no. 7, pp. 2749–2766, 2016, doi: https://doi.org/10.1617/s11527-015-0683-6

[238] Y. Aoki, S. Rasiah, and H. Khabbaz, "Properties of pervious concrete containing fly ash," Road Materials and Pavement Design, vol. 13, pp. 1–11, Mar. 2012, doi: https://doi.org/10.1080/14680629.2011.651834

[239] H. Liu, G. Luo, L. Wang, and Y. Gong, "Strength Time–Varying and Freeze–Thaw Durability of Sustainable Pervious Concrete Pavement Material Containing Waste Fly Ash," Sustainability, vol. 11, no. 1, 2019, doi: https://doi.org/10.3390/su11010176

[240] B. Wang and B. Pang, "Mechanical property and toughening mechanism of water reducing agents modified graphene nanoplatelets reinforced cement composites," Constr Build Mater, vol. 226, pp. 699–711, 2019, doi: https://doi.org/10.1016/j.conbuildmat.2019.07.229

[241] W. Baomin and D. Shuang, "Effect and mechanism of graphene nanoplatelets on hydration reaction, mechanical properties and microstructure of cement composites," Constr Build Mater, vol. 228, p. 116720, Dec. 2019, doi: https://doi.org/10.1016/j.conbuildmat.2019.116720

[242] R. Dandautiya and A. P. Singh, “Utilization potential of fly ash and copper tailings in concrete as partial replacement of cement along with life cycle assessment,” Waste Management, vol. 99, pp. 90–101, 2019, doi: https://doi.org/10.1016/j.wasman.2019.08.036

[243] M. Gesoğlu, E. Güneyisi, M. E. Kocabağ, V. Bayram, and K. Mermerdaş, “Fresh and hardened characteristics of self compacting concretes made with combined use of marble powder, limestone filler, and fly ash,” Constr Build Mater, vol. 37, pp. 160–170, 2012, doi: https://doi.org/10.1016/j.conbuildmat.2012.07.092

[244] P. V. R. K. Reddy and R. P. Darapureddi, “Synergetic Effect Of Graphene Oxide And Fly Ash On Workability, Mechanical And Microstructural Properties Of High-strength Concrete,” Jordan Journal of Civil Engineering, vol. 16, pp. 507–517, Jun. 2022. https://www.researchgate.net/publication/362155934

[245] M. M. Hulagabali, G. R. Vesmawala, and Y. D. Patil, “Synthesis, characterization, and application of graphene oxide and reduced graphene oxide and its influence on rheology, microstructure, and mechanical strength of cement paste,” Journal of Building Engineering, vol. 71, p. 106586, 2023, doi: https://doi.org/10.1016/j.jobe.2023.106586

[246] S. Zhai et al., “Investigation on preparation and multifunctionality of reduced graphene oxide cement mortar,” Constr Build Mater, vol. 275, p. 122119, 2021, doi: https://doi.org/10.1016/j.conbuildmat.2020.122119

[247] G. Jing et al., “From graphene oxide to reduced graphene oxide: Enhanced hydration and compressive strength of cement composites,” Constr Build Mater, vol. 248, p. 118699, 2020, doi: https://doi.org/10.1016/j.conbuildmat.2020.118699

[248] T. Shanmuga Priya, A. Mehra, S. Jain, and K. Kakria, “Effect of graphene oxide on high-strength concrete induced with rice husk ash: mechanical and durability performance,” Innovative Infrastructure Solutions, vol. 6, no. 1, p. 5, 2020, doi: https://doi.org/10.1007/s41062-020-00378-9

[249] P. Nath and P. Sarker, “Effect of Fly Ash on the Durability Properties of High Strength Concrete,” Procedia Eng, vol. 14, pp. 1149–1156, 2011, doi: https://doi.org/10.1016/j.proeng.2011.07.144

[250] S. P. Dalal and P. Dalal, “Experimental Investigation on Strength and Durability of Graphene Nanoengineered Concrete,” Constr Build Mater, vol. 276, p. 122236, 2021, doi: https://doi.org/10.1016/j.conbuildmat.2020.122236

[251] A. Khoshakhlagh, A. Nazari, and G. Khalaj, “Effects of Fe2O3 Nanoparticles on Water Permeability and Strength Assessments of High Strength Self-Compacting Concrete,” J Mater Sci Technol, vol. 28, no. 1, pp. 73–82, 2012, doi: https://doi.org/10.1016/S1005-0302(12)60026-7

[252] N. Sowmith and P. Anjaneya Babu, “Influence of Fly Ash on the Performance of Recycled Aggregate Concrete,” International Journal of Science and Research (IJSR), pp. 2319–7064, Jun. 2016, doi: https://doi.org/10.21275/v5i6.NOV164600

[253] S. Mishra and A. Jena, “Effect of fly ash on properties of pervious concrete,” May 2018. https://www.researchgate.net/publication/325301246

[254] H. Wang, H. Li, X. Liang, H. Zhou, N. Xie, and Z. Dai, “Investigation on the mechanical properties and environmental impacts of pervious concrete containing fly ash based on the cement-aggregate ratio,” Constr Build Mater, vol. 202, pp. 387–395, 2019, doi: https://doi.org/10.1016/j.conbuildmat.2019.01.044

[255] J. Endawati, R. Utami, and R. Rochaeti, “The Influence of Fly Ash and Aggregates Composition on Pervious Concrete Characteristics,” Materials Science Forum, vol. 917, pp. 297–302, Mar. 2018, doi: https://doi.org/10.4028/www.scientific.net/MSF.917.297

[256] E. Septiandini, I. Widiasanti, C. A. Pamungkas, A. S. S. Putri, T. Mulyono, and N. Z. P. Abdul, “Compressive strength of pervious concrete paving blocks for pavement with the addition of fly ash,” IOP Conf Ser Mater Sci Eng, vol. 1098, no. 2, p. 022046, 2021, doi: https://doi.org/10.1088/1757-899X/1098/2/022046

[257] H. Zibara, R. D. Hooton, M. D. A. Thomas, and K. Stanish, “Influence of the C/S and C/A ratios of hydration products on the chloride ion binding capacity of lime-

SF and lime-MK mixtures," Cem Concr Res, vol. 38, no. 3, pp. 422–426, 2008, doi: https://doi.org/10.1016/j.cemconres.2007.08.024

[258] L. G. Li and A. K. H. Kwan, "Adding limestone fines as cementitious paste replacement to improve tensile strength, stiffness and durability of concrete," Cem Concr Compos, vol. 60, pp. 17–24, 2015, doi: https://doi.org/10.1016/j.cemconcomp.2015.02.006

[259] J. J. Chen, A. K. H. Kwan, and Y. Jiang, "Adding limestone fines as cement paste replacement to reduce water permeability and sorptivity of concrete," Constr Build Mater, vol. 56, pp. 87–93, 2014, doi: https://doi.org/10.1016/j.conbuildmat.2014.01.066

[260] S. C. Devi and R. A. Khan, "Effect of graphene oxide on mechanical and durability performance of concrete," Journal of building engineering, vol. 6, pp. 201–214, 20202.doi: https://doi.org/10.1016/j.jobe.2019.101007

[261] R. E. Rodríguez-Camacho and R. Uribe-Afif, "Importance of using the natural pozzolans on concrete durability," Cem Concr Res, vol. 32, no. 12, pp. 1851–1858, 2002, doi: https://doi.org/10.1016/S0008-8846(01)00714-1

[262] N. Ghafoori, R. Spitek, and M. Najimi, "Influence of limestone size and content on transport properties of self-consolidating concrete," Constr Build Mater, vol. 127, pp. 588–595, 2016, doi: https://doi.org/10.1016/j.conbuildmat.2016.10.051

[263] H. Peng, Y. Ge, C. S. Cai, Y. Zhang, and Z. Liu, "Mechanical properties and microstructure of graphene oxide cement-based composites," Constr Build Mater, vol. 194, pp. 102–109, 2019, doi: https://doi.org/10.1016/j.conbuildmat.2018.10.234

[264] K. Marar and Ö. Eren, "Effect of cement content and water/cement ratio on fresh concrete properties without admixtures," International Journal of Physical Sciences, vol. 6, Oct. 2011. https://www.researchgate.net/publication/266602831

[265] U. M. Muthaiyan and S. and Thirumalai, "Studies on the properties of pervious fly ash–cement concrete as a pavement material," Cogent Eng, vol. 4, no. 1, p. 1318802, Jan. 2017, doi: https://doi.org/10.1080/23311916.2017.1318802

[266] M. M. Hulagabali, G. R. Vesmawala, and Y. D. Patil, “Synthesis, characterization, and application of graphene oxide and reduced graphene oxide and its influence on rheology, microstructure, and mechanical strength of cement paste,” Journal of Building Engineering, vol. 71, p. 106586, 2023, doi: https://doi.org/10.1016/j.jobe.2023.106586

[267] S. Du, Z. Tang, J. Zhong, Y. Ge, and X. Shi, “Effect of admixing graphene oxide on abrasion resistance of ordinary portland cement concrete,” AIP Adv, vol. 9, no. 10, p. 105110, Oct. 2019, doi: https://doi.org/10.1063/1.5124388

[268] S. Du, Z. Tang, J. Zhong, Y. Ge, and X. Shi, “Effect of admixing graphene oxide on abrasion resistance of ordinary portland cement concrete,” AIP Adv, vol. 9, no. 10, p. 105110, Oct. 2019, doi: https://doi.org/10.1063/1.5124388

[269] T. R. Praveenkumar, M. M. Vijayalakshmi, and M. S. Meddah, “Strengths and durability performances of blended cement concrete with TiO2 nanoparticles and rice husk ash,” Constr Build Mater, vol. 217, pp. 343–351, 2019, doi: https://doi.org/10.1016/j.conbuildmat.2019.05.045

[270] H. Hornain, J. Marchand, V. Duhot, and M. Moranville-Regourd, “Diffusion of chloride ions in limestone filler blended cement pastes and mortars,” Cem Concr Res, vol. 25, no. 8, pp. 1667–1678, 1995, doi: https://doi.org/10.1016/0008-8846(95)00163-8

[271] Z. Lu, D. Hou, L. Meng, G. Sun, C. Lu, and Z. Li, “Mechanism of cement paste reinforced by graphene oxide/carbon nanotubes composites with enhanced mechanical properties,” RSC Adv, vol. 5, no. 122, pp. 100598–100605, 2015, doi: https://doi.org/10.1039/C5RA18602A

[272] S. Zhai et al., “Investigation on preparation and multifunctionality of reduced graphene oxide cement mortar,” Constr Build Mater, vol. 275, p. 122119, 2021, doi: https://doi.org/10.1016/j.conbuildmat.2020.122119

[273] F. Pacheco-Torgal, S. Miraldo, Y. Ding, and J. A. Labrincha, “Targeting HPC with the help of nanoparticles: An overview,” Constr Build Mater, vol. 38, pp. 365–370, 2013, doi: https://doi.org/10.1016/j.conbuildmat.2012.08.013

[274] I. Fonseka, D. Mohotti, K. Wijesooriya, C.-K. Lee, and P. Mendis, “Influence of Graphene oxide on abrasion resistance and strength of concrete,” Constr Build Mater, vol. 404, p. 133280, 2023, doi: https://doi.org/10.1016/j.conbuildmat.2023.133280

[275] A. Peyvandi, P. Soroushian, A. M. Balachandra, and K. Sobolev, “Enhancement of the durability characteristics of concrete nanocomposite pipes with modified graphite nanoplatelets,” Constr Build Mater, vol. 47, pp. 111–117, 2013, doi: https://doi.org/10.1016/j.conbuildmat.2013.05.002

[276] J.-L. Le, H. Du, and S. D. Pang, “Use of 2D Graphene Nanoplatelets (GNP) in cement composites for structural health evaluation,” Compos B Eng, vol. 67, pp. 555–563, 2014, doi: https://doi.org/10.1016/j.compositesb.2014.08.005

[277] A. Hunain, A.-O. Ahmed, C. A. H.-D., and L. Xiaobing, “Materials Genome for Graphene-Cement Nanocomposites,” J Nanomech Micromech, vol. 3, no. 3, pp. 67–77, Sep. 2013, doi: https://doi.org/10.1061/(ASCE)NM.2153-5477.0000055

[278] K. Scrivener, A. Ouzia, P. Juilland, and A. Kunhi Mohamed, “Advances in understanding cement hydration mechanisms,” Cem Concr Res, vol. 124, p. 105823, 2019, doi: https://doi.org/10.1016/j.cemconres.2019.105823

[279] Q. Fu, Z. Wang, Y. Xue, and D. Niu, “Catalysis and Regulation of Graphene Oxide on Hydration Properties and Microstructure of Cement-Based Materials,” ACS Sustain Chem Eng, vol. 11, no. 14, pp. 5626–5643, Apr. 2023, doi: https://doi.org/10.1021/acssuschemeng.3c00109

[280] I. Fonseka, D. Mohotti, K. Wijesooriya, C.-K. Lee, and P. Mendis, “Influence of Graphene oxide on abrasion resistance and strength of concrete,” Constr Build Mater, vol. 404, p. 133280, 2023, doi: https://doi.org/10.1016/j.conbuildmat.2023.133280

[281] J. E. Rossen, B. Lothenbach, and K. L. Scrivener, “Composition of C–S–H in pastes with increasing levels of silica fume addition,” Cem Concr Res, vol. 75, pp. 14–22, 2015, doi: https://doi.org/10.1016/j.cemconres.2015.04.016

[282] J. A. Abdalla, B. S. Thomas, R. A. Hawileh, J. Yang, B. B. Jindal, and E. Ariyachandra, “Influence of nano-TiO2, nano-Fe2O3, nanoclay and nano-CaCO3 on

the properties of cement/geopolymer concrete," Cleaner Materials, vol. 4, p. 100061, 2022, doi: https://doi.org/10.1016/j.clema.2022.100061

[283] Z. Li, Z. He, and X. Chen, "The Performance of Carbonation-Cured Concrete," Materials, vol. 12, no. 22, 2019, doi: https://doi.org/10.3390/ma12223729

List of Publications

1) Singh, N., Singh, J. Impact of graphene derivative and ferrock on strength and durability of concrete. *Innov. Infrastruct. Solut.* **10**, 231 (2025). https://doi.org/10.1007/s41062-025-02036-4
2) Singh, N., Singh, J. Mechanical and microstructural analysis of concrete with graphene as partial replacement of cement. *Multiscale and Multidiscip. Model. Exp. and Des.* 8, 148 (2025). https://doi.org/10.1007/s41939-025-00755-w
3) Singh, N., Singh, J. Characterization of Concrete with Ferrock as a Potential Cement Substitute: Mechanical Strength, Durability and Microstructure analysis. *Iran J Sci Technol Trans Civ Eng* (2025). https://doi.org/10.1007/s40996-025-01885-4
4) Singh, N., Singh, J. Strength characterization of ferrock and incorporating as potential substitute of cement. *Jordan Journal of Civ Eng* (2025) https://doi.org/10.14525/JJCE.v19i3.06
5) Singh, N., Singh, J. Strength and microstructural characterization of iron- based binder as carbon absorbing material for sustainable concrete. *Multiscale and Multidiscip. Model. Exp. and Des.* **8**, 331 (2024). https://doi.org/10.1007/s41939-025-00918-9
6) Singh, N., Sharma, V. & Kapoor, K. Graphene in construction: enhancing concrete and mortar properties for a sustainable future. *Innov. Infrastruct. Solut.* 9, 428 (2024). https://doi.org/10.1007/s41062-024-01719-8
7) Singh, N., Sharma, R.L. & Yadav, K. Sustainable Solutions: Exploring Supplementary Cementitious Materials in Construction. *Iran J Sci Technol Trans Civ Eng* (2024). https://doi.org/10.1007/s40996-024-01585-5
8) Singh, N., Sharma, R.L. & Yadav, K. Sustainable development by carbon emission reduction and its quantification: an overview of current methods and best practices. *Asian J Civ Eng* 24, 3797–3822 (2023). https://doi.org/10.1007/s42107-023-00732-z
9) Singh, N., Singh, J. Investigation on permeability characteristics and microstructural analysis of concrete made with graphene oxide. *Innov. Infrastruct. Solut.* **10**, 280 (2025). https://doi.org/10.1007/s41062-025-02077

10) Experimental Investigation of Reduced Graphene Oxide and Ferrock CO_2 cured concrete: A Sustainable CO_2 - negative Cement Alternative (**Under Review)**

Conference paper

11) Sustainable Improvement of Concrete Properties by Agricultural Waste Based Supplementary Cementitious Materials – Conference Paper **(Accepted)**

1- Impact of graphene derivative and ferrock on strength and durability of concrete

Innovative Infrastructure Solutions (2025) 10:231
https://doi.org/10.1007/s41062-025-02036-4

TECHNICAL PAPER

Impact of graphene derivative and ferrock on strength and durability of concrete

Neha Singh[1] · Jaspreet Singh[1]

Received: 11 February 2025 / Accepted: 18 April 2025

Abstract
As the building industry has developed, the increased production of cement has become a substantial source of carbon emissions encouraging global warming. The present study investigates, for the first time, the combined effect of reduced graphene oxide and ferrock in enhancing concrete strength and durability while promoting sustainability. Ferrock reacts with carbon dioxide to form iron carbonates, contributing to its superior binding properties. Five concrete mixes were prepared with 0.2% reduced graphene oxide and 5%, 10%, 15% and 20% ferrock as substitute of cement. The fresh properties of concrete evaluated using the slump cone test and compaction factor test, while the hardened property assessed through compressive strength test. Durability performance was examined through rapid chloride penetration, water penetration, total absorption, and initial surface absorption tests. The results were systematically compared and reported. The compressive strength improved by 58.36% at 90 days of curing by mix RG0.2F10. The results found reduction of chloride penetration, water penetration, total absorption and initial surface absorption reduced by 72.47%, 35.29%, 61.9% and 35.71% respectively. The results found optimum replacement ratio was 10% with 0.2% of reduce graphene oxide by mix RG0.2F10. The study demonstrates the potential of reduced graphene oxide and ferrock as sustainable cement substitutes, enhancing strength and durability while promoting waste recycling and reducing soil pollution leads towards sustainable development.

Keywords Ferrock · Reduced graphene oxide · Durability · Mechanical strength · CO_2 curing

Introduction

The construction industry significantly contributes to global Carbon Dioxide (CO_2) emissions, with cement production accounting for about 7% of total CO_2 emissions [1]. Production of cement adversely affects the ecosystem and contributes to climate change, as it releases a significant amount of CO_2 into the atmosphere [2, 3]. Researches are being conducted on the utilization of potential cement substitutes to reduce cement consumption through the incorporation of various waste materials or suitable Supplementary Cementitious Materials (SCMs) [4, 5].

Recent advancements in materials science and nanotechnology have shown that graphene is an effective nanomaterial for improving the properties of cementitious materials. Nanomaterials also enhance the cracking resistance of concrete by filling pores at the nano scale, thereby mitigating its inherent tensile weakness. Reduced Graphene Oxide (rGO) is a graphene derivative that enhances strength and provides denser cementitious materials matrix [6]. rGO is produced by the reduction of Graphene Oxide (GO), which has many benefits, including cost-effectiveness, high yield, and scalability, making it a promising method for graphene acquisition. Also, it is dispersible in water due to the presence of functional groups [6]. Therefore, it is essential to examine the impact of rGO incorporation on the functional enhancement of cement-based materials. They promote the ongoing improvement of the microstructure of cementitious materials by efficiently functioning as a nanofiller and redistributing stress within the mixture's microstructure [7]. Numerous research has been conducted to examine the effects of rGO as a cementitious material. The previous research found an optimal dose of 0.1% rGO enhances Compressive Strength (CS) by 47%, split Tensile Strength (TS) by

✉ Jaspreet Singh
jaspreet.16659@lpu.co.in

Neha Singh
neha.12209870@lpu.in

[1] School of Civil Engineering, Lovely Professional University, Punjab 144411, India

2- Mechanical and microstructural analysis of concrete with graphene as partial replacement of cement

Multiscale and Multidisciplinary Modeling, Experiments and Design (2025) 8:148
https://doi.org/10.1007/s41939-025-00755-w

ORIGINAL PAPER

Mechanical and microstructural analysis of concrete with graphene as partial replacement of cement

Neha Singh[1] · Jaspreet Singh[1]

Received: 19 November 2024 / Accepted: 16 January 2025

Abstract
With the development of construction industry there is a challenge of strength development in an ecofriendly way. Reduced graphene oxide (rGO) is a nano-material which is dispersible in water. Many researchers have studied the influence of rGO in mechanical strength of mortar-based matrix with different ratios of rGO but limited on concrete ratios. This paper studies the impact of various ratios of rGO on mechanical properties of concrete composites to optimize the ratio. Six mixes were prepared with rGO as a partial substitute of cement in concrete in ratios of 0, 0.1, 0.2, 0.4, 0.6 and 0.8%. Tests for fresh properties, compressive strength (CS), split tensile strength (TS) and flexural strength (FS) were performed, compared and reported. The mix with 0.2% rGO showed the highest increase in CS, TS and FS with 37.38, 49.77 and 29.06% respectively as compared with control sample. The highest and lowest strength mix sample was analyzed by Scanning Electron Microscopy (SEM) and Energy Dispersive X-ray Spectroscopy (EDS) on 28 days of curing period. A one-way analysis of variance (ANOVA) was employed to determine whether the means of the mechanical strength of concrete were impacted by varying graphene ratios. Regression analysis showed good fit correlation between TS and FS of concrete. Obtained results showed that incorporation of rGO showed better strength than control mix and using rGO in concrete is an alternative nano material to enhance strength and leads to sustainable construction.

Keywords Reduced graphene oxide · Mechanical strength · Cement composites · Nano materials · ANOVA

1 Introduction

Concrete is one of the most utilized materials globally which has been utilized in the construction industry for over a century, primarily in structures such as buildings, roads, and bridges. Concrete industry accounts for around 5% of global greenhouse gas emissions (Lippiatt et al. 2020), which significantly contributes to climate change. Statistics show that cement production, which exceeds 4 billion tons per year, is responsible for over 4 billion tons of carbon emissions (Huang et al. 2023). This has increased atmospheric carbon concentrations to roughly 380 ppm, with forecasts indicating a rise to 800 ppm by 2100. In addition, the most recent report from the Intergovernmental Panel on Climate Change (2022) highlights the need to keep global warming to 1.5 °C, predicts that carbon emissions will peak by 2030, and states that carbon neutrality will be reached by 2060 (Barcelo et al. 2014). In response, sustainable construction practices have arisen as a significant area of research, with the goal of helping to fulfill these carbon reduction targets (Worrell et al. 2001).

The usage of cement in the construction industry can be reduced by using additives or alternatives for cement which is eco-friendly or materials with low carbon emissions (Wang et al. 2023). While traditional concrete has a high compressive strength (CS), frequently lacks the flexural strength (FS), split tensile strength (TS) and durability required to satisfy the needs of modern infrastructure due to cracking and poor fracture resistance (Zhang et al. 2022). To overcome these problems recent research suggests that use of nanoparticles, with cementitious materials, have an important role in controlling crack formation. Nanomaterials such as graphene oxide (GO), nano-TiO_2, and nano-SiO_2 have grown in popularity in construction due to their distinct characteristics, such as ultra-fine particles which favorable impact on the

✉ Jaspreet Singh
jaspreet.16659@lpu.co.in

Neha Singh
neha.12209870@lpu.in

[1] School of Civil Engineering, Lovely Professional University, Punjab 144411, India

Published online: 27 January 2025

3- Characterization of Concrete with Ferrock as a Potential Cement Substitute: Mechanical Strength, Durability and Microstructure analysis

Iranian Journal of Science and Technology, Transactions of Civil Engineering
https://doi.org/10.1007/s40996-025-01885-4

RESEARCH PAPER

Characterization of Concrete with Ferrock as a Potential Cement Substitute: Mechanical Strength, Durability and Microstructure analysis

Neha Singh[1] · Jaspreet Singh[1]

Received: 14 February 2025 / Accepted: 26 April 2025

Abstract
The present study investigates ferrock as binder, composed of iron oxide, waste dust of steel industries, as a partial substitute for cement, focusing on its carbon-absorbing properties and potential to enhance concrete's performance. The study aimed to find optimum ratio and investigate concrete mixes with ferrock as a substitute of cement in ratio of 0%, 5%, 10%, 15% and 20%. The slump cone and compaction factor tests evaluate the fresh properties of concrete, while compressive strength split tensile strength, and flexural strength tests were conducted to evaluate hardened properties of concrete. Durability analyzed further through water absorption, initial surface absorption, water penetration, and rapid chloride penetration tests. Microstructural analysis was performed to analyze the effects of ferrock incorporation on concrete microstructure. The carbonation test was done with phenolphthalein as an indicator for visual representation of carbonated parts in concrete. The samples were prepared according to the standard size recommended for testing and were initially cured for 4 days in a carbon dioxide environment, followed by water curing. The results demonstrated that 10% replacement of cement with ferrock yielded optimum performance, with an increase of 36.51% in compressive strength, 19.38% in flexural strength and 37.55% in split tensile strength. Microstructural analysis showed a denser micro- structure with more silica content and less iron due to complex iron carbonate formation in carbon dioxide presence. The results found ferrock a carbon-negative, eco-friendly material that recycles industrial waste, reduces cement use, enhances strength, and enables carbon-absorbing structures for sustainable construction.

Keywords Ferrock · Carbonation · Mechanical properties · Micro-structure · Iron oxide · Fly ash · Sustainable concrete · Cement replacement

1 Introduction

The rapid rate of infrastructure development in many parts of the world has resulted in an enormous demand for portland cement. The construction sector is significant in global resource extraction, consuming 40% of materials and contributing 50% of global greenhouse gas emissions. The significant increase in population causes consumption of non-renewable resources and increases the infrastructural demand (Amin et al. 2024a, b). The construction and building sector contribute significantly to global climate change, emitting 39% of global Carbon dioxide (CO_2) emissions and consuming raw materials (Soumya Pradhan et al. 2023). A significant portion of these emissions originated from cement production about one ton of CO_2 emits on production of one ton of cement (Verma et al. 2022a). CO_2 is the main greenhouse gas generate during cement preparation (Pradhan et al. 2023a). The conversion of limestone to lime—a process that inherently releases CO_2 as a byproduct—contributes heavily to global CO_2 levels (Xu et al. 2022). Additionally, the energy-intensive nature of cement manufacturing, largely fueled by fossil fuels, further exacerbates its contribution to anthropogenic emissions (Kumar et al. 2021). The study focuses to mitigate CO_2 emissions by minimizing cement usage through the incorporation of potential substitute. As this business advances, ecofriendly methods

✉ Jaspreet Singh
jaspreet.166598@lpu.co.in

Neha Singh
neha.12209870@lpu.in

[1] School of Civil Engineering, Lovely Professional University, Punjab 144411, India

Published online: 22 May 2025

4- Strength characterization of ferrock and incorporating as potential substitute of cement

Jordan Journal of Civil Engineering, Volume 19, No. 3, 2025
DOI: https://doi.org/10.14525/JJCE.v19i3.06

Jordan Journal of Civil Engineering

Journal homepage: https://jjce.just.edu.jo

Strength Characterization of Ferrock Incorporated As a Potential Substitute of Cement

Neha Singh[1], *Jaspreet Singh*[2]*

[1] School of Civil Engineering, Lovely Professional University, Punjab, 144411, India. E-Mail: neha.12209870@lpu.in
[2] School of Civil Engineering, Lovely Professional University, Punjab, 144411, India.
* Corresponding Author. E-Mail: jaspreet.16659@lpu.co.in

ARTICLE INFO

Article History:
Received: 16/1/2025
Accepted: 22/4/2025

ABSTRACT

The global construction sector is contributing to global warming through cement manufacturing, necessitating the search for eco-friendly, low-carbon materials as alternatives. Iron dust waste generated by steel industries is often disposed of through landfilling, which contributes to soil pollution. Ferrock is made up of iron dust which is produced in steel industries along with other supplementary cementitious materials to improve the performance of concrete. It is a carbon negative material which absorbs carbon during its reactions. Concrete mixes were prepared with ferrock at 0%, 5%, 10%, 15% and 20% replacement of cement. The compressive, split tensile and flexural strength tests were evaluated and their findings revealed that 10% is the optimum ratio which enhanced the aforementioned strengths by 37.4%, 37.5% and 19.4%, respectively, at 28 days of curing as compared with the control mix. Carbonation tests showed that concrete with ferrock had a higher carbonated area than the control mix without ferrock. Ferrock enhances concrete strength, reduces cement usage, and absorbs carbon dioxide from the environment, promoting sustainable development by recycling steel waste dust and reducing carbon emissions.

Keywords: Ferrock, Sustainable construction, Mechanical strength, Carbonation test, Industrial waste, Phenolphthalein.

INTRODUCTION

The growth of the building sector significantly contributes to increasing the level of carbon emissions and the demand for raw materials (Barcelo et al., 2014). This sector currently accounts for around 39% of carbon emissions worldwide, highlighting its significant influence on climate change. A substantial fraction of these emissions emits from cement manufacturing, wherein the transformation of limestone (LS) into lime—a process that intrinsically emits Carbon Dioxide (CO_2) as a by-product—substantially adds to world CO_2 concentrations (Kadawo et al., 2023; Alani et al., 2025). Cement is one of the main ingredients and acts as a binder in concrete (Liu et al., 2023). It also leaves large carbon footprints behind that can be smaller by limiting the use of cement with the help of abundant quantities of available materials (Chen et al., 2023). Incorporation of waste is increasingly being included in concrete composites by recent research studies. These wastes greatly reduce the environmental impact caused by cement manufacturing, along with conserving resources and reducing waste.

The Ministry of Steel reports that India has risen to the position of the world's second-biggest steel manufacturer, generating 99.56 tons of steel in 2020-

5- Strength and microstructural characterization of iron- based binder as carbon absorbing material for sustainable concrete

Multiscale and Multidisciplinary Modeling, Experiments and Design (2025) 8:331
https://doi.org/10.1007/s41939-025-00918-9

ORIGINAL PAPER

Strength and microstructural characterization of iron- based binder as carbon absorbing material for sustainable concrete

Neha Singh[1] · Jaspreet Singh[1]

Received: 18 January 2025 / Accepted: 17 May 2025

Abstract
The study utilized iron oxide, a waste byproduct from steel manufacturing, as the primary binding material. The concept involves the reaction of iron oxide with CO_2 in the presence of a weak acid, resulting in the formation of iron carbonates, which exhibit binding properties. The novelty of this study lies in the optimised ratios of raw materials, incorporating varying levels of oxalic acid and CO_2 utilisation. It further incorporates detailed microstructural analysis to identify optimum mix. Sixteen mixes were investigated with varying raw materials ratios and carbon curing duration as 2, 3, 4, 5, and 6 days followed by 3 air curing days. The Unconfined Compressive Strength (UCS) test was conducted to identify the optimum mix ratio along with carbon curing day corresponding to highest strength. Energy Dispersive X-ray Spectroscopy (EDS) provided insights into the elemental composition of raw materials and the iron carbonate binder, revealing a significant reduction in iron oxide after 4 days of carbon curing compared to 2 days, indicating its reaction with CO_2. X-ray Diffraction (XRD) analysis identified the mineral phases, and Scanning Electron Microscopy (SEM) visualized the microstructural development of the composites. A carbonation test confirmed the absorption of CO_2 by the iron-based binder during hardening. Results show iron carbonate binder not only provides substantial binding ability and compressive strength but also serves as a sustainable solution for CO_2 sequestration. This innovative approach offers a significant potential substitute for cement for enhanced strength and carbon negative structures. Use of ferrock promotes environmental sustainability through reduced usage of cement and the utilization of industrial waste.

Keywords Iron powder · Carbonation · Carbon curing · Compressive strength · Microstructural analysis · Sustainable concrete

1 Introduction

The global climate is changing because of Carbon Dioxide (CO_2) emissions, which could have possibly permanent negative effects on ecosystems and societies. According to a UN report, 38% of CO_2 emissions come from the construction industry, contributing to climate change (Jeffy Pravitha et al. 2023; Barcelo et al. 2014). Concrete's ease of use and versatility make it a popular choice for construction projects worldwide, however, it has impacts on the environment (Huang et al. 2018; Bellum et al. 2024). Today, cement is the world's second most widely used substance after water and serves as a binder. It is also the fourth greatest source of anthropogenic CO_2 emissions (Barcelo et al. 2014; Amran et al. 2022). The production of one ton of cement emits one ton of CO_2 indicating alarming situation in polluting the environment (Sun et al. 2022; Hay et al. 2021). When cement is produced, toxic fumes are released into the environment, which can be dangerous (Huang et al. 2023). Much research on going to lower atmospheric greenhouse gases, such as CO_2 (Liu et al. 2023). Climate change has alarmed scientists to search for new and sustainable alternatives for major emitting sources such as cement (Lippiatt et al. 2020).

Numerous steel mills across the nation fully contribute to the nation's demand for steel, which is produced on a

✉ Jaspreet Singh
jaspreet.16659@lpu.co.in

6- Graphene in construction: enhancing concrete and mortar properties for a sustainable future

Innovative Infrastructure Solutions (2024) 9:428
https://doi.org/10.1007/s41062-024-01719-8

REVIEW

Graphene in construction: enhancing concrete and mortar properties for a sustainable future

Neha Singh[1] · Vaibhav Sharma[1] · Kanish Kapoor[2]

Received: 4 May 2024 / Accepted: 14 September 2024

Abstract
Concrete is an important part of construction with good compressive strength but weak in tensile strength. Many nanomaterials have been used to improve characteristics of concrete. Graphene has been found to be the most promising nanomaterial because of its excellent properties like tensile strength and large surface area. The aim of this analysis is to review the revolutionary potential of graphene in concrete, which is a single-layer carbon allotrope, as an addition or partial replacement for cement in concrete. The objective is to improve the material's strength, workability, and environmental sustainability. The study takes use of graphene's extraordinary mechanical strength, thermal and electrical conductivity to undertake an in-depth investigation of the multiple forms of graphene. The review extensively explores various manifestations of graphene and reveals that even a minute addition of 0.1% graphene leads to notable substantial increases of up to 10–15%, 20–25%, and 20–30% in compressive strength (CS), tensile strength (TS), and flexural strength (FS), respectively. The review highlights challenges like scalability, economic viability, and regulatory adherence in graphene's utilization in construction. Informing researchers, policymakers, and industry professionals, this comprehensive review underscores graphene's significant promise in enhancing concrete properties, contingent on the quantity used, in the construction sector.

Keywords Graphene production · Environmental sustainability · Carbon emissions · Graphene concrete · Concrete performance improvements · Graphene nanoengineered construction

Introduction

According to projections made by the World Business Council for Sustainable Development (WBCSD), the worldwide output of cement will surpass 3.6 billion tons and is anticipated to fall somewhere in the range of 3.7 to 4.4 billion tons by the year 2050. This growth is fueled by urbanization and a rising demand for construction and infrastructure [1–3]. Until the year 2050, in order to achieve the goals specified in the Paris Agreement and to achieve zero carbon emissions, there is a necessity to reduce current emissions from 2.2 to 1.5 gigatons of carbon per years [4]. The contemporary focus on the cement industry is notably heightened, considering that cement serves as the principal constituent in concrete, facilitating particle cohesion through hydration with water [5]. The carbon emission profile of cement production is significant, with approximately one ton of carbon released per ton of cement manufactured. This emission arises predominantly from the chemical reactions that are important in the production of the primary constituents of cement. Lime (CaO) is produced when limestone ($CaCO_3$) is converted to calcareous or clinkering process, accounting for around 60% of these emissions. The majority of the remaining 40% can be ascribed to the fossil fuel combustion required to achieve the clinkerization temperature of 1450 °C [6]. Indeed, between 5% and 7% of the total pollution that is created by human activities is contributed by the cement sector [7]. The process of making

✉ Neha Singh
neha.12209870@lpu.in

Vaibhav Sharma
vaibhav.26569@lpu.co.in; civil.vaibhav.sharma@gmail.com

Kanish Kapoor
kapoork@nitj.ac.in

[1] School of Civil Engineering, Lovely Professional University, Phagwara, Punjab 144411, India

[2] Department of Civil Engineering, Dr. B R Ambedkar National Institute of Technology, Jalandhar, India

Published online: 23 October 2024

7- Sustainable Solutions: Exploring Supplementary Cementitious Materials in Construction

Iranian Journal of Science and Technology, Transactions of Civil Engineering
https://doi.org/10.1007/s40996-024-01585-5

REVIEW PAPER

Sustainable Solutions: Exploring Supplementary Cementitious Materials in Construction

Neha Singh[1] · R. L. Sharma[1] · Kundan Yadav[1]

Received: 13 November 2023 / Accepted: 8 August 2024

Abstract
Despite advancements in energy efficiency, the construction and operation of our built environment remains responsible for 34% of global energy demand and 37% of CO_2 emissions, exacerbating environmental challenges. Climate indicators are worsening; carbon dioxide levels continue to rise, putting the world on a trajectory for a 2% annual increase. Every country, city, organization, and company need to adopt net-zero plans to combat this crisis. The construction industry requires innovative and sustainable solutions, including the exploration of eco-friendly construction materials, to achieve carbon neutrality by 2050. The use of supplementary cementitious materials (SCMs) to partially replace cement in concrete production is a significant stride towards sustainable construction practices, effectively addressing waste generation and environmental concerns associated with traditional cement usage. SCMs help in recycling industrial by-products and agricultural wastes, significantly reducing landfill waste and promoting resource efficiency. Additionally, partial replacement of cement with SCMs can lower CO_2 emissions from cement production, contributing to the construction sector's net-zero goals. Moreover, SCMs can improve the durability and lifespan of concrete structures, reducing the need for frequent repairs and maintenance, thus saving costs and resources over time. This study summarizes diverse SCMs for partial cement replacement, explores their compositions, and emphasizes their crucial role in achieving carbon neutrality by 2050. It evaluates key characteristics such as compressive strength, durability, workability, and environmental impact to assess the performance, advantages, and challenges associated with these materials. This analysis guides practitioners in making informed decisions about their implementation in construction projects. Our review guides the construction industry towards more eco-friendly practices, contributing to the long-term sustainability and resilience of concrete structures. By mitigating the environmental footprint of cement production, we promote the creation of more sustainable and high-performance concrete structures.

Keywords Sustainable construction · Supplementary cementitious materials (SCMs) · Carbon neutrality · Comparative analysis · Environmental impact

1 Introduction

In recent years, the construction sector has seen a notable movement towards the adoption of sustainable methods and environmentally friendly solutions (Karhunmaa 2019; Gupta and Garg 2020). An essential element of this transition is the adoption of alternative materials, known as Supplementary Cementitious Materials (SCMs), that have the potential to partly substitute traditional cement in various building applications (Soni et al. 2022). Cement is a fundamental constituent and principal binder in the composition of concrete and plays a significant role in contributing to a considerable proportion of worldwide carbon emissions and energy consumption (Dahal et al. 2018; L. U. O. H.-L. Zhang Ya-Xin Wang Can n.d.). The ingredient in question is a costly substance used in the manufacturing of concrete and is associated with significant carbon footprints, which can be reduced by limiting cement usage (Juenger and Siddique 2015; Prakash Chandar and Santhosh 2022). The concrete industry requires a vast number of natural resources and heavily depends on freshwater and natural aggregates.

✉ Kundan Yadav
en.kundan@gmail.com

Neha Singh
neha707867@gmail.com

R. L. Sharma
rl78sharma@gmail.com

[1] School of Civil Engineering, Lovely Professional University, Phagwara, Punjab 144411, India

Published online: 22 August 2024

8- Sustainable development by carbon emission reduction and its quantification: an overview of current methods and best practices

Asian Journal of Civil Engineering (2023) 24:3797–3822
https://doi.org/10.1007/s42107-023-00732-z

REVIEW

Sustainable development by carbon emission reduction and its quantification: an overview of current methods and best practices

Neha Singh[1] · R. L. Sharma[1] · Kundan Yadav[1]

Received: 15 May 2023 / Accepted: 22 May 2023 / Published online: 1 June 2023

Abstract
The construction sector accounts for 36% of global energy consumption and 39% of global carbon dioxide emissions. Sustainable development, which entails reducing and quantifying carbon emissions, is essential to address climate change and the depletion of non-renewable resources. This review paper examines a range of strategies and methodologies, including green building rating systems, sustainable materials and renewable energy, smart building management systems, carbon capture and storage, life cycle assessments, and greenhouse protocols, that can facilitate sustainable development by reducing and quantifying carbon emissions. The paper underscores the need for up-to-date information and more precise techniques to achieve sustainable development goals. Additionally, the paper highlights the potential advantages of sustainable construction practices, such as lower energy costs, better indoor air quality, and more efficient use of resources.

Keywords Construction sector · Carbon dioxide emissions · Quantifying carbon emissions · Sustainable construction practices · Efficient use of resources

Introduction

India is a rapidly developing country with a large population, urbanization, and increasing wealth, leading to high energy consumption and greenhouse gas emissions (Zhang et al., 2023). Population growth is the leading cause of carbon emissions and greenhouses (Li et al., 2017). Sustainable development (SD) is one of the global environmental movement's orientations, with the goal of conserving and repairing the environment and it includes economic, environmental, and social impacts (GhaffarianHoseini et al., 2013; Peng et al., 2023; Zhao et al., 2021). According to the World Commission on Environment and Development (WCED) report, sustainable development is the "development that meets the need of the present without compromising the ability of future generations to meet their [own] needs" (Bruntland, 1987). The carbon footprint is the "total GHG emissions generated directly or indirectly by a person, event, organization, or product, resulting mostly in CO_2 emissions." According to the Intergovernmental Panel on Climate Change (IPCC), the generation of GHG from burning fossil fuels is a major factor in global warming (Jafary Nasab et al., 2020). Developed countries such as the United States, the United Kingdom, and Japan have committed to becoming carbon neutral by 2050 (Al-Obaidy et al., 2022). In India, construction and operation play a vital role in the economy, consuming 35% of global energy and contributing 29% of CO_2 emissions (Mahasenan et al., 2003). The construction sector is responsible for 30–40% of industrial CO_2 emissions globally, although this represents less than 7% of total global CO_2 emissions (Chen et al., 2010; Scrivener & Kirkpatrick, 2008; Worrell et al., 2001). Around 80% of energy usage and GHG (Qin & Kaewunruen, 2022) emissions are caused by building operations (including heating, cooling, ventilation, lighting, and appliances), whereas only 10–20% are caused by material manufacture, construction, and demolition (Nag & Parikh, 2000).

Carbon Footprint Analysis: Promoting Sustainable Development. Available from: https://www.researchgate.net/publication/348390830_Carbon_Footprint_Analysis_Promoting_Sustainable_Development [accessed Apr 24 2023].

✉ Neha Singh
neha707867@gmail.com

R. L. Sharma
sharma.23743@lpu.co.in

Kundan Yadav
en.kundan@gmail.com

[1] School of Civil Engineering, Lovely Professional University, Phagwara, Punjab 144411, India

9. Investigation on permeability properties and microstructural analysis of concrete made with reduced graphene oxide

Innovative Infrastructure Solutions (2025) 10:280
https://doi.org/10.1007/s41062-025-02077-9

TECHNICAL PAPER

Investigation on permeability characteristics and microstructural analysis of concrete made with graphene oxide

Neha Singh[1] · Jaspreet Singh[1]

Received: 2 November 2024 / Accepted: 16 May 2025

Abstract
Present research aimed to investigate the impact of reduced graphene oxide (rGO) as partial replacement of cement on compressive strength, permeability and microstructural properties. The concrete mixes prepared with 0, 0.1, 0.2, 0.4, 0.6 and 0.8% replacement of cement with rGO. Permeability properties were determined by water absorption, water permeability, initial surface absorption and rapid chloride penetration tests at 28, 56, and 90 curing days. Microstructure analysis performed by x-ray diffraction, scanning electron microscopy and energy dispersive x-ray spectroscopy. The results indicate that the increase in ratio of rGO enhances the compressive strength of concrete. The optimum ratio of replacement for compressive strength was found to be 0.2% with an improvement of 37.3, 34.09 and 32.91% at 28, 56 and 90 days of curing. The results indicate that water absorption, water penetration, initial surface absorption and chloride penetration reduced by 43.5, 56.39, 26.78 and 55.89% at 90 days of curing. The microstructural analysis revealed morphology is denser and compacted. Regression and analyses of variance were performed to establish correlation and analyze the difference between the means. Results of this investigation concluded that each mix containing rGO showed better strength and improved permeability as compared to control sample. Using rGO can be used in concrete to improve properties and leads toward sustainable construction.

Keywords Reduced graphene oxide · Sustainable construction · ANOVA · Water permeability test · Microstructural analysis

Abbreviations

CO_2	Carbon dioxide
rGO	Reduced graphene oxide
GO	Graphene oxide
OPC	Ordinary portland cement
SEM	Scanning electron microscope
XRD	X-ray diffraction
EDS	Energy dispersive x-ray spectroscopy
ASTM	American society for testing and materials
NaOH	Sodium hydroxide
NaCl	Sodium chloride
RCPT	Rapid chloride penetration test
ISAT	Initial surface absorption test
CSH	Calcium silicate hydrate
C_2S	Dicalcium silicate
C_3S	Tricalcium silicate
ANOVA	Analysis of variance

✉ Jaspreet Singh
jaspreet.16859@lpu.co.in

Neha Singh
neha.12209870@lpu.in

[1] School of Civil Engineering, Lovely Professional University, Punjab 144411, India

Published online: 13 June 2025

Introduction

Concrete is the most extensively utilized material in construction due to its superior structural stability. Large-scale production of cement is accompanied by significant environmental concerns, as Carbon Dioxide (CO_2) emissions from India's cement industry are projected to reach around 835 million tons by 2050—5.1 times higher than current levels [1]. India ranks as the second-largest cement producer globally, accounting for approximately 7–8% of total cement production, with an annual capacity of 234 million tons [2, 3]. Research indicates that manufacturing 1 kg of cement generates approximately 0.95 kg of CO_2 emissions [4]. Out of this, 0.55 kg is emitted directly during cement production, and an additional 0.40 kg results from the fuel required for combustion [5]. The extensive exploitation of natural resources for cement production has led to environmental degradation [6, 7]. To meet these demands while mitigating

List of Conferences

1. Poster Presentation-

Graphene-Infused Concrete: Improving Strength and Durability in Construction - **International Conference "Engineered Materials for Sustainable Development (EMSD- 2024)**

2. Paper Presentation-

Sustainable improvement of concrete properties by Agro- industrial waste based supplementary cementitious materials- **2nd International Conference on Sustainable Experimentation and Modelling in Civil Engineering (SEMCE-2024)**

1- Poster Presentation

PEC
EXPLORE INNOVATE EXCEL
SINCE 1921

INTERNATIONAL CONFERENCE
ON
ENGINEERED MATERIALS FOR SUSTAINABLE DEVELOPMENT
EMSD 2024

CERTIFICATE OF PARTICIPATION

Presented to

Mr./Miss./Dr. Neha Singh for Poster Presentation participated in
International Conference On Engineered Materials For Sustainable Development (EMSD 2024)
Jointly organised by
Punjab Engineering College (Deemed to be University), Chandigarh
And
National Agri-Food Biotechnology Institute (NABI), Mohali
from July 24-26, 2024

Prof. Sandeep Kumar
Conference Convenor, PEC, Chandigarh

Prof. Nitin Kumar Singhal
Conference Convenor, NABI, Mohali

2- Paper Presentation

SEMCE

SCHOOL OF CIVIL ENGINEERING

ThinkBIG

NAAC A++

Certificate No. 357345

Certificate of Presentation

This is to certify that Mr./Ms. **Neha Singh** of Lovely Professional University presented the paper titled *Sustainable improvement of concrete properties by Agro- Industrial based supplementary cementitious materials in the* **2nd International Conference on Sustainable Experimentation and Modelling in Civil Engineering (SEMCE-2024) held** from 13th to 14th November 2024, organized by **School of Civil Engineering** at Lovely Professional University, Punjab.

Date of Issue : 30-11-2024
Place : Phagwara (Punjab), India

Prepared by
(Administrative Officer-Records)

Organizing Secretary
(School of Civil Engineering)

Head of School
School of Civil Engineering

Copyright-

Graphical Abstract- Sustainable Improvement of Concrete Properties by Agricultural Waste Based Supplementary Cementitious Materials (Granted)

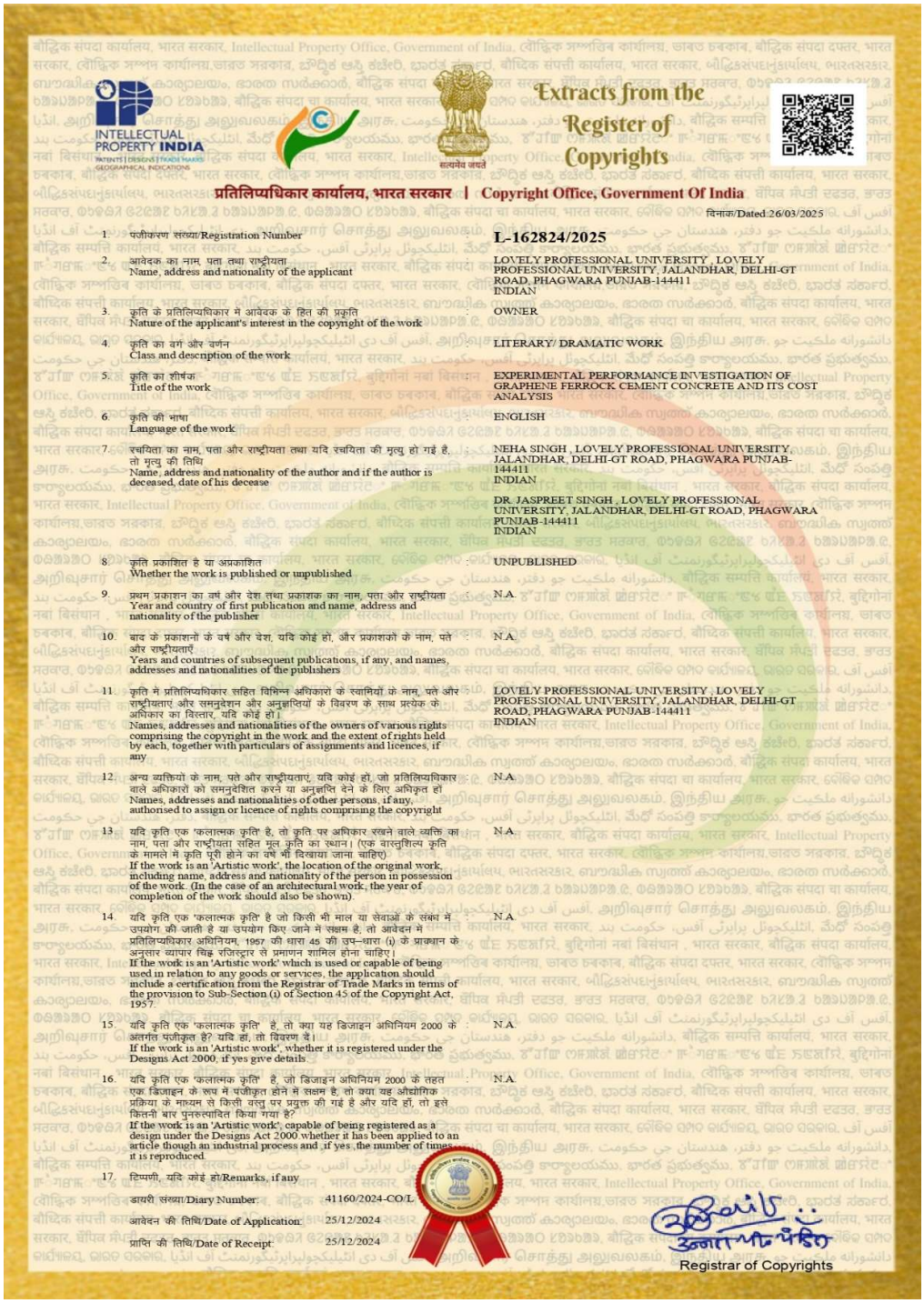

INTELLECTUAL PROPERTY INDIA
PATENTS | DESIGNS | TRADE MARKS | GEOGRAPHICAL INDICATIONS

सत्यमेव जयते

Extracts from the Register of Copyrights

प्रतिलिप्यधिकार कार्यालय, भारत सरकार | Copyright Office, Government Of India

दिनांक/Dated 26/03/2025

1.	पंजीकरण संख्या/Registration Number	**L-162824/2025**
2.	आवेदक का नाम, पता तथा राष्ट्रीयता Name, address and nationality of the applicant	LOVELY PROFESSIONAL UNIVERSITY , LOVELY PROFESSIONAL UNIVERSITY, JALANDHAR, DELHI-GT ROAD, PHAGWARA PUNJAB-144411 INDIAN
3.	कृति के प्रतिलिप्यधिकार में आवेदक के हित की प्रकृति Nature of the applicant's interest in the copyright of the work	OWNER
4.	कृति का वर्ग और वर्णन Class and description of the work	LITERARY/ DRAMATIC WORK
5.	कृति का शीर्षक Title of the work	EXPERIMENTAL PERFORMANCE INVESTIGATION OF GRAPHENE FERROCK CEMENT CONCRETE AND ITS COST ANALYSIS
6.	कृति की भाषा Language of the work	ENGLISH
7.	रचयिता का नाम, पता और राष्ट्रीयता तथा यदि रचयिता की मृत्यु हो गई है, तो मृत्यु की तिथि Name, address and nationality of the author and if the author is deceased, date of his decease	NEHA SINGH , LOVELY PROFESSIONAL UNIVERSITY, JALANDHAR, DELHI-GT ROAD, PHAGWARA PUNJAB-144411 INDIAN DR. JASPREET SINGH , LOVELY PROFESSIONAL UNIVERSITY, JALANDHAR, DELHI-GT ROAD, PHAGWARA PUNJAB-144411 INDIAN
8.	कृति प्रकाशित है या अप्रकाशित Whether the work is published or unpublished	UNPUBLISHED
9.	प्रथम प्रकाशन का वर्ष और देश तथा प्रकाशक का नाम, पता और राष्ट्रीयता Year and country of first publication and name, address and nationality of the publisher	N.A.
10.	बाद के प्रकाशनों के वर्ष और देश, यदि कोई हों, और प्रकाशकों के नाम, पते और राष्ट्रीयताएँ Years and countries of subsequent publications, if any, and names, addresses and nationalities of the publishers	N.A.
11.	कृति में प्रतिलिप्यधिकार सहित विभिन्न अधिकारों के स्वामियों के नाम, पते और राष्ट्रीयताएं और समनुदेशन और अनुज्ञप्तियों के विवरण के साथ प्रत्येक के अधिकार का विस्तार, यदि कोई हों। Names, addresses and nationalities of the owners of various rights comprising the copyright in the work and the extent of rights held by each, together with particulars of assignments and licences, if any	LOVELY PROFESSIONAL UNIVERSITY , LOVELY PROFESSIONAL UNIVERSITY, JALANDHAR, DELHI-GT ROAD, PHAGWARA PUNJAB-144411 INDIAN
12.	अन्य व्यक्तियों के नाम, पते और राष्ट्रीयताएं, यदि कोई हों, जो प्रतिलिप्यधिकार वाले अधिकारों को समनुदेशित करने या अनुज्ञप्ति देने के लिए अधिकृत हों Names, addresses and nationalities of other persons, if any, authorised to assign or licence of rights comprising the copyright	N.A.
13.	यदि कृति एक 'कलात्मक कृति' है, तो कृति पर अधिकार रखने वाले व्यक्ति का नाम, पता और राष्ट्रीयता सहित मूल कृति का स्थान। (एक वास्तुशिल्प कृति के मामले में कृति पूरी होने का वर्ष भी दिखाया जाना चाहिए) If the work is an 'Artistic work', the location of the original work, including name, address and nationality of the person in possession of the work. (In the case of an architectural work, the year of completion of the work should also be shown).	N.A.
14.	यदि कृति एक 'कलात्मक कृति' है जो किसी भी माल या सेवाओं के संबंध में उपयोग की जाती है या उपयोग किए जाने में सक्षम है, तो आवेदन में प्रतिलिप्यधिकार अधिनियम, 1957 की धारा 45 की उप–धारा (1) के प्रावधान के अनुसार व्यापार चिह्न रजिस्ट्रार से प्रमाणन शामिल होना चाहिए। If the work is an 'Artistic work' which is used or capable of being used in relation to any goods or services, the application should include a certification from the Registrar of Trade Marks in terms of the provision to Sub-Section (1) of Section 45 of the Copyright Act, 1957.	N.A.
15.	यदि कृति एक 'कलात्मक कृति' है, तो क्या यह डिजाइन अधिनियम 2000 के अंतर्गत पंजीकृत है? यदि हां, तो विवरण दें। If the work is an 'Artistic work', whether it is registered under the Designs Act 2000, if yes give details.	N.A.
16.	यदि कृति एक 'कलात्मक कृति' है, जो डिजाइन अधिनियम 2000 के तहत एक डिजाइन के रूप में पंजीकृत होने में सक्षम है, तो क्या यह औद्योगिक प्रक्रिया के माध्यम से किसी वस्तु पर प्रयुक्त की गई है और यदि हाँ, तो इसे कितनी बार पुनरुत्पादित किया गया है? If the work is an 'Artistic work', capable of being registered as a design under the Designs Act 2000 whether it has been applied to an article though an industrial process and ,if yes ,the number of times it is reproduced.	N.A.
17.	टिप्पणी, यदि कोई हो/Remarks, if any	

डायरी संख्या/Diary Number: 41160/2024-CO/L

आवेदन की तिथि/Date of Application: 25/12/2024

प्राप्ति की तिथि/Date of Receipt: 25/12/2024

उमा शंकर पंडित
Registrar of Copyrights

Graphical Abstract: